

Synthesis, conformational investigations and applications of α -peptides containing *cis*- β -aminocyclopropane dicarboxylic acids

Dissertation

zur Erlangung des Doktorgrades
der Naturwissenschaften (Dr. rer. nat.)
der Fakultät für Chemie und Pharmazie
der Universität Regensburg



vorgelegt von

Silvia De Pol

aus

Venezia

Regensburg 2006

Die Arbeit wurde angeleitet von : Prof. Dr. O. Reiser

Promotionsgesuch eingereicht am: 6. Februar 2006

Promotionskolloquium am: 16. März 2006

Prüfungsausschuß:

- Vorsitzender: Prof. Dr. S. Elz
- 1. Gutachter: Prof. Dr. O. Reiser
- 2. Gutachter Prof. Dr. B. König
- 3. Prüfer: Prof. Dr. A. Buschauer

Die vorliegende Arbeit wurde in der Zeit von Januar 2002 bis Januar 2006 am Institut für Organische Chemie der Universität Regensburg unter der Leitung von Prof. Dr. O. Reiser angefertigt.

Meinem Lehrer, Herrn Prof. Dr. O. Reiser, danke ich herzlich für die Überlassung des interessanten Themas, die Möglichkeit zur Durchführung dieser Arbeit und seine stetige Unterstützung.

*To Gerda, Santina,
Federico and Guerrino.*

Index

A. Introduction	1
A.1 About α -Peptides...	3
A.2 β -amino acids and β -Peptides	10
A.3 β -amino acids incorporated into α -Peptides	12
B. Model Peptides containing β-ACC: Synthesis and Conformational Investigations	17
B.1 Synthesis	17
B.2 Conformational Investigations	25
B.2.1 Circular dichroism	25
B.2.2 NMR investigation	26
B.2.2.1 Information from 1D-proton NMR spectra	27
B.2.2.2 Information from 2D-proton NMR data	28
B.2.2.3 Structure calculations from NOE data	30
B.2.3 FT-IR spectroscopy	30
B.3 Results on alternated α -Xaa/ β -ACC peptides	32
B.3.1 Alternated α -L-Ala/(-) β -ACC peptides	36
B.3.2 Alternated α -L-Ala/(+) β -ACC peptides	46
B.3.3 Alternated α -L-Xaa/(-) β -ACC peptide	50
C. β-ACC units into Biologically Active α-Peptides	57
C.1 RGD analogues	57
C.1.1 Introduction	57
C.1.2 RGD peptides containing β -ACC units	64
C.2 Conformational investigation on a β -ACC-NPY analogues	67
C.2.1 Introduction	67
C.2.2 NPY analogues containing β -ACC units	73

D. Summary	83
E. Experimental part	89
E.1. Instruments and general techniques	89
E.2 Solution Synthesis	92
E.2.1 Peptides containing (+)- β ACC units	92
E.2.2 Peptides containing (–)- β ACC units	101
E.3 Solid-phase synthesis	113
F. Appendix of NMR and X-Ray Data	115

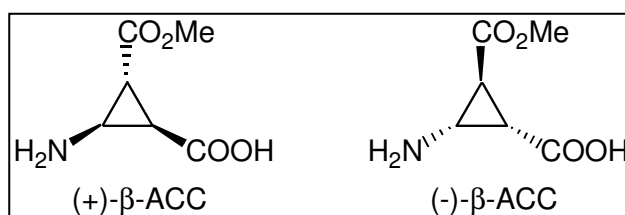
Abbreviations

Ac	Acetyl	min.	minutes
ACN	Acetonitrile	MS	Mass Spectroscopy
Alloc	Allyloxycarbonyl	NMR	Nuclear Magnetic Resonance
Ar	Aryl	NOE	Nuclear Overhauser Effect
Bn	Benzyl	PG	Protecting group
Boc	tert-Butyl	Ph	Phenyl
Bu	Butyl	ppb	Part per billion
c-	cyclo	Py	Pyridine
CD	Circular Dichroism	quant.	quantitative
COSY	Correlation Spectroscopy	RMSD	Root Mean Square Deviation
DIC	Diisopropylcarbodiimide	ROESY	Rotating Frame NOE
DIPEA	Diisopropylethylamine		spectroscopy
DMAP	Dimethylaminopyridine	r.t.	room temperature
DMF	Dimethylformamide	sat.	saturated
DMSO	Dimethylsulfoxide	tert	tertiary
EDC	Ethyl-N,N-dimethyl-3-aminopropylcarbodiimide	TFA	Trifluoro acetic acid
		TFE	Trifluoroethanol
Et	Ethyl	TOCSY	Total Correlation Spectroscopy
eq.	equivalents	UV	Ultraviolet Spectroscopy
Fmoc	9-Fluorenylmethoxycarbonyl		
h	hours		
HBTU	O-benzotriazole-N,N,N',N'-tetramethyluronium-hexafluoro-phosphate		
HB	Hydrogen Bond		
HFA	Hexafluoroacetone		
HOBt	Hydroxybenzotriazole		
IR	Infrared Spectroscopy		
MALDI	Matrix-assisted laser desorption ionization		
MeOH	Methanol		
Me	Methyl		

Amino acids:

<i>Amino acid</i>	<i>One-letter code</i>	<i>Three-letter code</i>
Alanine	A	Ala
Arginine	R	Arg
Asparagine	N	Asn
Aspartic acid	D	Asp
Cysteine	C	Cys
Glutamine	Q	Gln
Glutamic acid	E	Glu
Glycine	G	Gly
Histidine	H	His
Isoleucine	I	Ile
Leucine	L	Leu
Lysine	K	Lys
Methionine	M	Met
Phenylalanine	F	Phe
Proline	P	Pro
Serine	S	Ser
Threonine	T	Thr
Tryptophan	W	Trp
Tyrosine	Y	Tyr
Valine	V	Val
Unspecified amino acid	X	Xaa, Yaa

D-amino acids are described by D-Xaa in the three-letter code and with the small letter in the one-letter code.



A. Introduction

*“Almost all aspects of life are engineered
at the molecular level,
and without understanding molecules we can only have
a sketchy understanding of life itself”*

Francis Crick

4.6 billion years ago our Earth was a lifeless, inhospitable place. A billion years later life began, and its development to today's known complexity continues to generate fascinating conjectures and ingenious experiments. In the early 1950s *Miller* and *Urey* did the first experiment designed to clarify the chemical reactions that probably occurred on the primitive earth with a reducing atmosphere. From an atmosphere consisting of methane, ammonia, hydrogen, water vapor, and electrical discharge they obtained many amino acids as products.¹ Recent investigations indicate that the Earth's atmosphere was never reducing as *Urey* and *Miller* presumed, and under oxidizing conditions no amino acids are formed.² As an alternative it was proposed that the amino acids and the nitrogen-containing bases needed for the life might have been delivered by interstellar dust, meteorites and comets.³



Figure 1. Comet Hale-Bopp, spring 1997.⁴

Spectroscopic studies have shown that comets contain organic material including components of amino acids, and moreover they carry water as well.

Bernstein and coworkers reproduced interstellar/cometary ice and irradiated it with ultraviolet photons, similar to the ones emitted from stars, at very low temperature and pressure. The bonds of simple molecules like hydrogen, methanol and ammonia were broken and more elaborate molecules were formed.⁵

Blank and coworkers simulated comets impact with Earth in presence of amino acids and found that not only a good fraction of the amino acids survived but also many amino acids polymerized into small peptides.⁶

In the dusty interstellar clouds that form solar systems, starlight tends to get polarized, so it is possible that somehow, some way, one-handed light has produced left-handed amino acids that end up on Earth, and lead to the amazing characteristic of the life that is the one-handedness of its molecules.⁷ Amino acids, mostly left-handed, have been found in meteorites⁸ that are just fragments of old comets, suggesting that this idea might be right.

These simple molecules would have accumulated in the early oceans providing the raw material for subsequent prebiotic polymerization⁹ to give the first self-replicating entities, RNA analogues or peptide nucleic acid molecules¹⁰ that began the life and create the complexity that we are trying to understand now.

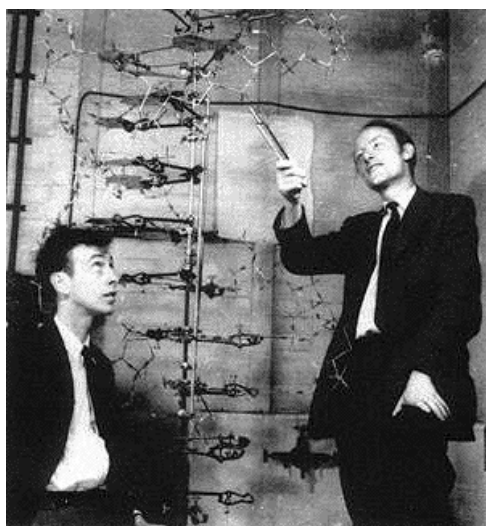


Figure 2. Francis Crick and James Watson with a model of DNA¹¹ (left), Crystal structure of a protein with unknown function from *Leishmania major*, a parasite of the human immune system¹² (right).

A.1 About α -Peptides...

In nature, polymers composed of only 20 different amino acids are enough to provide molecules capable of innumerable activities. Structural proteins such as collagen or elastin provide support in organisms. Defensive proteins such as antibodies provide protection. Proteins, called enzymes, are used as catalysts in various chemical reactions. Besides this, proteins can be used to transport small molecules or to regulate metabolic processes.

The key factor that determines the unique function of a protein is its 3-dimensional shape. Experiments have shown that the amino acid sequence itself contains all the instructions needed for proper folding.¹³

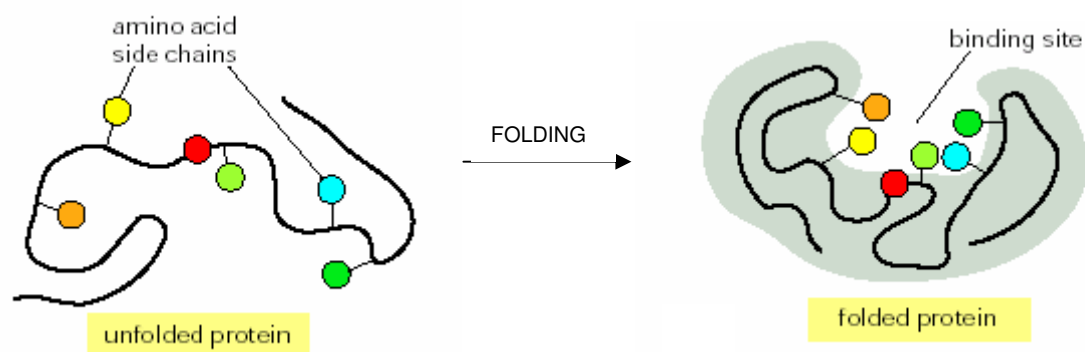


Figure 3. The folding of the polypeptide chain.¹⁴

The discovery of peptide hormones, growth factors and neuropeptides implicated in vital biological functions of our organism has increased interest in peptides, peptide analogues and peptide mimetics to further understand their molecular mechanism of action and to use them as therapeutic drugs. The development of peptides as clinically useful drugs however, has to overcome their poor metabolic stability and to increase their low bioavailability, due in part to their inability to cross biological membrane barriers.

Name	Sequence	Biological function
Insulin	Chains A (21 length) and B (30 length) S-S (A7-B7, A20-B19, A6-A11)	Decreases glucose level in blood
Somatostatin	Ala-Gly-Cys-Lys-Asn-Phe-Phe-Trp-Lys-Thr-Phe-Thr-Ser-Cys (S-S, 3-14)	Inhibit the secretion of growth hormone, insulin and glucagon
Oxytocin	Cys-Tyr-Ile-Gln-Asn-Cys-Pro-Leu-Gly-NH ₂ (S-S, 1-6)	Induce contraction of smooth muscles, especially uterine muscle for oxytocin. VP is also used as an antidiuretic hormone
Vasopressin (VP)	Cys-Tyr-Phe-Gln-Asn-Cys-Pro-Arg-Gly-NH ₂ (S-S, 1-6; Arg ⁸ or Lys ⁸)	
Neurotensin	pGlu-Leu-Tyr-Glu-Asn-Lys-Pro-Arg-Arg-Pro-Tyr-Ile-Leu	Cause constriction of blood vessels
Angiotensin II	Asp-Arg-Val-Tyr-Ile-His-Pro-Phe	
Met-enkephalin	Tyr-Gly-Gly-Phe-Met	Morphine-like properties, analgesic
Leu-enkephalin	Tyr-Gly-Gly-Phe-Leu	

Table 1. Some examples of biologically active endogenous peptides.

Therefore it is necessary to perform chemical modifications to arrive at peptidomimetics that maximize enzymatic stability and bioavailability while simultaneously preserving or even enhancing the potency and selectivity of the bioactive peptide.¹⁵

Specificity is also a problem: peptide receptors can be widely distributed in organisms and their stimulation results in a variety of desired and undesired effects, especially, when the peptide is conformationally flexible and hence able to interact with alternative receptors.¹⁶

Peptide modifications are a useful tool to investigate how the secondary structure can affect activity and using this knowledge it may be possible to regulate it.

Moreover, the introduction of new restricted building-blocks with discrete and predictable folding properties into peptides can allow to mimic the spatial orientation of the functional groups in the active site of enzymes and will help to design low molecular weight catalyst.

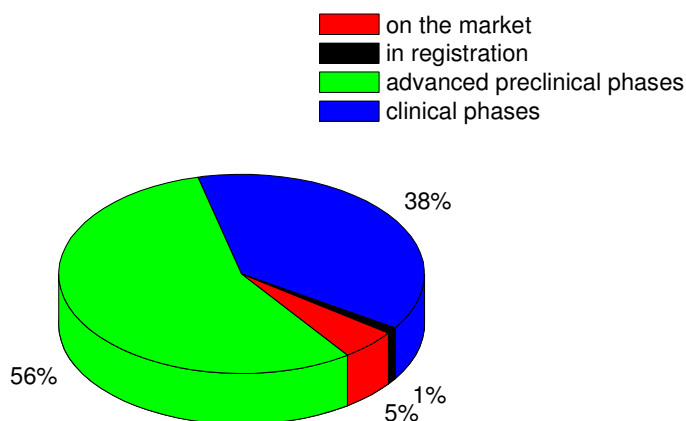


Figure 4. Development of peptide drugs.¹⁷

Polymers of α -amino acids present a well known set of secondary structures, characterized by precise hydrogen-bond patterns and torsional angles along their backbone.

A repeated hydrogen-bond between residue $i+4$ and residue i leads to the α -helix. In the 3_{10} -helix the hydrogen-bond is between the $i+3$ residue and the i residue.

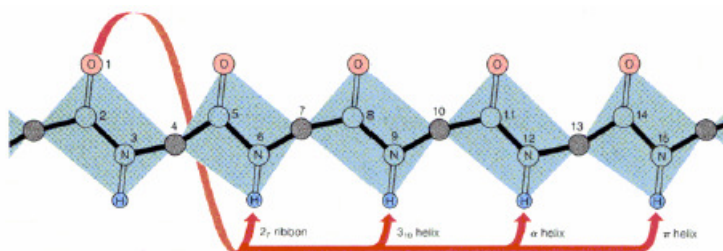


Figure 5. Some possible Hydrogen-bonds patterns in α -Peptides helices.¹⁸

Turns are required along the backbone to change the direction and are often involved in the recognition sites of the peptide/protein ligands with receptors.¹⁹ Figure 6 shows the most common turns present in proteins. A γ -turn involves 3 amino acids with a $i \leftarrow i+2$ hydrogen-bond. β -turns involve 4 amino acids with a $i \leftarrow i+3$ hydrogen-bond.

The repeating of the β -turn type III along the peptide chain leads to a 3_{10} -helix.

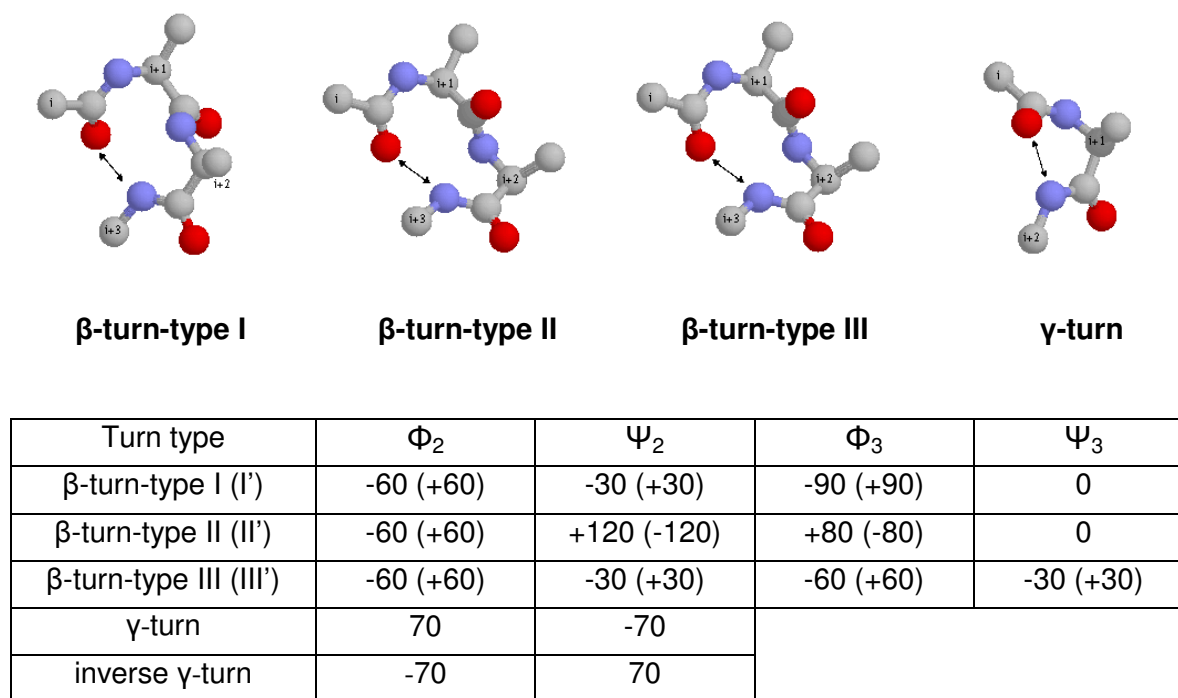


Figure 6. Torsional angles of β -turns and γ -turns.

To improve enzymatic stability, at least against the exopeptidases, one of the most simple strategies is end-protection. For example, the *in vivo* half-life in plasma of the N-terminal acetylated somatostatin, whose sequence is shown in Table 1, was improved from 3 minutes for the natural peptide, to more than 400 minutes.²⁰

To also increase stability against the endopeptidases, the peptide should be modified in its sequence, in the recognition site of the enzyme.

Some common modifications are the methylation of amide nitrogen, the introduction of a number of key amide bond isosters or the substitution of some L-amino acids in the sequence with D-amino acids, C $^\alpha$ Alkyl-amino acids or dehydroamino acids.

All these modification can have significant consequences on molecular flexibility. The methylation of amide nitrogen, can change the network of the *intra*-molecular hydrogen bonds and promotes *cis*-amide conformation.

The introduction of amide bond isosters completely prevents protease degradation of the amide bond and it may also significantly modify the biochemical properties of a peptide, particularly its conformation and its hydrophobicity. Those are used to investigate the role and function of backbone peptide bonds and to modify the properties of the parent peptides.²¹

Figure 7 lists some examples.

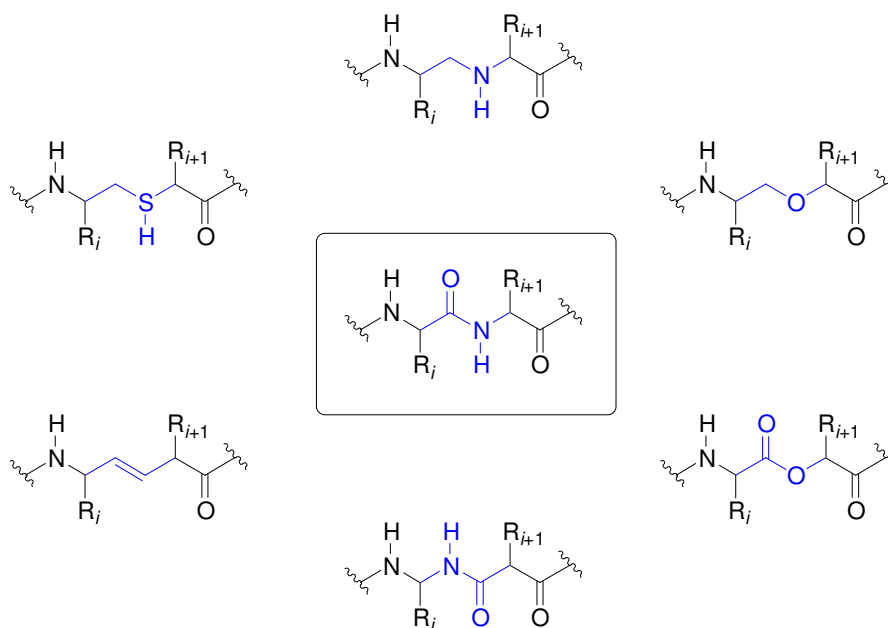


Figure 7. Some examples of amide bond surrogates, $\psi(\text{CONH})$ replacements.

The replacement of CONH with a CH_2NH or CH_2SH can help to investigate the possible functional role of the carbonyl group.

The replacement with a $\text{CH}=\text{CH}$ is the best replacement to maintain the planarity and rigidity of the amide bond. Enkephalin analogues with the $\text{CH}=\text{CH}$ N-terminus amide bond surrogate were found to have similar activity to the original peptide, simultaneously providing protection from degradation.²²

There are also some examples of replacement of CONH with the retro amide NHCO ²³. Chorev, Goodman, and co-workers synthesized the first highly bioactive, partially modified retro-inverso peptides, i.e. some enkephalin analogues that display higher activity than Met-enkephalin and prolonged duration of action in vitro and in vivo.²⁴

Among the modifications of the backbone, arguably the most common one is the substitution of the native sequence with other amino acids.

The single exchange of each residue with amino acids like L-Ala or L-Pro can be useful in understanding the function of each part of the ligand in the interaction with a receptor. This so called Ala or Pro scan can be used on bioactive peptides that present for example no selectivity to different receptors, as in the case of neuropeptide Y.²⁵

To prevent the proteolytic degradation by enzymes or to stabilize a particular turn it is also useful to introduce a D-amino acid into a bioactive sequence as already demonstrated by

Kessler et al. who synthesized the *cyclo*(-RGDfV-), a peptide integrin $\alpha_V\beta_3$ -receptor selective antagonist.²⁶ D-Phe promoted a β -turn that oriented the side chain of the -RGD-sequence into a position that caused it to interact selectively with this receptor subtype.

Nowadays, protein residues are often replaced with C^α -tetrasubstituted α -amino acids. The introduction of a further α -Alkyl group, strongly effects the available conformational space. Approximately 70% of the conformational space available to glycine is precluded by the addition of one methyl group (Ala). The addition of a second methyl group (Aib, α -aminoisobutyric acid or $C^{\alpha,\alpha}$ -dimethylglycine) eliminates an additional 20%.²⁷

Toniolo et al. summarized the conformational preference of the C^α -tetrasubstituted α -Amino Acids.²⁸ Aib is the simplest achiral amino acid of this family. It promotes type III/III' β -turns and 3_{10} and α helices.

Amino Acid Residue	Backbone Conformation Preference
$\begin{array}{c} \text{H}_3\text{C} \quad \text{CH}_3 \\ \diagdown \quad \diagup \\ -\text{HN} \quad \text{CO}- \\ \text{Aib} \end{array}, \quad \begin{array}{c} \text{H}_2\text{C} \quad (\text{CH}_2)_{n-2} \\ \diagdown \quad \diagup \\ -\text{HN} \quad \text{CO}- \\ \text{Ac}_n\text{C}, (n = 4-12) \end{array}$	regular 3_{10} / α -helices; $i+1$ position type I/I' β -turn $i+1$ and $i+2$ position type III/III' β -turn
$\begin{array}{c} \triangle \\ \diagdown \quad \diagup \\ -\text{HN} \quad \text{CO}- \\ \text{Ac}_3\text{C} \end{array}$	distorted 3_{10} / α -helices; $i+2$ position type I/I' β -turn $i+2$ position type II/II' β -turn
$\begin{array}{c} \text{R}_1-\text{H}_2\text{C} \quad \text{CH}_2-\text{R}_2 \\ \diagdown \quad \diagup \\ -\text{HN} \quad \text{CO}- \\ \text{R}_1 = \text{R}_2 \neq \text{H} \end{array}$	fully extended (C_5)

Table 2. Preferred backbone conformation of Achiral C^α -Tetrasubstituted α -Amino Acids.²⁸

In peptides containing achiral $C^{\alpha,\alpha}$ tetrasubstituted amino acids and also C^β -substituents, the energy difference between the helical and the fully extended conformation is smaller. For example, Deg ($C^{\alpha,\alpha}$ -diethylglycine), Dp^ng ($C^{\alpha,\alpha}$ -di- n -propylglycine) rich peptides can adopt either the fully extended or the helical conformation depending upon physical state.

The structural preferences imposed by 1-amino-1-cyclopropane carboxylic acid (Ac_3C) are for the position $i+2$ of type I/I' and type II/II' β -turns or distorted type III/III' β -turns and 3_{10}

helices. The preferences imposed by 1-amino-1-cycloalkane carboxylic acids (Ac_nC , $n=4-12$) containing peptides are similar to the corresponding ones containing Aib's (Table 2).

The addition of another carbon between the nitrogen atom and the carboxyl group of α -amino acid leads to the β -amino acids class.

The conformational preferences imposed by these amino acids has been extensively studied, in particular by the groups of *Seebach* and *Gellman*.

A.2 β -Amino acids and β -Peptides

β -amino acids and β -peptides have been extensively investigated in recent years with increasing interest because of their stability towards proteases, including pepsin, chymotrypsin, trypsin and carboxypeptidase.²⁹ Moreover they show stable secondary structures in short peptides, containing only six or seven β -amino acids.³⁰

The conformation of β -peptides can be analyzed in terms of the main chain torsional angles, which are depicted with the angles ω , ϕ , θ and ψ (Figure 8) using Balaram's conventions.³¹

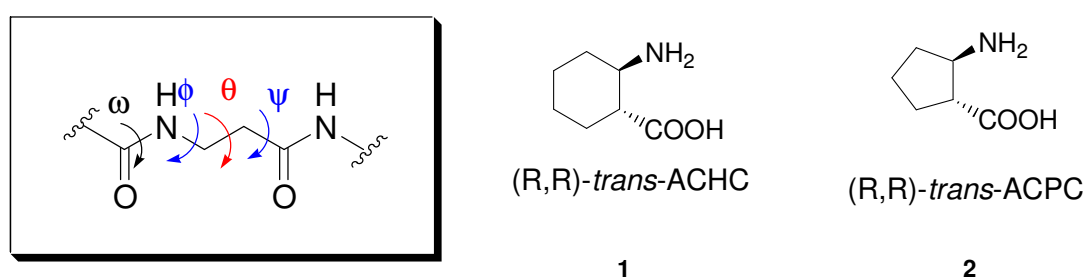


Figure 8. Definition for the torsional angles in β -peptides (left); β -amino acids used by *Gellman* and coworkers (right).

Folded helical or turn-like structures require a gauche conformation about the θ torsional angle. A very modest alteration of this value can switch between two completely different β -peptides helices as found by *Gellman* and coworker.³²

β -peptides containing the conformationally fixed cyclic *trans*-2-aminocyclohexane carboxylic acid (ACHC, **1**), with $\theta = \pm 60^\circ$, show a 3_{14} -helix. The smaller ring size of the *trans*-2-aminocyclopentanecarboxylic acid (ACPC, **2**) has a θ which is biased towards larger values and a 2.5_{12} -helix is stabilized.

Acyclic residues with different side chains investigated by *Seebach* and coworkers also adopt the 3_{14} -helix depending on the positions and on the stereochemistry of the side chains. The β^2 -amino acids form a less stable 3_{14} -helix than the corresponding all- β^3 -peptides. In β -peptides made up of alternating β^2 - and β^3 -building blocks a mixed $2,7_{10,12}$ -helix is obtained.³³

There are several examples where the ability of β -peptides to adopt stable conformations has been used for the synthesis of potent bioactive peptides.

The cyclic β -tetrapeptide shown in Figure 9 (right), with the side chains Phe, Trp, Lys and Thr, can mimic the natural peptide hormone somatostatin and also displays biological activity and micromolar affinity for human receptors.³⁴

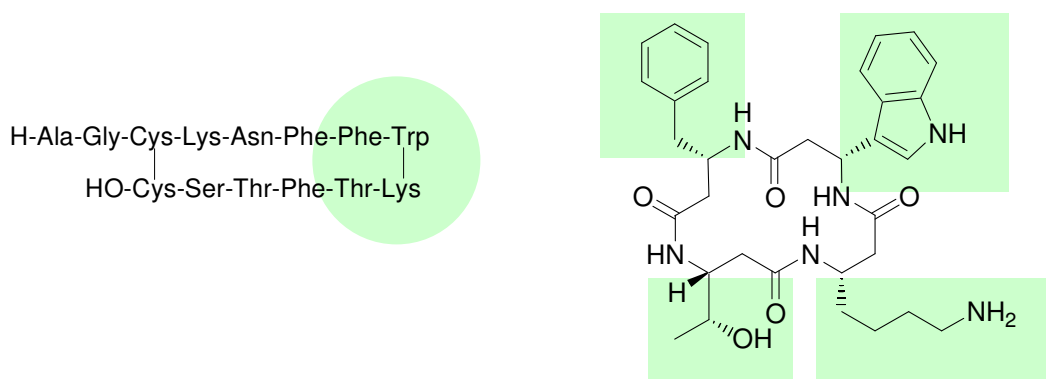


Figure 9. The α -peptide hormone somatostatin (left) and the cyclic β -tetrapeptide analogue (right).³⁴

Cyclic β^3 -tetrapeptides subunits can form nanotube-like structures, which can create transmembrane ion channels with ion conductance levels similar to those observed with gramicidin A and D (Figure 8, left).³⁵

The β -17 peptide shown in Figure 10 (right) adopts a amphipathic 2.5_{12} -helix and shows an antimicrobial activity that is comparable to that of a well-characterized magainin derivative. But more significantly, it has a much lower hemolytic activity.³⁶

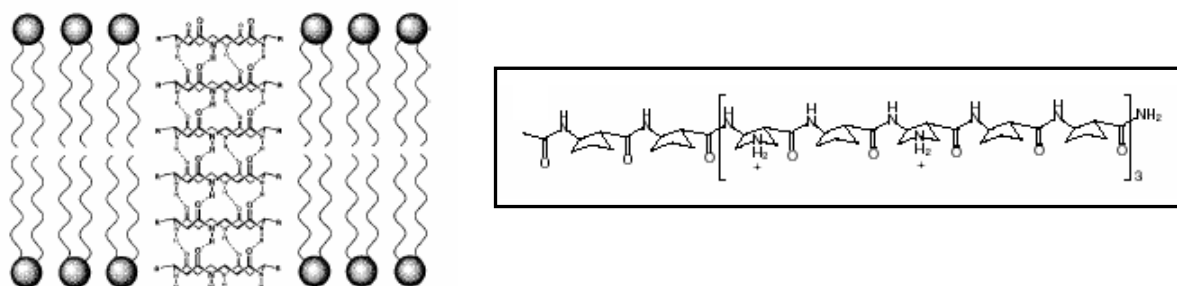


Figure 10. self-assembled transmembrane channels formed from cyclic β^3 -tetrapeptides (left); structure of the β -17 that mimic peptide antibiotic magainins (right).

A.3 β -amino acids incorporated into α -Peptides

Proteolytic stability in α -peptides can be enhanced by replacement of an α -amino acid with a β -residue at the specific cleavage site. In addition, the incorporation of β -residues has been found to be a successful peptidomimetic tool for obtaining potent biological activity, in some cases higher than the native peptide. The β -residue can be an analogue of the corresponding α -amino acid (same side chains) or a conformationally restricted β -amino acid, for example a cyclic β -residue, that can induce a specific conformation in the sequence.³⁷

Cyclic and bicyclic β -amino acids have been used to produce potent analogues of RGD-based molecules for the development of GPIIb/IIIa antagonists. Differences in ring size produced significant differences in the geometry of the resultant peptides and in the biological activity.³⁸

β -Peptides have been found to form β -hairpins. β -Amino acids can build β -peptide reverse turns, that allow for changes in the direction of the peptide backbone.³⁹

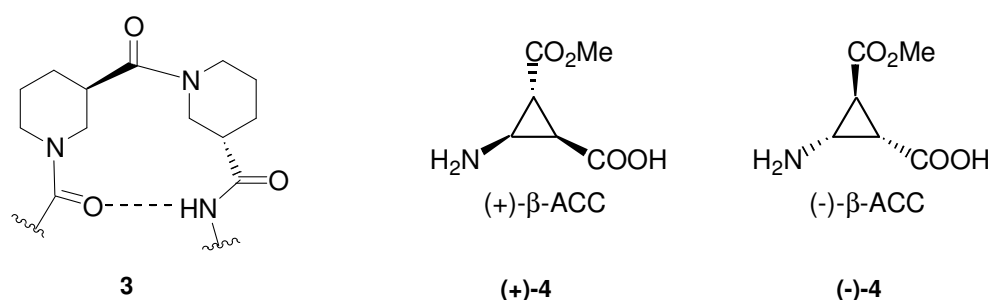


Figure 11. β -turn that promote β -hairpin found in β -peptides (left); The two enantiomers of β -ACC (right).

Cyclic β -amino acids were also used by *Gellman* and coworkers to generate a heterogeneous backbone with antimicrobial properties.⁴⁰ They built different α/β alternated foldamers that form an amphiphilic helix showing high antimicrobial activity with low eukaryotic cell toxicity.

RGD peptides modified by β -amino acids are active integrin $\alpha_{\text{IIb}}\beta_3$ and $\alpha_v\beta_3$ antagonists.⁴¹

The applications of unnatural building blocks that can induce a predictable conformation, require further investigation into their conformational preferences.

In our group we investigated the conformational preferences of the two enantiomers of a constrained cyclic β -alanine analogue, the β -aminocyclopropane dicarboxylic acids (+)-**4** and (–)-**4**, in which the amino and the carboxylic functions involved in the peptide bond are *cis* to each other.

The introduction of the (+)- β -ACC unit into the C-terminus of the NPY (Figure 12) was found to be active and selective for the Y_1 -receptor subtype.⁴²

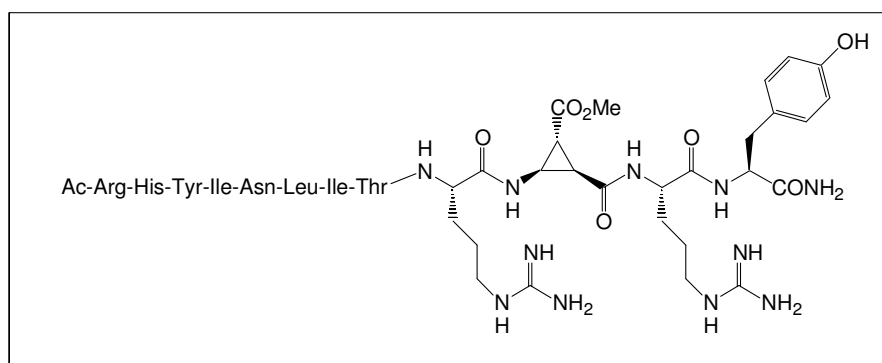


Figure 12. The most selective NPY analogue containing (+) β -ACC, Y_1 -receptor $K_i = 37 \pm 20$ nM; Y_5 -receptor $K_i = 724$ nM; Y_2 -receptor $K_i > 1000$ nM.

It is already known that α -pentapeptides containing only one β -ACC unit show stable turn like structures⁴³. The variety of these β -ACCs, which can be introduced as building blocks has been greatly extended, by synthesis β -ACCs with different side chains.⁴⁴

The aim of this work is to develop an understanding of the conformational preferences of these β -amino acids. Different mixed α -amino acids/ β -ACC peptides were synthesized and their conformation were investigated.

This knowledge will allow a projection of particular turns or structures that have discrete and predictable folding properties. Thereby helping to stabilize the conformation of biologically active α -peptide analogues, that may be used pharmacologically or in receptor-ligand interactions studies. The production of new building-blocks with particular conformational preferences could also be used for the design of spacer or low molecular weight catalysts, small molecules having a definite spatial orientation of functional groups.

-
- ¹ (a) Orgel, L. *Scientific American* **1994**, 271, 81. (b) Miller, S. L. *Science* **1953**, 117, 528-529.
- ² Carver, J. H. *Nature* **1981**, 292, 136-138
- ³ Oro, J. *Nature*, **1961**, 190, 389.
- ⁴ Foto by De Pol S. and Battaglia W. from Fastro, Italy.
- ⁵ (a) Bernstein, M. P.; Sandford, S. A.; Allamandola, L. J. *Le scienze*, **1999**, 373, 34-42. (b) Bernstein, M. P.; Sandford, S. A.; Allamandola, L.J., Chang, S., Scharberg, M. A. *Astrophys. J.* **1995**, 454, 327-344.
- ⁶ Gorman, J. *Science News Online* **2001**, 159, No. 20 and refs cited therein.
- ⁷ Shostak, S. <http://publish.seti.org/general/articles.php?id=65>
- ⁸ (a) Engel, M. H.; Macko, S. A. *Precambr. Res.* **2001**, 106, 35-45; (b) Engel, M. H.; Macko, S. A. *Nature* **1997**, 389, 265-268; (c) Cronin, J. R.; Pizzarello, S. *Science* **1997**, 275, 951-955.
- ⁹ (a) Ferris, J.P.; Hill, A. R.; Liu, R.; Orgel, L. E. *Nature* **1996**, 381, 59. (b) Kanavarioti, A.; Monnard, P. A.; Deamer, D. W. *Astrobiology* **2001**, 1, 271.
- ¹⁰ Bada, J. L.; Lazcano, A. *Science* **2002**, 296, 1982 and refs cited therein.
- ¹¹ <http://www.ba-education.demon.co.uk/for/science/dnamain.html>
- ¹² <http://www.nigms.nih.gov/news/releases/021005.html>
- ¹³ <http://gslc.genetics.utah.edu/units/basics/protein/>
- ¹⁴ http://www.accessexcellence.org/RC/VL/GG/garland_PDFs/Fig_5.24.pdf
- ¹⁵ Adessi, C.; Soto, C. *Curr. Med. Chem.* **2002**, 9, 963-978.
- ¹⁶ Giannis, A.; Kolter, T. *Angew. Chem. Int. Ed. Engl.* **1993**, 32, 1244-1267.
- ¹⁷ *Chemical & Engineering News* **2005**, 83, 11, 17-24.
- ¹⁸ Mathews, C. K.; van Holde, K.E. In *Biochemistry*, Second Edition. The Benjamin/Cummings Publishing Company, Inc.
- ¹⁹ Tyndall, J. D. A.; Pfeiffer, B.; Abbenante, G.; Fairlie, D. P. *Chem. Rev.* **2005**, 105, 793-826.
- ²⁰ Benuck, M.; Marks, N. *Life Sci.* **1976**, 19, 1271.
- ²¹ Spatola, A. F. In *Chemistry and Biochemistry of Peptides and Proteins*; Weinstein, B., Ed.; Marcel Dekker: New York, **1983**; Vol. 7, pp. 267-357.
- ²² (a) Metcalf, G. *Pharm. J.*, **1979**, 356; (b) Handa, B. K.; Land, A. C.; Lord, J. A.; Morgan, B. A.; Rance, M. J.; Smith, C. F. *Eur. J. Pharmacol.* **1981**, 70, 531.
- ²³ Fletcher, M. D.; Campbell, M. M. *Chem. Rev.* **1998**, 98, 763-795.
- ²⁴ Chorev, M.; Shavitz, R.; Goodman, M.; Minick, S.; Guillemin, R. *Science (Washington D.C.)* **1979**, 204, 1210-1212.
- ²⁵ Beck-Sickinger, A. G.; Wieland, H. A.; Wittneben, H.; Willim, K. D.; Rudolf, K.; Jung, G. *Eur. J. Biochem.* **1994**, 225, 947-958.

- ²⁶ Haubner, R.; Finsinger, D.; Kessler, H. *Angew. Chem.* **1997**, *109*, 1440-1456; *Angew. Chem. Int. Ed.* **1997**, *36*, 1374-1389.
- ²⁷ Nakanishi, H.; Kahn, M. In *Bioorganic chemistry: Peptides and Proteins*. Hecht, S. M.
- ²⁸ Toniolo, C.; Crisma, M.; Formaggio, F.; Peggion, C. *Biopolymers* **2001**, *60*, 396-419 and refs cited therein.
- ²⁹ (a) Seebach, D.; Abele, S., Schreiber, J. V., Martinoni, B.; Nussbaum, A. K.; Schild, H.; Schulz, H.; Hennecke, H.; Woessner, R.; Bitsch, F. *Chimia* **1998**, *52*, 734; (b) Hintermann, T.; Seebach, D. *Chimia* **1997**, *51*, 244.
- ³⁰ Seebach, D.; Matthews, J. L. *Chem. Commun.* **1997**, 2015.
- ³¹ Banerjee, A.; Balaram, P. *Curr. Science* **1997**, *73*, 1067.
- ³² Cheng, R. P.; Gellman, S. H.; DeGrado, W. F. *Chem. Rev.* **2001**, *101*, 3219-3232 and refs cited therein.
- ³³ Seebach, D.; Beck, A. K.; Bierbaum, D. J. *Chemistry & Biodiversity* **2004**, *1*, 1111-1239 and refs cited therein.
- ³⁴ Gademann, K.; Ernst, M.; Hoyer, D.; Seebach, D. *Angew. Chem. Int. Ed.* **1999**, *38*, 1223-1226.
- ³⁵ Clark, T. D.; Buehler, L. K.; Ghadiri, M. R. *J. Am. Chem. Soc.* **1998**, *120*, 651-656.
- ³⁶ Porter, E. A.; Wang, X.; Lee, H. S.; Weisblum, B.; Gellman, S. H. *Nature* **2000**, *404*, 565.
- ³⁷ (a) Gopi, H. N.; Ravindra, G.; Pal, P. P.; Pattanaik, P.; Balaram, H.; Balaram, P. *FEBS Letters* **2003**, *535*, 175-178; (b) Steer, D. L.; Lew, R. A.; Perlmutter, P.; Smith, A. I.; Aguillar, M. I. *Curr. Med. Chem.* **2002**, *9*, 811-822.
- ³⁸ (a) Thompson, P. E.; Steer, D. L.; Aguilar, M. I.; Hearn, M.T.W.; *Bioorg. Med. Chem. Lett.* **1998**, *8*, 2699-2704; (b) Klein, S. I.; Czekaj, M.; Molino, B. F.; Chu, V. *Bioorg. Med. Chem. Lett.* **1997**, *7*, 1773-1778.
- ³⁹ (a) Chung, Y. J.; Christianson, L. A.; Stanger, H. E.; Powell, D. R.; Gellman, S. H. *J. Am. Chem. Soc.*, **1998**, *120*, 10555-10556. (b) Daura, X.; Gademann, K.; Schäfer, H.; Jaun, B.; Seebach, D.; van Gunsteren, W. F. *J. Am. Chem. Soc.* **2001**, *123*, 2393-2404.
- ⁴⁰ Schmitt, M. A.; Weisblum, B.; Gellman, S. H. *J. Am. Chem. Soc.* **2004**, *126*, 6848-6849.
- ⁴¹ Schumann, F.; Müller, A.; Koksche, M.; Müller, G.; Sewald, N. *J. Am. Chem. Soc.* **2000**, *122*, 12009-12010.
- ⁴² Koglin, N.; Zorn, C.; Beumer, R.; Cabrele, C.; Sewald, N.; Reiser, O.; Beck-Sickinger, A. G. *Angew. Chem. Int. Ed.* **2003**, *42*, 202-205.
- ⁴³ Zorn, C. *Dissertation*, Regensburg **2001**.
- ⁴⁴ (a) Beumer, R.; Reiser, O. *Tetrahedron* **2001**, *57*, 6497-6503. (b) Gnad, F.; Poleschak, M.; Reiser, O. *Tetrahedron Lett.* **2004**, *45*, 4277-4280. (c) Gnad, F. *Dissertation*, Regensburg **2004**

B. Model Peptides containing β -ACC: Synthesis and Conformational Investigations

B.1 Synthesis

The model peptides containing either of the enantiomers of β -ACC that were synthesized and investigated in the course of this study are shown in Figure 13.

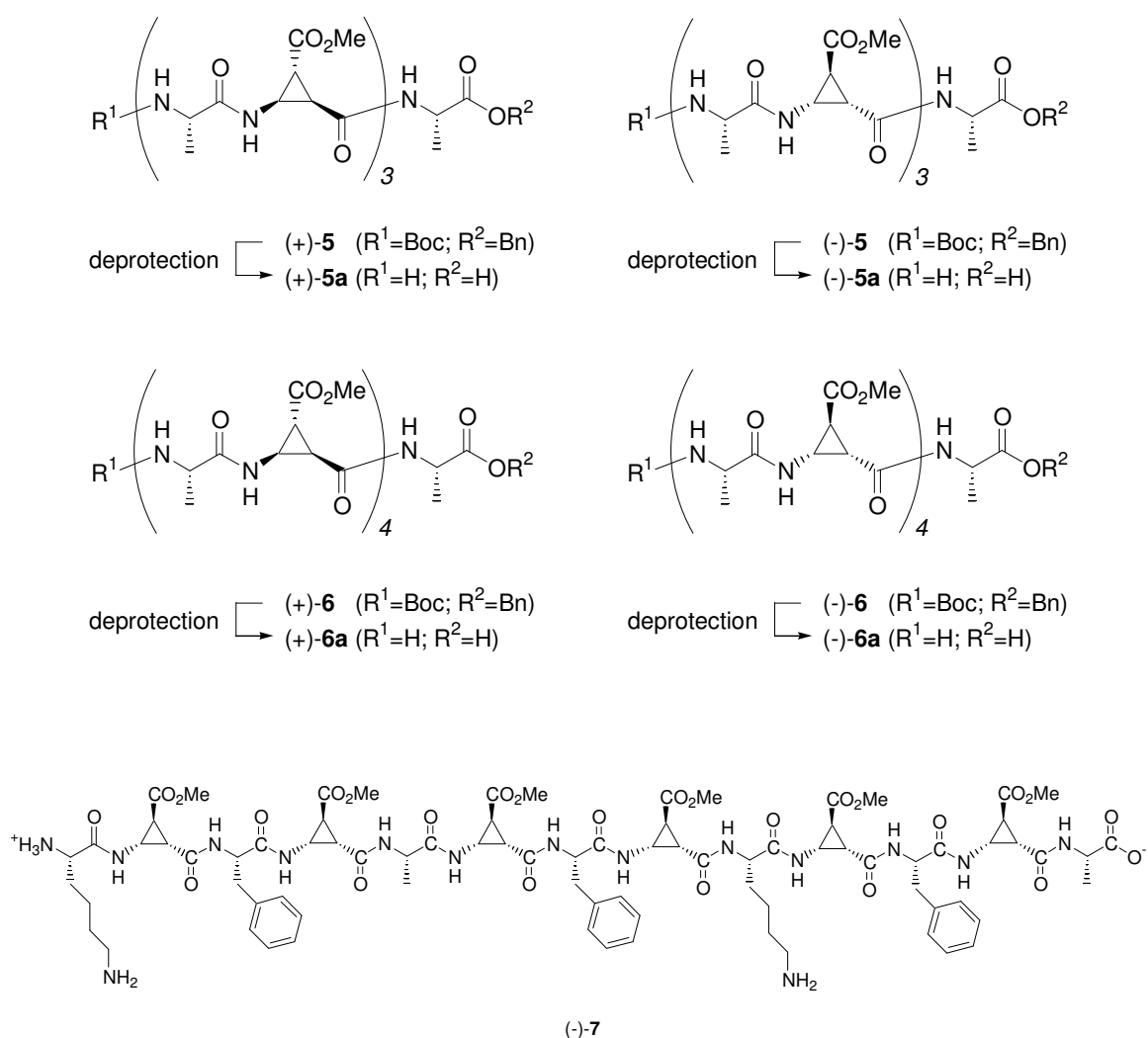


Figure 13. β -ACC containing peptides that have been synthesized and investigated in this work.

The synthesis of the β -ACC building blocks, being suitably functionalized to be introduced in peptides, has been carried out as developed in our group¹ from Boc-pyrrole in racemic or enantiomerically pure form. (Figure 14).

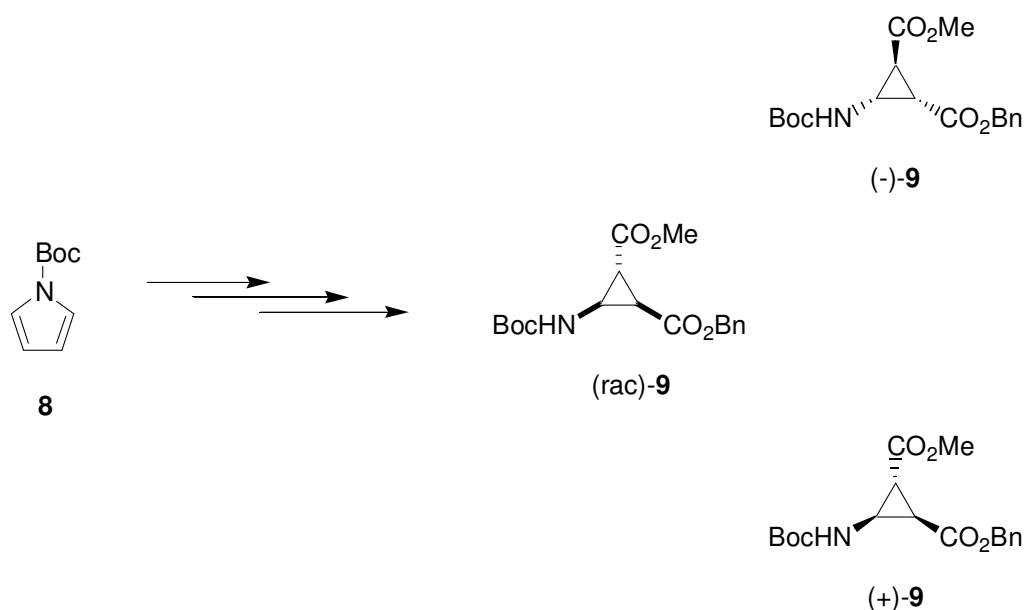


Figure 14. β -ACC building blocks for peptide synthesis.

The synthesis of peptides **5** and **6** was carried out in solution using Boc/OBn as orthogonal protecting groups.

As already described by Zorn², the β -ACC was deprotected at the N-terminus by treatment with HCl in ethyl acetate to afford the stable hydrochloride salt. The N-terminus of the protected β -ACC was reacted with a C-protected-L-alanine in the presence of the coupling reagents EDC and HOBt, using pyridine as base in dichloromethane.

The resulting diastereomeric dipeptides (+)-**10** and (-)-**10** were then separated by crystallization.

The C-terminal part of (+)-**10** or (-)-**10** was deprotected by hydrogenation in the presence of palladium charcoal and 1,4-cyclohexadiene in methanol. The carboxyl function was activated with EDC/HOBt and after the coupling with N-deprotected alanine it was possible to obtain the tripeptides (+)-**12** and (-)-**12** (Figure 15).

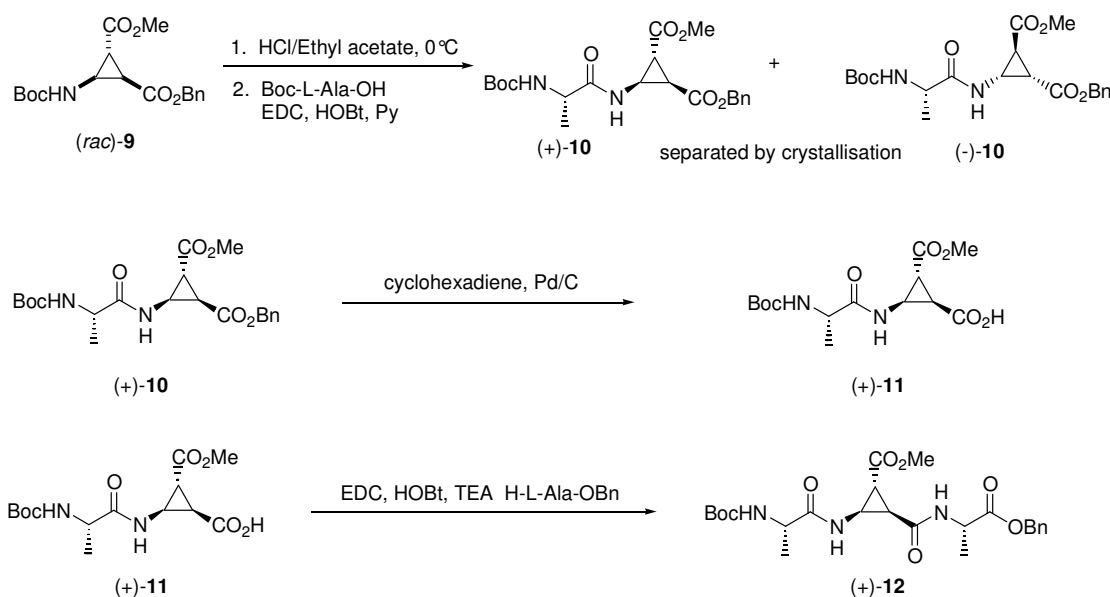
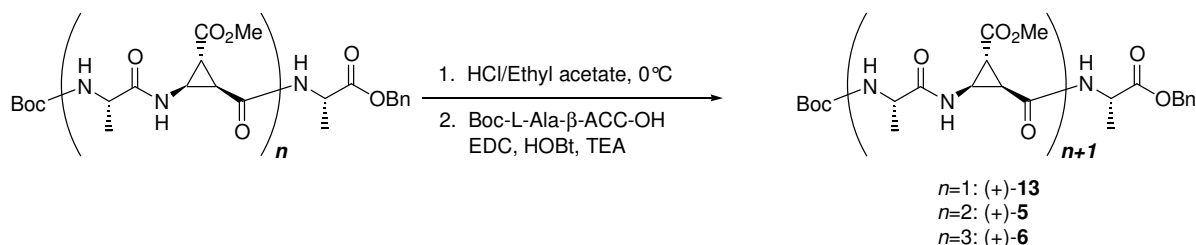


Figure 15. Introduction of β -ACC units into peptides.

Repeated N-terminus deprotections and couplings with the C-deprotected dipeptide Boc-L-Ala- β -ACC-OH were carried out to afford the heptapeptides (+)-**5** and (-)-**5** and nonapeptides (+)-**6** and (-)-**6** as shown in Figure 16.



The same synthetic strategy was carried out with (-)-**10** form to obtain peptides (-)-**13**, (-)-**5** and (-)-**6**.

Figure 16. Solution synthesis of the protected hepta- and nonapeptides **5** and **6**.

The synthesis of the (-)- β -ACC containing peptides and the (+)-heptapeptide (+)-**5** was carried out with good yield and without epimerisation. However epimerisation did occur when peptide (+)-**5** was elongated to afford the nonapeptide (+)-**6**. The $^1\text{H-NMR}$ spectra of the peptide after column chromatography purification showed more than one Boc-signal indicating the presence of epimers or at least rotamers. When the NMR spectra was measured at higher temperature no changes were observed, excluding the hypothesis of rotamers. After

recrystallization with ethyl acetate and petroleum ether it was possible to isolate the required peptide (+)-**6**, the purity of which was determined by HPLC to be greater than 90%.

The deprotection of the final peptides was achieved by treatment first with a saturated solution of HCl in ethyl acetate to remove the Boc-group. Next the benzyl ester deprotection was performed. This involved an overnight hydrogenation using a solution of cyclohexadiene in pentane in the presence of Pd/C in methanol. (Figure 17).

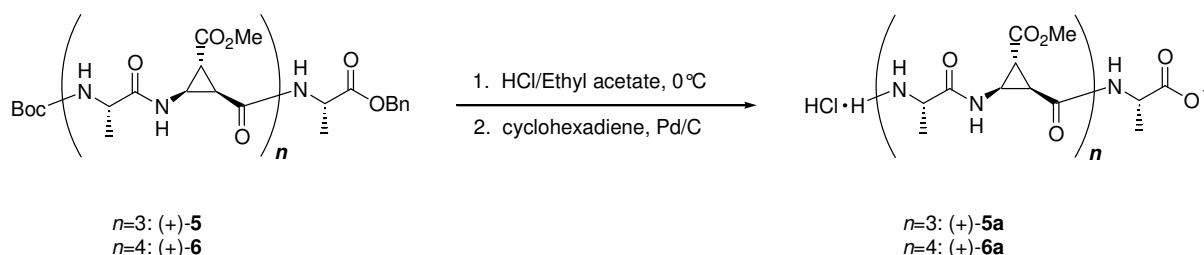
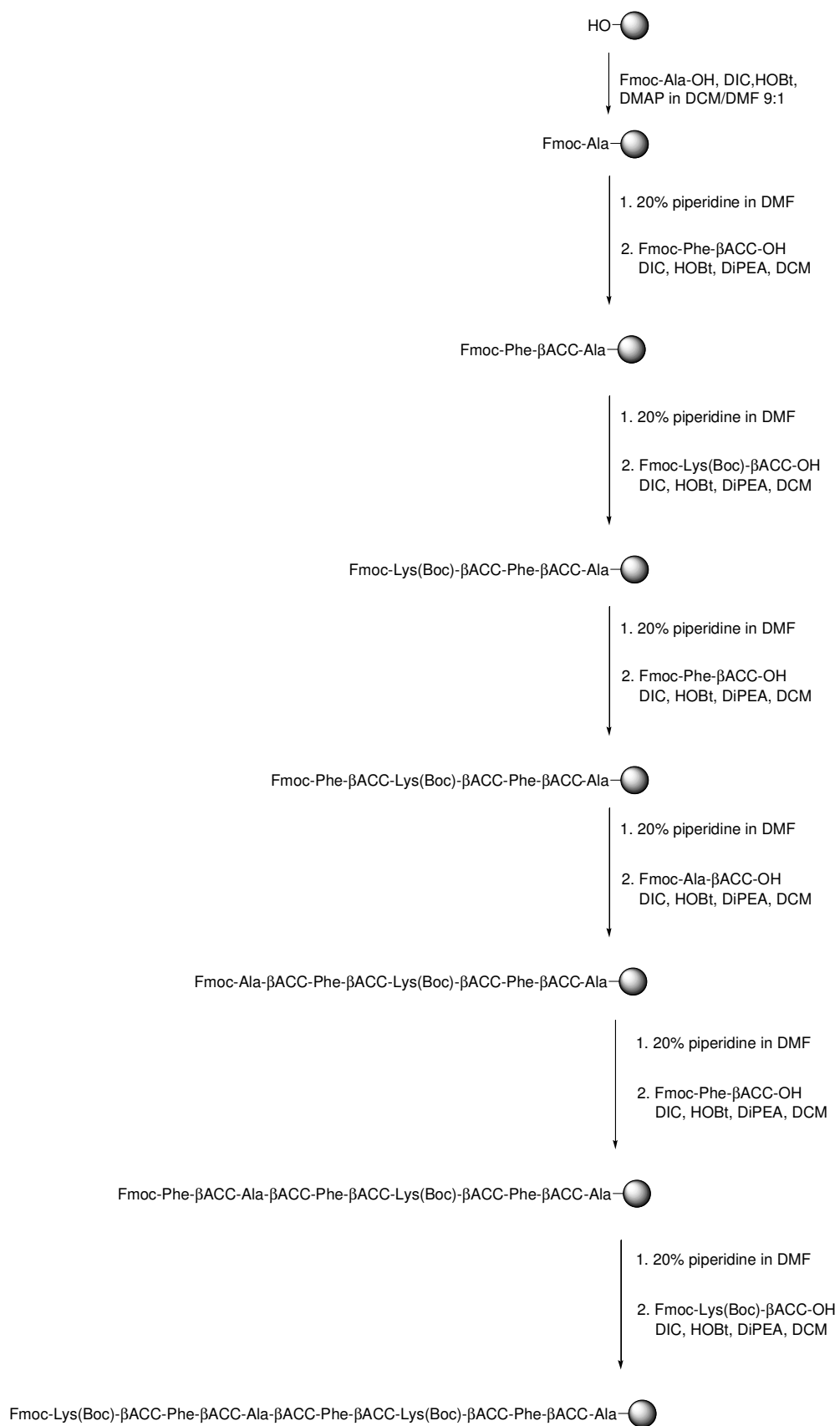
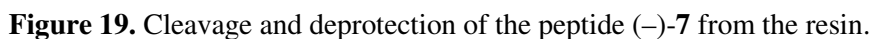


Figure 17. Deprotection of the peptides (+)-**5** and (+)-**6**. The same procedure was carried out for the hepta- and nonapeptide containing the (–)- β -ACC unit.

The peptide (–)-**7** was synthesized as shown in Figure 18 using a solid phase protocol. It was carried out by manual coupling using Fmoc/^tBu strategy on the acid labile HMPA-AM resin. The first amino acid, alanine, was attached activating the carboxylic function with DIC and HOBt in the presence of DMAP as catalyst and stirring overnight. The loading of the resin was determined spectrophotometrically by Fmoc cleavage with piperidine in DMF.³ After capping by treatment with acetic anhydride and DIPEA in DMF, the peptide chain was assembled by single manual coupling of the dipeptides Fmoc-Xaa- β ACC-OH activated by DIC/HOBt overnight in DCM/DMF 9:1 in the presence of DIPEA (Figure 18). After every two coupling-steps small scale cleavages were performed to control with analytical HPLC and mass analysis the growing peptide chain.

**Figure 18.** Solid phase synthesis of $(-)-7$.

The cleavage of the peptide from the resin with simultaneous side chains deprotection was achieved by treatment with a TFA/water/TIS mixture (95:5:5) for 2,5 hours (Figure 19). The peptide was precipitated from ice-cold diethyl ether and recovered by centrifugation. The purification was achieved by using RP-preparative HPLC and the product (–)-**7** was characterized by analytical HPLC and MALDI-MS spectroscopy.



For the synthesis of the peptide (–)-**7** by means of solid phase synthesis using an acid labile resin, Fmoc protected dipeptides (–)-**14a** and (–)-**15a** were prepared as shown in Figure 21. The enantiomerically pure (–)-**9** was deprotected at the N-terminus by treatment with HCl in ethyl acetate, followed by coupling with the corresponding Fmoc-protected amino acid to afford the protected dipeptide (–)-**14** and (–)-**15**. Final deprotection of the benzyl ester yielded (–)-**14a** and (–)-**15a**, respectively, being suitably functionalized for further coupling by treatment for 18 hours with cyclohexadiene and Pd/C.

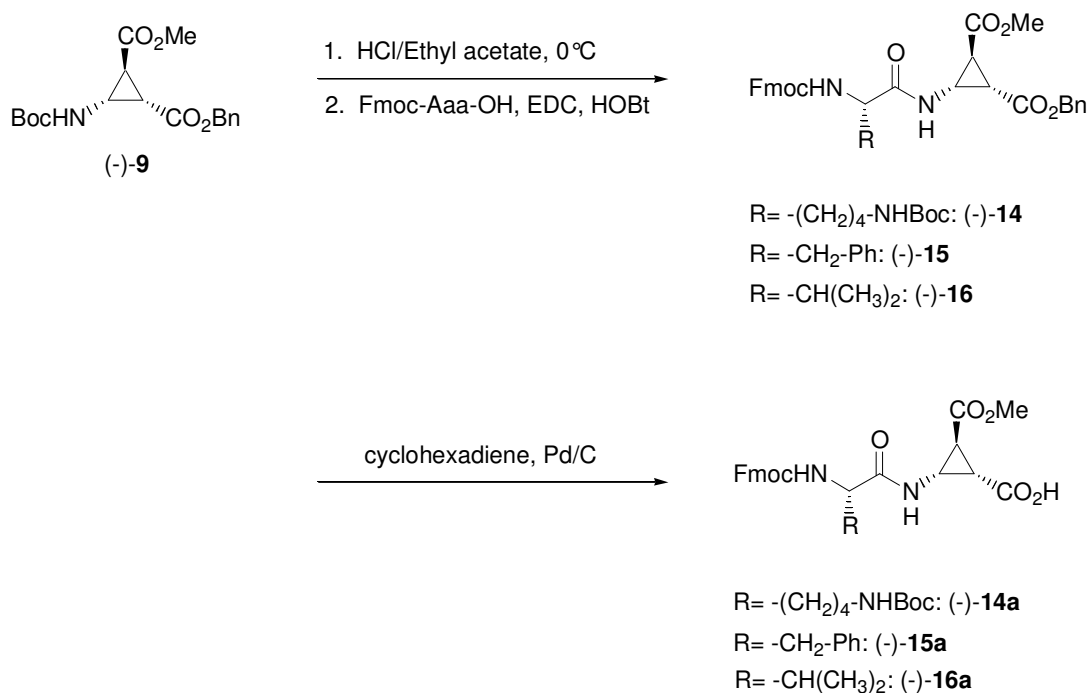


Figure 21. Synthesis of the Fmoc- β -ACC derivatives.

According to the same procedure the dipeptides (+)-**16a**, (–)-**16a**, (+)-**17a**, (–)-**17a**, (+)-**18a** shown in Figure 21 and 22 were synthesized as well, necessary in the synthesis of RGD-containing peptides and NPY-analogues (Chapter C).

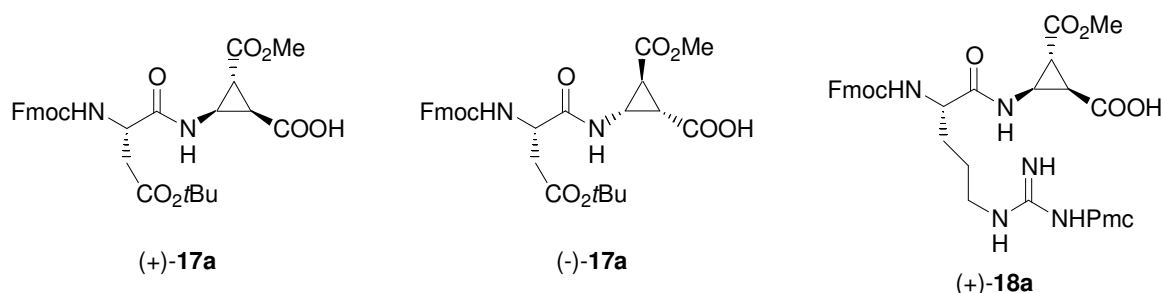


Figure 22. Dipeptides that were used in the synthesis of biological active analogues.

In the case of the dipeptide containing alanine **(-)-19a** the synthesis started from the Boc-protected dipeptide **(-)-10**. After deprotection at the N-terminus with HCl in ethyl acetate, treatment with Fmoc-OSu afforded the Fmoc derivative **(-)-19** in good yield, which was then deprotected at the C-terminus to yield **(-)-19a**, being ready for solid phase synthesis.

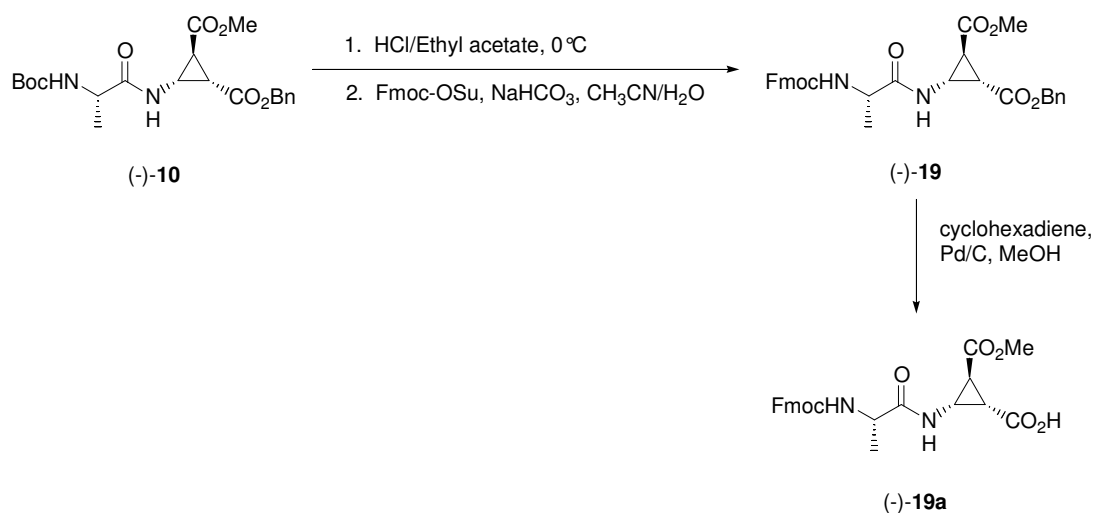


Figure 23. Synthesis of the Fmoc-protected dipeptide containing Alanine.

B.2 Conformational Investigations

The conformation of peptides depends in principal on the kind of amino acids that are present and their sequence. A knowledge of the three dimensional structure of a peptide is essential in understanding its physical, chemical and biological properties.

There are many techniques used to investigate the three dimensional structure of peptides. X-ray diffraction allows structural investigations at atomic resolution. However single crystals are needed and there always exists the possibility of a difference in the conformation between the solid state and the one seen in solution.

To gain information about the secondary structure of a peptide in solution, important tools such as circular dichroism spectroscopy, 1D and 2D NMR and FT-IR spectroscopy are employed.

B.2.1 Circular dichroism

Circular dichroism is an important spectroscopic technique, used to investigate the conformations of peptides and proteins. An optically active substance is able to interact with polarized light in a different way, depending on its “chirality”. UV-CD is based on planar polarized light. Planar polarized light is the sum of the left and the right circularly polarized light. When an optically active substance intercepts planar polarized light rays, the left and the right circularly polarized components are adsorbed by different amounts. When these are recombined, they appear as elliptically polarized light. The extent of this ellipticity is then measured.

The absorbance values of the peptide chromophore are due to a low energy $n\pi^*$ transition centered around 220 nm and a higher energy $\pi\pi^*$ transition around 190 nm.⁴

The advantage of CD measurements when investigating a polymer conformation is that the spectrum is no longer reflected by the absorbance of a single individual chromophore. The combination of the orientated chromophores in the three dimensional arrangement of the polymer gives rise to a new set of excited transitions. Therefore each type of peptide secondary structure has a unique and distinct CD spectrum.⁵

Additionally there can be some contributions from aromatic residues (Phe, Tyr, Trp and His) and disulfide bonds. If there are a significant number of aromatic residues present in a

molecule, the CD spectra can be affected in the region of far-UV. The contribution seen in near-UV is smaller. This region can be used to investigate changes of tertiary structures, for instance, those caused by ligand binding or folding/unfolding precesses.⁵

Shown below are the typical CD spectra seen for some secondary structures of α -peptides.

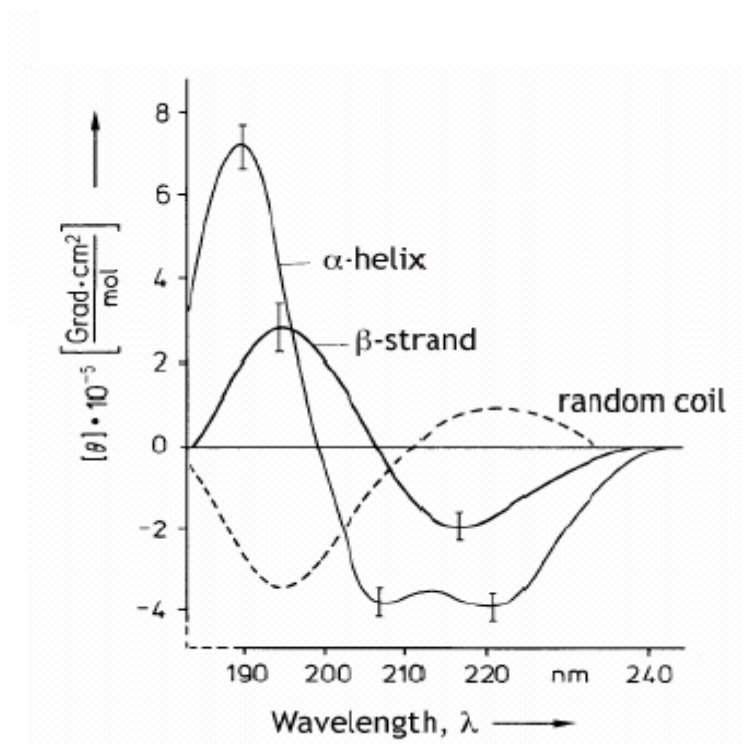


Figure 24. CD spectra of the common secondary structures seen for α -peptides.⁶

B.2.2 NMR investigation

The most common and useful tool used to investigate the secondary and tertiary structure of peptides and proteins in solution is Nuclear Magnetic Resonance (NMR) spectroscopy.

NMR spectroscopy allows an investigation of the structure of biopolymers on an atomic level in solution. Moreover, NMR investigations can highlight the presence of conformational equilibria. Important structural information can be obtained from both monodimensional and twodimensional NMR spectra.

B.2.2.1 Information from 1D-proton NMR spectra

Even though the NMR-spectra of biopolymers are derived from the nuclear spins of the constituent monomers, there is no straightforward correlation between the NMR spectra of the low molecular weight components and those of the whole polymer.⁷

A dispersion of nucleus's chemical shift values is the first indication of the presence of spatial folding in the polymer chain. When a polymer has a defined conformation in solution, a proton in the sequence will have a different microenvironment compared to those in a random coil structure. It will also be different from the same proton contained in an identical residue type at a different point in the sequence. This fact leads to different specific chemical shift values compared to those for an unfolded structure and to a good dispersion of the signals.

The presence of a secondary structure in solution can lead to a slower exchange rate for labile protons, which can be measured by time dependent NMR-spectroscopy, while in small molecules proton exchange is too fast to be observed. Moreover the slower diffusional motions of the macromolecule in solution can substantially affect the spin relaxation and the Nuclear Overhauser Enhancement (NOE).⁷

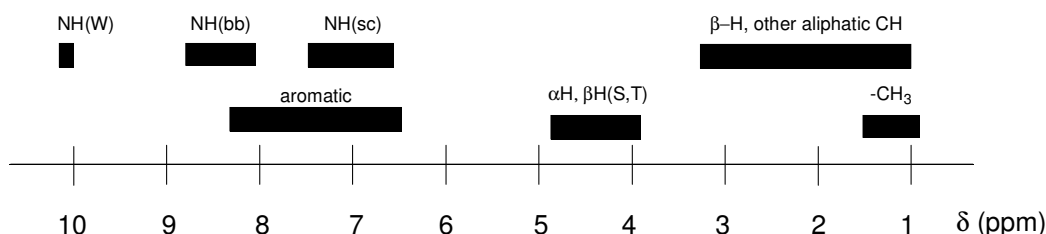


Figure 25. ^1H -chemical shift positions for α -peptides. Adapted from Ref. 7.

The presence of hydrogen-bonds can be detected in a 1D-NMR spectra. These techniques are based on the assumption that the NHs involved in a H-bond are less sensitive with respect to perturbations, such as changing of temperature, concentration or solvent, than the NHs that are exposed to the solvent.

Considering the NHs that are been exposed to the solvent, it has been established that the NH shift deviation with temperature ($\Delta\delta/\Delta T$) is less negative than -4 ppb/ $^\circ\text{C}$.⁸ However such data should be confirmed by other observations, because of possible errors in interpretation. For example, in the case of a conformational change towards a random coil structure with

increasing of temperature, when a small negative $\Delta\delta_{\text{NH}}/\Delta T$ is observed, the H-bonded NH should be downfield and the protection of H/D exchange should provide a more secure measurement of solvent access.⁹

The secondary structures of peptides are characterized by distinct torsion angles along the backbone. Since the size of the spin-spin coupling constant $^3J_{\text{HN}\alpha}$ depends on the torsion angle NH-CH α , the measurement of $^3J_{\text{HN}\alpha}$ is another approach that can give information on the torsion angle ϕ , and thus, on the peptide's conformation.^{7,10} Small values indicate turn or helical conformations, values bigger than 6 Hz correspond to an unordered structure or an extended conformation. Shown below (Figure 26) are the $^3J_{\text{HN}\alpha}$ values associated with some common peptide secondary structures.

Secondary structure	ϕ	$^3J_{\text{HN}\alpha}$ (Hz)
α -helix	- 57°	3.9
3_{10} -helix	- 60°	4.2
antiparallel β -sheet	- 139°	8.9
parallel β -sheet	- 119°	9.7



Figure 26: Table of the $^3J_{\text{HN}\alpha}$ -values in regular secondary structures⁷, also displayed are of the ϕ and ψ torsion angles present along the backbone of an α -peptide.

B.2.2.2 Information from 2D-proton NMR spectra

The most useful data relating to a peptide conformation is gained from 2D NMR investigation. Of particular interest are the DQF-COSY, TOCSY and NOESY/ROESY experiments.

The COSY displays [^1H - ^1H]-correlations due to scalar (through bond) couplings. The TOCSY reveals the proton cross peaks in the same spin system. With the help of these two experiments it is possible to assign completely all the chemical shifts of the protons in a peptide. The NOESY, Nuclear Overhauser Effect Spectroscopy, displays cross peaks due to dipolar coupling resulting from through *space* interactions.

NOESY cross peaks depend on the distance between two protons. Therefore it can connect pairs of hydrogen atoms in amino acids that may be far away along the peptide sequence but close together in space because of the presence of a stable three dimensional structure.

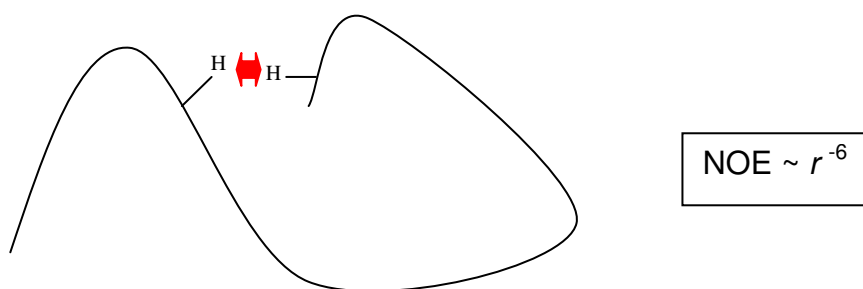


Figure 27. NOE signals can depend to the three dimensional structure of the peptide.

NOE cross peaks are normally defined as *sequential* distances when they are between backbone protons or between a backbone proton and a β proton in residues that are nearest neighbours in the sequence. *Medium-range* distances are all non-sequential signals between residues within a segment of five consecutive residues. *Long-range backbone* distances are between backbone protons in residues that are at least six position away in the sequence.⁷

Depending on the torsion angles that characterize the secondary structure of a peptide, *sequential* and *medium-range* ^1H - ^1H -distances will have different values.

For instance the *sequential* NH-NH and CH_α -NH contacts for a regular α -helix are about 2.8 Å and 3.5 Å respectively. The CH_β -NH contacts, since they depend also on the torsion angle on the side chain χ_i , vary between 2.5 and 4.1 Å for a α -helix.⁷

In the case of peptides, including proline or non proteinogenic amino acids there exists an increased possibility of *cis-trans* isomerization of the peptide bond. The influence of the *cis-trans* isomerization on the sequential ^1H - ^1H -distances allows closer $\text{CH}_\alpha(i)$ - $\text{CH}_\alpha(i+1)$ and NH(*i*)- $\text{CH}_\alpha(i+1)$ contacts in the *cis* form whereas shorter $\text{CH}_\alpha(i)$ - $\text{CH}_\delta(i+1)$ and NH(*i*)- $\text{CH}_\delta(i+1)$ contacts are observed for the *trans* form.⁷

Medium-range distances indicating helical-structures are *i,i+2*, *i,i+3* and *i,i+4* contacts. In particular *i,i+4* contacts are especially useful since they are present in a regular α -helix and not in a 3_{10} -helix. Tight turns have close *i,i+2* values. In the case of β -structure short *medium-range* distances are not observed, since the polypeptide segments are almost fully extended.⁷

Table 3 lists short *sequential* and *medium-range* distances that are found in known α -peptide conformations.

<i>Distance</i>	<i>α-helix</i>	<i>3_{10}-helix</i>	<i>β-sheet</i>
$d_{\alpha N}$	3.5	3.4	2.2
$d_{\alpha N}(i, i+2)$	4.4	3.8	
$d_{\alpha N}(i, i+3)$	3.4	3.3	
$d_{\alpha N}(i, i+4)$	4.2		
d_{NN}	2.8	2.6	4.2-4.3
$d_{NN}(i, i+2)$	4.2	4.1	
$d_{\beta N}$	2.5-4.1	2.9-4.4	3.2-4.7
$d_{\alpha\beta}(i, i+3)$	2.5-4.4	3.1-5.1	

Table 3. Short *sequential* and *medium-range* ^1H - ^1H distance in some common secondary structures in α -peptides.⁷

B.2.2.3 Structure calculations from NOE data

The NMR data can be finally used as an indirect source of structural information, from which the overall 3D structure can be calculated.

Programs like DYANA¹¹ are used for these structural calculations. DYANA performs simulated annealing by molecular dynamics in torsion angle space using conformational restraints obtained from the volumes of the corresponding NOE crosspeaks. It starts from conformers that possess random torsion angle values and fits them to the conformational restraints collected from the NMR measurements.¹²

Among the 50 calculated structures, the resulting 20 best ones were selected according to the lowest values of their target function.

B.2.3 FT-IR spectroscopy

Infrared light is energetic enough to excite molecular vibrations to higher energy levels. The main characteristic bands of the peptide group are called amide A, amide I and amide II. Evidence exists, which suggest that the position of these bands is related to the conformation of the peptide.¹³ The amide A band is mainly due to the N-H stretching vibration. It is very sensitive to the strength of a hydrogen bond, thus providing an opportunity to gain information about any intra- or intermolecular hydrogen bond. Usually in a non polar solvent, non hydrogen-bonded NHs adsorb above 3400 cm^{-1} while NHs that are involved in hydrogen-bonds, absorb below 3400 cm^{-1} .¹⁴ The amide I and II bands are related to the

backbone conformation. The amide I is associated with the C=O stretching vibration, while the amide II results from the N–H bending and from C–N stretching vibrations.

	α -helix	3_{10} -helix	β -sheet
Amide I	1652	1666-1662	1648-1645
Amide II	1548	1533-1531	1533-1536

Table 4. Frequencies (cm^{-1}) of the Amide I and Amide II bands found for different α -peptide conformations.

B.3 Results on alternated α -Xaa/ β -ACC peptides

Reverse turns play a crucial role in the globular architecture of folded proteins. They are often implicated in the recognition motif, in protein-peptide interactions, especially regarding interactions with G-protein couple receptors.¹⁵

The discovery of small systems that mimic different types of turns or inducing modifications at specific sites in the bioactive sequence able to enhance its reverse-turn propensity is a fascinating and important field of research in developing biologically active molecules.

There are already some examples of the introduction of cyclopropane-derived peptidomimetics into bioactive peptides such as HIV-1 protease inhibitors¹⁶, matrix metalloprotease inhibitors¹⁷ or enkephalin analogues¹⁸.

Cyclopropane-containing dipeptide isosteres -Xaa Ψ [COcpCO]Yaa- and -Xaa Ψ [NHcpNH]Yaa- were synthesized as well. A *trans*-substituted cyclopropane was found to stabilize extended conformations in oligopeptides while molecular modeling studies suggested that the *cis*-backbone substituents could stabilize a reverse turn.¹⁸

The influence of β -amino acids in the secondary structure of β -peptides has been extensively studied by the groups of *Gellman* and *Seebach*. As reviewed by *Cheng et al.*¹⁹, the substituents on the β -amino acid backbone, strongly affect the torsion angle θ leading to different preferences in the secondary structure of the resulting β -peptide.

In our case the presence of the cyclopropane ring constrains the amine and the carboxyl functions used in the peptide bond in the *cis* (syn) conformation, providing a unique conformational preference for this β amino acid compared to those already reviewed.

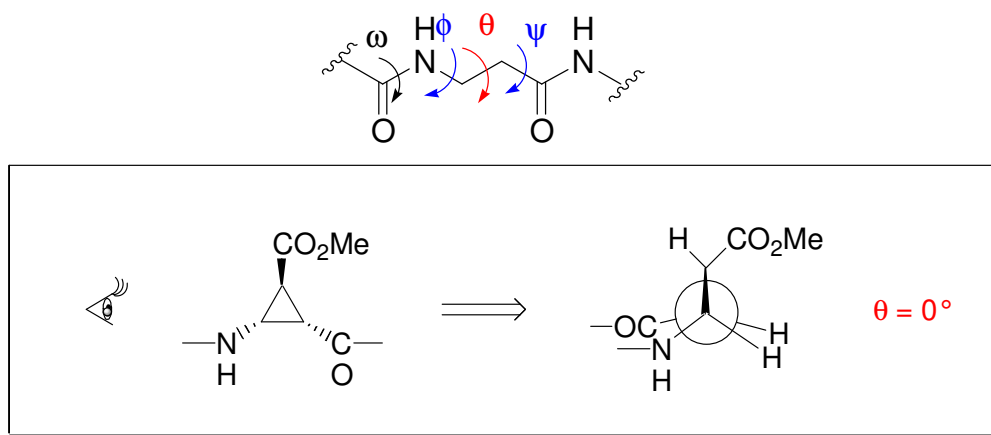


Figure 28. θ torsion angle in β -ACC.

Small model peptides containing only one β -ACC unit, (+)-**20** and (–)-**20**, were previously synthesized by Zorn². NMR investigations and molecular dynamic calculations on these peptides showed that they have a tendency to adopt a turn like structures as displayed in Figure 29.

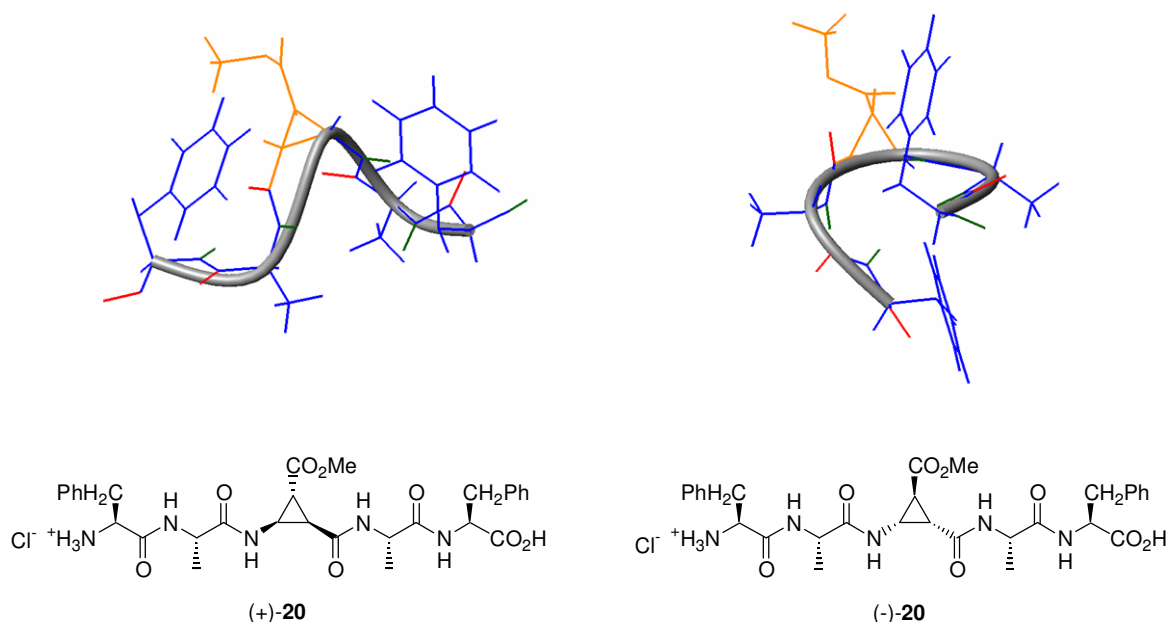


Figure 29. Structures of model peptides containing only one β -ACC unit.²

Moreover it was found with molecular modelling calculations and IR investigations in dichloromethane that the β -ACC unit could close a 6-membered ring (C_6) via an intermolecular H-bond.²

In this chapter the influence of the β -ACC units on the secondary structure of longer peptides, in which the β -unit is alternated with α -amino acids are described.

The possible H-bond patterns that can be found theoretically in helices, in which α -amino acids are alternated with β -amino acids are shown in Figure 30. Mixed 14/15- and 11-helices were found by Gellman *et al.*²⁰ in small α/β -peptides containing cyclic β -amino acids.

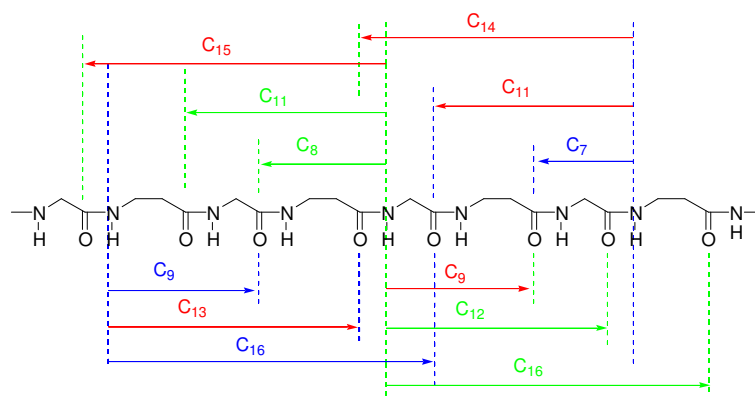


Figure 30. Possible helices in α -/ β - alternated peptides.

Computer calculations on a alternating Gly- β ACC nonapeptide was performed in vacuum by *Baldauf et al.*²¹ Through these studies it was possible to show that this peptide should adopt a mixed helix C9/C11 with $i \rightarrow i+1$ / $i \leftarrow i+3$ interactions. (Figure 31)

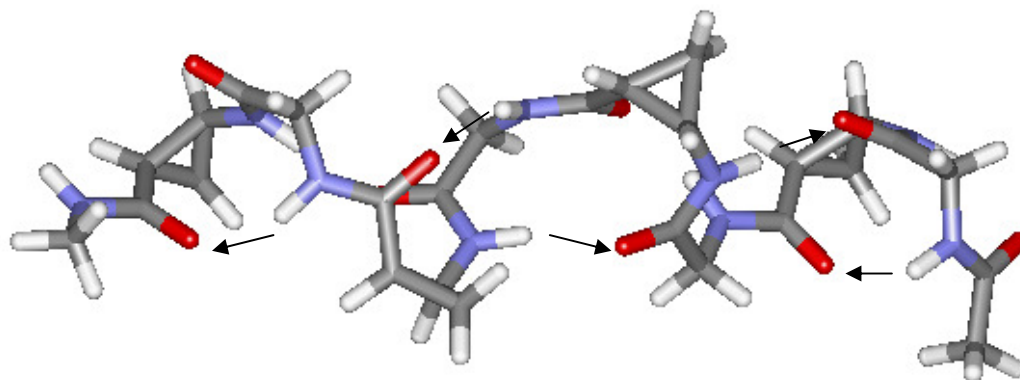


Figure 31. *Baldauf et al.* were able to predict the most stable helix in vacuum for an alternating Gly- β ACC nonapeptide using computer calculations.²¹

The β -ACC containing peptides were investigated with 2D-NMR, CD and FT-IR spectroscopy.

While structure determination of smaller globular proteins using NMR spectroscopy is well-established, particular care must be taken with smaller peptides. In this class of molecules folded conformations are possibly in (fast) exchange with extended forms, or differently folded forms may rapidly interconvert. It was therefore tried to monitor a number of

parameters in order to determine whether a single, well-folded conformation predominates. The following approach was used in order to determine predominant structures of the heptapeptides (–)-**5a**, (+)-**5a** and the nonapeptides (–)-**6a**, (+)-**6a** in methanol and to quantify to what extent these peptides are folded. Structures were calculated according to conventional methodology using NOE-derived distance restraints as the sole source of (upper) distance limits. It was assumed that a peptide adopts a well-folded form predominantly when the following three criteria are fulfilled: (1) No consistent restraint violations of the distant restraints are found; (2) A uniform calibration (NOE volume integral-distance conversion) can be used, and known distances adopt reasonable values; (3) All distances shorter than 3.5 Å that occur in more than half of the low-energy DYANA structures give rise to crosspeaks in the NOESY spectrum. It was found that the third criterion was particularly useful in determining whether a single conformer predominates. If NOE-derived distance restraints are due to two different conformers, the calculated structure representing only a single conformer usually displays short distances for which no NOEs can be found in the spectra.

To further verify that the proposed conformers are realistic, molecular dynamics (MD) simulations were conducted. The NMR structures were subjected to extensive temperature cycling in order to extensively screen conformational space and to perform statistical analysis on the resulting low-energy structures. For the structures that fulfilled the criteria described above, well-folded conformers resulted that were in agreement with the NMR data.

All investigated peptides displayed helical conformations, as is apparent from the presence of NOEs between sequential amide protons. However, they largely differ in the extent to which they are *uniquely* folded.

B.3.1 Alternated α -L-Ala/(-) β -ACC peptides

The peptides which contained the (-) β -ACC unit were less subject to conformational averaging. They are structurally best defined. A representative conformer from the low-energy NMR structures computed from the NOESY data with the program DYANA is displayed in Figure 32 (left).

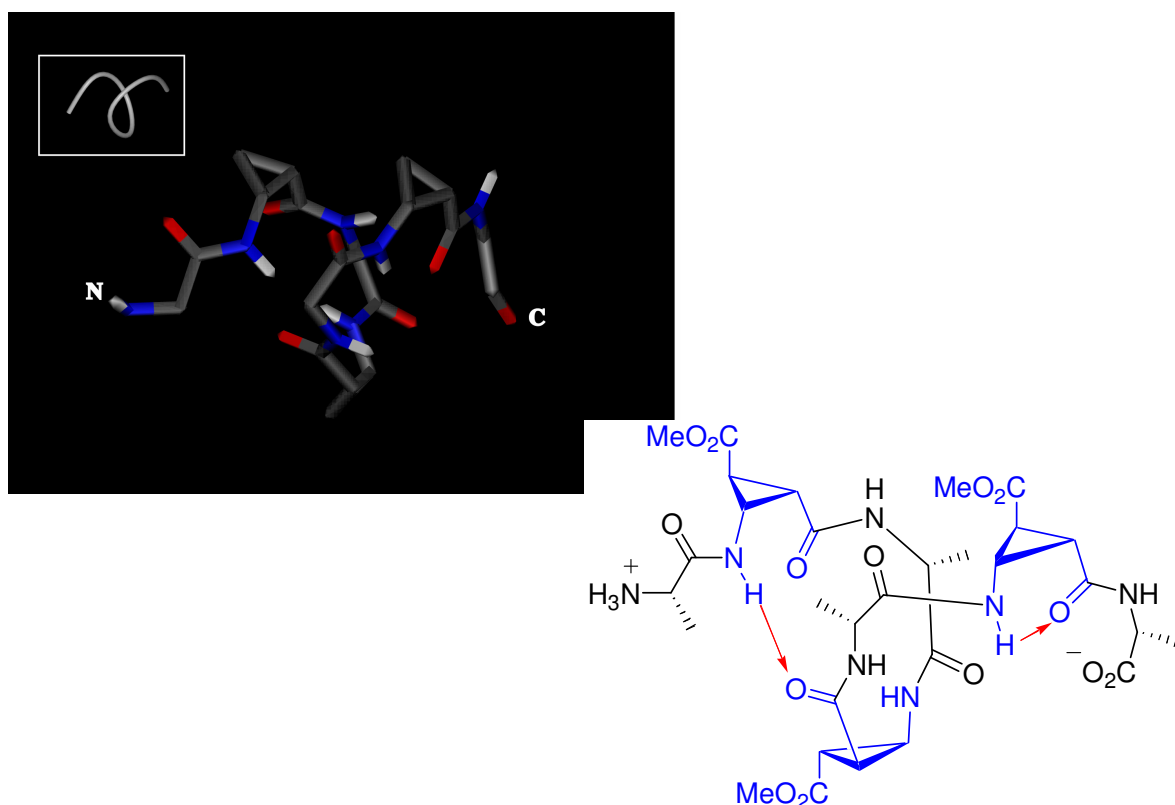


Figure 32. Structure calculated for the heptapeptide (-)-**5a**.

The heptapeptide (-)-**5a** forms a left-handed 3_{13} -helix. Hydrogen bonds occur between the amide proton of the β -ACC in position 2 and the carbonyl oxygen of the β -ACC in position 4. An intrasidual hydrogen bond between amide proton and carbonyl oxygen of the β -ACC in position 6 occurs in most of the low-energy structures²² (Figure 32, right). This structure was surprisingly well defined for a non-cyclic heptapeptide without disulfide bonds or other constraints. The helical fold²³ was supported by a larger number of *medium-range* NOEs, in particular by a range of $i, i+3$ contacts (Table 5).

Peptide	Contacts			Contacts	
(-)-5a	Ala ¹ HA	Ala ⁵ HA		Ala ³ HN	ACC ⁶ HG
	Ala ¹ HA	ACC ⁴ HG		Ala ³ HA	ACC ⁶ HG
	Ala ¹ QB	ACC ⁴ HA		Ala ³ HA	Ala ⁷ HA
	Ala ¹ HA	Ala ⁵ HA		Ala ³ QB	Ala ⁷ HA
	ACC ² HB	Ala ⁵ HA		ACC ⁴ HN	Ala ⁷ HA
	ACC ² HN	Ala ⁵ HA		ACC ⁴ HB	ACC ⁶ HN
	ACC ² HN	ACC ⁴ HG		ACC ⁴ HA	Ala ⁷ HA
(-)-6a	Ala ⁵ HN	ACC ⁸ HG		ACC ⁴ HA	Ala ⁷ HA
	ACC ⁴ HA	ACC ⁸ HN		ACC ⁶ HA	Ala ⁹ HA
	Ala ³ HN	Ala ⁷ HA		Ala ⁵ HA	ACC ⁸ HG
	ACC ² HN	Ala ⁵ HA		Ala ³ HA	ACC ⁶ HG
	Ala ¹ HA	Ala ⁵ HA		ACC ⁴ HN	Ala ⁷ HA
	Ala ³ HA	Ala ⁷ HA		ACC ⁶ HN	Ala ⁹ HA
	Ala ⁵ HA	Ala ⁹ HA		Ala ¹ QB	ACC ⁴ HA
	ACC ⁴ HA	ACC ⁸ HG		Ala ⁵ QB	ACC ⁸ HG
	Ala ³ QB	ACC ⁶ HG		Ala ¹ QB	ACC ⁴ HG

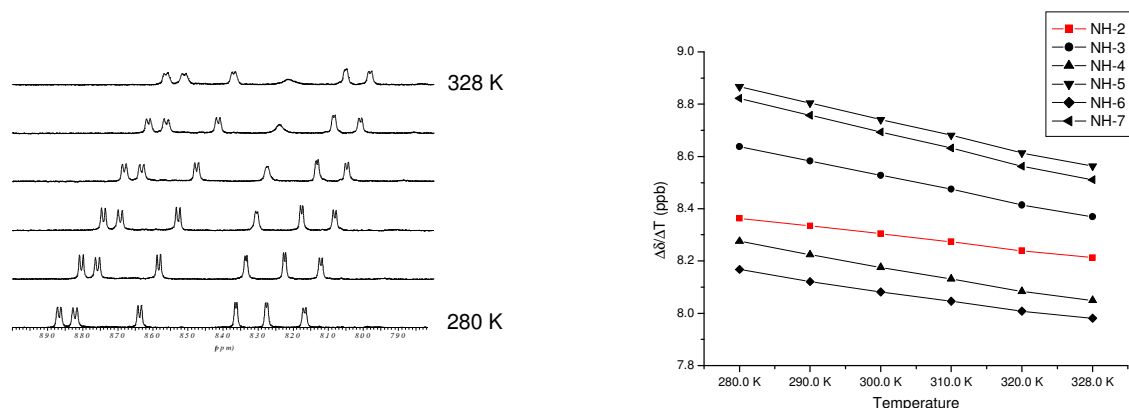
Table 5. Medium-range NOEs for the peptides **(-)-5a** and **(-)-6a**. In the table, A= α ; B= β , G= γ , D= δ , E= ϵ . The letter Q instead of H is used when there is a signal due to more than one hydrogen and it is not possible to distinguish between them, for example the CH₃ of Alanine.

Moreover, in the heptapeptide **(-)-5a** the $^3J_{\text{HN}\alpha}$ scalar coupling constants were less than 4.2 Hz (Table 6). All NOESY cross peaks due to intraresidual distances smaller than 3.5 Å in the 20 low-energy DYANA structures of the heptapeptide **(-)-5a** were found in the NOESY spectrum. In the spectra no i , $i+1$ H ^{α} , H ^{α} peaks were found indicating the absence of any *cis* Xaa-ACC bonds. In order to detect possible aggregation effects and to exclude intermolecular NOEs from the analysis, the sample was diluted to approx. 0.8 mM. Chemical shifts remained constant during dilution and the same NOE cross peaks were observed in the NOESY spectrum at this lower concentration. Signals were sufficiently separated so that all the NOESY crosspeaks could be assigned unambiguously.

(-)-5a	$^3J_{\text{HN}\alpha}$ (Hz)	(-)-6a	$^3J_{\text{HN}\alpha}$ (Hz)
NH-2	3.4	NH-2	3.9
NH-3	6.4	NH-3	6.0
NH-4	3.4	NH-4	3.4
NH-5	6.0	NH-5	5.9
NH-6	4.2	NH-6	3.5
NH-7	7.2	NH-7	6.7
		NH-8	5.6
		NH-9	6.8

Table 6. Vicinal coupling constants for H^N, H ^{α} in CD₃OH for peptide **(-)-5a** and **(-)-6a**.

The temperature coefficients ($\Delta\delta/\Delta T$) for the heptapeptide (–)-**5a** were also measured (Figure 33). Although any reduced temperature coefficient should be interpreted with care, together with a 2D-NMR investigation we confirmed that the NH of the β -ACC in position 2 was involved in a hydrogen-bond leading to the most downfielded chemical shift among the β -ACC-NHs and to a temperature coefficients $\Delta\delta/\Delta T$ less negative than -4 ppb/ $^{\circ}\text{C}$.



Temperature	NH-2	NH-3	NH-4	NH-5	NH-6	NH-7
280.0 K	8.3630	8.6373	8.2756	8.8667	8.1678	8.8216
290.0 K	8.3344	8.5829	8.2244	8.8037	8.1213	8.7576
300.0 K	8.3042	8.5277	8.1757	8.7409	8.0816	8.6930
310.0 K	8.2739	8.4750	8.1320	8.6816	8.0470	8.6320
320.0 K	8.2391	8.4140	8.0838	8.6129	8.0082	8.5621
328.0 K	8.2124	8.3693	8.0492	8.5626	7.9809	8.5108
$\Delta\delta/\Delta T$ (ppb)	- 3.14	- 5.58	- 4.72	- 6.34	- 3.90	- 6.48

Figure 33. Temperature coefficient for the NHs in the heptapeptide (–)-**5a**.

The structure of the nonapeptide (–)-**6a** was found to be similar to that of the heptapeptide (–)-**5a**. It displayed a 3_{13} helical fold (Figure 34, right) and no indications for significant conformational averaging in this peptide are found. Low scalar couplings and a high number of *medium-range* NOEs indicate that this peptide is well structured.

The CD investigations performed in methanol (Figure 34, left) stressed that the heptapeptide (–)-**5a** and the nonapeptide (–)-**6a** adopt the same conformation. Both peptides show a minima at about 200 nm that correspond probably to the Cotton effect associated with this

kind of turn. There is unfortunately no CD-reference for α -/ β -alternated peptides that adopt a 3_{13} -turn conformation.

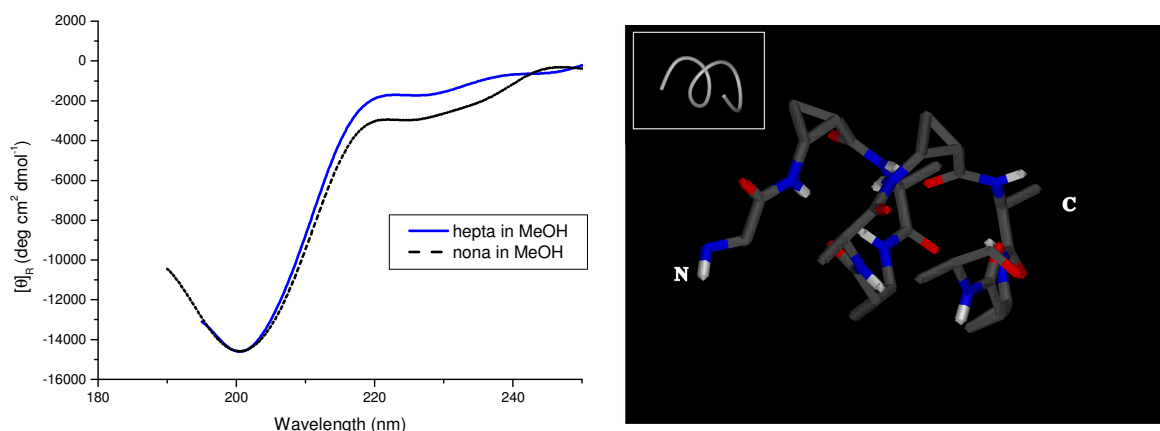


Figure 34. CD spectra of the heptapeptide (-)-5a and the nonapeptide (-)-6a in methanol and the NMR structure of (-)-6a.

The structure of the alternated α -Ala/(-)- β ACC peptides was found to be solvent dependent. The CD spectra of these peptides in different solvents, as shown in Figures 35 and 36, display the instability of the helix-turn that was found from NMR investigations by changing the environment. The intensity at 200 nm decreases, indicating an unfolding process or a conformational change. TFE are known to be a helix-inducing solvent. However it has been also found for proteins that the preferred conformation in TFE it is not necessarily correlated with the one in the native state.²⁴ Since TFE can disrupt the native state of proteins, for example in loop or β -sheet regions, to induce α -helices, it is possible that for our peptides TFE is not able to stabilize the 3_{13} -helix.

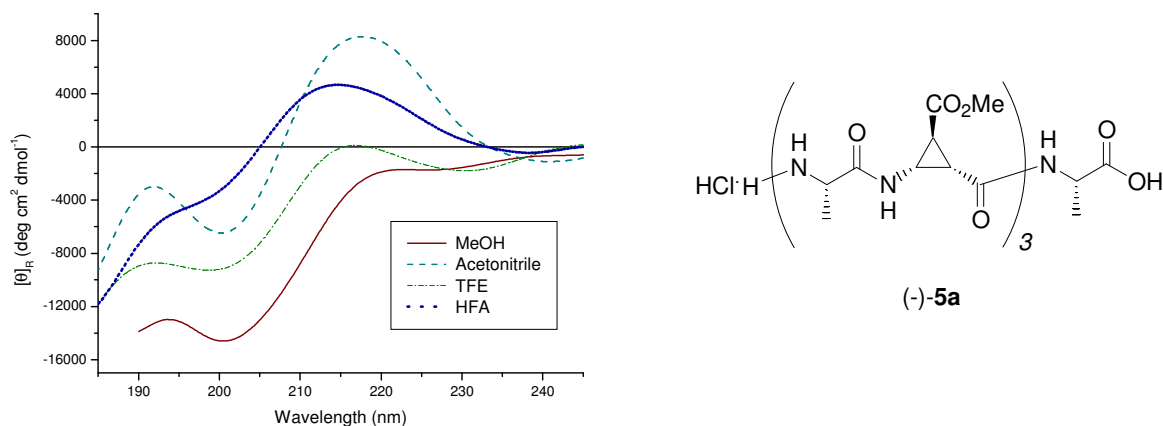


Figure 35. CD spectra of the heptapeptide (-)-5a in different solvents.

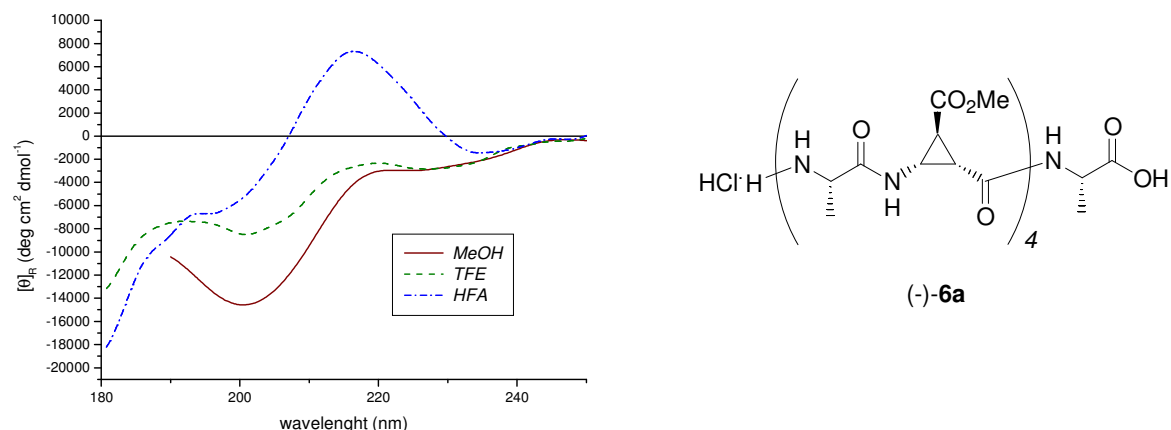


Figure 36. CD spectra of the nonapeptide **(-)-6a** in different solvents.

Although a slightly red-shift is present, the intensity of the ellipticity at 200 nm does not vary significantly over the concentration range of 330 μ M and 1 mM in methanol indicating no conformational changes or eventual aggregation effects. (Figure 37)

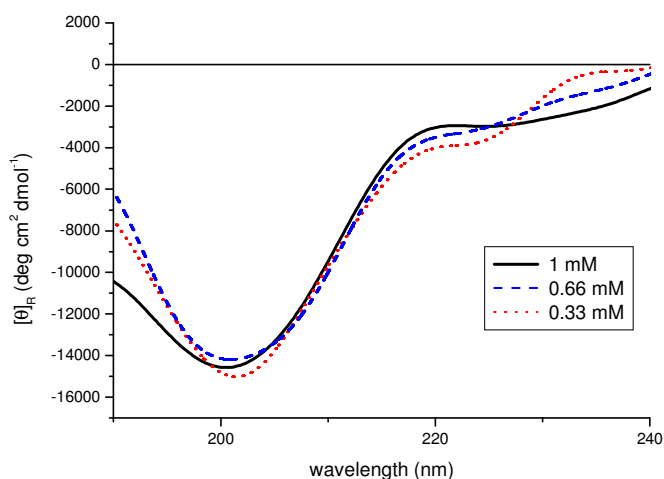


Figure 37. CD spectra of the nonapeptide **(-)-6a** measured in methanol at different concentrations.

In HFA the peptides show a maximum at about 216 nm, which is probably due to a different conformation. To further investigate the conformational changes on the secondary structure of the peptides containing the **(-)- β ACC** moiety, we measured the CD spectra in methanol in the presence of varying amounts of HFA. (Figure 38)

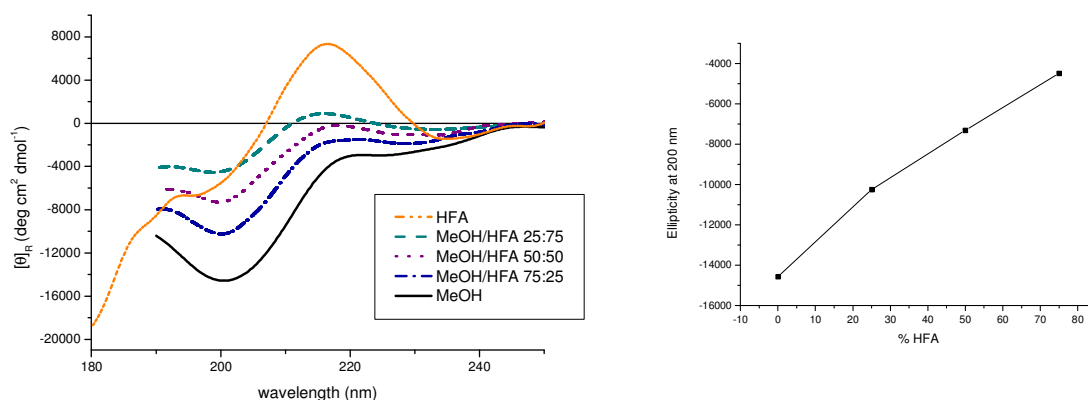


Figure 38. CD spectra of (–)-**6a** in methanol in the presence of different amounts of HFA.

By addition of HFA the 200 nm band intensity decreases and the new band at 216 nm is forming. Since there is no isodichroic point, it can be assumed that the structure found in methanol is in equilibrium with at least two different conformations in HFA. It is likely that in HFA the peptide is unfolded. The addition of this solvent to the folded peptide in methanol leads to a “melting” process of the structure. This process carried out *via* non-cooperative mechanism since the intensity at 200 nm with the amount of HFA has a almost linear dependence (Figure 38, right). Similar results were found also investigating the “melting” mechanism of the secondary structure for β -peptides.²⁵

The peptide at concentration of 1 mM in methanol were studied in the presence of increasing ratios of water. When the temperature is increased or urea, guanidinium hydrochloride, or water are added, the secondary structure of α -peptides generally collapses. As shown in Figure 39, increasing amount of water does not decrease the ellipticity at 200 nm, as expected for a unfolding process, but instead an increase was observed. Superficial NMR investigation on the peptide in water suggests a conformational change from methanol to water. Either the helical fold adopted in water is similar to that found in methanol, with a similar CD pattern or, more likely, a smaller amount of methanol, less than 100%, is better to stabilize the 3_{13} helix-turn.

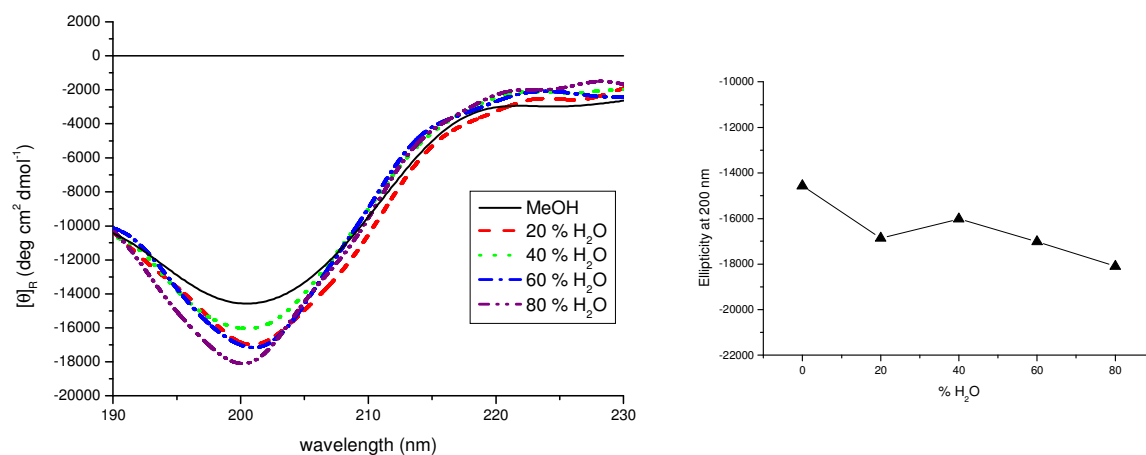


Figure 39. CD spectra of the nonapeptide (–)-**6a** in methanol with different amount of water. Right the behaviour of the ellipticity at 200 nm by increasing of percentage of water.

Shown below, in Figure 40, is the IR spectra of the peptide (–)-**6a** measured in methanol. It highlights the Amide I region.

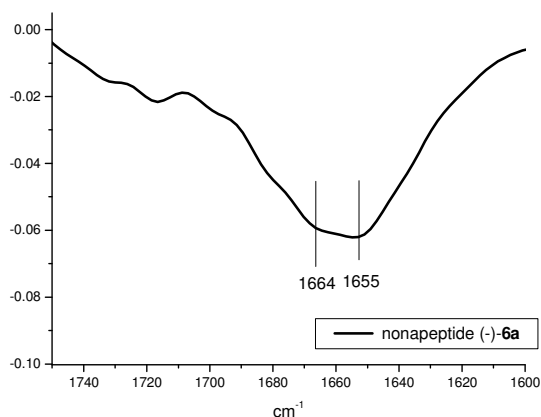


Figure 40. Amide I region of IR spectra of (–)-**6a** in methanol.

α -Helices are generally assumed to absorb in D₂O at around 1652 cm^{-1} . However intrinsic absorbencies, even for the same secondary structure-type, are not the same.²⁶

By calculating the second derivative, it was possible to identify the position of each component of the Amide I band. There are two maxima at about 1655 and 1664 cm^{-1} and a shoulder at around 1650 cm^{-1} that probably characterized the 3_{13} helix-turn previously found by NMR investigation.

According to computer calculations presented in Figure 31, the alternated α -Xxx/ β -ACC peptides could have undergone a conformational change depending on the solvent polarity. The CD spectra of (–)-**6** were then measured when different amounts of methanol and cyclohexane were added to the same volume of 1,2 dichloroethane. The presence of 1,2 dichloroethane was necessary for the solubility and the solution homogeneity. The peptide shows a different pattern depending on the ratio of polar and non polar solvents.

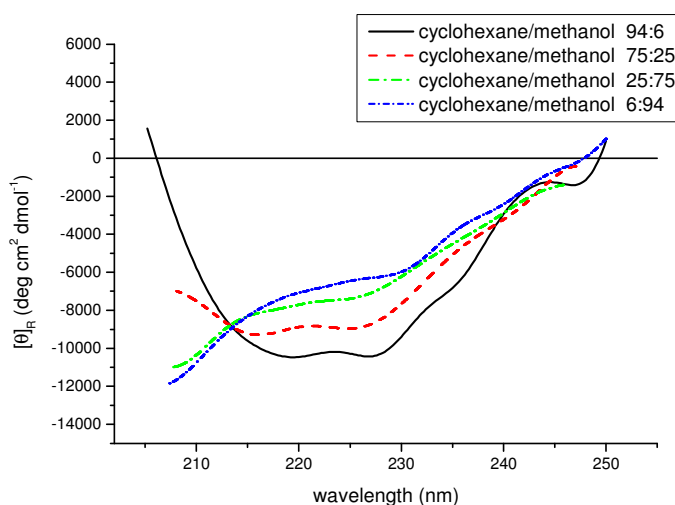


Figure 41. CD spectra of the nonapeptide (–)-**6** with different ratio of polar and non polar solvent.

The isodichroic point (Figure 41) suggests that an equilibrium exists between the two conformational states. In a non polar solvent a peptide's secondary structure is stabilized. Its CD pattern has two minima at about 218 and 227 nm and a maximum at a wavelength lower than 205 nm. Due to the high absorbance associated with the solvent-mixture itself, it was not possible to extend these measurements beyond this value.

NMR investigation of the peptide (–)-**6** was performed in the non polar solvent CDCl_3 . Measuring the proton NMR at different temperatures it was possible to observe a splitting in some of the signals, especially in the case of some NHs. This decrease in temperature was probably responsible for the formation of a different rotamer (Figure 42). Further conformational investigations were carried out at 300 K. At this temperature the above phenomena became negligible and the best signal dispersion was seen.

COSY and TOCSY experiments were used to assign the chemical shifts of all the protons. A ROESY spectrum was then implemented in order to understand the connectivity of the amino acids in the sequence. Finally the non sequential interresidue contacts were found.

Table 7 and Figure 42 show the *medium range* NOEs and some of the $i,i+3$ and $i,i+4$ contacts found for this peptide in CDCl_3 respectively.

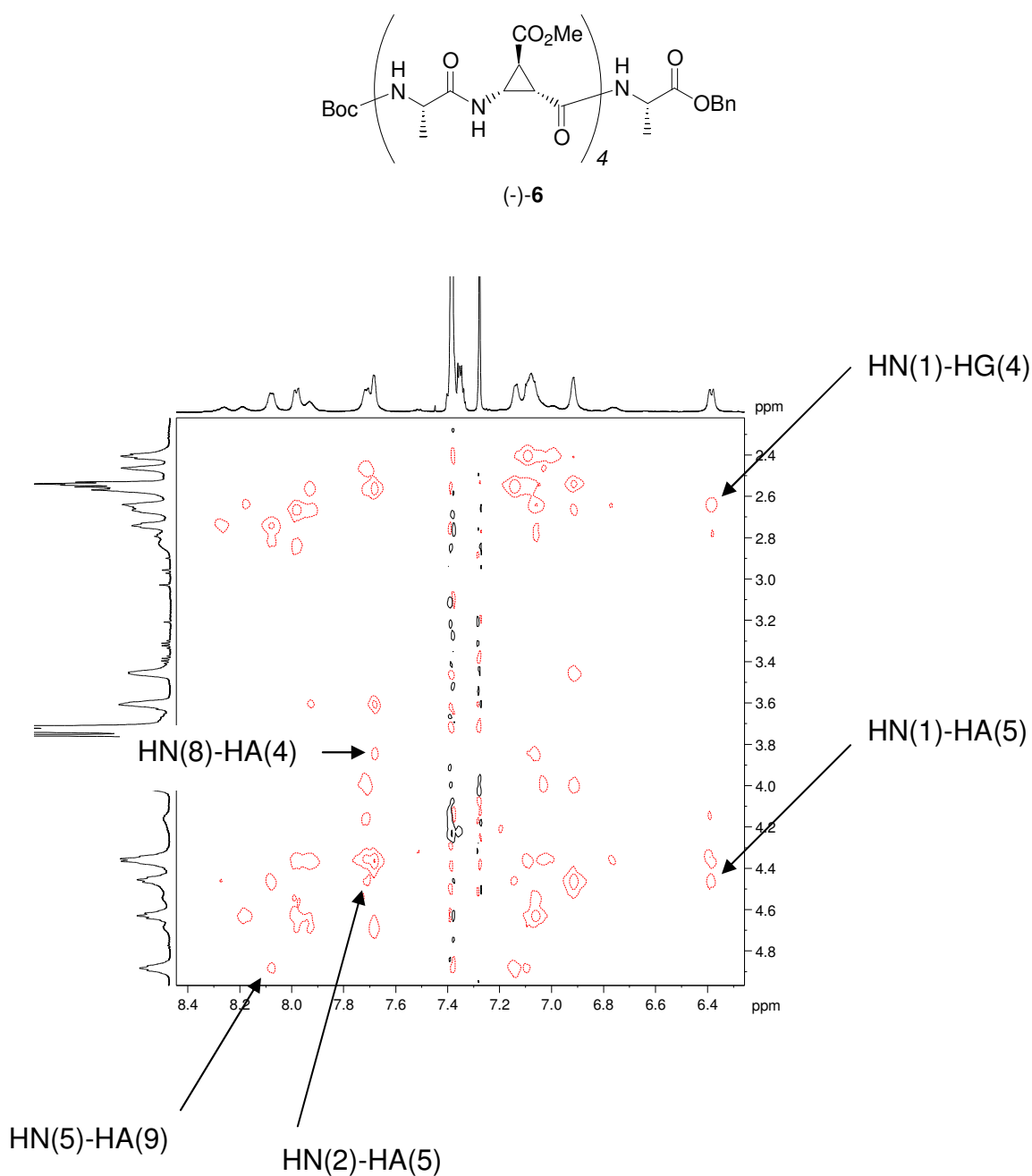


Figure 42. Some *Medium-range* NOEs for the peptide (-)-6 in the ROESY spectra, in CDCl_3 .

Peptide	Contacts			Contacts	
(-)-6	Ala ¹ HN	ACC ⁴ HG		ACC ⁶ HN	ACC ² HB
	Ala ¹ HN	ACC ⁴ HN		ACC ⁶ HN	ACC ² HG
	Ala ¹ HN	Ala ⁵ HA		ACC ⁶ HN	ACC ² HA
	ACC ² HN	Ala ⁵ HA		ACC ⁶ HA	ACC ² HB
	ACC ² HA	ACC ⁶ HG		Ala ⁷ HN	Ala ⁹ HA
	Ala ³ HA	ACC ⁸ HA		ACC ⁸ HN	ACC ⁴ HA
	ACC ⁴ HG	Ala ¹ HG		ACC ⁸ HA	ACC ⁴ HB
	ACC ⁴ HG	Ala ⁹ HG		ACC ⁸ HA	ACC ⁴ HG
	ACC ⁴ HB	Ala ⁹ HG		Ala ⁹ HN	Ala ⁵ HA
	Ala ⁵ HA	ACC ² HA		Ala ⁹ HA	Ala ⁵ HG
	Ala ⁵ HA	ACC ² HB			

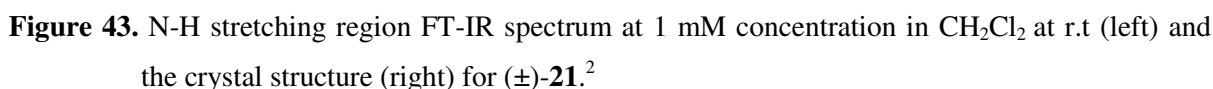
Table 7. Medium-range NOEs for the peptide **(-)-6** found in CDCl₃.

Temperature	NH-1	NH-2	NH-3	NH-4	NH-5	NH-6	NH-7	NH-8	NH-9
300 K	6.3851	7.7134	7.9819	7.0666	8.0781	6.9161	7.0878	7.6843	7.1376
310 K	6.3356	7.6858	7.9198	7.0180	8.0084	6.8905	7.0180	7.6471	7.0797
320 K	6.2797	7.6474	7.8533	6.9522	7.9346	6.8649	6.9522	7.6094	7.0194
$\Delta\delta/\Delta T$ (ppb)	-5.3	-3.3	-6.4	-5.7	-7.2	-2.6	-6.8	-3.7	-5.9

Table 8. Temperature coefficients for the NHs in the nonapeptide **(-)-6** in CDCl₃.

Temperature coefficients and the two dimensional NMR investigation suggested that a helical conformation was present. This probably involved a hydrogen bond NH→CO from the NH of the residue 2 in the same direction of the peptide chain. As well as a hydrogen bond CO←NH in the opposite direction from either the residue 6 or 8. It was also important to keep in mind that at a lower temperature than 300 K, a mixture of rotamers would be present. It is likely that chloroform is not able to stabilize the well defined structure, which was suggested by the CD investigations done using 1,2 dichloroethane and cyclohexane mixture.

Previous results by Zorn² suggest that the β -ACC moiety is able to reside in a hydrogen-bonded conformation in solution of dichloromethane as shown for the compound (\pm)-**21** in Figure 43. The strong hydrogen-bond acceptor capability of a tertiary amide carbonyl overcomes the not optimal N-H...O geometry and allows the hydrogen-bond highlighted by the main absorption at 3364 cm⁻¹. However, in the solid state this C₆ conformation is no longer favoured, which became evident in the X-ray structure in Figure 43 (right).



Unfortunately, in this work it was not possible to obtain crystals of the longer peptides with incorporated β -ACC units. We could only measure the X-ray structure for the C-terminal deprotected (+)-**11** dipeptide (Figure 44). From this data we could get no information on the conformational preference of the β -ACC, since the dipeptide has a extended spatial structure in a dimeric crystal packing with no *intramolecular* H-bond present.

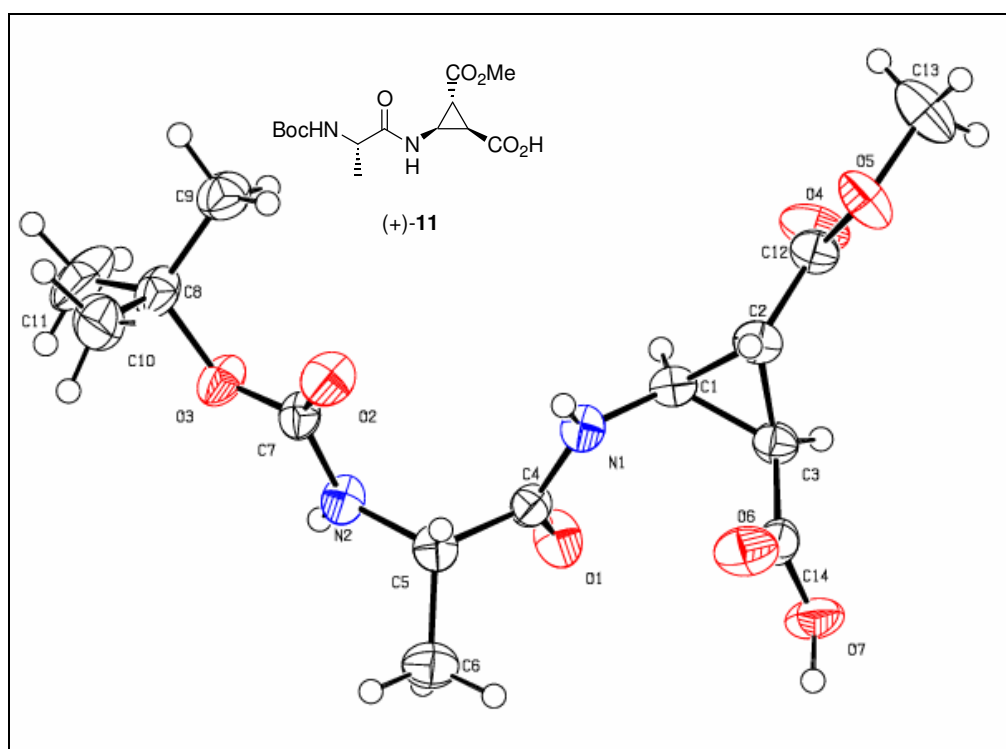


Figure 44. Crystal structure of the C-terminal deprotected dipeptide Boc-L-Ala-(+) β -ACC-OH.

The IR investigation of the amide A region of the heptapeptide (+)-**5** being carried out in the non polar solvent dichloromethane is shown in Figure 45. The main absorption at 3296 cm^{-1} suggested that the peptide should adopt a secondary structure in which almost all NHs are involved in an *intramolecular* H-bond.

However this result was not confirmed in a polar solvent such as methanol.

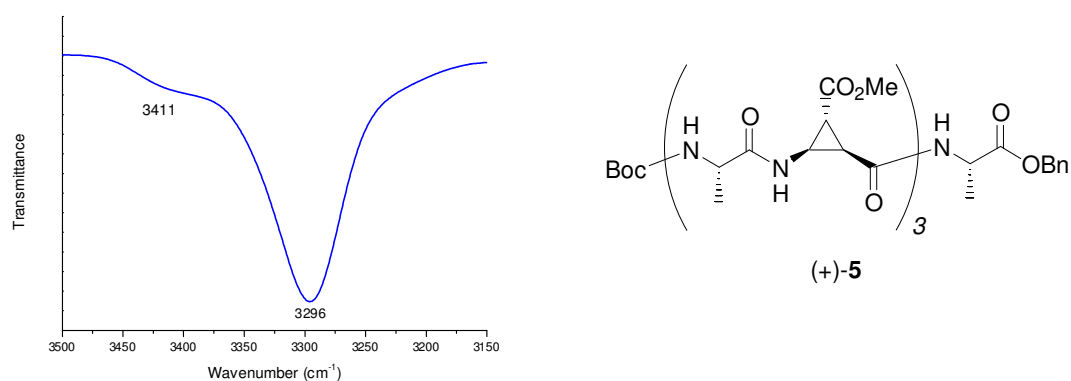


Figure 45. N-H stretching region FT-IR spectra for (+)-**5** at 1 mM concentration in CH_2Cl_2 at r.t.

The conformation in methanol of the heptapeptide (+)-**5a**, having (+)- β -ACC unit incorporated in its sequence, is less well defined than the corresponding (–)-**5a**. Although a number of medium-range NOE correlations could be found in the spectra (Table 10) and structures of reasonable energy may be computed from the NMR data. A large number of cross peaks corresponding to non sequential distances smaller than 3.5 Å were actually missing in the NMR spectra. This indicates that the NOEs are not due to a single, predominant conformation but rather a set of conformers which rapidly interconvert on the NMR timescale. This view is supported by the magnitude of the vicinal H^N , H^α coupling, which, for all the residues, except for the β -ACC in position 2, adopted values in the range of 6-7 Hz (Table 9), indicating rotationally-averaged ϕ backbone angles.

(+)- 5a	$^3J_{HN\alpha}$ (Hz)	(+)- 6a	$^3J_{HN\alpha}$ (Hz)
NH-2	4.6	NH-2	4.5
NH-3	6.2	NH-3	5.3
NH-4	6.3	NH-4	6.8
NH-5	6.5	NH-5	5.8
NH-6	7.2	NH-6	6.9
NH-7	8.0	NH-7	6.3
		NH-8	7.3
		NH-9	7.4

Table 9. Vicinal coupling constants for H^N , H^α in CD_3OH for peptide (+)-**5a** and (+)-**6a**.

Considering that most medium-range contacts were found in the first half of the sequence and that rather strong NOEs occurred between sequential amide protons, give rise to the conclusion that predominantly helical portions interconvert locally with extended conformations so that the full helix is unable to persist. This view is related to the observation that *medium-range* NOEs such as $\alpha(i)$, $\beta(i+3)$ correlations are required to distinguish stably-folded α -helices from nascent helices.²³

Peptides	Contacts			Contacts	
(+)-5a	ACC ⁴ HB	ACC ² HA		Ala ¹ QB	ACC ⁴ HG
	ACC ² HB	Ala ⁵ HA		Ala ¹ QB	ACC ⁴ HN
	ACC ⁴ HG	Ala ⁷ HA			
(+)-6a	Ala ¹ QB	Ala ³ HA		ACC ⁶ HG	Ala ⁹ HA
	ACC ⁴ HG	Ala ⁷ HA		ACC ⁶ HA	Ala ⁹ QB
	ACC ² HG	Ala ⁵ HA		ACC ⁶ HG	Ala ⁹ QB
	Ala ³ QB	ACC ⁶ HB		ACC ⁴ HG	Ala ⁷ QB
	Ala ⁵ QB	ACC ² HG			

Table 10. Medium-range NOEs found for the peptide containing the (+)- β -ACC unit.

The CD spectra of these two peptides in different solvents are shown in Figure 46. Both peptides show a minima with different intensities at about 204-205 nm with the exception of a shoulder at around 223 nm in HFA. NMR investigation in methanol suggested that a set of conformers is present. Despite this, the conformation of these peptides was unaffected when the solvents was changed. The solvents in question were unable to stabilize one conformation with respect to another one.

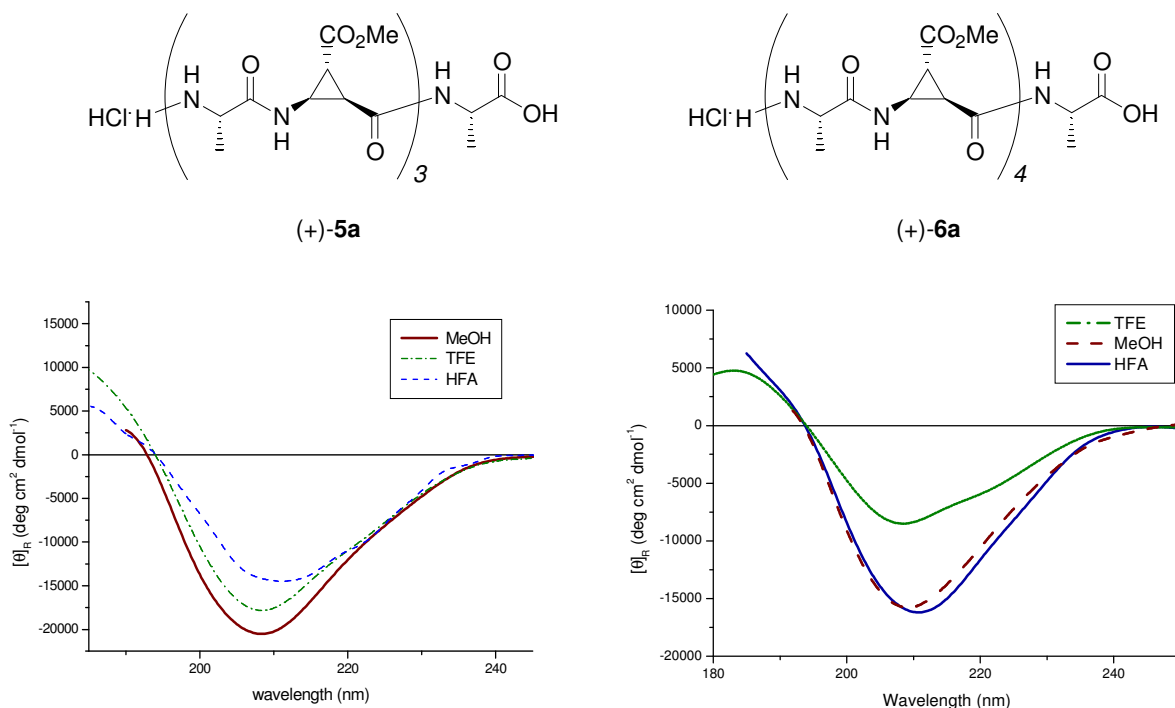


Figure 46. CD spectra of peptides (+)-5a and (+)-6a in different solvents.

B.3.3 Alternated α -L-Xaa/(-)- β -ACC peptide

The trideca peptide (-)-**7a** was synthesized in order to investigate what effect the (-)- β -ACC unit elicits when contained in a longer α -/ β -alternated peptide. Different α -amino acids were incorporated with the view to achieve a better understanding of the NMR signals. Two lysines were chosen to improve the solubility of the final peptide and three phenylalanine residues were introduced at positions 3, 7 and 11. In Figure 47 the positions 3 and 7 of the nonapeptide (-)-**5a** are highlighted. The side chains of the amino acids at these positions along the 3_{13} helix, were discovered to be on the same side and aligned one over another. Phenylalanine in these positions should cause a stabilizing effect on the overall structure through phenyl ring stacking.

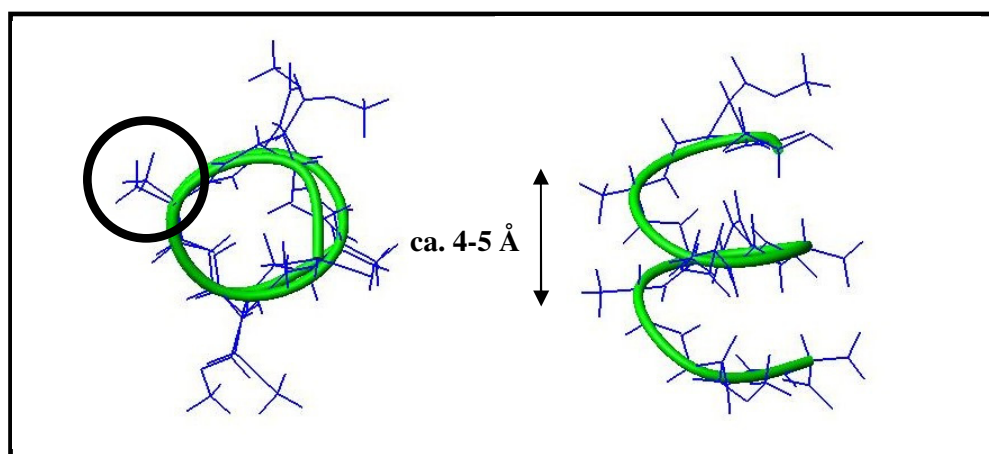
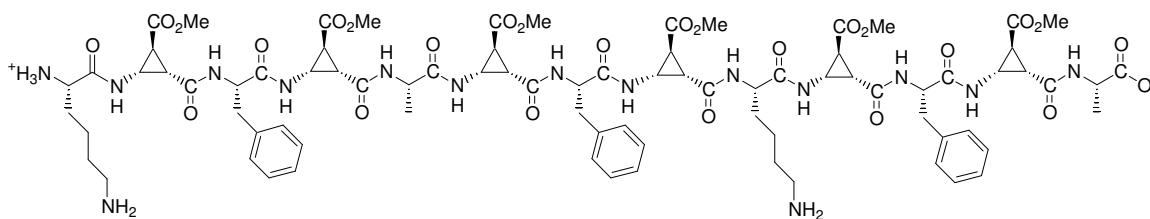


Figure 47. Upper and lateral view of the (-)-**6a**.

As for the shorter peptides, all NMR investigations involving the trideca peptide (-)-**7a** were performed in methanol. The *medium-range* NOE cross-peaks are summarized in Table 11. In the N-terminus of the sequence only very weak helical contacts are present, while in the region from residue 4 along the all sequence, strong $i,i+3$ and $i,i+4$ contacts were found. Excepted for the N-terminus, $\text{NH}(i)\text{-NH}(i+1)$; $\text{HA}(i)\text{-NH}(i+1)$ and $\text{HB}(i)\text{-NH}(i+1)$ contacts were seen for the Xaa-ACC segment and $\text{HA}(i)\text{-NH}(i+1)$ and $\text{HB}(i)\text{-NH}(i+1)$ were seen for the ACC-Xaa segment along the entire length of the sequence. These findings provide strong evidence for the presence of a helical conformation.

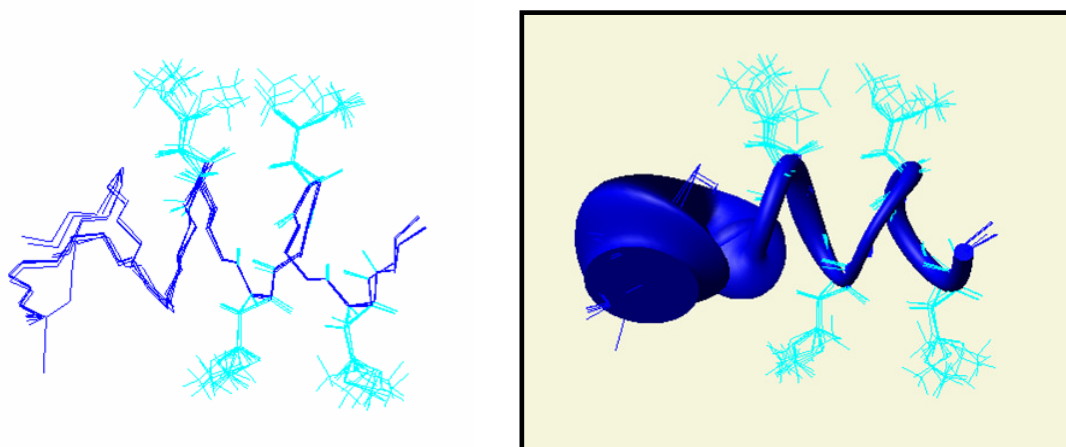


(-)-7

Peptide	Contacts			Contacts	
(-)-7a	Lys ¹ QB	ACC ⁴ HG		Ala ⁵ QB	ACC ⁸ HA
	Lys ¹ QG	ACC ⁴ HG		Ala ⁵ QB	ACC ⁸ HG
	Lys ¹ QD	ACC ⁴ HG		Ala ⁵ QB	Lys ⁹ HA
	ACC ² HN	Ala ⁵ HA		ACC ⁶ HN	ACC ⁸ HN
	Phe ³ HN	ACC ⁶ HG		ACC ⁶ HB	ACC ⁸ HN
	Phe ³ HA	Ala ⁵ QB		ACC ⁸ HN	ACC ¹² HN
	Phe ³ HA	Phe ⁷ HA		ACC ⁸ HA	ACC ¹² HG
	ACC ⁴ HN	ACC ⁶ HN		Lys ⁹ QB	Ala ¹³ HA
	ACC ⁴ HN	Phe ⁷ HA		Lys ⁹ QB	ACC ¹² HG
	Ala ⁵ HA	Phe ⁷ HN		Lys ⁹ QB	Ala ¹³ HN
	Ala ⁵ QB	Phe ⁷ HN		Lys ⁹ QB	Ala ¹³ HA
	Ala ⁵ QB	ACC ⁸ HN		ACC ¹⁰ HN	Ala ¹³ HA

Table 11. Medium-range NOE cross-peaks found for peptide (-)-7a.

The structure calculated with DYANA shows a helical conformation which is well defined from residue 4. The N-terminal part remains partially unfolded as displayed in Figure 48.

**Figure 48.** Lateral view (left) and the sausage display (right) of backbone atoms of 10 minimized superimposed structures. In both representation, the β -ACCs at position 6, 8, 10 and 12 are shown.

The instability of the secondary structure in methanol is probably due to the N-terminal deprotonated Lys¹. The presence of two positive charges does not allow the peptide to

undergo folding. Changes in the ionization degree of the peptides could affect inter-residual interactions and thereby cause conformational changes. CD studies confirmed that some conformational changes occur depending on the solvent or in the case of water solution, on the pH.

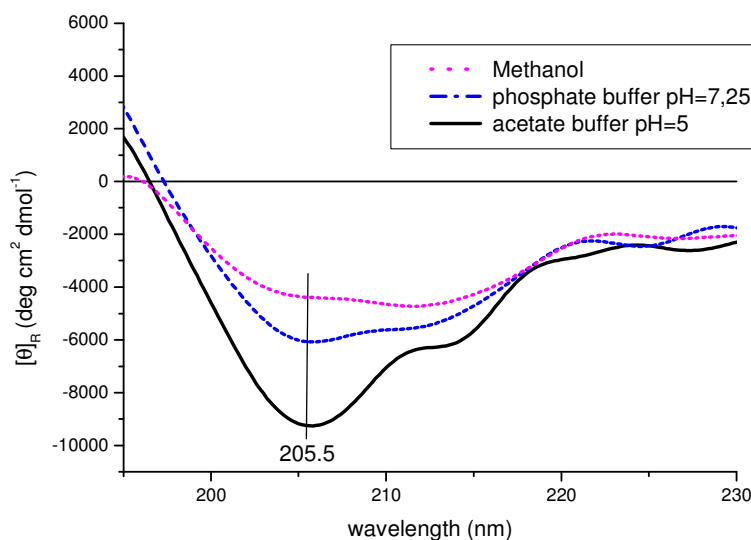


Figure 49. CD spectra of (–)-**7a** in methanol and in water at different pH.

The CD spectrum performed in methanol shows two bands of virtually the same intensity at about 205 and 212 nm (Figure 49). When the peptide was in a water solution, the relative intensities of the two bands were found to change, depending on the pH of the solution. At an acidic pH value the negative Cotton effect at ca. 205 nm became more relevant. NMR investigation in acetate buffer highlighted a destabilization of the secondary structure found in methanol, thus, supporting the idea that the two proximal positive charges at the N-terminus were responsible for the observed instability.

The CD spectrum of this peptide cannot be compared directly to those of the shorter alternated α -L-Ala/ β -ACC peptides, due to the presence of the phenylalanine residues. Three phenylalanine in thirteen total residues represent the 23 % of aromatic amino acids in the sequence. Moreover the position of these residues was chosen so as to give stacking in a 3_{13} helix.

In most cases values below 260 nm in a CD spectrum are predominantly governed by the amide chromophore, but the environment of the aromatic residues is also particularly important in determining the extent of their contributions. Strong coupling between aromatic transitions can occur if two or more aromatic rings are in close proximity. In proteins such interactions are more important in determining the aromatic CD than the number of aromatic

rings.²⁷ Calculations performed by *Sreerama et al.* showed that the phenylalanine transitions occurred at around 257 nm (L_b transition), 208 nm (L_a transition), and 188 nm (B transition). The latter is the strongest one because it couples strongly with the peptide transition. In many proteins with aromatic residues, a positive interfering band is also found at around 224 nm²⁸. In this case the transition B could have been the reason why there is no minima at 200 nm, expected for the turn-helix structure found in the shorter peptides. However the sensitivity of CD techniques to the relative orientations of the aromatic side chains is very high. Different orientations or various arrangements of the aromatic rings in the three-dimensional structure, leads to different CD spectra.²⁷

The helix-promoting solvent TFE, as already found for peptide (–)-**5a** and (–)-**6a**, does not stabilize any secondary structure. The CD pattern remains almost the same as in methanol but with a lower intensity probably due to an aggregation phenomena.

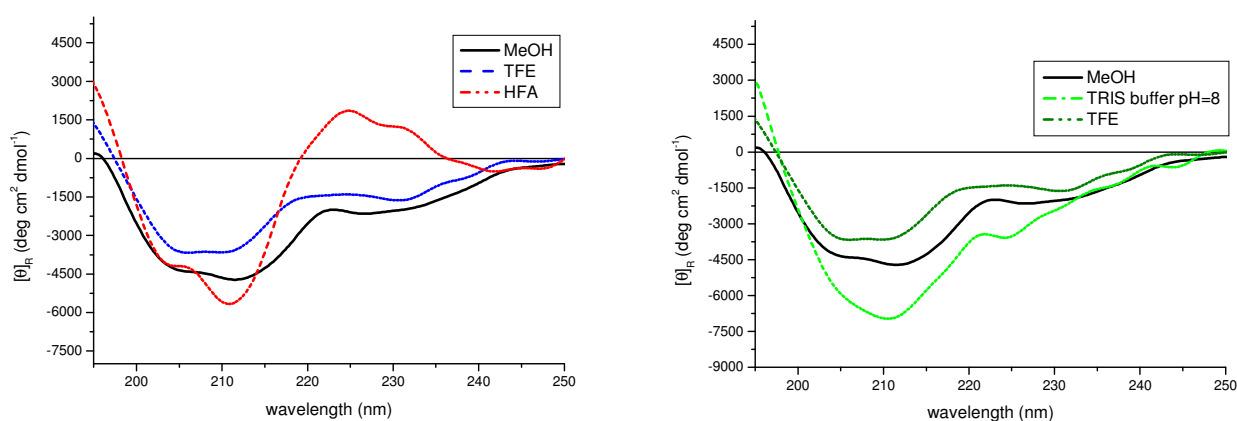


Figure 50. CD spectra of (–)-**7a** in different solvents.

In HFA the intensity of the negative band at 212 nm increases and a positive Cotton effect was observed around 224 nm (Figure 50). In water, under basic conditions, a negative Cotton effect at around 212 nm was seen to become more intense. While another band displaying a negative Cotton effect at around 224 nm was formed as shown in Figure 51.

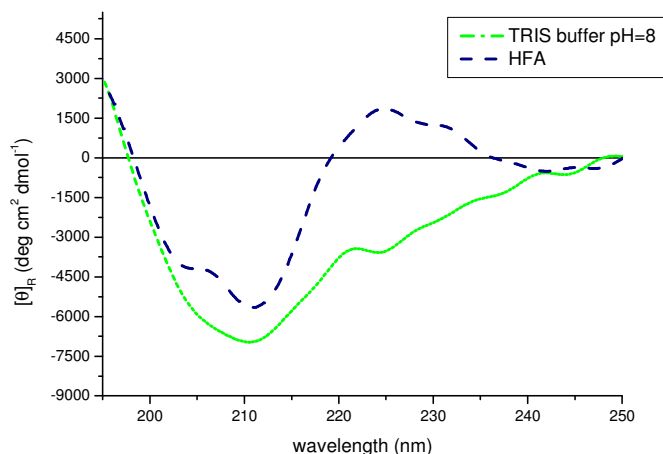


Figure 51. CD spectra of (–)-**7a** in water (pH=8) and in HFA.

The larger intensities of the CD spectra seen in HFA and in TRIS buffer could have been attributed to the presence of the phenylalanines. Different solvents could affect the solvation of the aromatic rings, possibly promoting aromatic ring stacking²⁹, and leading to different CD patterns.

Even for the β -peptides, a class which has been extensively studied, no clearly and unambiguously CD-“fingerprints” for certain secondary structure is yet possible.³⁰ A lot of work still has to be done in this area in order to achieve a complete understanding of the CD spectra of α -/ β -alternated peptides.

All CD spectra for peptide (–)-**7**, even if not shown, were recorded from 190 or 200 nm to 260 nm, depending on the solvents absorbance. The samples in methanol and in water at pH = 8.5 were also investigated in the near UV, from 260 to 300 nm and no bands could be detected in this part of the spectra.

The IR spectra of the Amide I region in methanol presented new absorptions at about 1675 cm^{-1} , compared to the spectrum found for the nonapeptide (–)-**6a** in the same solvent. The presence of an additional phenyl ring and the protonated amino functions of lysine could not affect this region, since the absorbance of these two groups are found at lower values.¹³ Therefore the absorbance at ca. 1675 cm^{-1} in the Amide I region could have arisen from the contributions of the conformationally unfolded N-terminus.

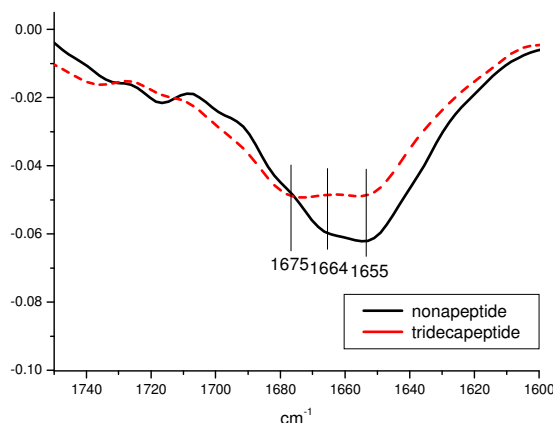


Figure 52. IR spectra in the Amide I region of the nonapeptide (—)-**6a** and the tridecapeptide (---)-**7a** measured in methanol.

¹ (a) Voigt, J.; Noltemeyer, M.; Reiser, O. *Synlett* **1997**, 202-204. (b) Bubert, C.; Cabrele, C.; Reiser, O. *Synlett* **1997**, 827-829. (c) Beumer, R.; Bubert, C.; Cabrele, C.; Vielhauer, O.; Pietzsch, M.; Reiser, O. *J. Org. Chem.* **2000**, *65*, 8960-8969.

² Zorn, C. *Dissertation*, Regensburg **2001**.

³ Meienhofen, J.; Waki, M.; Heimer, E. P.; Lambros, T. J.; Makofske, R. C.; Chang, C. D. *Int. J. Pept. Protein Res.* **1979**, *13*, 35-42.

⁴ Brahms, S.; Brahms, J. *J. Mol. Biol.* **1980**, *138*, 149-178.

⁵ Perczel, A.; Hollösi, M. in "Circular Dichroism and conformational Analysis of Biomolecules", Ed.: Fasman, G. D.; Plenum Press, New York, **1996**.

⁶ Greenfield, N.; Fasman, G. *Biochemistry*, **1969**, *8*, 4108.

⁷ Wüthrich, K. *NMR of Proteins and Nucleic Acids*, **1986**, New York: Wiley.

⁸ (a) Jiménez, M. A.; Nieto, J. L.; Rico, M.; Santoro, J.; Herranz, J.; Bermejo, F. J. *J. Mol. Struct.* **1986**, *143*, 435-438. (b) Zimmermann G. R.; Legault, P.; Selsted, M. E.; Pardi, A. *Biochemistry*, **1995**, *34*, 13663-13671.

⁹ Andersen, N. H.; Neidigh, J. W.; Harris, S. M.; Lee, G. M.; Liu, Z.; Tong, H. *J. Am. Chem. Soc.* **1997**, *119*, 8547-8561.

¹⁰ Pardi, A.; Billeter, M.; Wüthrich, K. *J. Mol. Biol.* **1984**, *180*, 741-751.

¹¹ Güntert, P.; Mumenthaler, C.; Wüthrich, K. *J. Mol. Biol.* **1997**, *273*, 283-298.

¹² Günter, P. *Quarterly Rev. Of Biophysics*, **1998**, *2*, 145-237.

¹³ http://www.imb-jena.de/ImgLibDoc/ftir/IMAGE_FTIR.html

¹⁴ (a) Gellman, S. H.; Dado, G. P.; Liang, G.-B.; Adams, B. R. *J. Am. Chem. Soc.* **1991**, *113*, 1164-1173. (b) Gellman, S. H.; Dado, G. P. *J. Am. Chem. Soc.* **1993**, *115*, 4228-4245.

- ¹⁵ (a) Tyndall, J. D. A.; Pfeiffer, B.; Abbenante, G.; Fairlie, D. P. *Chem. Rev.* **2005**, *105*, 793-826. (b) Marshall, G. R. *Biopolymers* **2001**, *60*, 246-277.
- ¹⁶ Martin, S. F.; Dorsey, G. O.; Gane, T.; Hiller, M. C.; Kessler, H.; Baur, M.; Marthä, B.; Erickson, J. W.; Bhat, T. N.; Munshi, S.; Gulnik, S. V.; Topol, I. A. *J. Med. Chem.* **1998**, *41*, 1581-1597.
- ¹⁷ Reichelt, A.; Gaul, C.; Frey, R. R.; Kennedy, A.; Martin, S. F. *J. Org. Chem.* **2002**, *67*, 4062-4075.
- ¹⁸ Martin, S. F.; Dwyer, M. P.; Hartmann, B.; Knight, K. S. *J. Org. Chem.* **2000**, *65*, 1305-1318.
- ¹⁹ Cheng, R. P.; Gellman, S. H.; DeGrado, W. F. *Chem. Rev.* **2001**, *101*, 3219-3232.
- ²⁰ Hayen, A.; Schmitt, M. A.; Ngassa, F. N.; Thomasson, K. A.; Gellman, S. H. *Angew. Chem. Int. Ed.* **2004**, *43*, 505-510.
- ²¹ Baldauf, C.; Hoffman, H.-J. unpublished results.
- ²² IR-investigation in solution of simple amides derived from β -ACC (CONEt₂ instead of CO₂Me, *N*-Ac instead of *N*-Boc indeed show complete intramolecular hydrogen bonding between CO and NH in *cis*-position. In contrast, the analogous β -alanine derivative does not show any hydrogen bonding, cf. G. P. Dado, S. H. Gellman, *J. Am. Chem. Soc.* **1994**, *116*, 1054.
- ²³ Dyson and Wright have established criteria by which partially folded shorter peptides can be identified (H.J. Dyson, M. Rance, R.A. Houghton, R.A. Lerner, P.E. Wright, *J. Mol. Biol.* **1988**, *201*, 161; H. J. Dyson, P.E. Wright, *Annu. Rev. Biophys. Biophys. Chem.* **1991**, *20*, 519).
- ²⁴ (a) Fan, P.; Bracken, C.; Baum, J. *Biochemistry*, **1993**, *32*, 1573-1582. (b) Sönnichsen, F. D.; Van Eyk, J. E.; Hodges, R. S.; Sykes, B. D. *Biochemistry*, **1992**, *31*, 8790-8798. (c) Luo, P.; Baldwin, R. L. *Biochemistry*, **1997**, *36*, 8413-8421.
- ²⁵ Gademann, K.; Jaun, B.; Seebach, D.; Perozzo, R.; Scapozza, L.; Folkers, G. *Helv. Chim. Acta* **1999**, *82*, 1-11.
- ²⁶ Brauner, J. W.; Flach, C. R.; Meldelsohn, R. *J. Am. Chem. Soc.* **2005**, *127*, 100-109.
- ²⁷ Sreerama, N.; Manning, M. C.; Powers, M. E.; Zhang, J.-X.; Goldenberg, D. P.; Woody, R. W. *Biochemistry* **1999**, *38*, 10814-10822.
- ²⁸ (a) Krittanai, C.; Johnson, W. C. Jr. *Anal. Biochem.* **1997**, *253*, 57-64. (b) Woody, R. W. *Eur. J. Biophys.* **1994**, *23*, 253-262.
- ²⁹ Salinas, R. K.; Shida, C. S.; Pertinhez, T. A.; Spisni, A.; Nakaie, C. R.; Paiva, A. C. M.; Schreier, S. *Biopolymers* **2002**, *65*, 21-31.
- ³⁰ Seebach, D.; Beck, A. K.; Bierbaum, D. J. *Chemistry & Biodiversity* **2004**, *1*, 1111-1239.

C. β -ACC units into Biologically Active α -Peptides

C.1 RGD-Analogues

C.1.1 Introduction

Cell adhesion is crucial for the three-dimensional tissue architecture of animals. The functional units mediating cell adhesion are multiprotein complexes arising by interaction of three general classes of proteins: the cell adhesion receptors, the extracellular matrix (ECM) proteins and the adhesion plaque proteins.¹

The cell adhesion receptors determine the specificity of cell-cell and cell-ECM recognition.² They are typically transmembrane glycoproteins that mediate binding to the components of the ECM or to counter-receptors on other neighboring cells. ECM proteins are usually large glycoproteins, including the collagens, fibronectins, laminins, and proteoglycans that assemble into fibrils or other complex macromolecular systems. The intracellular plaque proteins (or peripheral membrane proteins) provide structural and functional linkages between the adhesion systems and the cytoskeleton and transduce signals initiated on the cell surface by the adhesion receptors.¹

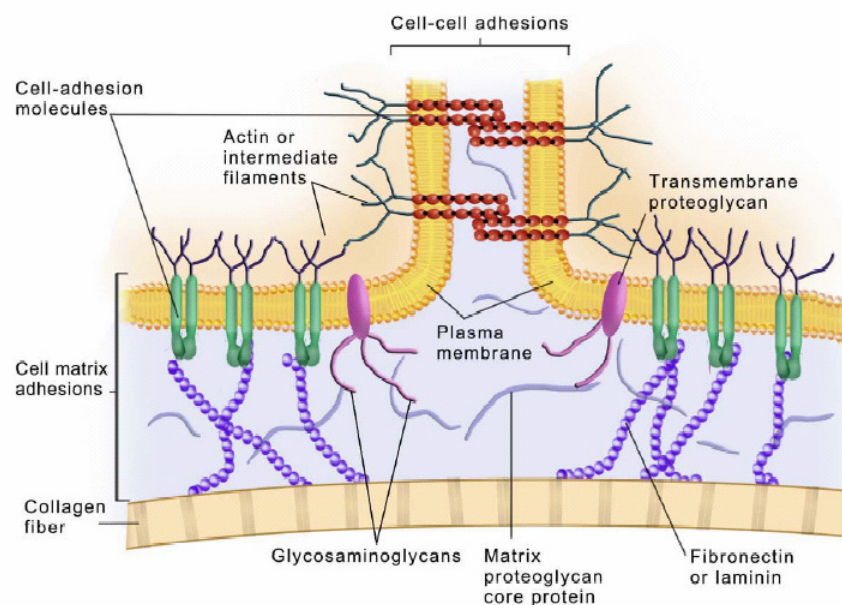


Figure 53. Overview of the macromolecular organization responsible for cell-cell and cell-matrix adhesions.³

Cell adhesion receptors include selectins, immunoglobulins, cadherins and integrins. In particular, integrins are involved in cell-cell adhesion processes and are the most important family of adhesion receptors that attach cells to their extracellular microenvironment.⁴ They are a class of heterodimeric transmembrane cell surface receptors made up of an α -subunit and a β -subunit. Each subunit presents a large extracellular domain, a single membrane-spanning region and, in most cases, a short cytoplasmatic domain.² Multiple combinations of the different 16 α - and 8 β -subunits lead to ligand binding specificity and different biological function of the distinct receptors.⁵ The α and β chains are both involved in ligand recognition. Common sequences in integrin ligands are found to be critical for the recognition by most integrins. A exposed aspartic acid or glutamic acid residue is required. Typical integrin-recognition are for example RGD, LDV, RDL and KQAGDV sequences (Table 12).⁶

Sequence	Integrin
RGD	$\alpha_5\beta_1$, $\alpha_8\beta_1$, $\alpha_v\beta_1$, $\alpha_v\beta_3$, $\alpha_v\beta_5$, $\alpha_v\beta_6$, $\alpha_v\beta_8$, $\alpha_{IIb}\beta_3$, $\alpha_2\beta_1$, $\alpha_3\beta_1$, $\alpha_4\beta_1$, $\alpha_7\beta_1$,
KQAGDV	$\alpha_5\beta_1$, $\alpha_{IIb}\beta_3$
LDV	$\alpha_5\beta_1$, $\alpha_4\beta_1$
RLD	$\alpha_v\beta_3$, $\alpha_M\beta_2$

Table 12. Some typical integrin-recognition sequence.

Each integrin can bind a number of divalent cations, including Ca^{2+} , Mg^{2+} and Mn^{2+} . Bound cations exert significant effects on integrin function. They can act as effectors, promoting ligand binding; as antagonists, inhibiting ligand binding or selectors, changing the ligand binding specificity. This influential role of the cations is explained by a probable sharing of a common binding pocket on the integrin with the ligand.⁷ The glutamic acid or aspartic acid in ligands form a ternary complex with the receptor-bound divalent cations.

The concentration of the divalent cations could have a regulation effect *in vivo*, given that Mg^{2+} and Mn^{2+} support physiological ligand binding at a broad range of concentrations while Ca^{2+} does so only at micromolar range. A millimolar concentrations of Ca^{2+} (as generally present in the plasma) is generally inhibitory for the integrin-ligand binding, increasing the rate of ligand dissociation.⁸ For example the adhesion of the osteoclast to the bone surface, mediated by $\alpha_v\beta_3$, must be tightly regulated to prevent excessive resorption. The regulation is controlled by the concentration of free Ca^{2+} , that increase beneath the osteoclast when mineralized bone is resorbed, inducing the detachment of the osteoclast with following cessation of resorption.⁷

Cell adhesion complexes are dynamic entities and are regulated by a two-way signaling system between the cell and its external environment.

Most integrins are present on the cell surface in the inactive form. Events within the cell can alter the conformation of the cytoplasmic domains. Conformational changes are then propagated through the molecule, increasing the integrin's affinity for an extracellular ligand. This "inside-out" regulation of integrin affinity protects the host from pathological integrin-mediated adhesion.⁴

Apart from cell-cell and cell-ECM recognition, integrins are involved in fundamental cellular processes such as migration, proliferation, differentiation and survival and contribute to the initiation and/or progression of many diseases including neoplasia, tumor metastasis, immune dysfunction and osteoporosis.⁹ They are implicated in an "outside-in" signaling allowing the transmission of signals from the external environment to the cell interior.⁴ In these cases the binding of a ligand to the receptor extracellular domain induces conformational changes at the cytoplasmic end altering the interaction of the integrin with the cytoplasmic proteins and a signal transduction cascade can be initiated.⁴

Integrins are involved in a variety of physiological and pathophysiological events and therefore are potential important pharmaceutical target. The integrin $\alpha_{IIb}\beta_3$, for instance, mediates the aggregation of platelet, antagonists to this receptor are effective antithrombotics. The $\alpha_2\beta_1$ is a receptor for collagen and laminin and it is required for the arrest of platelets under conditions of blood flow on the collagen fiber surface exposed as a consequence of injury.¹⁰ In particular, $\alpha_v\beta_3$ integrin is found to be involved in apoptosis, tumor growth, metastasis, control of bone density, and in general, α_v -integrins seems to be essential during angiogenesis and blood vessel formation and/or maturation in these tissues.^{11,12}

Recent studies have been focused the attention on anti-angiogenesis products as tumor treatment. When a solid tumor reaches a certain size and mass, it needs new blood vasculature to grow more, therefore it releases specific growth factors which stimulates the growth of new blood vessels. Several $\alpha_v\beta_3$ antagonists, such as Vitaxin¹³, a monoclonal antibody antagonist of $\alpha_v\beta_3$ now in Phase II, have been already found to perturb the growth and/or maturation of new blood vessels without detectably influencing the preexisting ones. In tumor models, not only tumor associated angiogenesis is blocked, but in some cases tumor regression is observed.¹¹

A schema of the integrin $\alpha_v\beta_3$ is outlined in Figure 54.

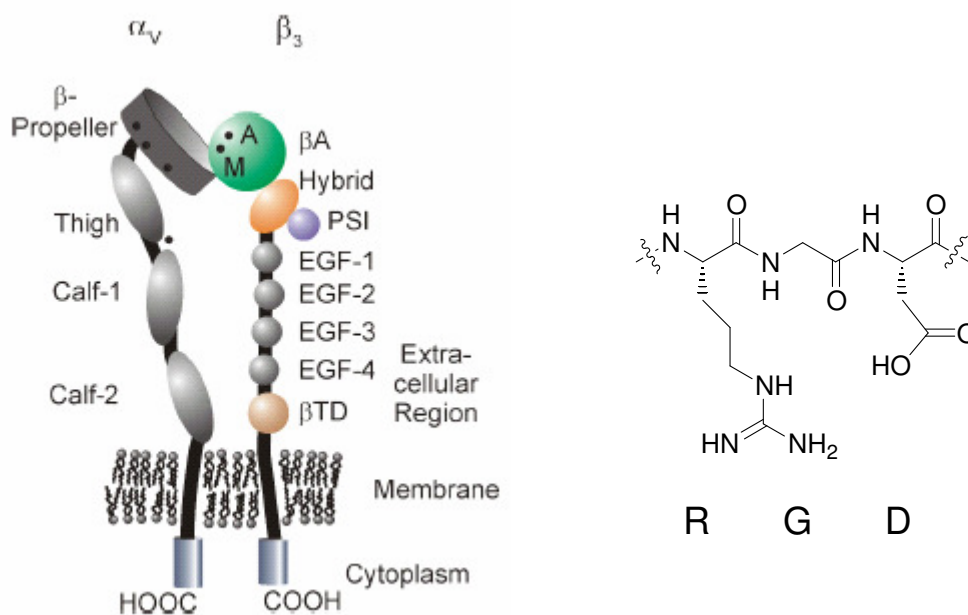


Figure 54. Schematic representation¹⁴ of the integrin dimer $\alpha_v\beta_3$ (left), and the formula of the RGD sequence (right).

Integrins are grouped into two classes based on the presence or absence of an extracellular A-type domain. This so called αA domain is involved in the ligand interaction. A metal ion is coordinated at the ligand-binding interface of αA through a conserved five amino acid motif, the Metal Ion-Dependent Adhesion Site (MIDAS), and the metal coordination is completed by the ligand. In αA -lacking integrins, ligand recognition requires an αA -like domain (βA) present in all integrin β subunits.¹⁵

The $\alpha_v\beta_3$ integrin is a αA -lacking integrin consisting of 12 domains assembled into a ovoid head and two “legs”.¹⁵

The tripeptide Arg-Gly-Asp is the most common sequence motif that is recognized by integrins. RGD-containing proteins that interact with integrins are for instance fibronectin, vitronectin, fibrinogen, von Willebrand factor, thrombospondin, laminin, entactin, tenascin, osteopontin, bone sialoprotein and, under some conditions, collagens.⁶ Interestingly the RGD sequence is also used by bacteria, viruses and yeasts to get into the host cell.¹⁶

The orientation of the Arg and Asp side chains and of the amide groups adjacent to Gly plays an important role for the recognition. The protein places conformational constraints on the pharmacophoric group Arg-Gly-Asp leading to the distinct orientation of the functional groups.¹⁷

The crystal structure¹⁵ of the extracellular segment of $\alpha_v\beta_3$ in complex with a RGD ligand, the pentapeptide c(Arg-Gly-Asp-D-Phe-N(Me)Val), reveals that the ligand is in a crevice

between the propeller and β A domain on the integrin head. Each residue of the RGD sequence participates extensively in the interaction. The Arg and Asp side chains point in the opposite directions, exclusively contacting the propeller and β A domain, respectively. The remaining two residues face away from the $\alpha\beta$ interface. Tertiary and quaternary changes in the integrin structure are observed. The “liganded” structure, compared to the “unliganded” one, held two Mn^{2+} more. One is in the MIDAS and the second one is near the MIDAS, into the so called Ligand-Associated Metal Binding Site (LIMBS). The coordination sphere for LIMBS does not exist in the “unliganded” complex. LIMBS does not contact directly the ligand but adds conformational stability and structural rigidity to the ligand-binding surface.¹⁵

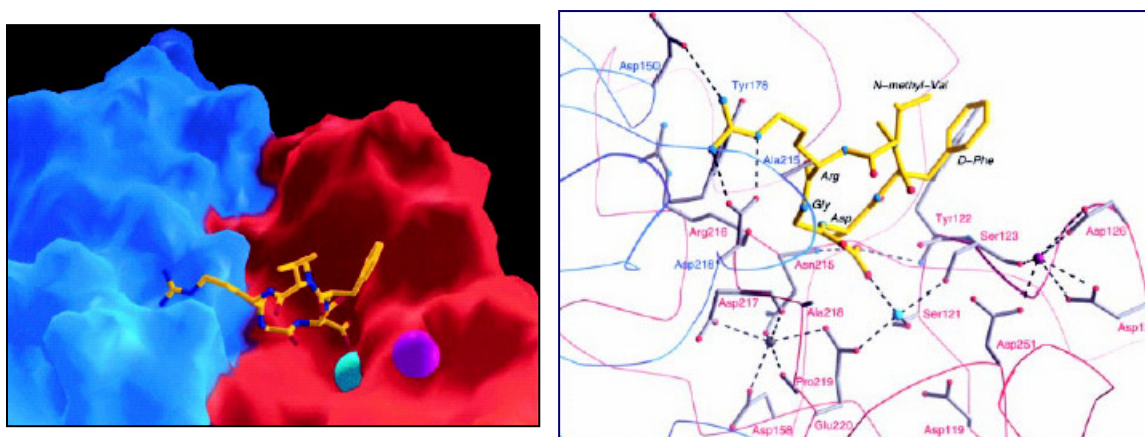


Figure 55. The ligand-integrin binding site from ref. 15. Left: surface representation of the ligand-binding site with the ligand peptide shown as ball-and-stick model in yellow. Right: the interactions between ligand and integrin. α V and β 3 residues are labelled blue and red, respectively. The Mn^{2+} ions in β 3 at MIDAS and LIMBS are shown as cyan and grey, respectively.

The finding that short RGD containing peptides could lead to the same effect observed with large ligands has intensified the search for selective small molecules as pharmacological tools. In linear peptides, the nature of residues flanking the RGD sequence highly influences receptor affinity and receptor selectivity, especially on the C-terminal side.⁶

However, cyclic peptides are generally much more potent and more specific than their linear counterparts. The cyclization induces a specific conformation on the RGD sequence leading to higher receptor specificity.¹⁶

Several cyclic RGD peptides were synthesized in the last years as fibrinogen receptor ($\alpha_{\text{IIb}}\beta_3$) antagonists or as $\alpha_v\beta_3$ integrin antagonists for treatment of human tumors, bone remodelling, osteoporosis, diabetic retinopathy or acute renal failure.¹⁶

The conformational preferences of a D-amino acid in cyclic peptides consisting of L-amino acids allowed the synthesis of biological active analogues. The hexapeptide c(Arg-Gly-Asp-D-Phe-Val-Gly) efficiently inhibits the binding of fibrinogen to the integrin $\alpha_{IIb}\beta_3$, while the cyclic pentapeptide c(Arg-Gly-Asp-D-Phe-Val) led to nanomolar IC₅₀ values at $\alpha_V\beta_3$ integrin.¹⁸ Kessler *et al.* further investigated the latter peptide by creating the retro-inverso isomers or by introducing the corresponding N-methylated amino acids.^{17,19} The N-methylation scan led to the peptide c(Arg-Gly-Asp-D-Phe-N(Me)Val) with biological activity in the subnanomolar range and increasing metabolic stability, being currently in clinical studies as drug against Kaposi's sarcoma, brain tumors and solid tumor by Merck KGaA, Darmstadt.

Recently, it was also found that a selective inhibition of the integrin receptors $\alpha_V\beta_3$ and $\alpha_V\beta_5$ through an antagonist such as c(Arg-Gly-Asp-D-Phe-Val) is able to inhibit retinal pigmented epithelial (RPE) cell attachment, migration and invasion.²⁰ These steps are important for the progression of proliferative vitreoretinopathy (PVR) suggesting the use of cyclic integrin antagonists as possible treatment of this disease.

Structure activity relationship studies on RGD peptides suggest that the interaction with $\alpha_V\beta_3$ integrin requires a kinked structure of the RGD fragment compare to a more stretched structure required from the $\alpha_{IIb}\beta_3$ integrin. Many cyclic peptides display a high selectivity to the vitronectin receptor if the RGD fragment occupies the positions i to $i+2$ of a regular γ -turn.

The tetrapeptide c(Arg-Gly-Asp-D- β -hPhe) synthesized by Sewald *et al.* is a selective $\alpha_V\beta_3$ antagonist and the β -amino acid acts as a pseudo γ -turn inducer.²¹

Nevertheless, the difference between the binding conformations for the $\alpha_{IIb}\beta_3$ or $\alpha_V\beta_3$ integrin receptors is probably very small.¹⁷ The introduction of the β -turn mimic dipeptide isosteric pyranoid δ -SAA in the peptide **22** (Figure 56) led to a loss of selectivity. The peptide shows good affinity to both $\alpha_{IIb}\beta_3$ and $\alpha_V\beta_3$ integrins probably due to a more flexible structure that is able to assume both binding conformations for the two different receptors.²²

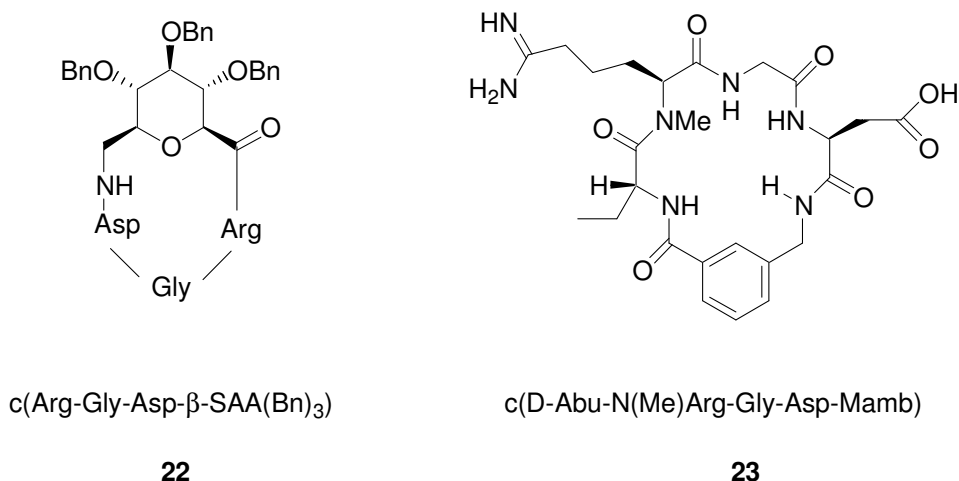


Figure 56. Formula of the peptide c(Arg-Gly-Asp- β -SAA(Bn)₃) containing a sugar amino acid unit and of the $\alpha_{IIb}\beta_3$ antagonist c(D-Abu-N(Me)Arg-Gly-Asp-Mamb).

The peptide c(D-Abu-N(Me)Arg-Gly-Asp-Mamb) shown in Figure 56 has a high affinity to $\alpha_{IIb}\beta_3$ integrin receptor.²³ Conformational investigation found a type II' β -turn centered at the D-Abu-N(Me)Arg dipeptide as expected for a dipeptide consisting of a D-amino acid followed by a N^α -methylamino acid. Replacement of the D-Abu-N(Me)Arg dipeptide with L-Ala-L-Arg or L-Pro-L-Arg resulted in a striking reversal of the selectivity.²⁴ These peptides have high affinity and selectivity to $\alpha_V\beta_3$ and NMR investigation evidences a shift from a type II' to a type I β -turn centered at the dipeptide L-Ala-L-Arg or L-Pro-L-Arg. The spatial relationship of the Arg and Asp side chains in the $\alpha_V\beta_3$ antagonist resulted in a closer approach compared to a $\alpha_{IIb}\beta_3$ integrin ligand even if the Arg-Gly-Asp segment does not occupy a regular γ -turn.

In Table 13 are summarized the IC₅₀ values of some integrin active peptides found in literature.

Peptide	Sequence	$\alpha_{IIb}\beta_3$	$\alpha_V\beta_3$
		IC ₅₀ (nM)	IC ₅₀ (nM)
24	c(Arg-Gly-Asp-D-Phe-N(Me)Val)	860	0.58
25	c(Arg-Gly-Asp-D- β -hPhe)	>300	63
22	c(Arg-Gly-Asp- β -SAA(Bn) ₃)	13.4	25
23	c(D-Abu-N(Me)Arg-Gly-Asp-Mamb)	2	500
26	c(L-Ala-Arg-Gly-Asp-Mamb)	18000	20
27	c(L-Pro-Arg-Gly-Asp-Mamb)	45000	13

Table 13. IC₅₀ values of some integrin active peptides found in literature.

C.1.2 RGD peptides containing β -ACC units

Different building blocks were used to induce the spatial requirements of the pharmacophore RGD with the aim to yield high affinity and selectivity to integrin receptors. α -Amino acids such as proline, D-amino acids, *N*-methylated analogues and other structures, such as sugar amino acids, β -, γ -, δ - amino acids etc. were introduced.

Accordingly, with the promising results obtained with the cyclopeptide c(Arg-Gly-Asp-(\pm)- β ACC-Val) containing β -ACC¹⁴ as racemate, the corresponding peptides with the enantiomerically pure β -ACCs were synthesized and tested in collaboration with the group of Prof. Sewald at the University of Bielefeld.

The β -ACC units were introduced as dipeptide building blocks Fmoc-Asp(O^tBu)- β -ACC-OH on the solid phase. Using the 2-chlorotrityl chloride resin the protected linear precursors were obtained. The peptides were then cyclized in solution under pseudo high dilution conditions using a dual syringe pump to avoid dimerization.²⁵ After cleavage of the side chain protecting groups the peptides were purified by RP-HPLC and characterized using MALDI-TOF MS and NMR techniques.

The biological activity of the peptides was investigated choosing the cyclic pentapeptide c(Arg-Gly-Asp-D-Phe-Val) as reference. Table 14 summarizes the results obtained measuring the ability of the RGD peptides to inhibit the binding of vitronectin to the $\alpha_v\beta_3$ integrin receptor expressed on human melanoma skin cells.

<i>Peptide</i>	<i>Sequence</i>	$\alpha_v\beta_3$ IC ₅₀ (nM)
(-)- 28	c(Arg-Gly-Asp(-)- β ACC-Val)	630
(+)- 28	c(Arg-Gly-Asp(+)- βACC -Val)	21
29	c(Arg-Gly-Asp-D-Phe-Val)	197

Table 14. Biological results obtained with cyclic peptides containing β -ACC units using human melanoma skin cells and vitronectin.

Combining their conformational bias and their already mentioned proteolytic stability, β -amino acids are potential interesting building blocks to create small bioactive α -peptide analogues with a predictable conformation.

Different non cyclic β -amino acids incorporated by *Sewald et al.* into cyclic peptides act as a turn mimetic, adopting a pseudo γ -turn conformation.²¹ The dipeptide *R*-nipecotic acid-*S*-nipecotic acid incorporated into an enzyme mimic in the position of a β -turn is able to mimic the β -turn maintaining unchanged the enzyme activity.²⁶ 2-Amino cyclohexane carboxylic acids into cyclic penta- and hexapeptides are found in pseudo γ -turn conformation but also in β -turns, in particular the *cis*-stereoisomer is predominantly found in the position *i* of different β -turns.²⁷

As already described in the Chapter B, β -ACC units have been found to induce helical conformations in peptides containing more than one β -ACC units in an alternated mode. The conformational preference induced by a single β -ACC moiety in an α -peptide, especially in cyclic peptides, is still under investigation.

NMR investigations on the most active peptide (+)-**28** show the Arg-Gly-Asp segment in the positions *i* to *i*+2 of a type II' β -turn in which the (+) β -ACC moiety occupies the position *i*+3 (Figure 57).

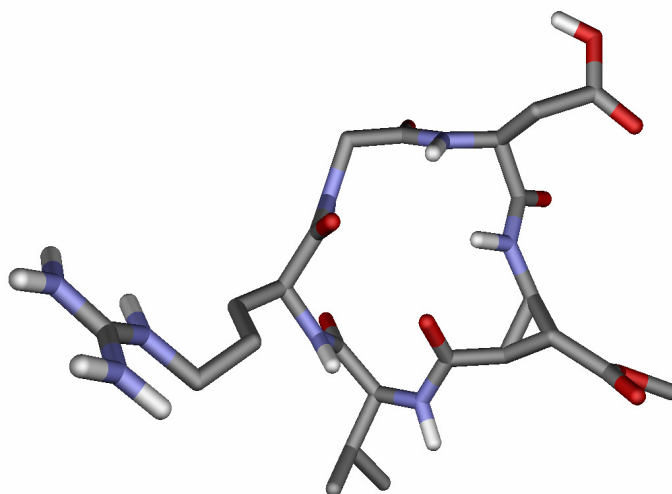


Figure 57. NMR structure found for the peptide (+)-**28**.

Further work is currently in progress to explore the selectivity of the β -ACC containing RGD peptides for their possible use as pharmacological tools and to further investigate the conformational bias of β -ACCs. Further knowledge could probably establish general principles for their application as a building block able to induce a reproducible conformation in small cyclic α -peptides analogues.

C.2 Conformational investigation on a β -ACC containing NPY analogue

C.2.1 Introduction

Neuropeptide Y (NPY) is one of the most abundant neuropeptide in the brain and was first isolated in the porcine brain.²⁸ It is a member of a peptide family consisting of NPY, peptide YY (PYY) and pancreatic polypeptide (PP). All three peptides consist of 36 residues, have a high content of tyrosine residues and are C-terminally amidated. PP and PYY are mainly synthesized and released by intestinal and pancreatic cells. NPY is localized in the nervous system, high level are detected in the cerebral cortex. Peripherally, it is abundant in the sympathetic nervous system and it is also expressed in liver, heart spleen and in endothelial cells of blood vessels.²⁹

hNPY	YPSKPDNPGEDAPAEDMARYYSALRHYNLITRQRY-NH ₂
hPYY	YPIKPEAPGEDASPEELNRYYSALRHYNLITRQRY-NH ₂
hPP	APLEPVYPGDNATPEQMAQYAADLRRYINMLTRPRY-NH ₂

Figure 58. Amino acid sequences of human NPY (hNPY), human peptide YY (hPYY), and human pancreatic polypeptide (hPP).

PP has found to have a hairpin-like three-dimensional structure (Figure 59, right), the so called PP-fold. A type II β -turn connects a polyproline-like type II helix (residues 1 to 9) to an amphiphilic α -helix (residues 14 to 30). The C-terminal end is a flexible turn projecting away from the hairpin loop.³⁰

Based on the high sequence homology, this secondary structure was assumed to be common to the whole NPY family peptides.

Although NPY is thought to be entirely monomeric at physiological conditions, recent NMR studies show a dimeric NPY structure at high concentrations, in which the C-terminal part of the peptide (residues 14-36) adopts an α -helical conformation which is stabilized in the dimer by intermolecular hydrophobic interactions and there is no polyproline helix on the N-terminus. Decrease of the concentration shift the dimerization equilibrium towards the monomeric form of NPY in which the N-terminus remain unfolded (residues 1-13).³¹ In Figure 59 a comparison between the two structures is shown.

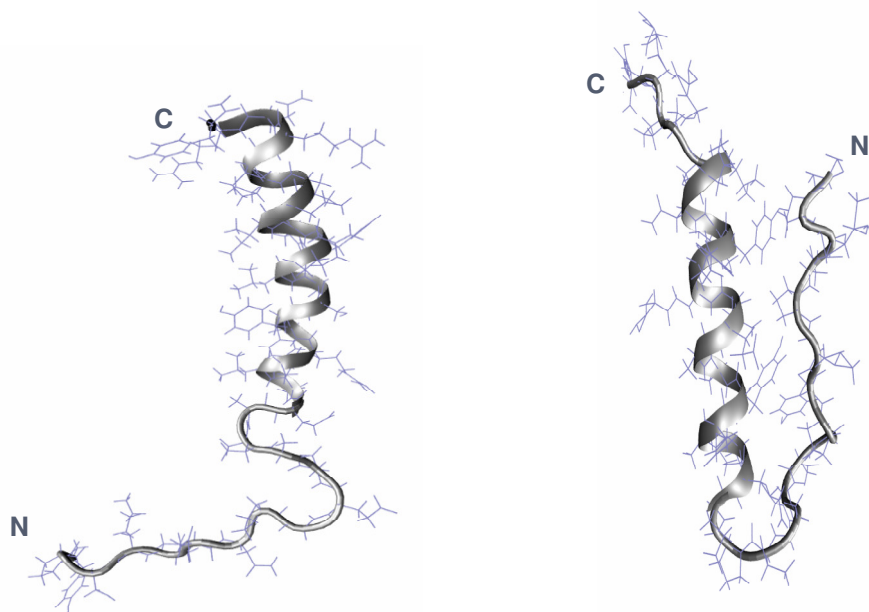


Figure 59: Comparison of structures of NPY (left) bound to micelles and the typical PP-fold (right) of the bovine pancreatic polypeptide.³²

NPY performs its biological activity through the interaction with different heptahelical G-protein-coupled receptors, the so called Y receptors that belong to a rhodopsin like superfamily (class 1) of G-protein-coupled receptors.

Five distinct subtypes of NPY receptor have been cloned in mammals, Y₁, Y₂, Y₄, Y₅ and y₆. These can be sorted into three distinct subfamilies based upon their degree of amino acid sequence identity. The subfamilies are Y₁, Y₂ and Y₅ from their first member. These three receptors differ more from each other than any other G-protein-coupled receptors that can respond to the same peptide ligand. The Y₁ subfamily includes the Y₁, Y₄ and y₆.³³ An additional putative receptor Y₃ has been pharmacologically described but it has not been cloned and no specific agonists and antagonists are known. In primates the y₆ receptor has not been found although its mRNA is present in several human tissues. Its gene may have become non functional during evolution.³⁴

NPY and PYY have high affinity to Y₁, Y₂ and Y₅ receptor subtypes, the Y₄ is the PP-preferring receptor.³⁵

NPY is able to bind equally potently different receptor subtypes. The conformation of the peptide is probably enough flexible to allow more than one energetically favourable structure induced by different receptors, and it is likely that at concentrations at which hNPY is found to be active *in vivo*, it adopts the monomer form with the PP-fold required for the receptor interaction.³⁶

NMR investigations on NPY in the presence of micelles, produced with the predominant phospholipid in animal cell membranes, the zwitterionic detergent phosphatidylcholine, show that the NPY could interact with the cell membrane before the receptor recognition.^{37,38} NPY associates to DPC-micelles mainly through hydrophobic interactions which stabilized the α -helical conformation at the C-terminus of the monomer. The N-terminus remains flexible and does not interact with the micelles (Figure 59, left).

The pre-adsorption of the ligand to the cell membrane increases the effective peptide concentration in vicinity of the receptor and special conformations may be induced. Through two-dimensional diffusion on the cell membrane surface the peptide will be recognized from the receptor. In the case of NPY it is so far unclear how the secondary and the tertiary structure change into the bioactive conformation for the interaction to the corresponding receptor subtype.

	Y₁	Y₂	Y₄	Y₅
Preferred endogenous ligand	NPY, PYY	NPY, PYY, NPY(3-36), PYY(3-36)	PP	NPY, PYY, NPY(3-36), PYY(3-36)
Expression profile	Cerebral cortex, thalamus, brain stem, smooth muscle of blood vessels	Hippocampus, brain stem nuclei, hypothalamus, gastrointestinal tract, smooth muscle of blood vessels	Colon, small intestine, prostate, very low in brain, paraventricular hypothalamus, interpeduncular nucleus	Hippocampus, plexiform cortex of the olfactory bulb, suprachiasmatic and arcuate nuclei
Physiological function	Vasoconstriction, regulation of food intake, anxiety-related behaviours, regulation of transmitter release, circadian rhythms	Inhibition of glutamate release, inhibition of noradrenaline release, learning and memory, circadian rhythms	Possible in regulation of LH secretion	Possible regulation of food intake, circadian rhythms

Table 15: Binding preferences, distribution and physiological functions of the NPY human-receptors. Adapted from ref. 39.

NPY is involved in several physiological functions including stimulation of feeding, regulation of blood pressure, anxiety and related behaviours, stress, depression, circadian rhythms, memory and learning processes.⁴⁰

It is not fully clear yet, which NPY receptor subtype regulate each function. Tabelle 15 summarizes physiological functions of the NPY human-receptors.

Studies using selective agonists and antagonists and knockout mice suggest that Y_2 receptor subtype facilitate learning and memory⁴¹, it is involved in energy homeostasis, in body weight regulation,⁴² it may play a role in the regulation of bone formation⁴³, and it play an important role in diabetic retinopathy and retinal neovascularization.⁴⁴

About physiological roles of the Y_4 receptor subtype there are limited informations. It is probably involved in LH secretion⁴⁵ and it may inhibit reproductive function.⁴⁶

The Y_5 subtype can play a key role in regulating energy homeostasis. A chronic activation of this subtype produces hyperphagia and obesity probably due to metabolic changes.⁴⁷ [D-Trp³⁴]NPY and [Ala³¹, Aib³²] NPY, that are selective for this receptor subtype, shown that Y_5 is also involved in feeding behaviour.⁴⁸ The Ala-Aib substitution induced a 3₁₀-helical turn at the C-terminus which seems to be the key motif for Y_5 selectivity.

The Y_1 receptor subtype was the first Y receptor cloned.⁴⁹ Strong evidences support the involvement of the NPY Y_1 receptor subtype in the regulation of blood pressure, regulation of anxiety, and in feeding behaviour.^{50,51} Y_1 antagonists might be useful for treatment of obesity.⁵²

Moreover recent investigations showed that the Y_1 and Y_2 subtypes can play an important role in different tumors.⁵³

Y_1 receptor subtype is expressed in breast carcinomas, moreover the addition of NPY to Y_1 -expressing human SK-N-MC tumor cells inhibit the cell growth suggesting a potential antiproliferation effect of NPY mediated by Y_1 subtype receptor.⁵⁴ NPY receptors are therefore potential new molecular target for diagnosis and therapy of several cancers, and specifically radiolabelled NPY analogues could be used as tumor imaging agents.⁵⁵

[Arg⁶,Pro³⁴]-pNPY show a good affinity and selectivity to the Y₁ subtype.⁶⁰ Also the substitution with the corresponding D-amino acid at either position 25 or 26 of NPY, [D-Arg²⁵]-NPY, [D-His²⁶]-NPY and the shorter cyclic Pro³⁴-analogue Des-AA¹¹⁻¹⁸[Cys^{7,21}, D-Lys⁹(Ac), D-His²⁶, Pro³⁴]-NPY, results in good selectivity.⁶¹

The cyclic peptide c[D-Cys²⁹-L-Cys³⁴]NPY Ac-29-36, that mimic the C-terminal part of hNPY, exhibit high affinity and selectivity for the Y₁ subtype showing that the lack of the N-terminal part of the NPY is not required, as previously thought, at least for the binding to this subtype (Figure 61).⁶²

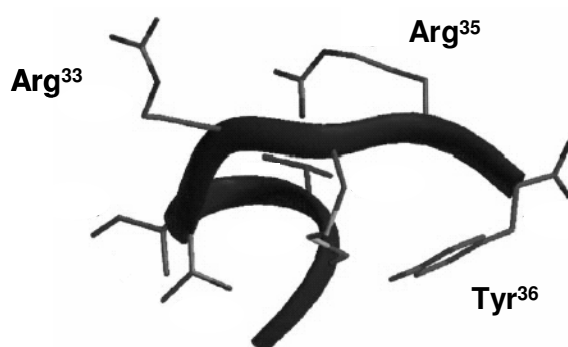


Figure 61. The modelled structure for the cyclic peptide c[D-Cys²⁹-L-Cys³⁴]NPY Ac-29-36, that mimic the C-terminal part of hNPY, exhibit high affinity and selectivity for the Y₁ subtype. Adapted from Ref.62.

C.2.2 NPY analogues containing β -ACC units

The introduction of a (+)- β ACC moiety leads to dodecapeptide NPY analogues that present high selectivity to the Y_1 receptor subtype. The two enantiomers of β -ACC were introduced in the C-terminus (residues 25-36) of the NPY in position 32 and/or 34.⁶³ Depending on the position of the substitution and the absolute configuration of the respective β -ACC derivate, these short NPY analogues present good affinity and good selectivity to the Y_1 receptor subtype. Table 16 reports the most active peptides found.

Peptide	Sequence	Y_1	Y_2 K_i (nM)	Y_5	Selectivity $Y_1:Y_5$
34	NPY ^a	0.52(\pm 0.02)	0.23(\pm 0.02)	2.21(\pm 0.03)	1:2
35	Ac-RHYINLITRQRY-NH ₂	>1000	21	>1000	N/A
36	Ac-RHYINL-IT-R \blacktriangle RY-NH ₂	37(\pm 20)	>1000	724	1:20
37	Ac-RHYINL-IT-R \blacktriangledown RY-NH ₂	>1000	>1000	>1000	N/A
38	Ac-RHYINLI \blacktriangle RQRY-NH ₂	>1000	>1000	>1000	N/A
39	Ac-RHYINLI \blacktriangledown RQRY-NH ₂	>1000	>1000	>1000	N/A
40	Ac-RHYINL-I \blacktriangle -R \blacktriangle RY-NH ₂	50(\pm 10)	>1000	617	1:12
41	Ac-RHYINL-R \blacktriangle -R \blacktriangle RY-NH ₂	29(\pm 13)	>1000	118	1:4

Table 16. Representative β -ACC containing NPY analogues (where \blacktriangle =(+) β -ACC; \blacktriangledown =(-) β ACC) tested by Koglin *et al.*⁶³ (^a Data from Ref. 64)

The truncated peptide **35**, having the native sequence of NPY, shows no affinity for Y_1 or Y_5 . The replacement of a single residue, in position 34, with (+)-configured β -ACC (peptide **36**) leads to a nanomolar biological affinity at the Y_1 -receptor with high selectivity. The absolute configuration of the β -ACC moiety plays a crucial role in the affinity since the peptide **37** with the (-)-configured β -ACC in the same position is biologically inactive. The substitution with β -ACC only in position 32 (peptides **38** and **39**) are inactive in both configurations, identifying the introduction of a turn-inducing residue in position 34 as crucial for selectivity at the Y_1 -receptor. The introduction of two (+)-configured β -ACC moieties, in positions 32 and 34, (peptide **40**) leads to significant affinity for Y_5 , probably due to a more helical conformation on the C-terminus, a structural feature being found in α -, β -peptide sequences, with cyclic β -amino acids⁶⁵ and especially with β -ACC residues, as described in Chapter B. As seen with peptide **41**, a successive replacement of the Ile³¹ with

arginine increases further the Y₅ affinity probably due to a new ionic interaction of the arginine side chain with the Y₅ receptor.

Accordingly, the conformation of the most selective of these NPY analogues which contain the (+)-configuration β -ACC-moiety in position 34 (Figure 62) was investigated in water in the presence of dodecylphosphocholine micelles as a model of the cell membrane using NMR spectroscopy.⁶⁶

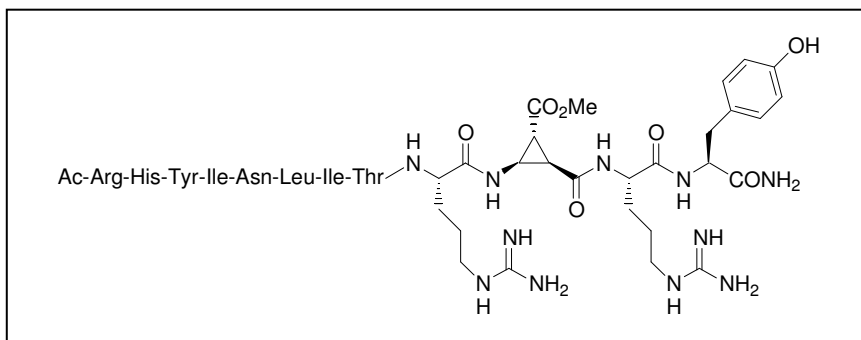


Figure 62. NPY analogue containing (+) β -ACC, peptide **36**, synthesized and investigated.

The determination of the conformation in the presence of a membrane mimetic reveals information about the secondary structure of the membrane-bound species that is recognized by the receptor.

The peptides was synthesized by solid-phase technique on Rink amide resin by using the orthogonal Fmoc/*t*Bu strategy. The enantiomeric pure (+)- β -ACC was introduced in the growing peptide chain as dipeptide building block Fmoc-Arg(Pmc)-(+)- β -ACC-OH, (+)-**18a**, after activation by manual coupling as described by *Koglin et al.*⁶³ The subsequent elongation was achieved by automated coupling steps. After cleavage from the resin and removal of the protecting groups by using TFA, the peptides were purified by preparative HPLC on a RP C-18 column. The peptide was analyzed by MALDI-TOF mass spectrometry, which confirmed the intact cyclopropyl ring system, and by analytical reversed phase HPLC.

The NMR assignments were made according to the sequence-specific sequential resonance assignment procedure as described in Chapter B, using COSY, TOCSY and NOESY experiments with the support of the XEASY software package.⁶⁷

The one-dimensional NMR spectrum of (+)- β -ACC³⁴-NPY (25-36) displays good dispersion of amide proton chemical shifts indicating that the peptide is folded to some extent.

residue	NH	CH _{α}	CH _{β}	CH _{γ}	CH _{δ}	others
Arg ¹	8.98	3.86	2.14	1.83; 1.68	3.20	
His ²	7.53	4.34	2.79			
Tyr ³	7.54	4.25	2.92; 3.03			7.01; 6.86
Ile ⁴	7.71	3.79	1.97	1.62; 1.25		
			γ CH ₃ 0.94	δ CH ₃ 0.87		
Asn ⁵	7.97	4.50	2.79			γ NH ₂ 6.85
Leu ⁶	7.60	4.14	1.94; 1.78	1.61	0.96; 0.88	
Ile ⁷	7.58	4.10	2.08	1.71; 1.32		
			γ CH ₃ 1.00	δ CH ₃ 0.89		
Thr ⁸	7.88	4.35	4.09	CH ₃ 1.24		
Arg ⁹	7.80	4.22	1.91; 1.82	1.68		
β -ACC ¹⁰	8.04	3.58	2.51	2.70		CH ₃ 3.72
Arg ¹¹	8.36	4.32	1.70; 1.62	1.48	3.15	
Tyr ¹²	8.16	4.47	3.03; 2.81			7.06; 6.76

Table 17. Chemical shifts found at 310K, referenced to the water signal at 4.63 ppm.

In the segment encompassing residues His² to β -ACC¹⁰ sequential contacts between amide protons are present in the 2D NOESY spectrum, suggesting a helically folded conformation. The helical conformation is supported by a series of medium-range *i,i+2* and *i,i+3* NOE contacts. Although the structure is not well-defined enough to unambiguously define the type of helix the absence of *i,i+4* contacts suggests it to be a 3_{10} -helix rather than an α -helix. No *i,i+1*-H ^{α} -H ^{α} peaks are observed throughout the sequence indicating the absence of *cis*-amide bonds, in particular for the Arg— β -ACC amide bond. Figure 63 summarized the sequential and medium-range NOEs found.

The incorporation of the β -ACC moiety is still compatible with a turn of a helical conformation in the segment comprising Arg33 and Arg35, two residues believed to be directly involved in forming contacts with the receptor.

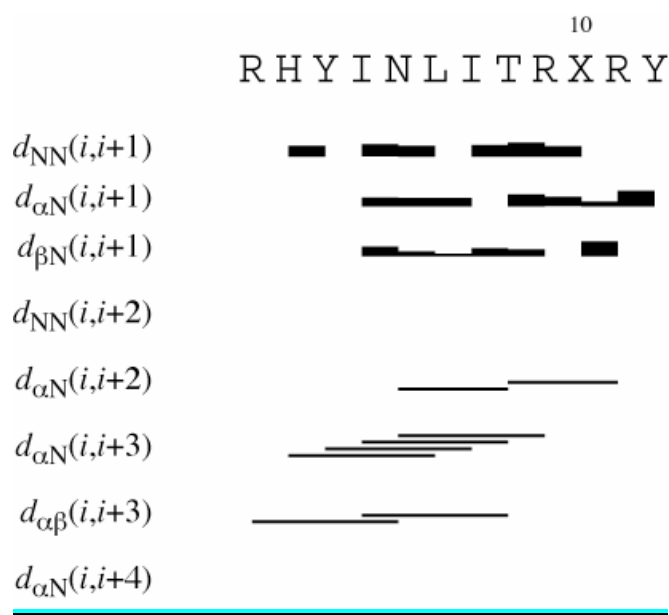


Figure 63. Summary of sequential and medium-range NOEs for β -ACC³⁴-NPY (25-36) measured in the presence of DPC micelles, (where X = (+) β -ACC). The thickness of the lines is proportional to the integral value in the NOESY spectrum.

From the NOESY data, using the program DYANA, the 20 structures with the lowest target function values were selected to present the NMR ensemble. The residue-specific atomic root-mean-square deviations (RMSD) for the backbone heavy atoms were 0.89 ± 0.36 Å for the Arg¹-Tyr¹² peptide and 0.35 ± 0.17 Å for the 3_{10} helical Ile⁴-Arg⁹ segment.

The NMR ensemble reveals backbone dihedrals compatible with a helical conformation between Arg¹ and ACC¹⁰ (Figure 64). Hydrogen bonds are present in the majority of computed structures corresponding to $i,i+3$ NH \rightarrow CO hydrogen bonds for carbonyl atoms of residues 3,4 and 6. At the C terminus around the ACC residue no fixed H bond is observed. However, amide protons of both residues of Tyr¹² and ACC¹⁰ need to be only slightly shifted in position to form hydrogen bonds to the carbonyl of Ile⁷ resulting in 10 or 17 membered rings. Considering the increased RMSD in the C-terminal segment Ile⁷ to Tyr¹² (1.21 ± 0.5 Å) it is possible that the CO of Ile⁷ is forming time-shared hydrogen bonds to both amide protons of ACC¹⁰ and Tyr¹².

Peptide	Contacts		Contacts	
36	2 Arg+ HA	5 Ile HB	5 Ile QG1	7 Leu QGD
	2 Arg+ QB	4 Tyr HN	6 Asn HA	8 Ile HN
	2 Arg+ QB	4 Tyr QD	6 Asn HA	9 Thr HN
	2 Arg+ QB	4 Tyr QE	8 Ile HN	12 Arg+ QB
	3 His+ HA	6 Asn HN	8 Ile HA	12 Arg+ QB
	4 Tyr HA	7 Leu HN	8 Ile HB	12 Arg+ QB
	4 Tyr QD	7 Leu QD1	8 Ile QG2	10 Arg+ HN
	4 Tyr QD	7 Leu QD2	8 Ile QG2	11 ACC HN
	4 Tyr QD	7 Leu QGD	8 Ile QG2	11 ACC HG
	4 Tyr QE	7 Leu QD1	8 Ile QG2	12 Arg+ QB
	4 Tyr QE	7 Leu QD2	8 Ile QG1	12 Arg+ QB
	5 Ile HA	8 Ile HN	8 Ile QD1	12 Arg+ QB
	5 Ile HA	8 Ile HB	9 Thr HA	11 ACC HN
	5 Ile HA	8 Ile QG2	11 ACC HG	13 Tyr QE

Table 18. Non-sequential restraints used for the structure calculation. In the table, A= α ; B= β , G= γ , D= δ , E= ϵ . The letter Q instead of H is used when there is a signal due to more than one hydrogen and it is not possible to distinguish between them, for example in the presence of a CH₂ in the β position of Arginine. QQ is used in the case of two CH₃ as for example in Leucine when it is not possible to distinguish them in the NMR spectra.

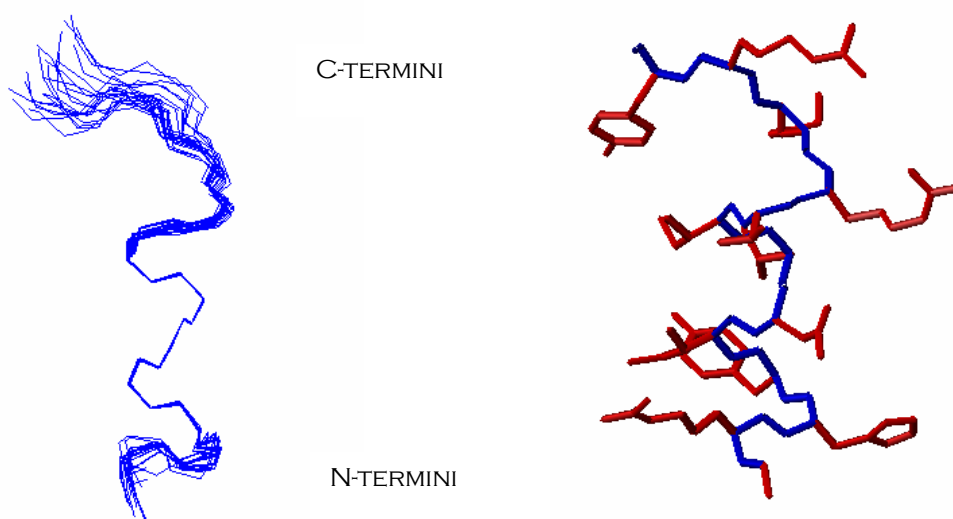


Figure 64. Superposition of low-energy conformers of (+) β -ACC³⁴-NPY (25-36) **36** as determined in the presence of DPC micelles displaying bonds involving backbone atoms only (left). Single conformer displaying bonds between backbone atoms in blue and between side chain atoms in red (right). Hydrogen atoms are omitted.

The C-terminus of NPY from residues 17 to 36 shows an α -helical structure in the presence of DPC micelles⁶⁸, the C-terminus of NPY from residue 25 to 36, as reported by *Koglin et al*⁶³ shows the typical CD spectrum of a random peptide in buffer but it is able to adopt a structure with high α -helical content in the presence of the α -helical-promoting additive 2,2,2 trifluoroethanol (TFE).

The structure of (+) β -ACC NPY analogue results in an amphiphilic helix that exposes hydrophobic sidechains including the aromatic (Tyr) residues on one side, presumably forming the micelle-binding interface. In particular, Arg residues corresponding to positions 33 and 35 in full-length NPY are positioned on the other, solvent exposed side of the helix as shown in Figure 64.

The different receptor subtypes share the C terminus of NPY as one common recognition site. Previously studies suggested the need of a turn-like structure at the C-Terminus for the Y_1 receptor selectivity (Figure 65).⁶⁹

Substitutions in this region can have subtype-specific effects on binding affinity. A structure elucidation of a peptide hormone in solution in the absence of the target receptor can deliver limited information into the bioactive conformation.

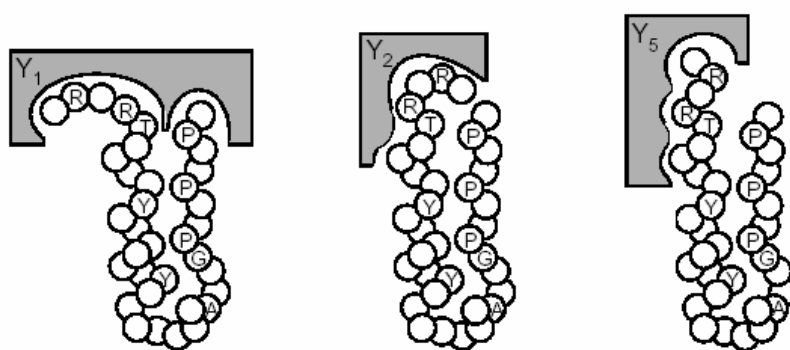


Figure 65. Model of the binding mode of NPY at the different receptor subtypes.⁶⁹

However, keeping in mind that the NPY is probably first recognized from the cell membrane, the solution structure of (+) β -ACC³⁴-NPY (25-36) analogue in the presence of micelles provides an idea about the conformation that is recognized by the receptor.

The presence of the (+) β -ACC unit in the shorted NPY analogue herein investigated imposed a defined turn-structure at the C-Terminus that could be responsible for the selectivity of this peptide.

Further investigation on these peptide analogues are currently in progress in order to explore an eventual use of these peptides as pharmacological tool.

¹ Gumbiner, B. M. *Cell* **1996**, 84, 345-357.

² Aplin, A. E.; Howe, A.; Alahari, S. K.; Juliano, R. L. *Pharmacol. Rev.* **1998**, 50, 197-263.

³ http://ocw.mit.edu/NR/rdonlyres/Biological-Engineering-Division/BE-410JSpring2003/5732AE5F-AE62-448E-BB43-9710DE60DCD6/0/lec_25_slides.pdf

⁴ Karp, G. “*Cell and Molecular biology*”, Chapter 7, **2005**, Wiley.

⁵ Horton, M. A. *Int. J. Biochem. Cell Biol.* **1997**, 29, 721-725.

⁶ Ruoslahti, E. *Annu. Rev. Cell Dev. Biol.*, **1996**, 12, 697-715.

⁷ Plow, E. F.; Haas, T. A.; Zhang, L.; Loftus, J.; Smith, J. W. *J. Biol. Chem.* **2000**, 275, 21785-21788.

⁸ Arnaout, M. A.; Goodman, S. L.; Xiong, J.-P. *Curr. Opin. Cell Biol.* **2002**, 14, 641-651.

⁹ Xiong, J.-P.; Stehle, T.; Diefenbach, B.; Zhang, R.; Dunker, R.; Scott, D. L.; Joachimiak, A.; Goodman, S. L. Arnaout, M. A. *Science* **2001**, 294, 339-345.

¹⁰ Emsley, J., Knight, C. G.; Farndale, R. W.; Barnes, M. J.; Liddington, R. C. *Cell* **2000**, 101, 47-56.

¹¹ Eliceiri, B. P.; Cheresh, D. A. *J. Clin. Invest.* **1999**, 103, 1227-1230.

¹² Strömblad, S.; Cheresh, D. A. *Chemistry & Biology* **1996**, 3, 881-885.

¹³ www.medimmune.com/pipeline/vitaxin.asp

¹⁴ Malešević, M. *Dissertation* **2002**, Bielefeld.

¹⁵ Xiong, J.-P.; Stehle, T.; Zhang, R.; Joachimiak, A.; Frech, M.; Goodman, S. L.; Arnaout, M. A. *Science* **2002**, 296, 151-155.

¹⁶ Schaffner, P., Dard, M. M. *Cell. Mol. Life Sci.*, **2003**, 60, 119-132.

¹⁷ Dechantsreiter, M. A.; Planker, E.; Marthä, B.; Lohof, E.; Hölzemann, G.; Jonczyk, A.; Goodman, S. L.; Kessler, H. *J. Med. Chem.* **1999**, 42, 3033-3040.

¹⁸ Müller, G.; Gurrath, M.; Kessler, H.; Timpl, R. *Angew. Chem.* **1992**, 104, 341-343.

¹⁹ Wermuth, J.; Goodman, S. L.; Jonczyk, A.; Kessler, H. *J. Am. Chem. Soc.* **1997**, 119, 1328-1335.

²⁰ Hoffmann, S.; He, S.; Jin, M.; Ehren, M.; Wiedemann, P.; Ryan, S. J.; Hinton, D. R.; *BMC Ophthalmology* **2005**, 5, 16

²¹ Schumann, F.; Müller, A.; Koksche, M.; Müller, G.; Sewald, N. *J. Am. Chem. Soc.* **2000**, 122, 12009-12010.

²² Lohof, E.; Planker, E.; Mang, C.; Burkhart, R.; Dechantsreiter, M. A.; Haubner, R.; Wester, H.-J.; Schwaiger, M.; Hölzemann, G.; Goodman, S. L.; Kessler, H. *Angew. Chem. Int. Ed.* **2000**, 39, 2761-2764.

- ²³ Bach, A. C., II; Eyermann, C. J.; Gross, J. D.; Bower, M. J.; Harlow, R. L.; Weber, P. C.; DeGrado, W. F. *J. Am. Chem. Soc.* **1994**, *116*, 3207-3219.
- ²⁴ Bach, A. C., II; Espina, J. R.; Jackson, S. A.; Stouten, P. F. W.; Duke, J. L.; Mousa, S. A.; DeGrado, W. F. *J. Am. Chem. Soc.* **1996**, *118*, 293-294.
- ²⁵ M. Malesevic, U. Strijowski, D. Bächle, N. Sewald, *J. Biotechnol.* **2004**, *112*, 73 – 77.
- ²⁶ Arnold, U.; Hinderaker, M. P.; Nilsson, B. L.; Huck, B. R.; Gellman, S. H.; Raines, R. T. . *J. Am. Chem. Soc.* **2002**, *124*, 8522-8523.
- ²⁷ Strijowski, U.; Sewald, N. *Org. Biomol. Chem.* **2004**, *2*, 1105-1109.
- ²⁸ Tatemoto, K.; Carlquist, M.; Mutt, V. *Nature*, **1982**, *296*, 659-660.
- ²⁹ Gehlert, D.R. *Neuropeptides*, **2004**, *38*, 135-140.
- ³⁰ Glover, I.; Haneef, I.; Pitts, J.; Wood, D.; Tickle, I.; Blundell, T. *Biopolymers* **1983**, *22*, 293-304.
- ³¹ Mörl, K.; Beck-Sickinger, A. G.; *Handbook Exp. Pharm. Vol. 162*, (Ed. Michel, M. C.), Springer-Verlag Berlin, **2004**, 479-503 and refs cited therein.
- ³² Structural data are obtain from Protein Data Bank (<http://www.rcsb.org/pdb/>, PDB access code 1F8P and 1BBA respectively).
- ³³ Larhammar, D.; Salaneck, E. *Neuropeptides* **2004**, *38*, 141-151.
- ³⁴ Michael, M.C.; Beck-Sickinger, A. G.; Cox, H.; Doods, H. N.; Herzog, H.; Larhammar, D.; Quirion, R.; Schwartz, T.; Westfall, T. *Pharmacol. Rev.* **1998**, *50*, 143-150.
- ³⁵ Berglund, M. M.; Lundell, I.; Eriksson, H.; Söll, R.; Beck-Sickinger, A. G.; Larhammar, D. *Peptides* **2001**, *22*, 351-356.
- ³⁶ Nordmann, A.; Blommers, M. J. J.; Fretz, H.; Arvinte, T.; Drake, A. F. *Eur. J. Biochem.* **1999**, *261*, 216-226.
- ³⁷ Bader, R.; Bettio, A.; Beck-Sickinger, A. G.; Zerbe, O. *J. Mol. Biol.* **2001**, *305*, 307-329.
- ³⁸ (a) Lerch, M.; Gafner, V.; Bader, R.; Christen, B.; Folkers, G.; Zerbe, O. *J. Mol. Biol.* **2002**, *322*, 1117-1133. (b) Bader, R.; Zerbe, O. *ChemBioChem* **2005**, *6*(9), 1520-1534.
- ³⁹ (a) Redrobe, J. P.; Carvajal, C.; Kask, A.; Dumont, Y.; Quirion, R. *Handbook Exp. Pharm. Vol. 162*, (Ed. Michel, M. C.), Springer-Verlag Berlin, **2004**, 111-136. (b) Silva, A. P.; Cavadas, C.; Grouzmann, E. *Clinica Chimica Acta* **2002**, *326*, 3-25.
- ⁴⁰ Silva, A. P.; Cavadas, C.; Grouzmann, E. *Clinica Chimica Acta* **2002**, *326*, 3-25 and refs cited therein.
- ⁴¹ (a) Flood, J. F.; Hernandez, E. N.; Morley, J. E.; *Brain Res.* **1987**, *421*, 280-290. (b) Reprobe, J. P.; Dumont, Y.; St Pierre, J. A.; Quirion, R. *Brain Res.* **1999**, *848*, 153-166.
- ⁴² Sainsbury, A.; Schwarzer, C.; Couzens, M.; Fetissov, S.; Furtinger, S.; Jenkins, A.; Cox, H. M.; Sperk, G.; Hökfelt, T.; Herzog, H. *PNAS* **2002**, *99*, 8938-8943.
- ⁴³ Baldock, P. A.; Sainsbury, A.; Couzens, M.; Enriquez, R. F.; Thomas, G. P.; Gardiner, E. M.; Herzog, H. *J. Clin. Invest.* **2002**, *109*, 915-921.

- ⁴⁴ Koulu, M.; Movafagh, S.; Touhimaa, J.; Jaakkola, U.; Kallio, J.; Pesonen, U.; Geng, Y.; Karvonen, M. K.; Vaninio-Jylha, E.; Pöllönen, M.; Kaipio-Salmi, K.; Seppälä, H.; Lee, E. W.; Higgins, R. D.; Zukowska, Z. *Annals of Medicine* **2004**, *36*, 232-240.
- ⁴⁵ Rapisinho, P. D.; Broqua, P.; Hayward, A.; Akinsanya, K.; Galyean, R.; Schteingart, C.; Junien, J.-L.; Aubert, M. L. *Neuroendocrinology* **2000**, *71*, 2-7.
- ⁴⁶ Sainsbury, A.; Schwarzer, C.; Couzens, M.; Jenkins, A.; Oakes, S. R.; Ormandy, C. J.; Herzog, H. *Genes Dev* **2002**, *16*, 1077-1088.
- ⁴⁷ Mashiko, S.; Ishihara, A.; Iwaasa, H.; Sano, H.; Oda, Z.; Ito, J.; Yumoto, M.; Okawa, M.; Suzuki, J.; Fukuroda, T.; Jitsuoka, M.; Morin, N.; MacNeil, D. J.; Van der Ploeg, L. H. T.; Ihara, M.; Fukami, T.; Kanatani, A.; *Endocrinology* **2003**, *144*, 1793-1801.
- ⁴⁸ (a) Cabrele, C.; Langer, M.; Bader, R.; Wieland, H. A.; Doods, H. N.; Zerbe, O.; Beck-Sickinger, A. G. *J. Biol. Chem.* **2000**, *275*, 36043-36048. (b) Parker, E. M.; Balasubramaniam, A.; Guzzi, M.; Mullins, D. E.; Salisbury, B. G.; Sheriff, S.; Witten, M. B.; Hwa, J. J. *Peptides* **2000**, *21*, 393-399.
- ⁴⁹ Eva, C.; Keinänen, K.; Monyer, H.; Seeburg, P.; Sprengel, R. *FEBS Lett.* **1990**, *271*, 81-84.
- ⁵⁰ Kask, A.; Harro, J.; von Hörsten, S.; Redrobe, J. P.; Dumont, Y.; Quirion, R. *Neuroscience and Biobehavioral Rev.* **2002**, *26*, 259-283.
- ⁵¹ Gehlert, D. R. *Neuropeptides* **2004**, *38*, 135-140.
- ⁵² Ishihara, A.; Kanatani, A.; Okada, M.; Hidaka, M.; Tanaka, T.; Mashiko, S.; Gomori, A.; Kanno, T.; Hata, M.; Kanesaka, M.; Tominaga, Y.; Sato, N.; Kobayashi, M.; Murai, T.; Watanabe, K.; Ishii, Y.; Fukuroda, T.; Fukami, T.; Ihara, M. *British J. of Pharmacology* **2002**, *136*, 341-346.
- ⁵³ (a) Körner, M.; Waser, B.; Reubi, J. C. *Laboratory Investigation* **2004**, *84*, 71-80. (b) Körner, M.; Waser, B.; Reubi, J. C. *Clinical Cancer Res.* **2004**, *10*, 8426-8433.
- ⁵⁴ Reubi, J. C.; Gugger, M.; Waser, B.; Schaer, J.-C. *Cancer Res.* **2001**, *61*, 4636-4641.
- ⁵⁵ Langer, M.; La Bella, R.; Garcia-Garayoa, E.; Beck-Sickinger, A. G. *Bioconjugate Chem.* **2001**, *12*, 1028-1034.
- ⁵⁶ Brennauer, A.; Dove, S.; Buschauer, A. *Handb. Exp. Pharmacol.* 2004, Vol. 162. Michel, M.C. (ed). Berlin, Heidelberg, New York: Springer. Pp. 505-546.
- ⁵⁷ Beck-Sickinger, A. G.; Wieland, H. A.; Wittneben, H.; Willim, K. D.; Rudolf, K.; Jung, G. *Eur. J. Biochem.* **1994**, *225*, 947-958.
- ⁵⁸ Cabrele, C.; Beck-Sickinger, A. G. *J. Peptide Sci.* **2000**, *6*, 97-122.
- ⁵⁹ Hoffman, S.; Rist, B.; Videnov, G.; Jung, G.; Beck-Sickinger, A. G. *Regul. Pept.* **1996**, *65*, 61-70.
- ⁶⁰ Söll, R. M.; Dinger, M. C.; Lundell, I.; Larhammer, D.; Beck-Sickinger, A. G. *Eur. J. Biochem.* **2001**, *268*, 2828-2837.
- ⁶¹ Mullins, D.; Kirby, D.; Hwa, J.; Guzzi, M.; Rivier, J.; Parker, E. *Mol. Pharmacol.* **2001**, *60*, 534-540.
- ⁶² Takebayashi, Y.; Koga, H.; Togami, J.; Inui, A.; Kurihara, H.; Koshiya, K.; Furuya, T.; Tanaka, A.; Murase, K. *J. Peptide Res.* **2000**, *56*, 409-415.

- ⁶³ Koglin, N.; Zorn, C.; Beumer, R.; Cabrele, C.; Sewald, N.; Reiser, O.; Beck-Sickinger, A. G. *Angew. Chem. Int. Ed.* **2003**, *42*, 202-205.
- ⁶⁴ Balasubramaniam, A.; Dhawan, V. C.; Mullins, D. E.; Chance, W. T.; Sheriff, S.; Guzzi, M.; Prabhakaran, M.; Parker, E. M. *J. Med. Chem.* **2001**, *44*, 1479-1482.
- ⁶⁵ (a) Hayen, A.; Schmitt, M. A.; Ngassa, F. N.; Thomasson, K. A.; Gellman, S. H. *Angew. Chem. Int. Ed.* **2004**, *43*, 505-510. (b) Schmitt, M. A.; Weisblum, B.; Gellman, S. H. *J. Am. Chem. Soc.* **2004**, *126*, 6848-6849.
- ⁶⁶ Henry, G. D.; Sykes, B. D. *Methods Enzymol.* **1994**, *239*, 515-535.
- ⁶⁷ Bartels, C.; Xia, T.; Billeter, M.; Guenter, P.; Wüthrich, K. *J. Biomol. NMR* **1995**, *5*, 1-10.
- ⁶⁸ Lerch, M.; Mayrhofer, M.; Zerbe, O. *J. Mol. Biol.* **2004**, *339*, 1153-1168.
- ⁶⁹ Eckard, C. P.; Cabrale, C.; Wieland, H.A.; Beck-Sickinger, A. G. *Molecules* **2001**, *6*, 448-467.

D. Summary

The design of short conformationally constrained polymers, being able to display analogue functional properties found in large peptides or proteins, requires the identification of new polymeric backbones or building blocks with suitable folding properties. In this work different α -peptides containing two enantiomers of *cis*- β -amino cyclopropane carboxylic acid were synthesized in order to extend our knowledge regarding their conformational preferences.

Alternated peptides α -L-Xaa- β -ACC were synthesized and their conformations were investigated by IR, CD and NMR spectroscopy.

The synthesis of this compounds was carried out in solution or on the solid phase by adding the C-terminus deprotected dipeptide PG-Xaa- β -ACC-OH at each step as shown in Figure 66.

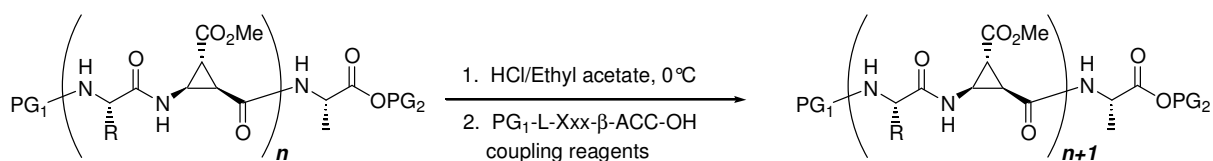


Figure 66. Elongation reaction of α -Xxx/ β -ACC alternated peptides.

Short L-Ala- β -ACC alternated peptides in a polar solvent like methanol adopt well defined helical secondary structures. When the (–) β -ACC is incorporated, the peptides showed a 3_{13} helix turn involving a hydrogen-bond between the NH of the first β -ACC and the C=O of the following β -ACC unit as shown for the heptapeptide (–)-**5a** in Figure 67.

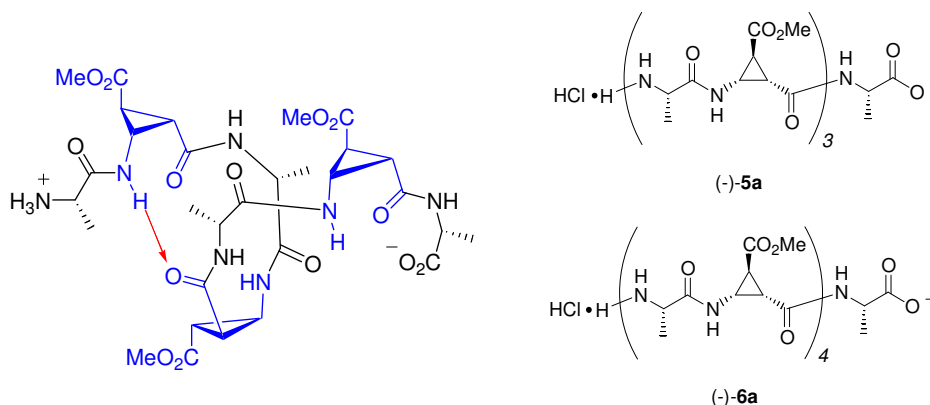


Figure 67. Schema of the structure calculated for the heptapeptide (–)-**5a**.

The CD spectrum corresponding to this structure shows a minimum at about 200 nm. CD spectra, which were measured in different solvents such as trifluoroethanol or hexafluoroacetone and in methanol with different amounts of water, suggest that the stability of the 3_{13} helix-turn found by NMR investigation in methanol, is strongly dependent on the environment.

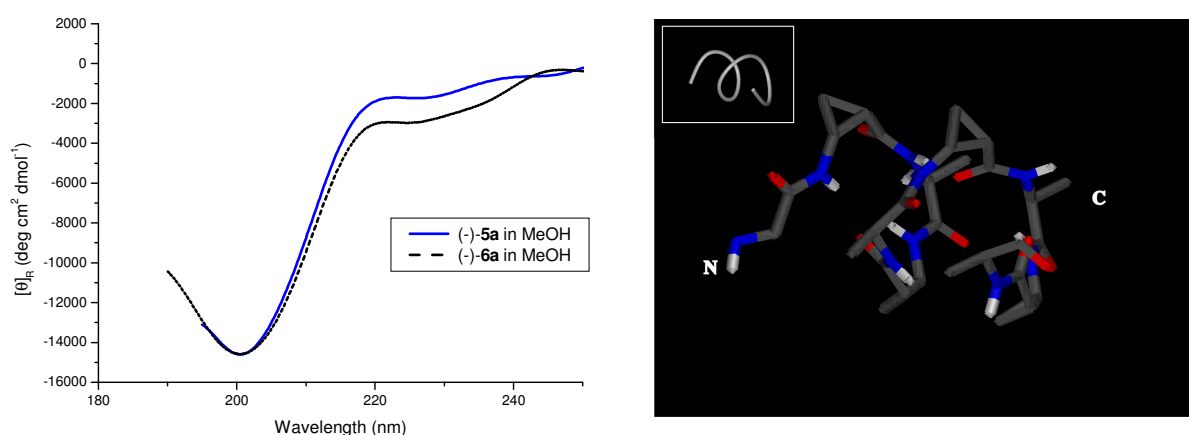


Figure 68. CD spectra of the heptapeptide (-)-**5a** and the nonapeptide (-)-**6a** in methanol and the NMR structure of (-)-**6a**.

It is likely that those peptides in a non polar environment adopt a different conformation, as suggested from the isodichroic point obtained in the CD spectra of the nonapeptide (-)-**6**. However conformational investigation in chloroform by NMR were not in agreement with a well defined folded secondary structure.

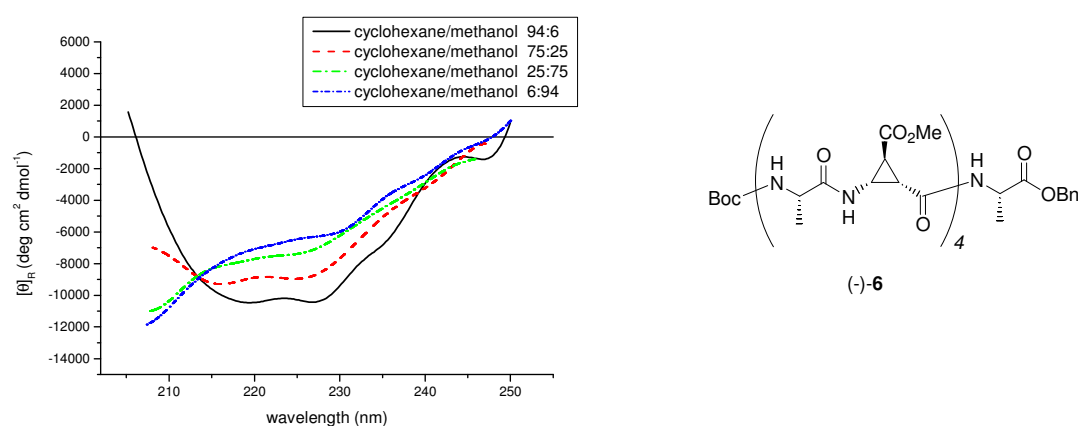


Figure 69. CD spectra of the nonapeptide (-)-**6** with different ratio of polar and non polar solvent.

The investigation on the longer peptide (–)-**7** in which different α -L-amino acid are alternated with (–)- β -ACC units confirm the presence of a helical conformation even if the N-terminus of the peptide is not well defined. This flexibility could be due to the presence of two positive charges at the N-terminal deprotected Lys¹. In fact, changes in the ionization degree of polypeptides, obtained by using different solvents or different pH values in water solutions, led to some conformational changes. In methanol the CD spectrum shows two bands, at about 205 and 212 nm. A more acidic environment increases the intensity at 205 nm compared with the 212 band. The opposite behaviour is found in a basic environment or in HFA (Figure 70).

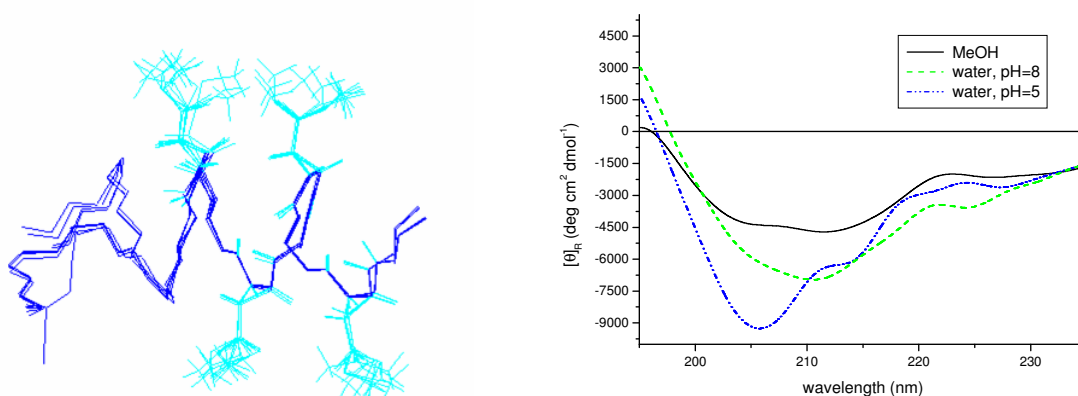


Figure 70. View of backbone atoms of 10 minimized superimposed structures for (–)-**7**, the β -ACCs in position 6, 8, 10 and 12 are shown (left). The CD spectra of (–)-**7** measured in different solvents (right).

The NMR data obtained from the analogues containing the (+) β -ACC moiety display a structure, which is less well defined than the corresponding (–) β -ACC derivatives. For the former, there is likely a set of conformers which rapidly interconvert on the NMR timescale. CD investigations in different solvents show patterns that are almost solvent independent. The solvents investigated are probably not able to stabilize one conformation with respect to another one.

In the second part of this PhD work, β -ACC units were used as building blocks in biological active analogues of neuropeptide Y and RGD peptides, inducing a particular spatial orientation of important side chains for the interaction. Some β -ACC containing peptides are found to be able to enhance the biological affinity to the corresponding receptor. Conformational investigation on them allowed us to collect more information about the

active conformation being responsible for the binding or at least on the conformation that is recognized by the receptor.

Cyclic pentapeptides containing the typical integrin recognition sequence Arg-Gly-Asp were synthesized and their affinities to the $\alpha_V\beta_3$ receptor were investigated. The $\alpha_V\beta_3$ integrin receptor subtype plays an important role in many physiological events and it is a potential pharmaceutical target for treatment of several diseases including tumors.

The stereochemistry of the β -ACC moiety is found to be decisive for the receptor affinity. The pentapeptide c(Arg-Gly-Asp-(+)- β -ACC-Val) is found to have a IC_{50} value in a nanomolar range, which is a higher affinity compared to the reference peptide c(Arg-Gly-Asp-D-Phe-Val) as shown in Table 19.

Peptide	Sequence	$\alpha_V\beta_3$ IC_{50} (nM)
(-)- 28	c(Arg-Gly-Asp(-)- β -ACC-Val)	630
(+)- 28	c(Arg-Gly-Asp-(+)- β-ACC -Val)	21
29	c(Arg-Gly-Asp-D-Phe-Val)	197

Table 19. Biological results obtained with cyclic peptides containing β -ACC units using human melanoma skin cells and vitronectin.

Conformational NMR investigation on (+)-**28** shows the Arg-Gly-Asp segment in the positions i to $i+2$ of a type II' β -turn in which the (+) β -ACC moiety occupies the position $i+3$.

The introduction of the (+)- β -ACC moiety in the C-terminal dodecapeptide of the NPY, at the position 10 (position 34 corresponding to the full length NPY) led to a shorter NPY analogue which is able to bind the Y_1 NPY receptor subtype with good affinity and selectivity.

The secondary structure of the most selective analogue **36** was investigated by 2D NMR in the presence of micelles that mimic the cell membrane, in order to gain information about the conformation that is recognized by the Y_1 receptor subtype after the absorption step on the cell membrane.

The observed secondary structure, differs substantially from the conformation present in the C-terminal part of the full length NPY, both from the helical structure found in solution in the presence of micelles, and from the typical PP-fold that has a flexible C-terminus (Figure 71).

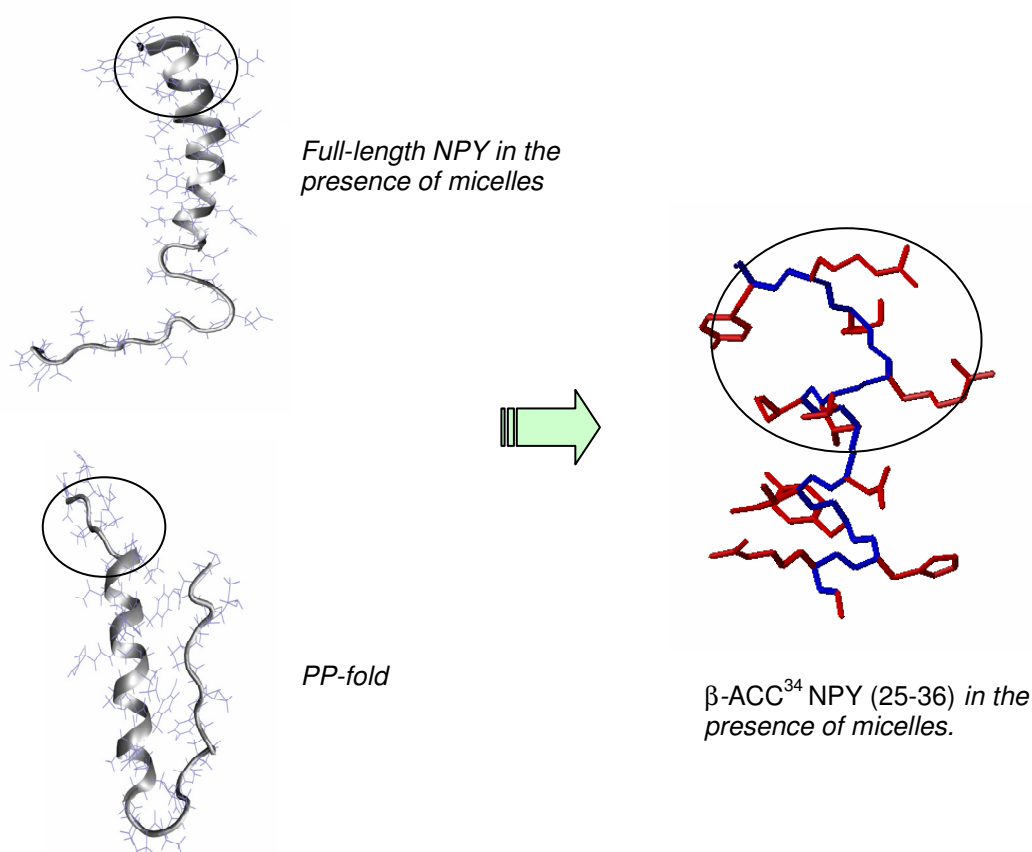


Figure 71. Comparison between the different conformations found concerning NPY. The C-termini are highlighted with a circle. The Hydrogen atoms in the β -ACC³⁴ NPY (25-36) are omitted.

As shown in Figure 71, the β -ACC-NPY analogue **36** adopts at the N-terminus an amphiphilic helix that exposes hydrophobic side chains on one side, presumably forming the micelle-binding interface. At the C-terminus, the (+) β -ACC moiety interrupts the helix and induced a turn-like structure. This conformation could be responsible for a particular orientation of the key side chains for the receptor recognition leading consequently to receptor selectivity.

In conclusion, β -ACC moieties are found to be able to induce a defined secondary structure in short α -/ β - mixed peptides. Alternated α -/ β - peptides show helical conformations, which are better defined when the (–) enantiomer is used. The effect of only one β -ACC unit

surrounded by α -amino acids has to be further investigated. However, the (+) enantiomer investigated in the cyclic-RGD peptide and in the linear NPY analogue displayed a strong influence on the overall conformation, inducing turn structures. In particular it induces a pseudo β -turn in the cyclic analogue and a pseudo β -turn time-shared with a more extended 17 membered-ring in the case of the NPY analogue.

E. Experimental part

E.1 Instruments and general techniques

NMR: Bruker Avance 600 (600.13 MHz), Bruker DRX-500, Bruker Avance 400 (400.13 MHz), Bruker Avance 300 (300.13 MHz) spectrometers were used. **¹H NMR:** The chemical shifts are reported in δ (ppm) relative to chloroform (CDCl₃, 7.26 ppm), dymethylsulfoxide (DMSO-d₆, 2.49 ppm), methanol (CD₃OD, 3.34 ppm) and tetramethylsilane (TMS, 0 ppm). The spectra were analysed by first order, the coupling constants are reported in Hertz (Hz). Characterisation of signals: s = singlet, d = doublet, t = triplet, q = quartet, m = multiplet, s br = broad singlet, dd = double douplet, dt = double triplet, dq = double quartet, ddd = double double doublet. Integration is determined as the relative number of atoms. Diastereomeric ratios were determined by comparing the integrals of corresponding protons in the ¹H NMR spectra. **¹³C NMR:** The chemical shifts are reported in δ (ppm) relative to chloroform (CDCl₃, 77.0 ppm), dymethylsulfoxide (DMSO-d₆, 36.9 ppm), methanol (CD₃OD, 49.0 ppm) and tetramethylsilane (TMS, 0 ppm). ¹³C NMR resonance assignment were aided by the use of the DEPT 135 (DEPT = distortionless enhancement by polarisation transfer) or HSQC (Heteronuclear Single Quantum Correlation) techniques to determine the number of hydrogens attached to each carbon atom and is declared as: + = primary or tertiary (positive DEPT signal intensity or straight line in HSQC), - = secondary (negative DEPT signal or dot line in HSQC) and quat = quaternary (no DEPT signal intensity) carbon atoms. In some cases DEPT 90 spectra were recorded to distinguish between primary and tertiary carbon atoms and HMBC (Heteronuclear Multiple Bond Correlation) to distinguish between quaternary carbon and aromatic CH. **2D-NMR:** The spectra were recorded using the solvent line (CD₃OH, ¹H δ 3.31 or CDCl₃, 7.26 ppm) for referencing. DQF-COSY, 80 ms-TOCSY and 500 ms-ROESY standard experiments were performed with suppression of the methanol OH line by low-power presaturation.

IR-spectra were recorded with a Bio-Rad Excalibur series FT-IR or a Tensor 27 Bruker.

MS-spectra: massspectroscopy department of the University of Regensburg.

Elemental analysis: microanalytical department of the University of Regensburg.

Melting points (mp) were determined with a Buchi SMP 20 and are uncorrected.

Thin layer chromatography (TLC) was performed on alumina plates coated with silica gel (Merck silica gel 60 F 254, layer thickness 0.2 mm). Visualisation was accomplished by UV-light (wavelength $\lambda = 254$ nm) and a Molybdotophosphoric acid solution.

Optical rotations were measured on a Perkin-Elmer-Polarimeter 241 with sodium lamp at 589 nm in the specified solvent. The optical rotation was calculated with the following formula:

$$[\alpha]_D^\theta = ([\alpha]_{\text{exp}} \times 100) / (c \times d)$$

θ = temperature (°C)

$[\alpha]_{\text{exp}}$ = measured value

c = concentration (g/100 ml)

d = length of the cuvette

CD spectra were measured on a JASCO model J-710/720 at the Institut für Bioanalytic und Sensorik of the University of Regensburg (research group of Prof. Dr. O. Wolfbeis) at 21° C between 300 and 200-180 nm in the specified solvent, the number of scans ranging between 10 and 50. The length of the cylindrical cuvettes was 0.1 mm, the resolution was 0.2 nm, the band width 1.0 nm, the sensitivity 20 mdeg, the response 0.25 s, the speed 20 nm/min. The background was subtracted to each spectrum. The absorption value is measured as Molar Ellipticity per Residue (deg cm² dmol⁻¹).

Column chromatography was performed on silica gel Geduran SI 60 (70-230 mesh) purchased from Merck and flash chromatography on flash-silica gel 60 (230-400 mesh ASTM) purchased from Merck.

Solvents were purified according to standard laboratory methods. THF, diethyl ether and toluene were distilled over sodium/benzophenone before use. Dichlormethane, DMSO and DMF were distilled over calcium hydride and acetonitrile over P₂O₅. Methanol was refluxed 2 h over magnesia, distilled and stored under nitrogen over 4 Å molecular sieves. The hexanes used had a boiling point of 40-60 °C. All solvents were distilled before use. Other chemicals were purchased from commercial suppliers and used as received.

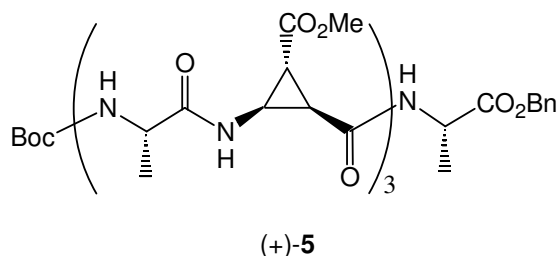
All reactions with oxygen or moisture sensitive reactants were performed under nitrogen atmosphere.

For the elongation of the NPY-analogue peptide, after the manual coupling with the β -ACC containing dipeptide, the peptide synthesiser Syro from MultiSynTech was used.

HPLC-chromatography: analytical and preparative reverse Phase HPLC was performed on Agilent equipment (Böblingen, Germany) by using the columns: Luna C18(2), 3 μm , 4.60 x 150 mm and the Luna C18(2), 90 μm , 21.2 x 250 mm (Phenomenex, Aschaffenburg, Germany). The flow rate was 1 mL/min for the analytical HPLC runs and 21 mL/min for preparative applications. The binary solvent system (A/B) was: (A) ACN, (B) 0.0059% TFA in water. The absorbance was detected at 220 nm.

E.2 Solution Synthesis

E.2.1 Peptides containing (+)- β ACC units

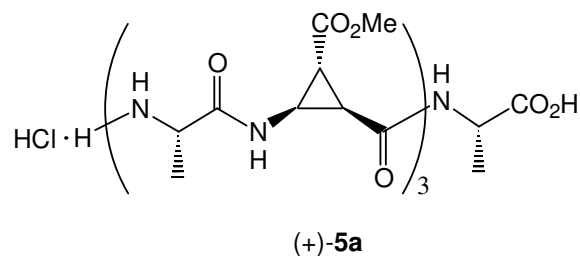


Boc-[Ala-(+)- β -ACC]₃-Ala-OBn, (+)-5:

methyl(1*R*,2*R*,3*R*)-2-[[[(1*S*)-2-[[[(1*R*,2*R*,3*R*)-2-[[[(1*S*)-2-[[[(1*R*,2*R*,3*R*)-2-[[[(1*S*)-2-(benzyloxy)-1-methyl-2-oxoethyl]amino}carbonyl)-3-(methoxycarbonyl)cyclopropyl]amino]-1-methyl-2-oxoethyl]amino]carbonyl]-3-(methoxycarbonyl)cyclopropyl]amino]-1-methyl-2-oxoethyl]amino]carbonyl]-3-((2*S*)-2-[(*tert*-butoxycarbonyl)amino]propanoyl) amino]cyclopropanecarboxylate;

(+)-**13** (970 mg, 1.38 mmol) was deprotected by treatment with HCl 3 M in ethyl acetate (52 ml) for 3 h at 0 °C. The solution was concentrated in vacuum, the salt was resuspended in CH₂Cl₂ (25 ml). Separately the (+)-**11** (500 mg, 1.52 mmol, 1.1 eq.) was dissolved in CH₂Cl₂ (20 ml) and cooled in an ice bath and activated with HOBt (205 mg, 1.52 mmol, 1.1 eq.) and EDC (292 mg, 1.52 mmol, 1.1 eq.). After 10 minutes the mixture of the deprotected (+)-**13** and triethylamine (0.29 ml, 2.07 mmol, 1.5 eq.) were added. The mixture was stirred at room temperature 80 h. The solution was then concentrated in vacuum and the product was obtained by chromatography (CH₂Cl₂/MeOH 25:2) as a white solid (874 mg, 70 %). *R_f* ((+)-**5**) = 0.6 in CH₂Cl₂/MeOH 9:1 - mp 185-187 °C. - [α]_D²¹ - 95.2 (c 0.5, CH₃OH). - ¹H NMR (CD₃OD, 300 MHz) δ 1.24 (d, *J* = 7.4 Hz, 3H, CH₃CH), 1.29 (d, *J* = 7.3 Hz, 3H, CH₃CH), 1.31 (d, *J* = 7.3 Hz, 3H, CH₃CH), 1.39 (d, *J* = 7.3 Hz, 3H, CH₃CH), 1.42 (s, 9H, (CH₃)₃C), 2.30-2.40 (m, 3H, cyclopropyl-CH), 2.46-2.52 (m, 3H, cyclopropyl-CH), 3.64 (s, 3H, CH₃O), 3.66-3.78 (m, 3H, cyclopropyl-CHN), 3.70 (s, 3H, CH₃O), 3.71 (s, 3H, CH₃O), 3.95-4.02 (m, 1H, Ala-CHN), 4.19-4.31 (m, 2H, Ala-CHN), 4.51 (q, *J* = 7.3 Hz, 1H, Ala-CHN), 5.12 (d, *J* = 12.3 Hz, 1H, CH₂O), 5.20 (d, *J* = 12.3 Hz, 1H, CH₂O), 7.33-7.36 (m, 5H, Ph-CH). - ¹³C NMR (CD₃OD, 75.5 MHz) δ 17.6 (+, CH₃CH), 17.7 (+, CH₃CH), 17.9 (+, CH₃CH), 18.2 (+, CH₃CH), 27.5 (+, cyclopropyl-CH), 27.6 (+, cyclopropyl-CH), 27.7 (+, cyclopropyl-CH),

28.4 (+, cyclopropyl-CH), 28.8 (+, (CH₃)₃C, 3C), 28.9 (+, cyclopropyl-CH), 29.0 (+, cyclopropyl-CH), 36.6 (+, cyclopropyl-CHN, 2C), 36.7 (+, cyclopropyl-CHN), 49.6 (+, Ala-CHN), 50.7 (+, Ala-CHN, 2C), 51.6 (+, Ala-CHN), 52.9 (+, CH₃O, 2C), 53.0 (+, CH₃O), 68.0 (-, CH₂O), 80.7 (C_{quat}, (CH₃)₃C), 129.3 (+, Ph-CH, 2C), 129.4 (+, Ph-CH), 129.6 (+, Ph-CH, 2C), 137.3 (C_{quat}, Ph-C), 157.7 (C_{quat}, N(CO)O), 169.7 (C_{quat}, C=O, 3C), 172.3 (C_{quat}, C=O, 2C), 172.4 (C_{quat}, C=O, 2C), 172.5 (C_{quat}, C=O), 173.9 (C_{quat}, C=O), 175.5 (C_{quat}, C=O), 175.7 (C_{quat}, C=O). - MS FAB (MeOH/Glycerin) *m/z* (%) 916 (MH⁺, 56), 816 (M⁺-Boc, 100), 726 (16). - IR (KBr) 3334, 2981, 1728, 1666, 1526, 1443, 1314 cm⁻¹. - HR MS calcd for C₄₂H₅₇N₇O₁₆ 916.39400, found 916.39183

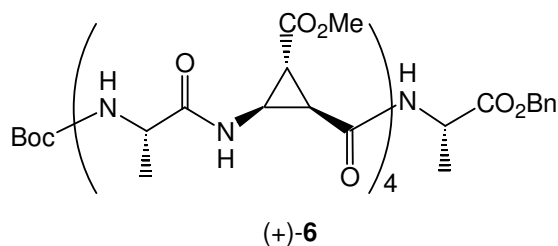


HCl·H-[Ala-(+)-β-ACC]₃-Ala-OH, (+)-5a:

(2S)-1-[[[(1R,2R,3R)-2-[[[(1S)-2-[[[(1R,2R,3R)-2-[[[(1S)-2-[[[(1S)-1-carboxyethyl]amino}carbonyl]-3-(methoxycarbonyl)cyclopropyl]amino]-1-methyl-2-oxoethyl]amino]carbonyl]-3-(methoxycarbonyl)cyclopropyl]amino]-1-methyl-2-oxoethyl]amino]carbonyl]-3-(methoxycarbonyl)cyclopropyl]amino]-1-oxo-2-propanaminiumchloride;

(+)-**5** (100 mg, 0.109 mmol) was stirred in HCl 3 M in ethyl acetate (2 ml) at 0°C for 3 h. The solution was then concentrated in vacuum and the salt redissolved in methanol (10 ml). Then Pd/C 10 % (20 mg) and cyclohexadiene (0.17 ml, 42 % in pentane) were added. The reaction mixture was stirred overnight, filtrated over a celite pad and concentrated in vacuum to afford the deprotected peptide as a white solid (75 mg, 90 %). - mp 190 °C decomposed. - $[\alpha]_D^{21}$ - 81.0 (c 0.5, MeOH). - ¹H NMR (CD₃OD, 300 MHz) δ 1.30 (d, *J* = 7.7 Hz, 3H, CH₃CH), 1.32 (d, *J* = 7.4 Hz, 3H, CH₃CH), 1.40 (d, *J* = 7.1 Hz, 3H, CH₃CH), 1.41 (d, *J* = 6.9 Hz, 3H, CH₃CH), 2.33-2.36(m, 1H, cyclopropyl-CH), 2.38-2.42 (m, 1H, cyclopropyl-CH), 2.47-2.56 (m, 4H, cyclopropyl-CH), 3.55 (dd, *J* = 7.8, 4.8 Hz, 1H, cyclopropyl-CHN),

3.67-3.79 (m, 2H, cyclopropyl-CHN), 3.72 (s, 3H, CH₃O), 3.73 (s, 3H, CH₃O), 3.73 (s, 3H, CH₃O), 3.89 (q, $J = 6.9$ Hz, 1H, Ala-CHN), 4.21 (q, $J = 7.2$ Hz, 1H, Ala-CHN), 4.28 (q, $J = 7.3$ Hz, 1H, Ala-CHN), 4.43 (q, $J = 7.2$ Hz, 1H, Ala-CHN). - ¹³C NMR (CD₃OD, 75.5 MHz) δ 16.1 (+, CH₃CH, 2C), 16.3 (+, CH₃CH), 16.4 (+, CH₃CH), 25.6 (+, cyclopropyl-CH), 26.0 (+, cyclopropyl-CH), 26.2 (+, cyclopropyl-CH), 27.0 (+, cyclopropyl-CH, 2C), 27.5 (+, cyclopropyl-CH), 28.3 (+, cyclopropyl-CH), 35.0 (+, cyclopropyl-CHN, 2C), 35.1 (+, cyclopropyl-CHN), 48.6 (+, CHN, 2C), 49.2 (+, CHN), 49.4 (+, CHN), 51.4 (+, CH₃O), 51.5 (+, CH₃O), 51.6 (+, CH₃O), 167.3 (C_{quat}, C=O), 168.1 (C_{quat}, C=O), 168.2 (C_{quat}, C=O), 170.6 (C_{quat}, C=O), 170.8 (C_{quat}, C=O), 170.9 (C_{quat}, C=O, 2C), 173.9 (C_{quat}, C=O), 174.2 (C_{quat}, C=O), 174.6 (C_{quat}, C=O). - MS FAB (MeOH/Glycerin) m/z (%) 726 (MH⁺, 100). - IR (KBr) 3360, 3054, 2980, 1731, 1654, 1533, 1450, 1315, 1209, 1174 cm⁻¹. - HR MS calcd for C₃₀H₄₃N₇O₁₄ + H 726.29462, found 726.29401.

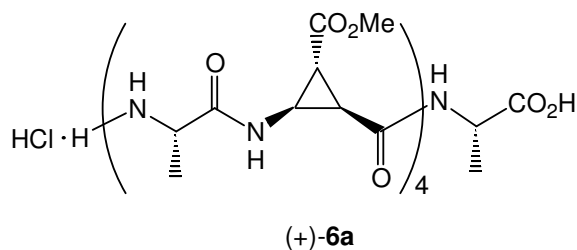


Boc-[Ala-(+)- β -ACC]₄-Ala-OBn, (+)-6:

methyl(1*R*,2*R*,3*R*)-2-[[[(1*S*)-2-[[[(1*R*,2*R*,3*R*)-2-[[[(1*S*)-2-[[[(1*S*)-2-(benzyloxy)-1-methyl-2-oxoethyl]amino}carbonyl]-3-(methoxycarbonyl)cyclopropyl]amino]-1-methyl-2-oxoethyl]amino]carbonyl]-3-(methoxycarbonyl)cyclopropyl]amino]-1-methyl-2-oxoethyl]amino]carbonyl]-3-[[[(2*S*)-2-[[[(1*R*,2*R*,3*R*)-2-[[[(2*S*)-2-[(*tert*-butoxycarbonyl)amino]propanoyl]amino)-3-(methoxycarbonyl)cyclopropyl]carbonyl]amino]propanoyl]amino}cyclopropanecarboxylate;

(+)-5 (200 mg, 0.22 mmol) was deprotected by treatment with HCl 3 M in ethyl acetate (9 ml) for 3h at 0 °C. The solution was concentrated in vacuum, the salt was resuspended in CH₂Cl₂ (20 ml). Separately the (+)-11 (100 mg, 0.30 mmol, 1.35 eq.) was dissolved in CH₂Cl₂ (20 ml) and cooled in an ice bath and activated with HOBt (41 mg, 0.30 mmol, 1.35 eq.) and EDC (58 mg, 0.30 mmol, 1.35 eq.). After 10 minutes the mixture of the deprotected (+)-5 and triethylamine (0.05 ml, 0.37 mmol, 1.70 eq.) were added. The mixture was stirred at room temperature 90 h. The solution was then concentrated in vacuum and the product was

obtained by chromatography ($\text{CH}_2\text{Cl}_2/\text{MeOH}$ 25:3; $R_f = 0.2$) as a white solid (135 mg, 55 %), 15 % epimerisation was observed. The product was isolated as a white solid by recrystallization from ethyl acetate/hexanes. - mp >200 °C. - $[\alpha]_D^{21} -50.0$ (c 1, CHCl_3). - ^1H NMR (DMSO-d_6 , 600 MHz) δ 1.09-1.12 (m, 6H, CH_3CH), 1.14 (d, $J = 7.2$ Hz, 3H, CH_3CH), 1.29 (d, $J = 7.4$ Hz, 3H, CH_3CH), 1.36 (s, 9H, $(\text{CH}_3)_3\text{C}$), 2.17 (m, 1H, cyclopropyl-CH), 2.21-2.26 (m, 3H, cyclopropyl-CH), 2.45-2.53 (m, 4H, cyclopropyl-CH) 3.44-3.50 (m, 2H, cyclopropyl-CHN), 3.54-3.60 (m, 2H, cyclopropyl-CHN), 3.60 (s, 3H, CH_3O), 3.65 (s, 3H, CH_3O), 3.65 (s, 3H, CH_3O), 3.66 (s, 3H, CH_3O), 3.84-3.90 (m, 1H, Ala-CHN), 4.11-4.19 (m, 3H, Ala-CHN), 4.32-4.38 (m, 1H, Ala-CHN), 5.09 (d, $J = 12.5$ Hz, 1H, CH_2O), 5.16 (d, $J = 12.3$ Hz, 1H, CH_2O), 7.06 (d, $J = 7.2$ Hz, 1H, NH), 7.32-7.40 (m, 5H, Ph-CH), 8.00 (d, $J = 7.2$ Hz, 1H, NH), 8.07 (d, $J = 6.4$ Hz, 1H, NH), 8.10 (d, $J = 6.7$ Hz, 1H, NH), 8.14 (d, $J = 6.4$ Hz, 1H, NH), 8.63 (d, $J = 7.2$ Hz, 1H, NH), 8.66 (d, $J = 7.7$ Hz, 1H, NH), 8.68 (d, $J = 7.2$ Hz, 1H, NH), 8.92 (d, $J = 7.4$ Hz, 1H, NH). - ^{13}C NMR (DMSO-d_6 , 100.6 MHz) δ 16.8 (+, CH_3CH), 17.5 (+, CH_3CH), 17.6 (+, CH_3CH), 17.7 (+, CH_3CH), 17.8 (+, CH_3CH), 25.2 (+, cyclopropyl-CH), 25.4 (+, cyclopropyl-CH), 25.6 (+, cyclopropyl-CH, 2C), 27.1 (+, cyclopropyl-CH, 2C) 27.4 (+, cyclopropyl-CH), 27.6 (+, cyclopropyl-CH) 28.0 (+, $(\text{CH}_3)_3\text{C}$), 35.1 (+, cyclopropyl-CHN, 3C), 35.2 (+, cyclopropyl-CHN), 48.2 (+, Ala-CHN), 48.4 (+, Ala-CHN, 3C), 49.6 (+, Ala-CHN), 52.0 (+, CH_3O), 52.0 (+, CH_3O , 2C), 52.1 (+, CH_3O), 65.9 (-, CH_2O), 78.0 (C_{quat} , $(\text{CH}_3)_3\text{C}$), 127.6 (+, Ph-CH, 2C), 128.0 (+, Ph-CH), 128.3 (+, Ph-CH, 2C), 135.8 (C_{quat} , Ph-C), 166.2 (C_{quat} , $\text{N}(\text{CO})\text{O}$), 166.4 (C_{quat} , $\text{C}=\text{O}$, 2C), 166.8 (C_{quat} , $\text{C}=\text{O}$, 2C), 169.3 (C_{quat} , $\text{C}=\text{O}$), 169.5 (C_{quat} , $\text{C}=\text{O}$), 170.5 (C_{quat} , $\text{C}=\text{O}$), 170.6 (C_{quat} , $\text{C}=\text{O}$), 170.6 (C_{quat} , $\text{C}=\text{O}$, 2C) 172.0 (C_{quat} , $\text{C}=\text{O}$), 172.5 (C_{quat} , $\text{C}=\text{O}$), 172.6 (C_{quat} , $\text{C}=\text{O}$). - MS FAB ($\text{MeOH}/\text{Glycerin}$) m/z (%) 1150 (MNa^+ , 64), 1128 (MH^+ , 14), 1028 (MH^+ -Boc, 100). - IR (KBr) 3305, 2966, 1731, 1649, 1522, 1447, 1199, 1169, 752 cm^{-1} . - HR MS calcd for $\text{C}_{51}\text{H}_{69}\text{N}_9\text{O}_{20} + \text{Na}$ 1150.45565, found 1150.45543

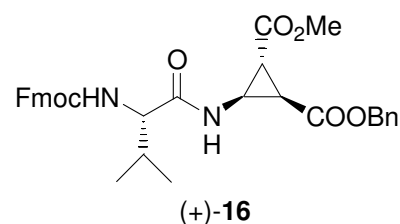


HCl·H-[Ala-(+)-β-ACC]₄-Ala-OH, (+)-6a:

(2S)-1-{[(1R,2R,3R)-2-{[(1S)-2-{[(1R,2R,3R)-2-{[(1S)-2-{[(1R,2R,3R)-2-{[(1S)-2-{[(1R,2R,3R)-2-{[(1S)-1-carboxyethyl]amino}carbonyl]-3-(methoxycarbonyl)cyclopropyl]amino}-1-methyl-2-oxoethyl)amino]carbonyl]-3-(methoxycarbonyl)cyclopropyl]amino}-1-methyl-2-oxoethyl)amino]carbonyl]-3-(methoxycarbonyl)cyclopropyl]amino}-1-methyl-2-oxoethyl)amino]carbonyl]-3-(methoxycarbonyl)cyclopropyl]amino}-1-oxo-2-propanaminium chloride;

(+)-**6** (30 mg, 0.027 mmol) was stirred in HCl 3 M in ethyl acetate (1 ml) at 0°C for 3 h. The solution was then concentrated in vacuum and the salt redissolved in methanol (5 ml). Then Pd/C 10 % (40 mg) and cyclohexadiene (0.03 ml, 42 % in pentane) were added. The reaction mixture was stirred overnight, filtrated over a celite pad and concentrated in vacuum to afford the deprotected peptide as a white solid (25 mg, 95 %). - mp 160 °C decomposed. - ¹H NMR (CD₃OD, 300 MHz) δ 1.25-1.31 (m, 9H, CH₃CH), 1.36 (d, *J* = 7.1 Hz, 3H, CH₃CH), 1.37 (d, *J* = 7.1 Hz, 3H, CH₃CH), 2.30-2.37 (m, 2H, cyclopropyl-CH), 2.43-2.54 (m, 6H, cyclopropyl-CH), 3.49-3.56 (m, 1H, cyclopropyl-CHN), 3.62-3.76 (m, 2H, cyclopropyl-CHN), 3.79-3.89 (m, 1H, cyclopropyl-CHN), 3.68 (s, 3H, CH₃O), 3.69 (s, 3H, CH₃O), 3.69 (s, 3H, CH₃O), 3.70 (s, 3H, CH₃O), 4.13-4.30 (m, 4H, Ala-CHN), 4.35-4.44 (m, 1H, Ala-CHN). - ¹³C NMR (CD₃OD, 75.5 MHz) δ 15.9 (+, CH₃CH), 16.0 (+, CH₃CH), 16.1 (+, CH₃CH), 16.2 (+, CH₃CH), 16.3 (+, CH₃CH), 26.2 (+, cyclopropyl-CH), 26.6 (+, cyclopropyl-CH), 27.2 (+, cyclopropyl-CH, 2C), 27.3 (+, cyclopropyl-CH), 27.4 (+, cyclopropyl-CH), 27.6 (+, cyclopropyl-CH), 27.9 (+, cyclopropyl-CH), 34.8 (+, cyclopropyl-CHN), 34.9 (+, cyclopropyl-CHN), 35.0 (+, cyclopropyl-CHN), 35.1 (+, cyclopropyl-CHN), 48.5 (+, Ala-CHN), 48.8 (+, Ala-CHN), 49.4 (+, Ala-CHN), 49.7 (+, Ala-CHN), 50.1 (+, Ala-CHN), 51.4 (+, CH₃O, 4C), 167.3 (C_{quat}, C=O), 167.9 (C_{quat}, C=O), 168.0 (C_{quat}, C=O, 2C), 170.7 (C_{quat}, C=O, 2C), 170.9 (C_{quat}, C=O), 171.0 (C_{quat}, C=O), 173.7 (C_{quat}, C=O), 174.3 (C_{quat}, C=O), 174.6 (C_{quat}, C=O), 174.8 (C_{quat}, C=O), 175.0 (C_{quat}, C=O). - FAB (MeOH/Glycerin) *m/z* (%) 938 (MH⁺, 100). - IR (KBr) 3362, 3060, 2960, 1725, 1645, 1520,

1440, 1315, 1210, 1120 cm^{-1} . - HR MS calcd for $\text{C}_{39}\text{H}_{55}\text{N}_9\text{O}_{18} + \text{H}$ 938.3743, found 938.3759.

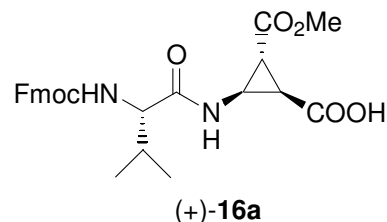


Fmoc-Val-(+)- β ACC-OBn, (+)-16:

1-methyl 2-phenyl (1*R*,2*R*,3*S*)-3-[[[(2*S*)-2-[(9*H*-fluoren-9-ylmethoxy)carbonyl]amino}-3-methylbutanoyl]amino]-1,2-cyclopropanedicarboxylate;

A solution of (+)-**9** (350 g, 1.0 mmol) in HCl 3 M in ethyl acetate (38 ml) was stirred at 0 °C for 3 h. The solvent was evaporated the solid was resuspended in CH_2Cl_2 (30 ml) Fmoc-Val-OH (441 mg, 1.3 mmol, 1.3 eq.), EDC (346 mg, 1.8 mmol, 1.8 eq) and pyridine (104 μl , 1.3 mmol, 1.3 eq.) were added. The mixture was stirred overnight at room temperature. The solution was washed with saturated NaHCO_3 (40 ml), 1 M KHSO_4 (40 ml) and saturated NaHCO_3 (40 ml). The organic phase was dried over Na_2SO_4 and concentrated. The product was purified by chromatography ($\text{CH}_2\text{Cl}_2/\text{MeOH}$ 50:1, R_f = 0.2). 493 mg, 86 % mp 164-166 °C. $[\alpha]_D^{21}$ - 20.37 (c 0.5, CHCl_3). - ^1H NMR (CDCl_3 , 300 MHz): δ 0.88 (d, J = 6.7 Hz, 3H, Val- CH_3), 0.91 (d, J = 6.6 Hz, 3H, Val- CH_3), 2.08 (dq, J = 6.5, 6.6, 6.7 Hz, 1H, Val- βCH), 2.32 (dd, J = 5.2, 4.9 Hz, 1H, cyclopropyl-CH), 2.57 (dd, J = 8.2, 5.2 Hz, 1H, cyclopropyl-CH), 3.70 (s, 3H, CH_3O), 3.99 (dd, J = 8.3, 6.5, 1H, Val- αCH) 4.16 (ddd, J = 8.2, 8.2, 4.9. 1H, cyclopropyl-CHN), 4.23 (t, J = 6.9 Hz, 1H, Fmoc-CH), 4.40 (d, J = 6.9 Hz, 2H, Fmoc- CH_2), 5.08 (d, J = 12.2 Hz, 1H, CH_2O), 5.13 (d, J = 12.2 Hz, 1H, CH_2O), 5.36 (d, J = 8.3 Hz, 1H, Val-NH), 6.70 (d, J = 8.2 Hz, 1H, cyclopropyl-NH), 7.29-7.43 (m, 9H, Ar-CH), 7.59-7.63 (m, 2H, Fmoc-Ar-CH), 7.75-7.78 (m, 2H, Fmoc-Ar-CH). - ^{13}C NMR (CDCl_3 , 75.5 MHz): δ 17.7 (+, Val- CH_3), 19.2 (+, Val- CH_3), 26.1 (+, cyclopropyl-CH), 28.7 (+, cyclopropyl-CH), 31.0 (+, Val- βCH), 36.0 (+, cyclopropyl-CHN), 47.2 (+, Fmoc-CH), 52.5 (+, CH_3O), 60.4 (+, Val-CHN), 67.2 (-, Fmoc- CH_2), 67.5 (-, Bn- CH_2), 120.0 (+, Fmoc-Ar-CH, 2C), 125.1 (+, Fmoc-Ar-CH, 2C), 127.1 (+, Ar-CH, 2C), 127.8 (+, Ar-CH, 2C), 128.4 (+, Ar-CH, 2C), 128.7 (+, Ar-CH), 128.7 (+, Ar-CH, 2C), 134.9 (C_{quat} , Ph-C), 141.3 (C_{quat} , Fmoc-Ar-C, 2C), 143.7 (C_{quat} , Fmoc-Ar-C, 2C), 156.4 (C_{quat} , N(CO)O), 169.8 (C_{quat} , C=O), 170.1 (C_{quat} , C=O), 171.8 (C_{quat} , C=O). - MS ESI (DCM/MeOH + 10 mmol/l NH_4Ac) m/z

(%) 593 (MNa^+ , 11), 588 (MNH_4^+ , 40) 571 (MH^+ , 100). - IR 3306, 2957, 1726, 1664, 1533, 1450, 1294, 1219, 1171, 771 cm^{-1} . - Anal. Calcd for $\text{C}_{33}\text{H}_{34}\text{N}_2\text{O}_7$ C, 69.46; H, 6.01; N, 4.91. Found: C, 68.92; H, 5.46; N, 4.40.



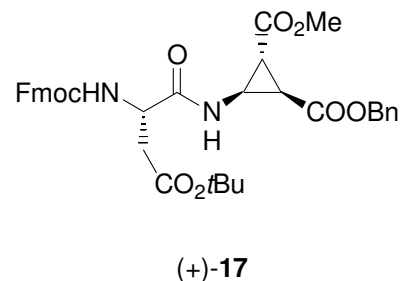
Fmoc-Val-(+)- β ACC-OH, (+)-16a**:**

(1*R*,2*R*,3*R*)-2-[[[(2*S*)-2-[(9*H*-fluoren-9-ylmethoxy)carbonyl]amino]-3-methylbutanoyl]amino]-3-(methoxycarbonyl)cyclopropanecarboxylic acid;

(+)-**16** (130 mg, 0.23 mmol) was dissolved under nitrogen atmosphere in MeOH (10 ml), then 1,4-cyclohexadiene 4M in pentane (216 μl , 5 eq) and Pd/C 5% (80 mg) were added. The reaction mixture was stirred under inert atmosphere overnight, then it was filtrated on a 2 cm celite pad and concentrated. The product was purified by chromatography (from CH_2Cl_2 to $\text{CH}_3\text{OH}/\text{CH}_2\text{Cl}_2$ 90:10; R_f = 0.4 in $\text{CH}_3\text{OH}/\text{CH}_2\text{Cl}_2$ 90:10) to afford the product as a white solid (99 mg, 90 %).

mp 185-187 $^{\circ}\text{C}$. $[\alpha]_D^{21}$ -17.8 (c 1, CH_3OH). - ^1H NMR ($\text{CD}_3\text{OD}/\text{CDCl}_3$ 10:1, 600 MHz): δ 0.91 (d, J = 6.2 Hz, 6H, Val- CH_3), 2.04-2.10 (m, 1H, Val- βCH), 2.25 (dd, J = 5.0, 4.6 Hz, 1H, cyclopropyl-CH), 2.30 (dd, J = 8.1, 5.0 Hz, 1H, cyclopropyl-CH), 3.66 (s, 3H, CH_3O), 3.66-3.68 (m, 1H, cyclopropyl-CHN), 3.87 (d, J = 7.0 Hz, 1H, Val- αCH), 4.20 (t, J = 7.1 Hz, 1H, Fmoc-CH), 4.31 (dd, J = 10.3, 7.1 Hz, 1H, Fmoc- CH_2), 4.40 (dd, J = 10.2, 7.1 Hz, 1H, Fmoc- CH_2), 7.27-7.38 (m, 4H, Ar-CH), 7.63 (pseudo t, J = 7.8 Hz, 2H, Fmoc-Ar-CH), 7.76 (pseudo d, J = 7.5 Hz, 2H, Fmoc-Ar-CH). - ^{13}C NMR ($\text{CD}_3\text{OD}/\text{CDCl}_3$ 10:1, 150.9 MHz): δ 18.7 (+, Val- CH_3), 20.0 (+, Val- CH_3), 28.9 (+, cyclopropyl-CH), 29.9 (+, cyclopropyl-CH), 31.5 (+, Val- βCH), 36.5 (+, cyclopropyl-CHN), 48.4 (+, Fmoc-CH), 52.8 (+, CH_3O), 62.3 (+, Val-CHN), 68.3 (-, Fmoc- CH_2), 121.0 (+, Fmoc-Ar-CH, 2C), 126.3 (+, Fmoc-Ar-CH, 2C), 128.2 (+, Fmoc-Ar-CH, 2C), 128.3 (+, Fmoc-Ar-CH, 2C), 128.9 (+, Fmoc-Ar-CH, 2C), 142.6 (C_{quat} , Fmoc-Ar-C, 2C), 145.1 (C_{quat} , Fmoc-Ar-C), 145.3 (C_{quat} , Fmoc-Ar-C), 158.8 (C_{quat} , N(CO)O), 172.8 (C_{quat} , C=O, CH_3O), 174.9 (C_{quat} , Val-C=O), 176.2 (C_{quat} , C=O, CO_2H). - MS FAB ($\text{MeOH}/\text{Glycerine}$) m/z (%) 999 ($2\text{M}+\text{K}^+$, 40), 961 ($2\text{M}+\text{H}^+$, 10), 519

(MK⁺, 20) 481 (MH⁺, 100). - IR 3320, 2957, 1718, 1670, 1450, 1275, 1171, 1034, 770 cm⁻¹. - HR MS calcd for C₂₆H₂₈N₂O₇ + H 481.1975, found 481.1975



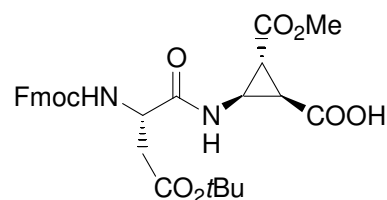
Fmoc-Asp(O^tBu)-(+)-βACC-OBn, (+)-17:

1-methyl 2-phenyl (1*R*,2*R*,3*S*)-3-[[[(2*S*)-4-(*tert*-butoxy)-2-[(9*H*-fluoren-9-ylmethoxy)carbonyl]amino]-4-oxobutanoyl]amino]-1,2-cyclopropanedicarboxylate;

A solution of (+)-9 (320 mg, 0.86 mmol) in HCl 3 M in ethyl acetate (33 ml) was stirred at 0 °C for 3 h. The solvent was evaporated the solid was resuspended in CH₂Cl₂ (30 ml) and a solution of Fmoc-Asp(O^tBu)-OH (708 mg, 1.72 mmol, 2 eq.), EDC (330 mg, 1.72 mmol, 2 eq) and HOBt (209 mg, 1.55 mmol, 1.8 eq.) in CH₂Cl₂ (40 ml) (previously stirred 1 h at 0 °C) was added. Pyridine (123 μl, 1.55 mmol, 1.8 eq.) was then added dropwise. The mixture was stirred overnight at room temperature. The solution was washed with saturated NaHCO₃ (50 ml), 1 M KHSO₄ (50 ml) and saturated NaHCO₃ (50 ml). The organic phase was dried over Na₂SO₄ and concentrated. The product was purified by chromatography (PE/EA 3:1 R_f = 0.1). 497 mg, 89 %.

mp 44-46 °C . $[\alpha]_D^{21}$ -15.0 (c 0.5, CH₃OH). - ¹H NMR (CDCl₃, 300 MHz): δ 1.46 (s, 9H, O^tBu), 2.32 (dd, *J* = 4.9, 4.9 Hz, 1H, cyclopropyl-CH), 2.55 (dd, *J* = 8.2, 5.2 Hz, 1H, cyclopropyl-CH), 2.53-2.60 (m, 1H, Asp-βCH₂), 2.89 (dd, *J* = 16.9, 4.5 Hz, 1H, Asp-βCH₂), 3.70 (s, 3H, CH₃O), 4.02 (ddd, *J* = 7.9, 7.9, 4.7 Hz, 1H, cyclopropyl-CHN), 4.22-4.27 (m, 1H, Fmoc-CH), 4.31-4.37 (m, 1H, Fmoc-CH₂), 4.45-4.51 (m, 2H, Fmoc-CH₂, Asp-αCH), 5.03 (d, *J* = 12.3 Hz, 1H, CH₂O), 5.10 (d, *J* = 12.3 Hz, 1H, CH₂O), 5.94 (d, *J* = 8.5 Hz, 1H, Asp-NH), 7.28-7.43 (m, 9H, Fmoc-Ar-CH, Bn-Ar-CH), 7.54-7.66 (m, 3H, Fmoc-Ar-CH, βACC-NH), 7.76 (pseudo d, *J* = 7.4 Hz, 2H, Fmoc-Ar-CH). - ¹³C NMR (CDCl₃, 75.5 MHz): δ 26.2 (+, cyclopropyl-CH), 28.1 (+, (CH₃)₃C), 28.7 (+, cyclopropyl-CH), 36.0 (+, cyclopropyl-CHN),

37.1 (-, Asp-CH₂), 47.1 (+, Fmoc-CH), 51.2 (+, Asp-CHN), 52.5 (+, CH₃O), 67.4 (-, Fmoc-CH₂, 1C), 68.8 (-, Bn-CH₂, 1C), 82.0 (C_{quat}, (CH₃)C), 120.0 (+, Ar-CH), 120.2 (+, Fmoc-Ar-CH), 124.4 (+, Ar-CH), 125.1 (+, Ar-CH), 125.2 (+, Ar-CH), 127.1 (+, Ar-CH), 127.8 (+, Ar-CH), 127.9 (+, Ar-CH), 128.4 (+, Ar-CH), 128.5 (+, Ar-CH), 128.6 (+, Ar-CH, 2C), 129.4 (+, Ar-CH), 135.0 (C_{quat}, Ph-Ar-C), 139.7 (C_{quat}, Fmoc-Ar-C), 141.3 (C_{quat}, Fmoc-Ar-C), 143.6 (C_{quat}, Fmoc-Ar-C), 143.9 (C_{quat}, Fmoc-Ar-C), 156.0 (C_{quat}, N(CO)O), 169.7 (C_{quat}, C=O), 169.9 (C_{quat}, C=O), 171.1 (C_{quat}, C=O), 171.2 (C_{quat}, C=O). - MS FAB (MeOH/Glycerine) 643 (MH⁺, 86), 587 (100). - IR 3329, 2978, 1718, 1522, 1308, 1217, 1169, 1051, 741 cm⁻¹. - HR MS calcd for C₃₆H₃₈N₂O₉ + H 643.2656, found 643.2650.



(+)-**17a**

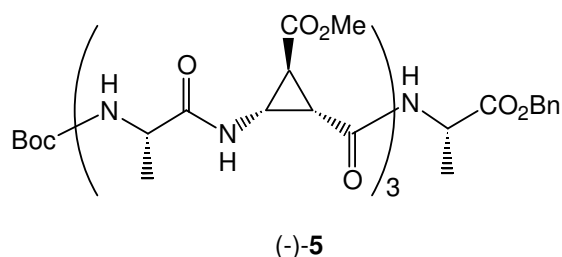
Fmoc-Asp(O^tBu)-(+)-βACC-OH, (+)-17a**:**

(1*R*,2*R*,3*R*)-2-[[((2*S*)-4-(*tert*-butoxy)-2-[(9*H*-fluoren-9-ylmethoxy)carbonyl]amino}-4-oxobutanoyl)amino]-3-(methoxycarbonyl)cyclopropanecarboxylic acid;

(+)-**17** (497mg, 0.77 mmol) was dissolved under nitrogen atmosphere in MeOH (20 ml), then 1,4-cyclohexadiene (0.49 ml, 4M in pentane, 5 eq) and Pd/C 5 % (100 mg) were added. The reaction mixture was stirred under inert atmosphere overnight, then it was filtrated on a 2 cm celite pad and concentrated to afford the product as a white solid (353 mg, 83 %). mp 88-90 °C . $[\alpha]_D^{21}$ - 21.7 (c 0.5, CH₃OH). - ¹H NMR (CD₃OD, 300 MHz): δ 1.42 (s, 9H, O^tBu), 2.37 (m, 2H, cyclopropyl-CH), 2.53 (dd, *J* = 16.2, 9.2 Hz, 1H, Asp-βCH₂), 2.75 (dd, *J* = 16.2, 4.7 Hz, 1H, Asp-βCH₂), 3.65-3.70 (m, 1H, cyclopropyl-CHN) 3.71 (s, 3H, CH₃O), 4.20-4.24 (m, 2H, Fmoc-CH₂), 4.33-4.35 (d, *J* = 6.6 Hz, 1H, Fmoc-CH), 4.47-4.51 (m, 1H, Asp-αCH), 7.29-7.40 (m, 4H, Fmoc-Ar-CH), 7.63-7.67 (m, 2H, Fmoc-Ar-CH), 7.77-7.79 (m, 2H, Fmoc-Ar-CH). - ¹³C NMR (CD₃OD, 75.5 MHz): δ 28.5 (+, cyclopropyl-CH), 28.7 (+, cyclopropyl-CH), 36.7 (+, cyclopropyl-CHN), 38.6 (-, Asp-CH₂), 48.4 (+, Fmoc-CH), 53.0 (+, CH₃O), 53.1 (+, Asp-CHN), 68.3 (-, Fmoc-CH₂), 82.5 (C_{quat}, (CH₃)C), 121.0 (+, Fmoc-Ar-CH, 2C),

126.3 (+, Fmoc-Ar-CH, 2C), 128.2 (+, Fmoc-Ar-CH, 2C), 128.8 (+, Fmoc-Ar-CH, 2C), 142.6 (C_{quat}, Fmoc-Ar-C, 2C), 145.2 (C_{quat}, Fmoc-Ar-C), 145.4 (C_{quat}, Fmoc-Ar-C), 158.4 (C_{quat}, N(CO)O), 170.7 (C_{quat}, C=O), 171.3 (C_{quat}, C=O), 175.0 (C_{quat}, C=O), 172.1 (C_{quat}, C=O), 174.5 (C_{quat}, C=O). - MS ESI (DCM/MeOH + 10 mmol/l NH₄Ac) *m/z* (%) 570.3 (MNH₄⁺, 100), 553.3 (MH⁺, 78), 497.1 (MH⁺-C₄H₈, 30). - IR 3329, 2980, 1717, 1522, 1450, 1302, 1217, 1157, 756 cm⁻¹. - HR MS calcd for C₂₉H₃₂N₂O₉+H 553.21861, found 553.21846.

E.2.2 Peptides containing (-)-βACC unit.

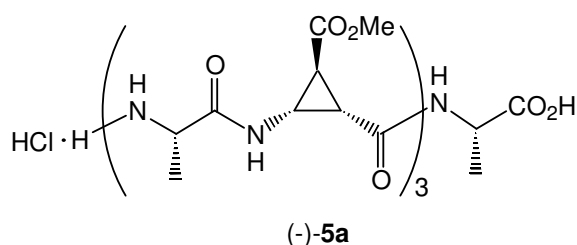


Boc-[Ala(-)-β-ACC]₃-Ala-OBn, (-)-5:

methyl(1S,2S,3S)-2-[[[(1S)-2-[[[(1S,2S,3S)-2-[[[(1S)-2-[[[(1S,2S,3S)-2-[[[(1S)-2-(benzyloxy)-1-methyl-2-oxoethyl]amino}carbonyl]-3-(methoxycarbonyl)cyclopropyl]amino]-1-methyl-2-oxoethyl]amino]carbonyl]-3-(methoxycarbonyl)cyclopropyl]amino]-1-methyl-2-oxoethyl]amino]carbonyl]-3-[(2S)-2-[(*tert*-butoxycarbonyl)amino]propanoyl]amino) cyclopropanecarboxylate;

(-)-**13** (536 mg, 0.76 mmol) was deprotected by treatment with HCl 3 M in ethyl acetate (10 ml) for 3 h at 0 °C. The solution was concentrated in vacuum, the salt was resuspended in CH₂Cl₂ (20 ml). Separately the (-)-**11** (284 mg, 0.86 mmol, 1.13 eq.) was dissolved in CH₂Cl₂ (20 ml) and cooled in an ice bath and activated with HOBt (116 mg, 0.86 mmol, 1.13 eq.) and EDC (166 mg, 0.86 mmol, 1.13 eq.). After 10 minutes the mixture of the deprotected (-)-**13** and triethylamine (0.16 ml, 1.17 mmol, 1.53 eq.) were added. The mixture was stirred at room temperature 80 h. The solution was then concentrated in vacuum and the product was obtained by chromatography (CH₂Cl₂/MeOH 25:2; R_f = 0.4) as a white solid (578 mg, 83 %). - mp 132-134 °C. - $[\alpha]_D^{21}$ -137.4 (c 1, CH₃OH). - ¹H NMR (CD₃OD, 300 MHz) δ 1.23 (d, *J* = 7.2 Hz, 3H, CH₃CH), 1.32 (d, *J* = 7.2 Hz, 3H, CH₃CH), 1.32 (d, *J* = 7.2 Hz, 3H, CH₃CH), 1.40 (d, *J* = 7.4 Hz, 3H, CH₃CH), 1.43 (s, 9H, (CH₃)₃C), 2.27 (dd, *J*

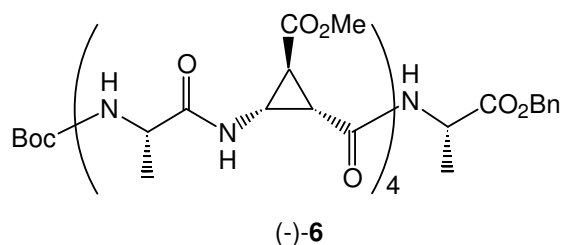
=5.2, 4.6 Hz, 1H, cyclopropyl-CH), 2.35-2.56 (m, 5H, cyclopropyl-CH), 3.48 (dd, $J = 8.2$, 4.3 Hz 1H, cyclopropyl-CHN), 3.56-3.66 (m, 2H, cyclopropyl-CHN), 3.70 (s, 3H, CH₃O), 3.71 (s, 3H, CH₃O), 3.71 (s, 3H, CH₃O), 3.96-4.05 (m, 1H, Ala-CHN), 4.25-4.37 (m, 2H, Ala-CHN), 4.51 (q, $J = 7.3$ Hz, 1H, Ala-CHN), 5.15 (d, $J = 12.3$ Hz, 1H, CH₂O), 5.22 (d, $J = 12.3$ Hz, 1H, CH₂O), 7.31-7.39 (m, 5H, Ph-CH). - ¹³C NMR (CD₃OD, 75.5 MHz) δ 16.0 (+, CH₃CH, 3C), 16.9 (+, CH₃CH), 26.4 (+, cyclopropyl-CH), 26.8 (+, cyclopropyl-CH), 26.9 (+, cyclopropyl-CH), 27.2 (+, cyclopropyl-CH, (CH₃)₃C, 6C), 35.1 (+, cyclopropyl-CHN, 2C), 35.2 (+, cyclopropyl-CHN), 48.4 (+, Ala-CHN), 49.3 (+, Ala-CHN), 49.4 (+, Ala-CHN), 50.3 (+, Ala-CHN), 51.4 (+, CH₃O, 2C), 51.4 (+, CH₃O), 66.7 (-, CH₂O), 79.3 (C_{quat}, (CH₃)₃C), 127.8 (+, Ph-CH, 2C), 128.0 (+, Ph-CH), 128.2 (+, Ph-CH, 2C), 135.7 (C_{quat}, Ph-C), 156.0 (C_{quat}, N(CO)O), 167.9 (C_{quat}, C=O), 168.1 (C_{quat}, C=O, 2C), 170.9 (C_{quat}, C=O, 2C), 171.1 (C_{quat}, C=O), 172.3 (C_{quat}, C=O), 174.3 (C_{quat}, C=O), 174.4 (C_{quat}, C=O). 175.4 (C_{quat}, C=O). - MS FAB (MeOH/Glycerin) m/z (%) 917 (MH⁺, 6), 817 (MH⁺-Boc, 100), 727 (MH⁺-Boc-Bn, 8). - IR (KBr) 3333, 2982, 1728, 1665, 1526, 1443, 1315 cm⁻¹ - HR MS calcd for C₄₂H₅₇N₇O₁₆ + H 916.39400, found 916.39560.



HCl·H-[Ala-(-)-β-ACC]₃-Ala-OH, (-)-5a:

(2S)-1-[[[(1S,2S,3S)-2-[[[(1S)-2-[[[(1S,2S,3S)-2-[[[(1S)-2-[[[(1S)-1-carboxy-ethyl]amino}carbonyl)-3-(methoxycarbonyl)cyclopropyl]amino}-1-methyl-2-oxoethyl)amino]carbonyl]-3-(methoxycarbonyl)cyclopropyl]amino}-1-methyl-2-oxoethyl)amino]carbonyl]-3-(methoxycarbonyl)cyclopropyl]amino}-1-oxo-2-propanaminium chloride; (-)-5 (100 mg, 0.109 mmol) was stirred in HCl 3 M in ethyl acetate (2 ml) at 0°C for 3 h. The solution was then concentrated in vacuum and the salt redissolved in methanol (10 ml). Then Pd/C 10 % (60 mg) and cyclohexadiene (0.17 ml, 42 % in pentane) were added. The reaction mixture was stirred overnight, filtrated over a celite pad and concentrated in vacuum to afford

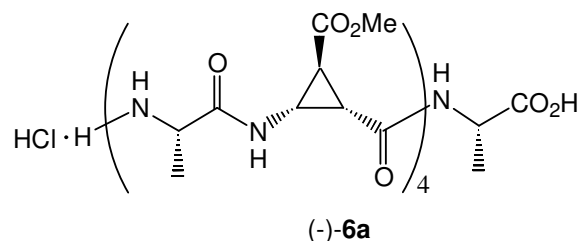
the deprotected peptide as a white solid (80 mg, 96 %). - mp 200 °C decomposed. - $[\alpha]_D^{21}$ - 168.8 (c 0.5, MeOH). - ^1H NMR (CD_3OD , 300 MHz) δ 1.32 (d, $J = 7.2$ Hz, 3H, CH_3CH), 1.35 (d, $J = 7.3$ Hz, 3H, CH_3CH), 1.44 (d, $J = 7.4$ Hz, 3H, CH_3CH), 1.46 (d, $J = 7.1$ Hz, 3H, CH_3CH), 2.28 (dd, $J = 5.4, 4.5$ Hz, 1H, cyclopropyl-CH), 2.36 (d, $J = 5.3, 4.3$ Hz, 1H, cyclopropyl-CH), 2.40 (dd, $J = 5.3, 4.7$ Hz, 1H, cyclopropyl-CH), 2.44-2.59 (m, 3H, cyclopropyl-CH), 3.40 (dd, $J = 8.3, 4.5$ Hz, 1H, cyclopropyl-CHN), 3.50-3.54 (m, 2H, cyclopropyl-CHN), 3.71 (s, 3H, CH_3O), 3.72 (s, 3H, CH_3O), 3.72 (s, 3H, CH_3O), 3.91 (q, $J = 7.0$ Hz, 1H, Ala-CHN), 4.22 (q, $J = 7.2$ Hz, 1H, Ala-CHN), 4.23 (q, $J = 7.3$ Hz, 1H, Ala-CHN), 4.39 (q, $J = 7.3$ Hz, 1H, Ala-CHN). - ^{13}C NMR (CD_3OD , 75.5 MHz) δ 17.4 (+, CH_3CH), 17.5 (+, CH_3CH), 17.6 (+, CH_3CH), 17.7 (+, CH_3CH), 27.9 (+, cyclopropyl-CH), 28.1 (+, cyclopropyl-CH), 28.7 (+, cyclopropyl-CH), 28.9 (+, cyclopropyl-CH, 2C), 29.5 (+, cyclopropyl-CH), 36.3 (+, cyclopropyl-CHN, 2C), 36.7 (+, cyclopropyl-CHN), 50.2 (+, CHN), 50.3 (+, CHN), 51.4 (+, CHN, 2C), 52.9 (+, CH_3O), 52.9 (+, CH_3O , 2C), 168.8 (C_{quat} , C=O), 169.3 (C_{quat} , C=O), 169.6 (C_{quat} , C=O), 172.4 (C_{quat} , C=O, 2C), 172.5 (C_{quat} , C=O, 2C), 176.2 (C_{quat} , C=O), 176.4 (C_{quat} , C=O), 176.6 (C_{quat} , C=O). - MS FAB (MeOH/Glycerin) m/z (%) 727 (MH^+ , 100), 369 (28), 277 (76). - IR (KBr) 3360, 3060, 2956, 1730, 1655, 1536, 1450, 1314, 1209, 1174 cm^{-1} . - HR MS calcd for $\text{C}_{30}\text{H}_{43}\text{N}_7\text{O}_{14} + \text{H}$ 726.29462, found 726.29456.



Boc-[Ala(-)-β-ACC]₄-Ala-OBn, (-)-6:

methyl (1*S*,2*S*,3*S*)-2-[[[(1*S*)-2-[[[(1*S*,2*S*,3*S*)-2-[[[(1*S*)-2-[[[(1*S*,2*S*,3*S*)-2-[[[(1*S*)-2-(benzyloxy)-1-methyl-2-oxoethyl]amino}carbonyl]-3-(methoxycarbonyl)cyclopropyl]amino]-1-methyl-2-oxoethyl]amino]carbonyl]-3-(methoxycarbonyl)cyclopropyl]amino]-1-methyl-2-oxoethyl]amino]carbonyl]-3-[[[(2*S*)-2-[[[(1*S*,2*S*,3*S*)-2-[[[(2*S*)-2-[(*tert*-butoxycarbonyl)amino]propanoyl]amino)-3-(methoxycarbonyl)cyclopropyl]carbonyl]amino)propanoyl]amino}cyclopropanecarboxylate;

(-)-**5** (200 mg, 0.22 mmol) was deprotected by treatment with HCl 3 M in ethyl acetate (10 ml) for 3 h at 0 °C. The solution was concentrated in vacuum, the salt was resuspended in CH₂Cl₂ (20 ml). Separately the (-)-**11** (100 mg, 0.30 mmol, 1.35 eq.) was dissolved in CH₂Cl₂ (20 ml) and cooled in an ice bath and activated with HOBt (41 mg, 0.30 mmol, 1.35 eq.) and EDC (58 mg, 0.30 mmol, 1.35 eq.). After 10 minutes the mixture of the deprotected (-)-**5** and triethylamine (0.052 ml, 0.32 mmol, 1.70 eq.) were added. The mixture was stirred at room temperature 48 h. The solution was then concentrated in vacuum and the product was obtained by chromatography (CH₂Cl₂/MeOH 25:2; R_f = 0.3) as a white solid (185 mg, 76%). - mp 149-151 °C. - $[\alpha]_D^{21}$ - 16.2 (c 0.5, CHCl₃). - ¹H NMR (CD₃OD, 300 MHz) δ 1.26 (d, *J* = 7.1 Hz, 3H, CH₃CH), 1.31 (d, *J* = 7.1 Hz, 3H, CH₃CH), 1.33 (d, *J* = 7.1 Hz, 3H, CH₃CH), 1.33 (d, *J* = 7.1 Hz, 3H, CH₃CH), 1.42 (d, *J* = 7.1 Hz, 3H, CH₃CH), 1.44 (s, 9H, (CH₃)₃C), 2.28 (dd, *J* = 5.2, 4.4 Hz, 1H, cyclopropyl-CH), 2.36-2.56 (m, 7H, cyclopropyl-CH), 3.46 (dd, *J* = 8.2, 4.4 Hz 1H, cyclopropyl-CHN), 3.52 (dd, *J* = 8.2, 4.4 Hz 1H, cyclopropyl-CHN), 3.58-3.66 (m, 2H, cyclopropyl-CHN), 3.71 (s, 3H, CH₃O), 3.71 (s, 3H, CH₃O), 3.71 (s, 3H, CH₃O), 3.72 (s, 3H, CH₃O), 4.05 (q, *J* = 7.1 Hz, 1H, Ala-CHN), 4.30 (q, *J* = 7.1 Hz, 1H, Ala-CHN), 4.33 (q, *J* = 7.1 Hz, 1H, Ala-CHN), 4.37 (q, *J* = 7.1 Hz, 1H, Ala-CHN), 4.53 (q, *J* = 7.1 Hz, 1H, Ala-CHN), 5.17 (d, *J* = 12.4 Hz, 1H, CH₂O), 5.24 (d, *J* = 12.3 Hz, 1H, CH₂O), 7.30-7.41 (m, 5H, Ph-CH). - ¹³C NMR (CD₃OD, 75.5 MHz) δ 16.0 (+, CH₃CH), 16.1 (+, CH₃CH), 16.1 (+, CH₃CH), 16.2 (+, CH₃CH), 16.9 (+, CH₃CH), 26.4 (+, cyclopropyl-CH), 26.7 (+, cyclopropyl-CH), 26.8 (+, cyclopropyl-CH), 26.9 (+, cyclopropyl-CH), 27.3 (+, cyclopropyl-CH, (CH₃)₃C, 3C), 27.3 (+, cyclopropyl-CH), 27.5 (+, cyclopropyl-CH), 27.6 (+, cyclopropyl-CH), 35.1 (+, cyclopropyl-CHN, 3C), 35.2 (+, cyclopropyl-CHN), 49.3 (+, Ala-CHN, 3C), 49.4 (+, Ala-CHN), 50.3 (+, Ala-CHN), 51.4 (+, CH₃O, 2C), 51.4 (+, CH₃O, 2C), 66.6 (-, CH₂O), 79.3 (C_{quat}, (CH₃)₃C), 127.7 (+, Ph-CH, 2C), 128.0 (+, Ph-CH), 128.2 (+, Ph-CH, 2C), 135.7 (C_{quat}, Ph-C), 156.0 (C_{quat}, N(CO)O), 167.9 (C_{quat}, C=O), 168.0 (C_{quat}, C=O), 168.1 (C_{quat}, C=O, 2C), 170.9 (C_{quat}, C=O, 2C), 171.0 (C_{quat}, C=O, 2C), 172.3 (C_{quat}, C=O), 174.3 (C_{quat}, C=O), 174.4 (C_{quat}, C=O, 2C), 175.4 (C_{quat}, C=O). - MS FAB (MeOH/Glycerin) *m/z* (%) 1150 (MNa⁺, 2), 1128 (MH⁺, 4), 1028 (MH⁺-Boc, 100). - IR (KBr) 3304, 2963, 1730, 1649, 1523, 1447, 1313, 1169, 752 cm⁻¹. - HR MS calcd for C₅₁H₆₉N₉O₂₀ + H 1128.47390, found 1128.4737.

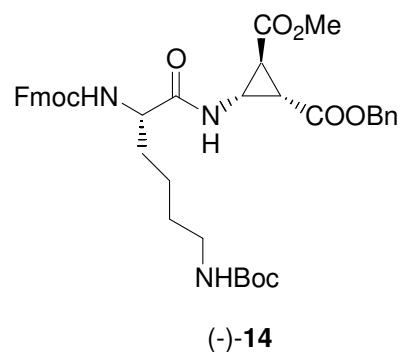


HClH-[Ala-(-)-β-ACC]₄-Ala-OH, (-)-6a:

(2S)-1-[[[(1S,2S,3S)-2-[[[(1S)-2-[[[(1S,2S,3S)-2-[[[(1S)-2-[[[(1S,2S,3S)-2-[[[(1S)-1-carboxyethyl]amino}carbonyl]-3-(methoxycarbonyl)cyclopropyl]amino}-1-methyl-2-oxoethyl)amino]carbonyl]-3-(methoxycarbonyl)cyclopropyl]amino}-1-methyl-2-oxoethyl)amino]carbonyl]-3-(methoxycarbonyl)cyclopropyl]amino}-1-methyl-2-oxoethyl)amino]carbonyl]-3-(methoxycarbonyl)cyclopropyl]amino}-1-oxo-2-propan-aminium chloride

(-)-6 (100 mg, 0.09 mmol) was stirred in HCl 3 M in ethyl acetate (2 ml) at 0°C for 3 h. The solution was then concentrated in vacuum and the salt redissolved in methanol (10 ml). Then Pd/C 10 % (30 mg) and cyclohexadiene (0.14 ml, 42 % in pentane) were added. The reaction mixture was stirred overnight, filtrated over a celite pad and concentrated in vacuum to afford the deprotected peptide as a white solid (80 mg, 96 %). - mp 170 °C decomposed. - $[\alpha]_D^{21}$ - 46.6 (c 0.5, CHCl₃). - ¹H NMR (CD₃OD, 300 MHz) δ 1.34 (d, *J* = 7.1 Hz, 3H, CH₃CH), 1.35 (d, *J* = 7.1 Hz, 3H, CH₃CH), 1.36 (d, *J* = 7.1 Hz, 3H, CH₃CH), 1.44 (d, *J* = 7.4 Hz, 3H, CH₃CH), 1.48 (d, *J* = 7.1 Hz, 3H, CH₃CH), 2.30-2.33 (m, 2H, cyclopropyl-CH), 2.37-2.42 (m, 2H, cyclopropyl-CH), 2.47-2.60 (m, 4H, cyclopropyl-CH), 3.42 (dd, *J* = 6.3, 4.5 Hz, 1H, cyclopropyl-CHN), 3.45 (dd, *J* = 6.6, 4.4 Hz, 1H, cyclopropyl-CHN), 3.57 (dd, *J* = 8.4, 4.8 Hz, 1H, cyclopropyl-CHN), 3.61 (dd, *J* = 8.5, 4.4 Hz, 1H, cyclopropyl-CHN), 3.73 (s, 3H, CH₃O), 3.73 (s, 3H, CH₃O), 3.73 (s, 3H, CH₃O), 3.73 (s, 3H, CH₃O), 3.93 (q, *J* = 7.0 Hz, 1H, Ala-CHN), 4.21 (q, *J* = 7.2 Hz, 1H, Ala-CHN), 4.22 (q, *J* = 7.2 Hz, 1H, Ala-CHN), 4.38 (q, *J* = 7.1 Hz, 1H, Ala-CHN), 4.40 (q, *J* = 7.5 Hz, 1H, Ala-CHN). - ¹³C NMR (CD₃OD, 75.5 MHz) δ 15.9 (+, CH₃CH), 16.0 (+, CH₃CH), 16.1 (+, CH₃CH), 16.1 (+, CH₃CH), 16.2 (+, CH₃CH), 26.2 (+, cyclopropyl-CH), 26.6 (+, cyclopropyl-CH), 27.2 (+, cyclopropyl-CH, 2C), 27.3 (+, cyclopropyl-CH), 27.4 (+, cyclopropyl-CH), 27.6 (+, cyclopropyl-CH), 27.9 (+, cyclopropyl-CH), 34.8 (+, cyclopropyl-CHN), 34.9 (+, cyclopropyl-CHN), 35.0 (+, cyclopropyl-CHN), 35.0 (+, cyclopropyl-CHN), 48.5 (+, Ala-CHN), 48.8 (+, Ala-CHN), 49.4 (+, Ala-CHN), 49.7 (+, Ala-CHN), 50.1 (+, Ala-CHN), 51.4 (+, CH₃O, 4C), 167.3 (C_{quat},

C=O), 167.9 (C_{quat}, C=O), 168.0 (C_{quat}, C=O, 2C), 170.7 (C_{quat}, C=O, 2C), 170.9 (C_{quat}, C=O), 171.0 (C_{quat}, C=O), 173.7 (C_{quat}, C=O), 174.3 (C_{quat}, C=O), 174.6 (C_{quat}, C=O), 174.8 (C_{quat}, C=O), 174.9 (C_{quat}, C=O).-MS FAB (MeOH/Glycerin) *m/z* (%) 938 (MH⁺, 100). - IR (KBr) 3362, 3060, 2960, 1725, 1645, 1520, 1440, 1315, 1210, 1120 cm⁻¹. - HR MS calcd for C₃₉H₅₅N₉O₁₈ + H 938.3743, found 938.3759.



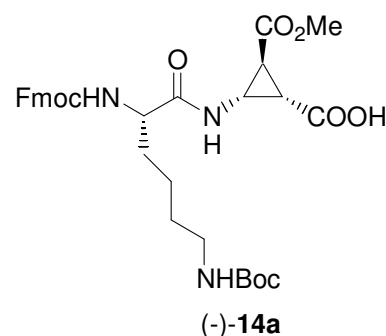
Fmoc-Lys(Boc)-(-)-βACC-OBn, (-)-14:

1-methyl 2-phenyl (1*S*,2*S*,3*R*)-3-[(*(2S)*-6-[(*tert*-butoxycarbonyl)amino]-2-[(*(9H*-fluoren-9-ylmethoxy)carbonyl]amino}hexanoyl)amino]-1,2-cyclopropanedicarboxylate;

A solution of (-)-9 (300 g, 0.86 mmol) in HCl 3 M in ethyl acetate (33 ml) was stirred at 0 °C for 3 h. The solvent was evaporated the solid was resuspended in CH₂Cl₂ (30ml) and a solution of Fmoc-Lys(Boc)-OH (806 mg, 1.72 mmol, 2 eq.), EDC (330 mg, 1.72 mmol, 2 eq) and HOBt (209 mg, 1.55 mmol, 1.8 eq.) in CH₂Cl₂ (50 ml) (previously stirred 1 h at 0 °C) was added. pyridine (123 μl, 1.55 mmol, 1.8 eq.) was then added dropwise. The mixture was stirred overnight at room temperature. The solution was washed with saturated NaHCO₃ (50 ml), 1 M KHSO₄ (50 ml) and saturated NaHCO₃ (50 ml). The organic phase was dried over Na₂SO₄ and concentrated. The product was purified by chromatography (CH₂Cl₂/MeOH 50:1; R_f = 0.2). 640 mg, 70 %.

mp 118-120 °C. $[\alpha]_D^{21}$ - 7.6 (c 0.5, CHCl₃). - ¹H NMR (CDCl₃, 300 MHz) δ 1.28-1.39 (m, 2H, Lys-γ-CH₂), 1.44 (s, 9H, Boc), 1.44-1.56 (m, 2H, Lys-δ-CH₂), 1.57-1.65 (m, 1H, Lys-β-CH₂), 1.81-1.88 (m, 1H, Lys-β-CH₂), 2.30 (dd, *J* = 5.0, 4.8 Hz, 1H, cyclopropyl-CH), 2.55 (dd, *J* = 8.2, 4.8 Hz, 1H, cyclopropyl-CH), 3.05-3.15 (m, 2H, Lys-ε-CH₂), 3.70 (s, 3H, CH₃O), 4.00-4.12 (m, 2H, cyclopropyl-CHN, Lys-α-CH) 4.24 (t, 1H, *J* = 7.1 Hz, Fmoc-CH), 4.37 (dd, *J* = 10.2, 7.1 Hz, 1H, Fmoc-CH₂), 4.48 (dd, *J* = 10.2, 7.1 Hz, 1H, Fmoc-CH₂), 4.58-4.63 (m, 1H,

NH), 5.03 (d, $J = 12.2$ Hz, 1H, CH₂O), 5.13 (d, $J = 12.2$ Hz, 1H, CH₂O), 7.11 (d, $J = 6.9$ Hz, 1H, NH), 7.28-7.42 (m, 9H, Ar-CH), 7.60-7.62 (m, 2H, Fmoc-Ar-CH), 7.75-7.78 (m, 2H, Fmoc-Ar-CH). - ¹³C NMR (CDCl₃, 75.5 MHz): δ 22.5 (-, Lys- γ -CH₂), 26.2 (+, cyclopropyl-CH), 28.4 (+, 3C, C(CH₃)₃) 28.7 (+, cyclopropyl-CH), 29.7 (-, Lys- δ -CH₂), 31.7 (-, Lys- β -CH₂), 35.9 (+, cyclopropyl-CHN), 39.9 (-, Lys- ϵ -CH₂), 47.2 (+, Fmoc-CH), 52.5 (+, CH₃O), 54.9 (+, Lys-CHN), 67.1 (-, Fmoc-CH₂), 67.4 (-, Bn-CH₂), 79.2 (C_{quat}, (CH₃)₃C), 120.0 (+, Fmoc-Ar-CH, 2C), 125.1 (+, Fmoc-Ar-CH, 2C), 127.1 (+, Fmoc-Ar-CH, 2C), 127.4 (+, Fmoc-Ar-CH, 2C), 128.5 (+, Bn-Ar-CH, 2C), 128.6 (+, Bn-Ar-CH), 128.7 (+, Bn-Ar-CH, 2C), 135.0 (C_{quat}, Bn-Ar-C), 141.3 (C_{quat}, Fmoc-Ar-C, 2C), 143.7 (C_{quat}, Fmoc-Ar-C), 144.0 (C_{quat}, Fmoc-Ar-C), 156.2 (C_{quat}, N(CO)O, 2C), 169.8 (C_{quat}, C=O), 169.9 (C_{quat}, C=O), 172.4 (C_{quat}, C=O). - MS ESI (DCM/MeOH + 10 mmol/l NH₄Ac) m/z (%) 700 (MH⁺, 50) 600 (MH⁺-Boc) - IR 3312, 2951, 1715, 1520, 1450, 1248, 1171, 758 cm⁻¹. - HR MS calcd for C₃₉H₄₅N₃O₉ + H 700.3234, found 700.3223.



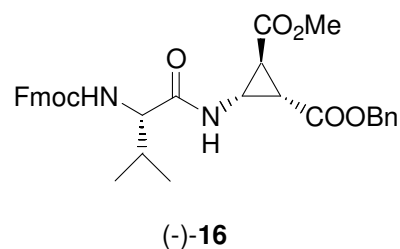
Fmoc-Lys(Boc)-(-)- β ACC-OH, (-)-**14a**:

(1S,2S,3S)-2-[(2S)-6-[(*tert*-butoxycarbonyl)amino]-2-[(9H-fluoren-9-ylmethoxy)carbonyl]amino}hexanoyl)amino]-3-(methoxycarbonyl)cyclopropanecarboxylic acid;

(-)-**14** (600 mg, 0.86 mmol) was dissolved under nitrogen atmosphere in MeOH (40 ml), then 1,4-cyclohexadiene 4M in pentane (1.1 ml, 5 eq.) and Pd/C 5 % (240 mg) were added. The reaction mixture was stirred under inert atmosphere overnight, then it was filtrated on a 2 cm celite pad and concentrated to afford the product as a white solid (420 mg, 80%).

mp 67-69 °C. [α]_D²¹ - 5.8 (c 0.5, CH₃OH). - ¹H NMR (CD₃OD, 300 MHz) δ 1.17-1.27 (m, 2H, Lys- γ -CH₂), 1.41 (s, 9H, Boc), 1.41-1.49 (m, 2H, Lys- δ -CH₂), 1.58-1.78 (m, 2H, Lys- β -CH₂), 2.29-2.41 (m, 2H, cyclopropyl-CH), 3.00-3.03 (m, 2H, Lys- ϵ -CH₂), 3.70 (s, 3H, CH₃O), 4.03 (dd, $J = 9.3, 5.2$ Hz, 1H, cyclopropyl-CHN) 4.09 (q, $J = 7.1$ Hz, 1H, Lys- α -CH), 4.15-4.23

(m, 1H, Fmoc-CH), 4.33-4.40 (m, 2H, Fmoc-CH₂), 7.28-7.40 (m, 4H, Ar-CH), 7.64-7.68 (m, 2H, Fmoc-Ar-CH), 7.77-7.80 (m, 2H, Fmoc-Ar-CH). - ¹³C NMR (CD₃OD, 75.5 MHz): δ 24.2 (-, Lys-γ-CH₂), 28.6 (+, cyclopropyl-CH), 28.8 (+, cyclopropyl-CH), 28.9 (+, 3C, C(CH₃)₃), 30.5 (-, Lys-δ-CH₂), 32.3 (-, Lys-β-CH₂, 1C), 32.8 (-, Lys-β-CH₂, 1C), 36.6 (+, cyclopropyl-CHN), 41.1 (-, Lys-ε-CH₂), 48.5 (+, Fmoc-CH), 52.9 (+, CH₃O), 56.7 (+, Lys-CHN), 68.0 (-, Fmoc-CH₂), 79.9 (C_{quat}, (CH₃)₃C), 121.0 (+, Fmoc-Ar-CH, 2C), 126.3 (+, Fmoc-Ar-CH, 2C), 128.2 (+, Fmoc-Ar-CH, 2C), 128.9 (+, Fmoc-Ar-CH, 2C), 142.7 (C_{quat}, Fmoc-Ar-C, 2C), 145.2 (C_{quat}, Fmoc-Ar-C), 145.4 (C_{quat}, Fmoc-Ar-C), 158.6 (C_{quat}, N(CO)O, 2C), 172.3 (C_{quat}, C=O), 174.7 (C_{quat}, C=O), 176.1 (C_{quat}, C=O). - MS FAB (MeOH/Glycerin) *m/z* (%) 610 (MH⁺, 10), 554 (15), 510 (M-Boc, 100) - IR 3338, 2951, 1707, 1522, 1450, 1366, 1250, 1171, 1043, 741 cm⁻¹. - HR MS calcd for C₃₂H₃₉N₃O₉ + H 610.2765, found 610.2757.

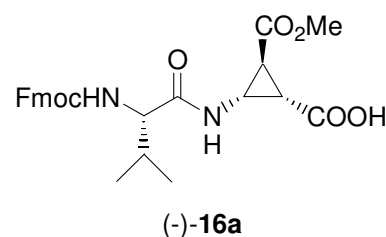


Fmoc-Val-(-)-βACC-OBn, (-)-16:

1-methyl 2-phenyl (1*S*,2*S*,3*R*)-3-[[[(2*S*)-2-[(9*H*-fluoren-9-ylmethoxy)carbonyl]amino]-3-methylbutanoyl]amino]-1,2-cyclopropanedicarboxylate;

A solution of (-)-9 (514 g, 1.47 mmol) in HCl 3 M in ethyl acetate (56 ml) was stirred at 0 °C for 3 h. The solvent was evaporated the solid was resuspended in CH₂Cl₂ (40 ml) Fmoc-Val-OH (650 mg, 1.91 mmol, 1.3 eq.), EDC (508 mg, 2.65 mmol, 1.8 eq) and pyridine (153 μl, 1.91 mmol, 1.3 eq.) were added. The mixture was stirred overnight at room temperature. The solution was washed with saturated NaHCO₃ (50 ml), 1 M KHSO₄ (50 ml) and saturated NaHCO₃ (50 ml). The organic phase was dried over Na₂SO₄ and concentrated. The product was purified by chromatography (CH₂Cl₂/MeOH 50:1; R_f = 0.2). 735 mg, 88 % - mp 175-177 °C. [α]_D²¹ -9.2 (c 0.5, CHCl₃). - ¹H NMR (CDCl₃, 300 MHz): δ 0.89 (d, *J* = 6.9 Hz, 3H,

Val-CH₃), 0.96 (d, $J = 6.9$ Hz, 3H, Val-CH₃), 2.09-2.20 (m, 1H, Val-βCH), 2.29 (dd, $J = 5.2, 4.8$ Hz, 1H, cyclopropyl-CH), 2.57 (dd, $J = 8.2, 5.2$ Hz, 1H, cyclopropyl-CH), 3.71 (s, 3H, CH₃O), 4.00 (dd, $J = 8.1, 5.9$, 1H, Val-αCH) 4.11 (m, 1H, cyclopropyl-CHN), 4.24 (t, $J = 6.9$ Hz, 1H, Fmoc-CH), 4.42 (d, $J = 6.9$ Hz, 2H, Fmoc-CH₂), 5.08 (d, $J = 12.2$ Hz, 1H, CH₂O), 5.17 (d, $J = 12.2$ Hz, 1H, CH₂O), 5.29 (d, $J = 8.1$ Hz, 1H, Val-NH), 6.97 (d, $J = 7.7$ Hz, 1H, cyclopropyl-NH), 7.29-7.43 (m, 9H, Ar-CH), 7.60-7.62 (m, 2H, Fmoc-Ar-CH), 7.75-7.78 (m, 2H, Fmoc-Ar-CH). - ¹³C NMR (CDCl₃, 75.5 MHz): δ 17.6 (+, Val-CH₃), 19.2 (+, Val-CH₃), 26.0 (+, cyclopropyl-CH), 28.9 (+, cyclopropyl-CH), 30.9 (+, Val-βCH), 35.9 (+, cyclopropyl-CHN), 47.2 (+, Fmoc-CH), 52.5 (+, CH₃O), 60.3 (+, Val-CHN), 67.1 (-, Fmoc-CH₂), 67.6 (-, Bn-CH₂), 120.0 (+, Fmoc-Ar-CH, 2C), 125.1 (+, Fmoc-Ar-CH, 2C), 127.1 (+, Ar-CH, 2C), 127.8 (+, Ar-CH, 2C), 128.5 (+, Ar-CH, 2C), 128.6 (+, Ar-CH), 128.7 (+, Ar-CH, 2C), 134.9 (C_{quat}, Ph-C), 141.3 (C_{quat}, Fmoc-Ar-C, 2C), 143.8 (C_{quat}, Fmoc-Ar-C, 2C), 156.4 (C_{quat}, N(CO)O), 169.8 (C_{quat}, C=O), 170.1 (C_{quat}, C=O), 171.9 (C_{quat}, C=O). - MS ESI (DCM/MeOH + 10 mmol/l NH₄Ac) m/z (%) 593 (MNa⁺, 11), 588 (MNH₄⁺, 40) 571 (MH⁺, 100). - IR 3306, 2957, 1726, 1664, 1533, 1450, 1294, 1219, 1171, 771 cm⁻¹. - Anal. Calcd for C₃₃H₃₄N₂O₇ C, 69.46; H, 6.01; N, 4.91. Found: C, 68.85; H, 5.77; N, 4.54.

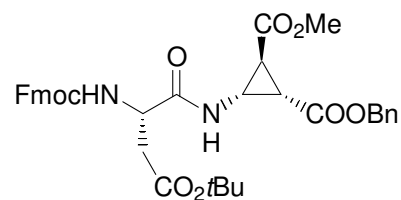


Fmoc-Val-(-)-βACC-OH, (-)-16a:

(1S,2S,3S)-2-[(2S)-2-[(9H-fluoren-9-ylmethoxy)carbonyl]amino]-3-methylbutanoyl) amino]-3-(methoxycarbonyl)cyclopropanecarboxylic acid;

(-)-**16** (150 mg, 0.35 mmol) was dissolved under nitrogen atmosphere in MeOH (20 ml), then 1,4-cyclohexadiene 4M in pentane (332 μl, 5 eq) and Pd/C 5% (80 mg) were added. The reaction mixture was stirred under inert atmosphere overnight, then it was filtrated on a 2 cm celite pad and concentrated to afford the product as a white solid (156 mg, 93 %).

mp 180 decomposed °C . $[\alpha]_D^{21}$ - 26.7 (c 0.5, CH₃OH). - ¹H NMR (CD₃OD, 600 MHz): δ 0.93 (d, *J* = 5.5 Hz, 6H, Val-CH₃), 2.07-2.11 (m, 1H, Val-βCH), 2.25 (dd, *J* = 5.3, 4.2 Hz, 1H, cyclopropyl-CH), 2.29 (dd, *J* = 7.8, 5.3 Hz, 1H, cyclopropyl-CH), 3.68 (s, 3H, CH₃O), 3.72 (dd, *J* = 7.8, 4.2 Hz, 1H, cyclopropyl-CHN), 3.85 (d, *J* = 7.2 Hz, 1H, Val-αCH), 4.22 (t, *J* = 7.1 Hz, 1H, Fmoc-CH), 4.34 (dd, *J* = 10.2, 7.1 Hz, 1H, Fmoc-CH₂), 4.41 (dd, *J* = 10.2, 7.1 Hz, 1H, Fmoc-CH₂), 7.29-7.40 (m, 4H, Ar-CH), 7.66 (m, 2H, Fmoc-Ar-CH), 7.79 (m, 2H, Fmoc-Ar-CH). - ¹³C NMR (CD₃OD, 150.9 MHz): δ 18.6 (+, Val-CH₃), 19.8 (+, Val-CH₃), 28.6 (+, cyclopropyl-CH), 29.9 (+, cyclopropyl-CH), 31.5 (+, Val-βCH), 36.4 (+, cyclopropyl-CHN), 48.4 (+, Fmoc-CH), 52.7 (+, CH₃O), 62.5 (+, Val-CHN), 68.2 (-, Fmoc-CH₂), 120.9 (+, Fmoc-Ar-CH, 2C), 126.3 (+, Fmoc-Ar-CH, 2C), 128.1 (+, Fmoc-Ar-CH, 2C), 128.2 (+, Fmoc-Ar-CH, 2C), 128.8 (+, Fmoc-Ar-CH, 2C), 142.6 (C_{quat}, Fmoc-Ar-C, 2C), 145.0 (C_{quat}, Fmoc-Ar-C), 145.3 (C_{quat}, Fmoc-Ar-C) 158.8 (C_{quat}, N(CO)O), 172.8 (C_{quat}, C=O, CH₃O), 174.8 (C_{quat}, Val-C=O), 176.5 (C_{quat}, C=O, CO₂H). - MS FAB (MeOH/Glycerine) *m/z* (%) 999 (2M+K⁺, 40), 961 (2M+H⁺, 10), 519 (MK⁺, 20) 481 (MH⁺, 100). - IR 3320, 2957, 1718, 1670, 1450, 1275, 1171, 1034, 770 cm⁻¹. - HR MS calcd for C₂₆H₂₈N₂O₇ + H 481.1975, found 481.1975



(-)-17

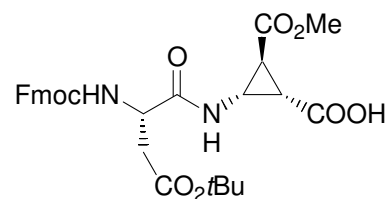
Fmoc-Asp(O^tBu)-(-)-βACC-OBn, (-)-17:

1-methyl 2-phenyl (1*S*,2*S*,3*R*)-3-[[[(2*S*)-4-(*tert*-butoxy)-2-[[[(9*H*-fluoren-9-ylmethoxy) carbonyl]amino]-4-oxobutanoyl]amino]-1,2-cyclopropanedicarboxylate;

A solution of (-)-**9** (300 g, 0.86 mmol) in HCl 3 M in ethyl acetate (35 ml) was stirred at 0 °C for 3 h. The solvent was evaporated the solid was resuspended in CH₂Cl₂ (30 ml) and a solution of Fmoc-Asp(O^tBu)-OH (708 mg, 1.72 mmol, 2 eq.), EDC (330 mg, 1.72 mmol, 2 eq) and HOBt (209 mg, 1.55 mmol, 1.8 eq.) in CH₂Cl₂ (40 ml) (previously stirred 1 h at 0 °C) was added. Pyridine (123 μl, 1.55 mmol, 1.8 eq.) was then added dropwise. The

mixture was stirred overnight at room temperature. The solution was washed with saturated NaHCO_3 (50 ml), 1 M KHSO_4 (50 ml) and saturated NaHCO_3 (50 ml). The organic phase was dried over Na_2SO_4 and concentrated. The product was purified by chromatography (PE/EA 3:1; $R_f = 0.1$). 408 mg, 74 %

mp 75-77 °C . $[\alpha]_D^{21} + 5.0$ (c 0.5, CH_3OH). - ^1H NMR (CDCl_3 , 300 MHz): δ 1.46 (s, 9H, *OtBu*), 2.32 (dd, $J = 5.1, 4.9$ Hz, 1H, cyclopropyl-CH), 2.56 (dd, $J = 8.2, 5.1$ Hz, 1H, cyclopropyl-CH), 2.62 (dd, $J = 16.9, 5.0$ Hz, 1H, Asp- βCH_2), 2.93 (dd, $J = 17.0, 4.7$ Hz, 1H, Asp- βCH_2), 3.70 (s, 3H, CH_3O), 4.06-4.13 (m, 1H, cyclopropyl-CHN), 4.25-4.30 (m, 1H, Fmoc-CH), 4.33-4.39 (m, 1H, Fmoc- CH_2), 4.47-4.55 (m, 2H, Fmoc- CH_2 , Asp- αCH), 5.03 (d, $J = 12.2$ Hz, 1H, CH_2O), 5.12 (d, $J = 12.2$ Hz, 1H, CH_2O), 5.86 (d, $J = 8.8$ Hz, 1H, Asp-NH), 7.29-7.43 (m, 4H, Fmoc-Ar-CH), 7.52 (d, $J = 8.0$ Hz, 1H, $\beta\text{ACC-NH}$), 7.61-7.64 (m, 2H, Fmoc-Ar-CH), 7.77 (pseudo d, $J = 7.7$ Hz, 2H, Fmoc-Ar-CH). - ^{13}C NMR (CDCl_3 , 75.5 MHz): δ 26.1 (+, cyclopropyl-CH), 28.1 (+, $(\text{CH}_3)_3\text{C}$), 28.6 (+, cyclopropyl-CH), 36.1 (+, cyclopropyl-CHN), 36.8 (-, Asp- CH_2), 47.1 (+, Fmoc-CH), 51.3 (+, Asp-CHN), 52.5 (+, CH_3O), 67.4 (-, Fmoc- CH_2 , 1C), 67.5 (-, Bn- CH_2 , 1C), 81.9 (C_{quat} , $(\text{CH}_3)_3\text{C}$), 120.0 (+, Fmoc-Ar-CH, 2C), 125.2 (+, Fmoc-Ar-CH, 2C), 127.1 (+, Fmoc-Ar-CH), 127.2 (+, Fmoc-Ar-CH), 127.8 (+, Ar-CH, 2C), 128.4 (+, Ar-CH, 2C), 128.5 (+, Ar-CH, 1C), 128.7 (+, Ar-CH, 2C), 135.0 (C_{quat} , Ph-Ar-C), 141.3 (C_{quat} , Fmoc-Ar-C, 2C), 143.7 (C_{quat} , Fmoc-Ar-C), 143.9 (C_{quat} , Fmoc-Ar-C), 156.2 (C_{quat} , $\text{N}(\text{CO})\text{O}$), 169.8 (C_{quat} , $\text{C}=\text{O}$), 169.9 (C_{quat} , $\text{C}=\text{O}$), 171.0 (C_{quat} , $\text{C}=\text{O}$), 172.2 (C_{quat} , $\text{C}=\text{O}$). - MS FAB (MeOH/Glycerine) 643 (MH^+ , 86), 587 (100). - IR 3329, 2978, 1718, 1522, 1308, 1217, 1169, 1051, 741 cm^{-1} . - HR MS calcd for $\text{C}_{36}\text{H}_{38}\text{N}_2\text{O}_9 + \text{H}$ 643.2656, found 643.2650.

(-)-**17a**

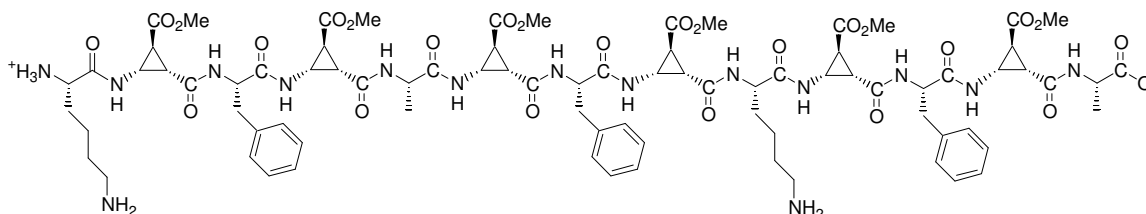
Fmoc-Asp(O^tBu)-(-)-βACC-OH, (-)-17a**:**

(1*S*,2*S*,3*S*)-2-(((2*S*)-4-(*tert*-butoxy)-2-[(9*H*-fluoren-9-ylmethoxy)carbonyl]amino)-4-oxobutanoyl)amino]-3-(methoxycarbonyl)cyclopropanecarboxylic acid;

(-)-**17** (300 mg, 0.47 mmol) was dissolved under nitrogen atmosphere in MeOH (30 ml), then 1,4-cyclohexadiene 4M in pentane (0.60 ml, 5 eq.) and Pd/C 5 % (120 mg) were added. The reaction mixture was stirred under inert atmosphere overnight, then it was filtrated on a 2 cm celite pad and concentrated to afford the product as a white solid (227 mg, 88.%).

mp 78-80 °C . $[\alpha]_D^{21}$ -10.42 (c 0.5, CH₃OH). - ¹H NMR (CD₃OD, 300 MHz): δ 1.42 (s, 9H, OtBu), 2.32-2.39 (m, 2H, cyclopropyl-CH), 2.54 (dd, *J* = 16.2, 8.8 Hz, 1H, , Asp-βCH₂), 2.78 (dd, *J* = 16.2, 5.2 Hz, 1H, , Asp-βCH₂), 3.65 (dd, *J* = 7.9, 4.9 Hz, 1H, cyclopropyl-CHN) 3.71 (s, 3H, CH₃O), 4.20-4.25 (m, 1H, Fmoc-CH), 4.33-4.38 (m, 2H, Fmoc-CH₂), 4.49 (dd, *J* = 8.7, 5.2 Hz, 1H, Asp-αCH), 7.27-7.40 (m, 4H, Fmoc-Ar-CH), 7.66 (pseudo t, *J* = 6.4 Hz, 2H, Fmoc-Ar-CH), 7.66 (pseudo d, *J* = 7.8 Hz, 2H, Fmoc-Ar-CH). - ¹³C NMR (CD₃OD, 75.5 MHz): δ 28.4 (+, cyclopropyl-CH), 28.8 (+, cyclopropyl-CH), 36.7 (+, cyclopropyl-CHN), 38.6 (-, Asp-CH₂), 48.4 (+, Fmoc-CH), 53.0 (+, CH₃O), 53.4 (+, Asp-CHN), 68.4 (-, Fmoc-CH₂), 82.5 (C_{quat}, (CH₃)C), 121.0 (+, Fmoc-Ar-CH, 2C), 128.3 (+, Fmoc-Ar-CH, 2C), 128.9 (+, Fmoc-Ar-CH, 2C), 129.9 (+, Fmoc-Ar-CH, 2C), 142.6 (C_{quat}, Fmoc-Ar-C, 2C), 145.2 (C_{quat}, Fmoc-Ar-C), 145.4 (C_{quat}, Fmoc-Ar-C), 158.4 (C_{quat}, N(CO)O), 171.3 (C_{quat}, C=O), 172.3 (C_{quat}, C=O), 172.8 (C_{quat}, C=O), 174.4 (C_{quat}, C=O), 174.5 (C_{quat}, C=O). - MS FAB (MeOH/Glycerine) *m/z* (%) 553 (MH⁺, 12), 497 (MH⁺-^tBu, 62), 275 (100). - IR 3337, 3066, 2979, 1724, 1530, 1449, 1370, 1302 cm⁻¹. - HR MS calcd for C₂₉H₃₂N₂O₉ + H 553.21861, found 553.21846.

E.3 Solid phase synthesis



H-Lys-(-)-βACC-Phe-(-)-βACC-Ala-(-)-βACC-Phe-(-)-βACC-Lys-(-)-βACC-Phe-(-)-βACC-Ala-OH

(-)-7

It was synthesized using a solid phase protocol. It was carried out by manual coupling using Fmoc/^tBu strategy on the acid labile HMPA-AM resin (130 mg).

The first amino acid, alanine (92 mg), was attached activating the carboxylic function with DIC (0.046 ml) and HOBt (40 mg) in the presence of DMAP (1.44 mg) in CH₂Cl₂/DMF 9:1, stirring overnight. The loading of the resin was determined spectrophotometrically by Fmoc cleavage with piperidine in DMF (theoretical loading: 0.91 mmol/gr; found: 0.6 mmol/gr). After capping by treatment with acetic anhydride and DIPEA in DMF, the peptide chain was assembled by single manual coupling of the dipeptides Fmoc-Xaa-βACC-OH (3-3.8 eq) activated by DIC/HOBt (1 eq in respect of the dipeptide) overnight in DCM/DMF 9:1 in the presence of DIPEA (2 eq in respect of dipeptide). The deprotection of the Fmoc was performed by treatment with 20% piperidine in DMF, one cycles of 10 and one of 15 minutes. After every two coupling-steps small scale cleavages were performed to control with analytical HPLC and mass analysis the growing peptide chain.

The cleavage of the peptide from the resin with simultaneous side chains deprotection was achieved by treatment with a TFA/water/TIS mixture (95:5:5) for 2,5 hours. The peptide was precipitated from ice-cold diethyl ether and recovered by centrifugation. The purification was achieved by using RP-preparative HPLC and the product (-)-7 was characterized by analytical HPLC and MALDI-MS spectroscopy.

MALDI MS: calcd for C₈₁H₁₀₅N₁₅O₂₆ + H 1705.8, found 1705.6.

F. Appendix of NMR and X-Ray Data

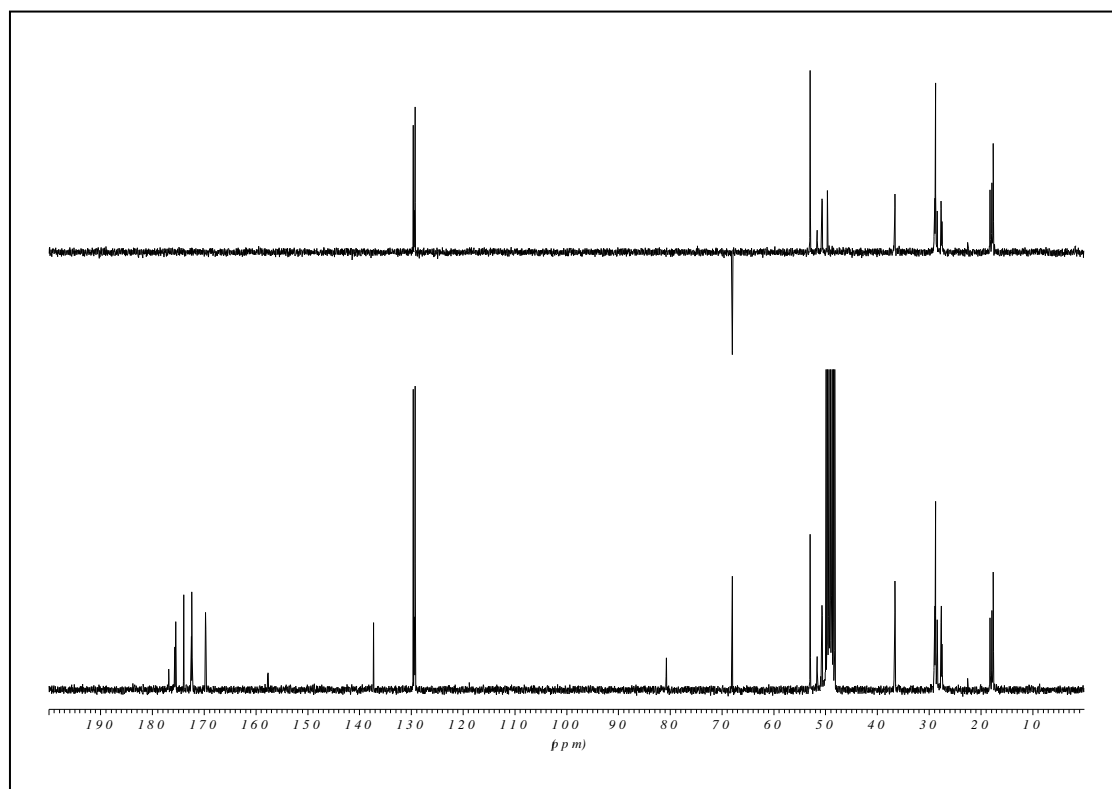
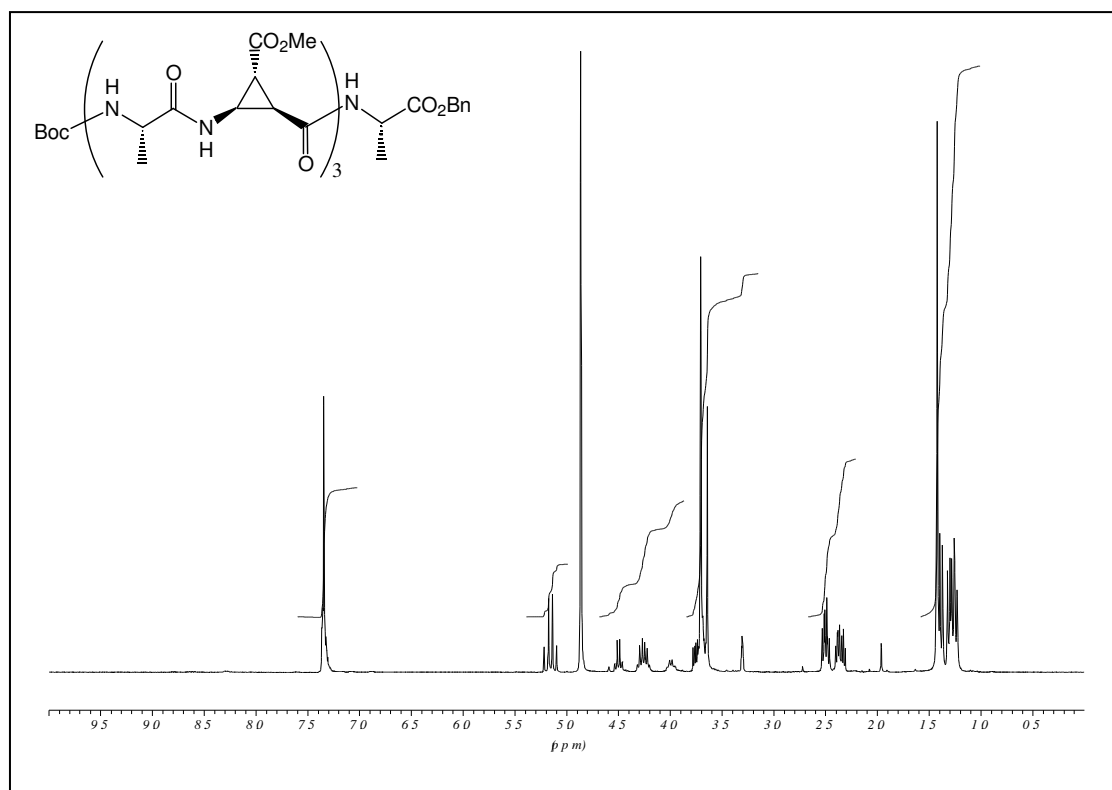
NMR

^1H -Spectra (top of the page)

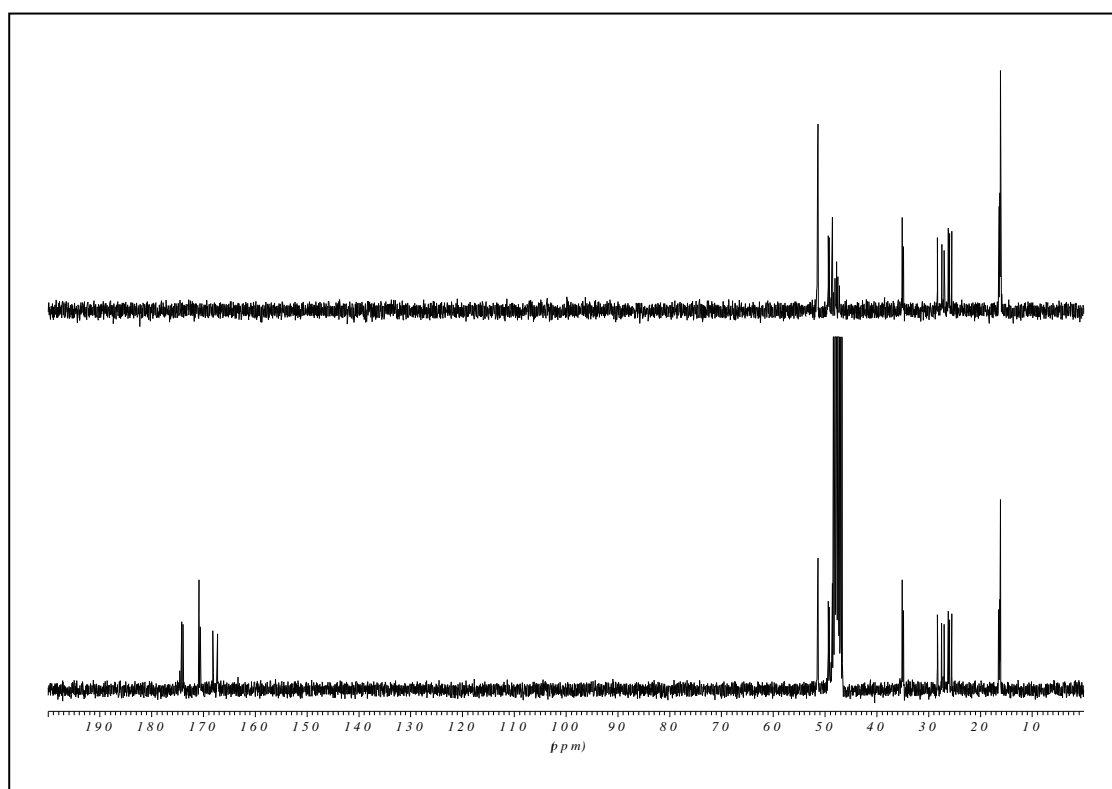
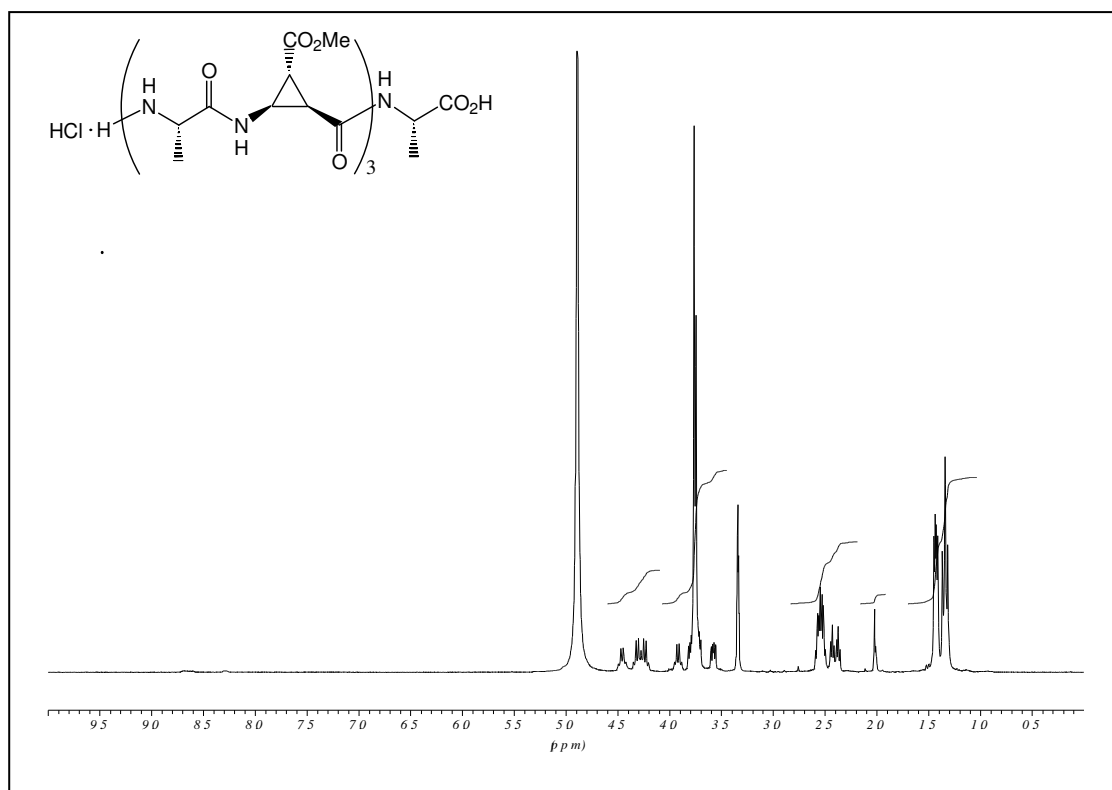
^{13}C -Spectra (bottom of the page)

For the peptide (–)-**7**, obtained by solid phase synthesis, the HPLC chromatogram after purification is given.

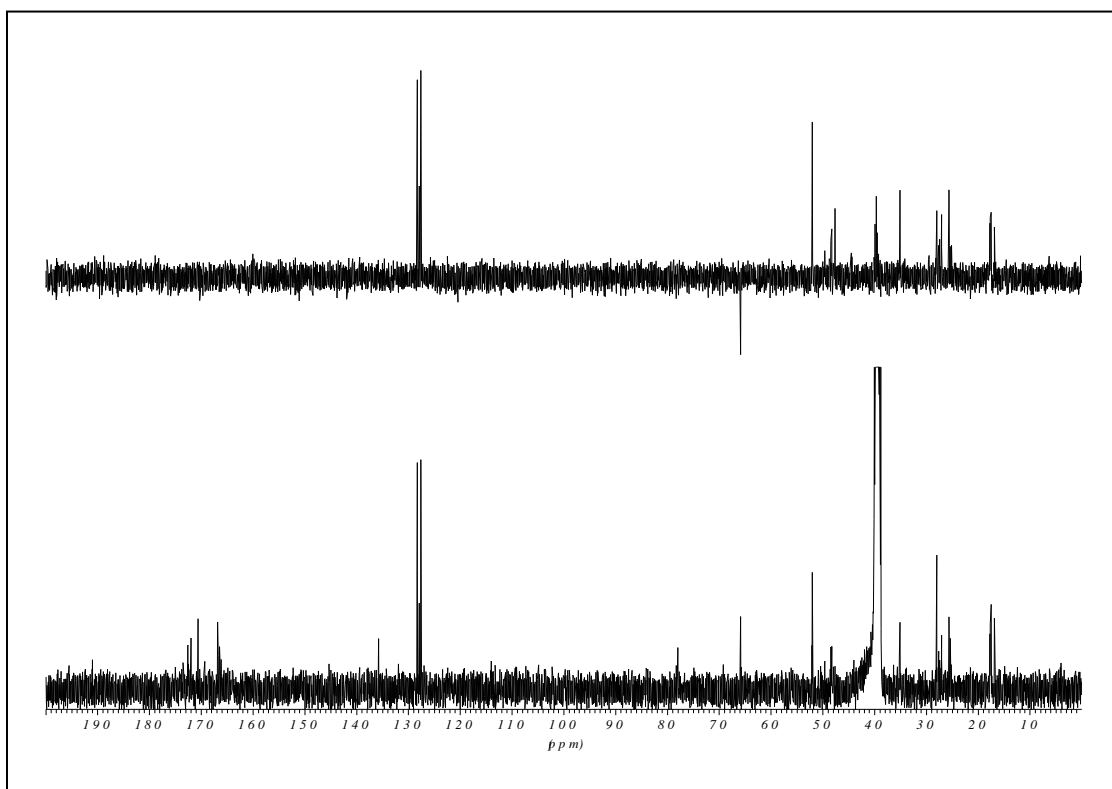
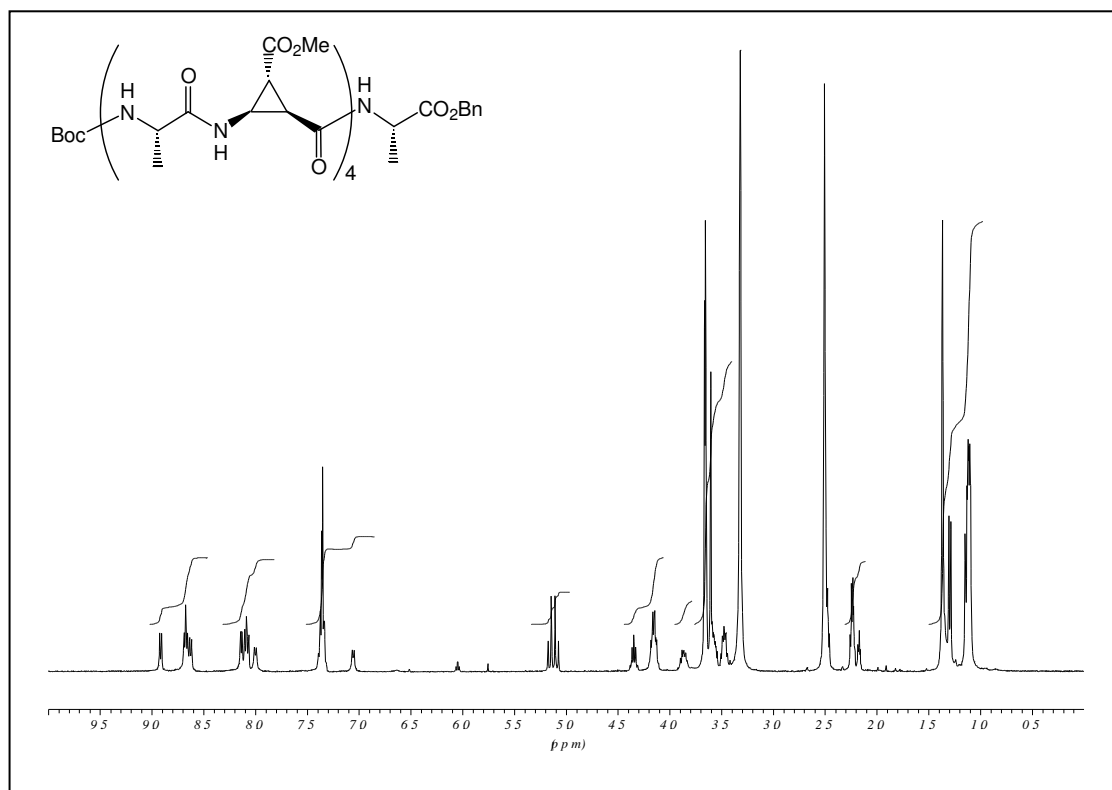
Boc-[Ala-(+)- β -ACC]₃-Ala-OBn, (+)-**5** measured in CD₃OD.



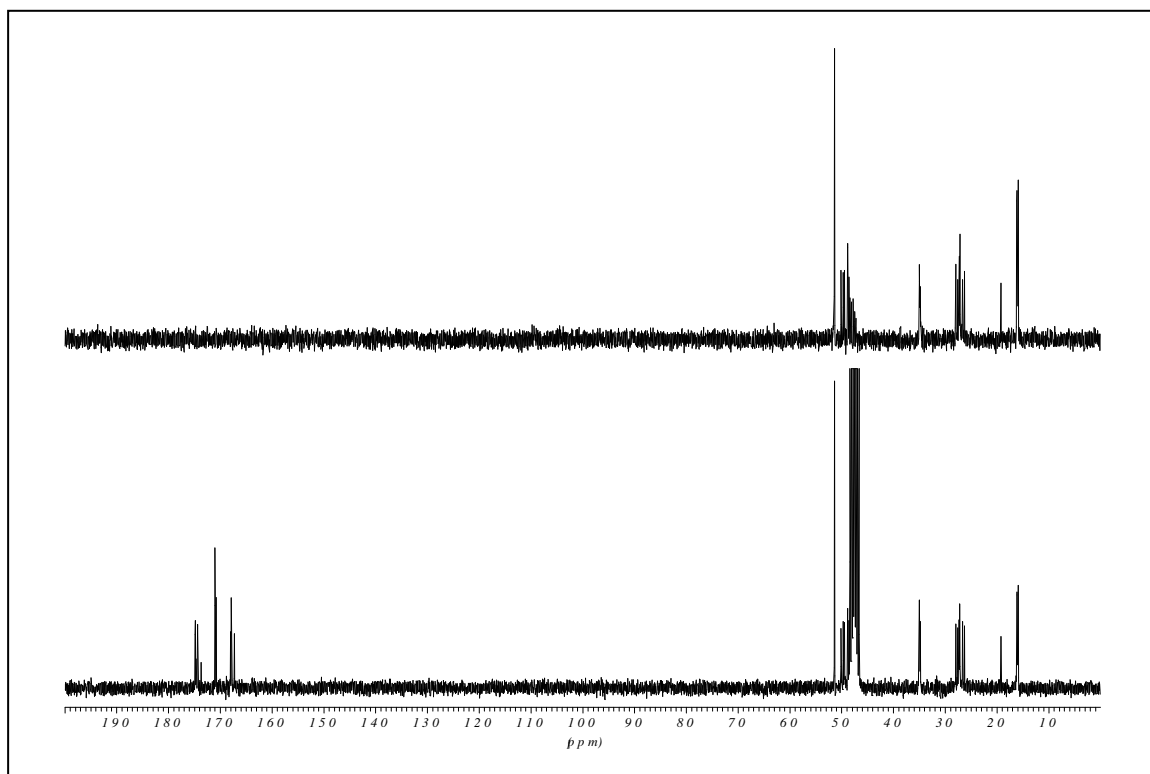
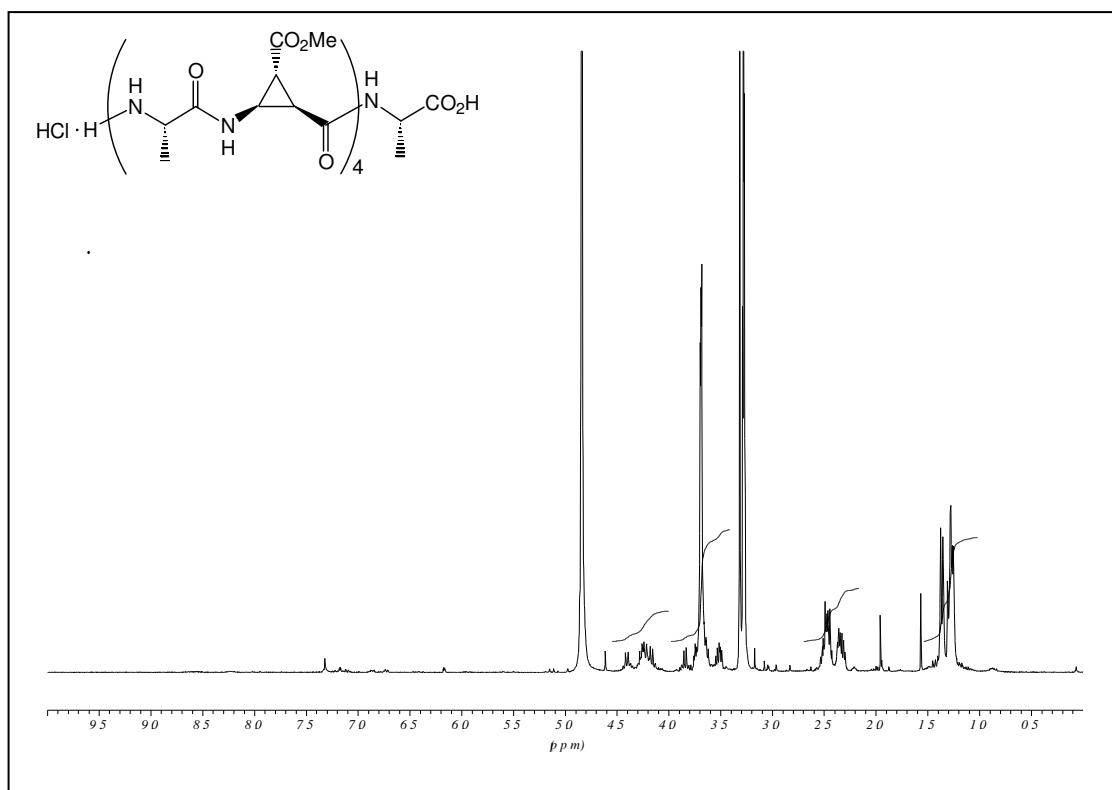
HCl·H-[Ala-(+)-β-ACC]₃-Ala-OH, (+)-**5a** measured in CD₃OD.



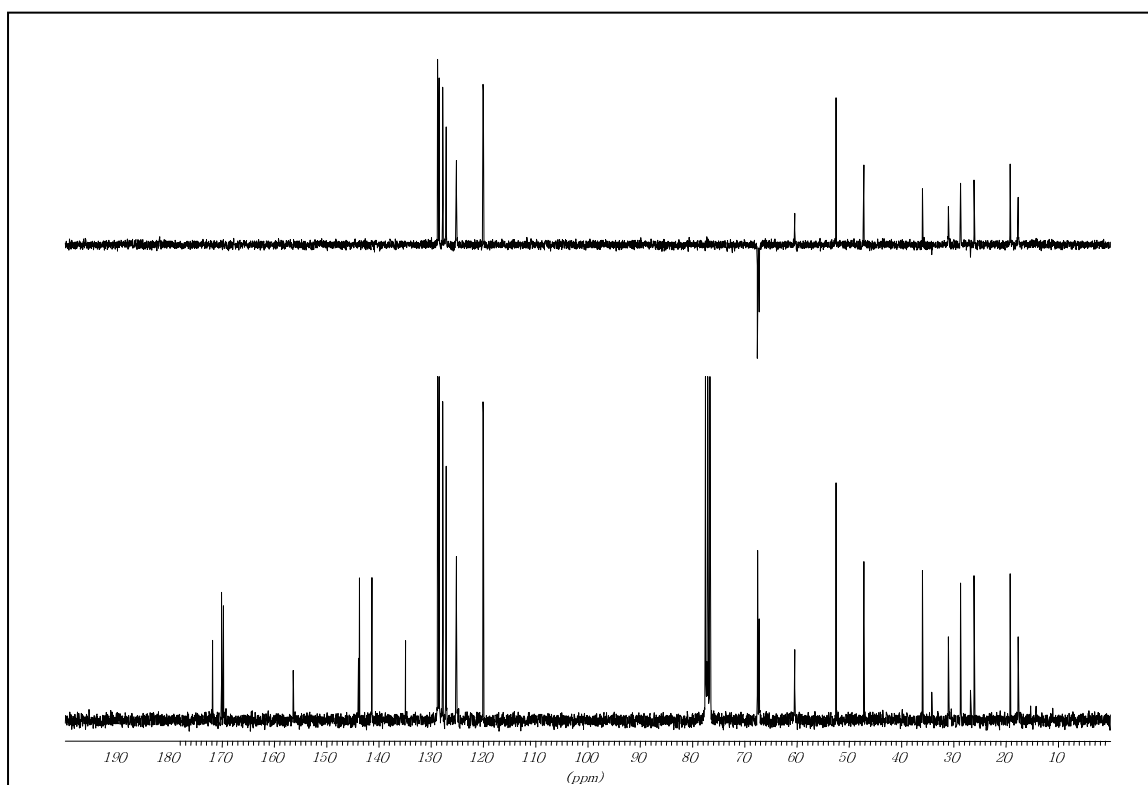
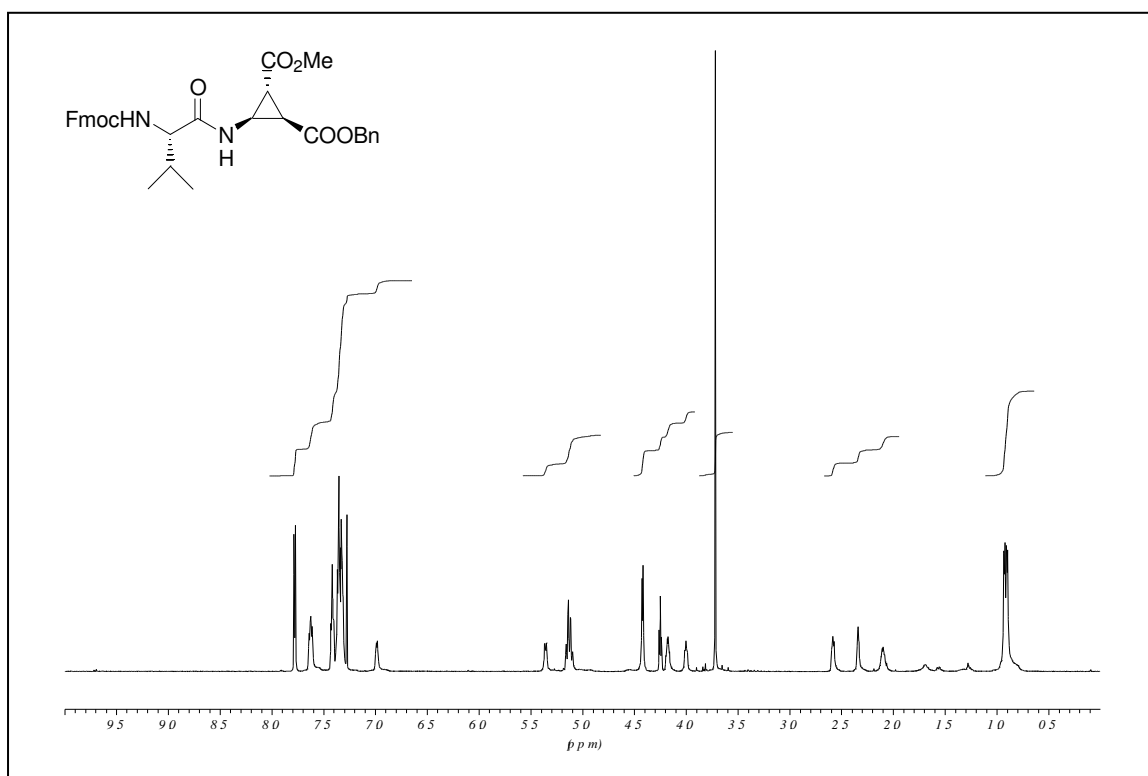
Boc-[Ala-(+)- β -ACC]₄-Ala-OBn, (+)-**6** measured in DMSO d⁶.



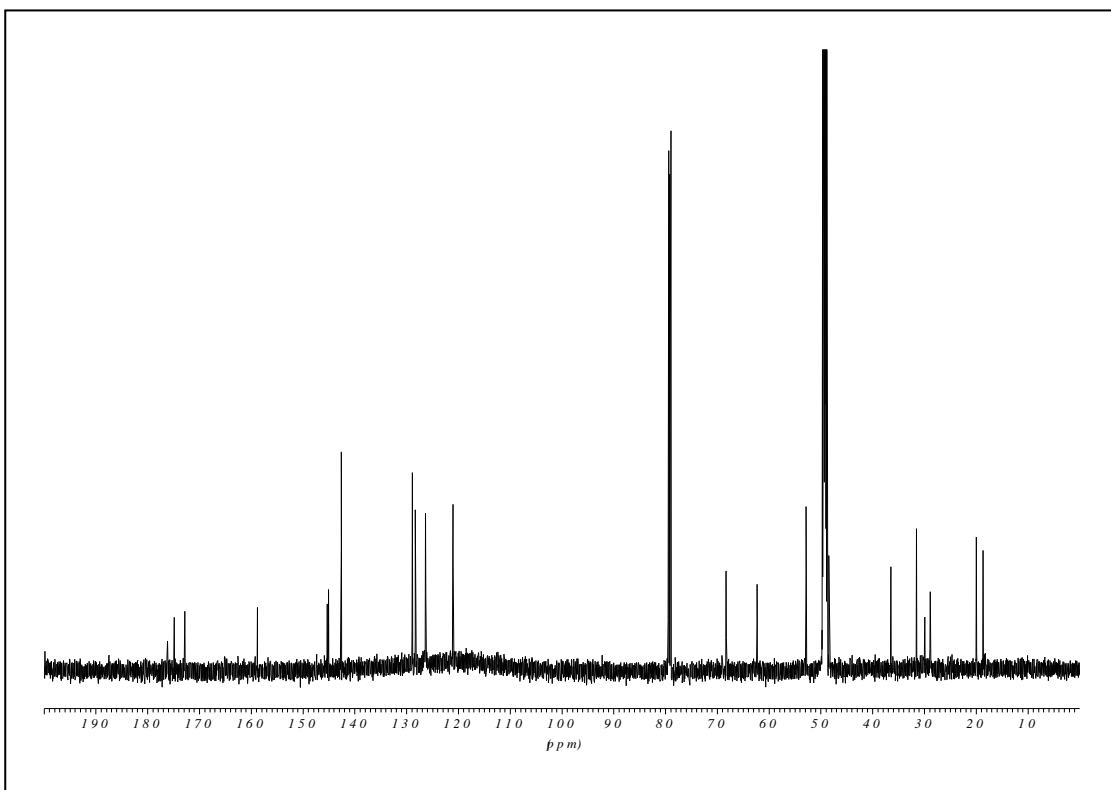
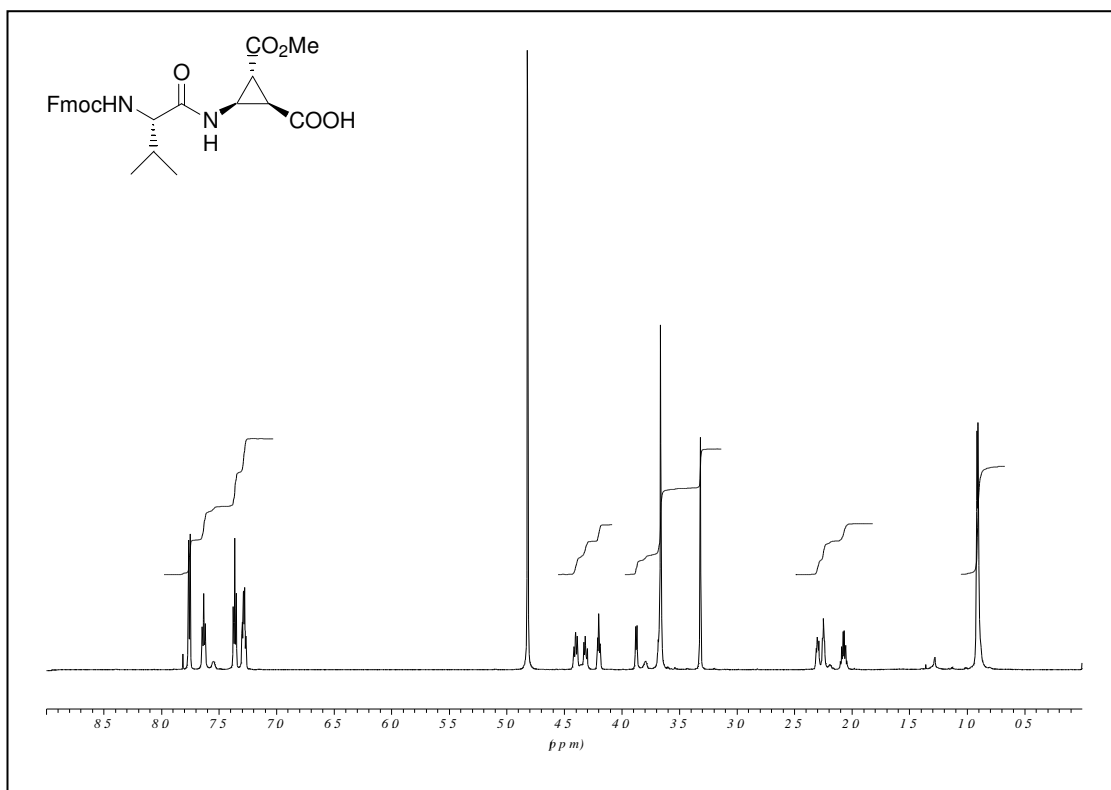
HCl·H-[Ala-(+)-β-ACC]₄-Ala-OH, (+)-**6a** measured in CD₃OD.



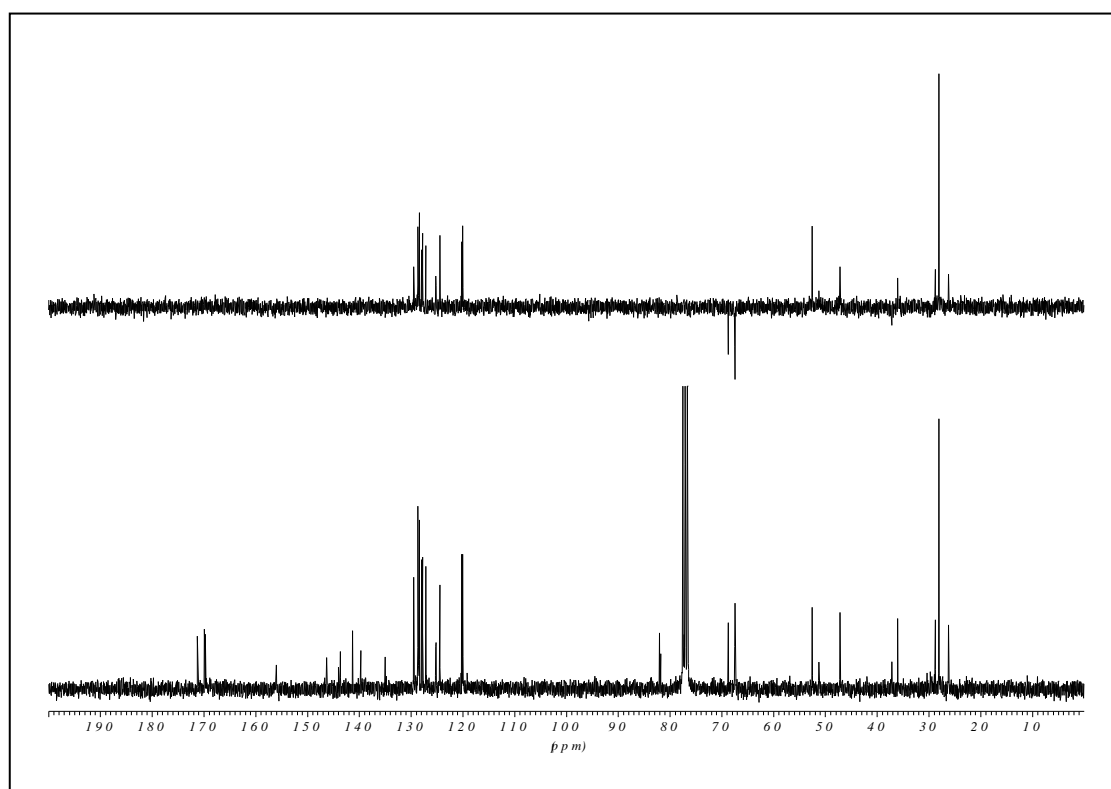
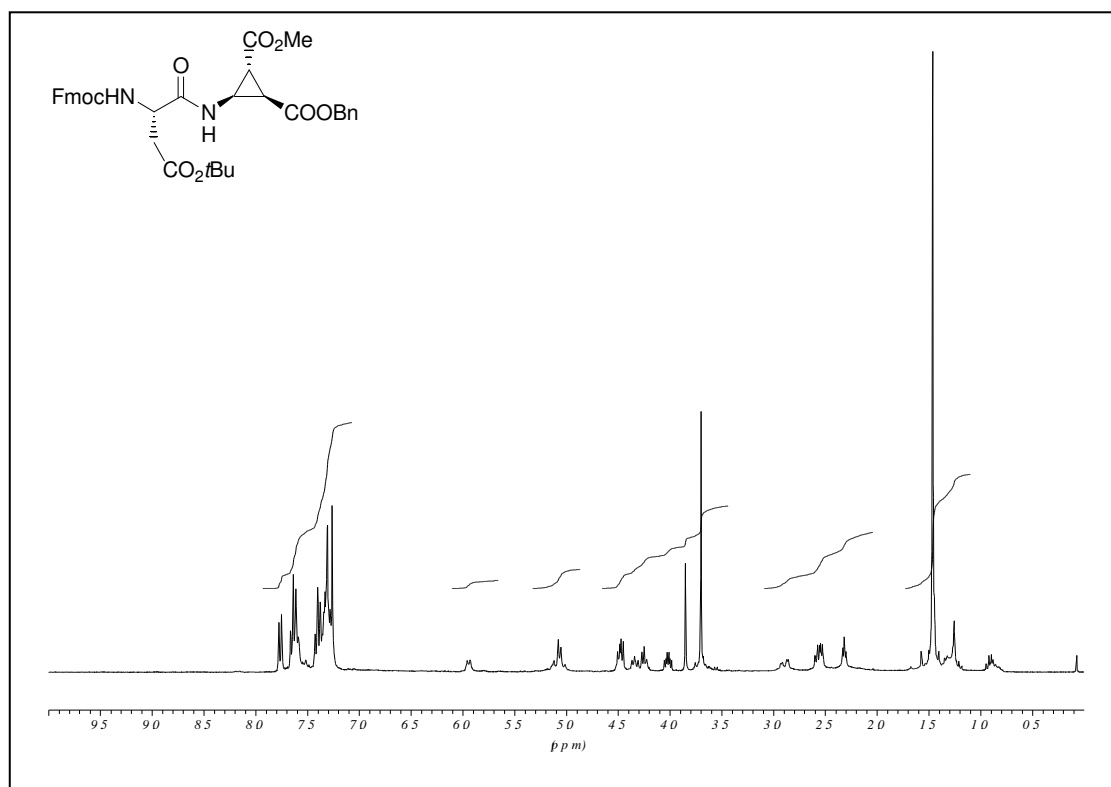
Fmoc-Val-(+)- β ACC-OBn, (+)-**16** measured in CDCl_3 .



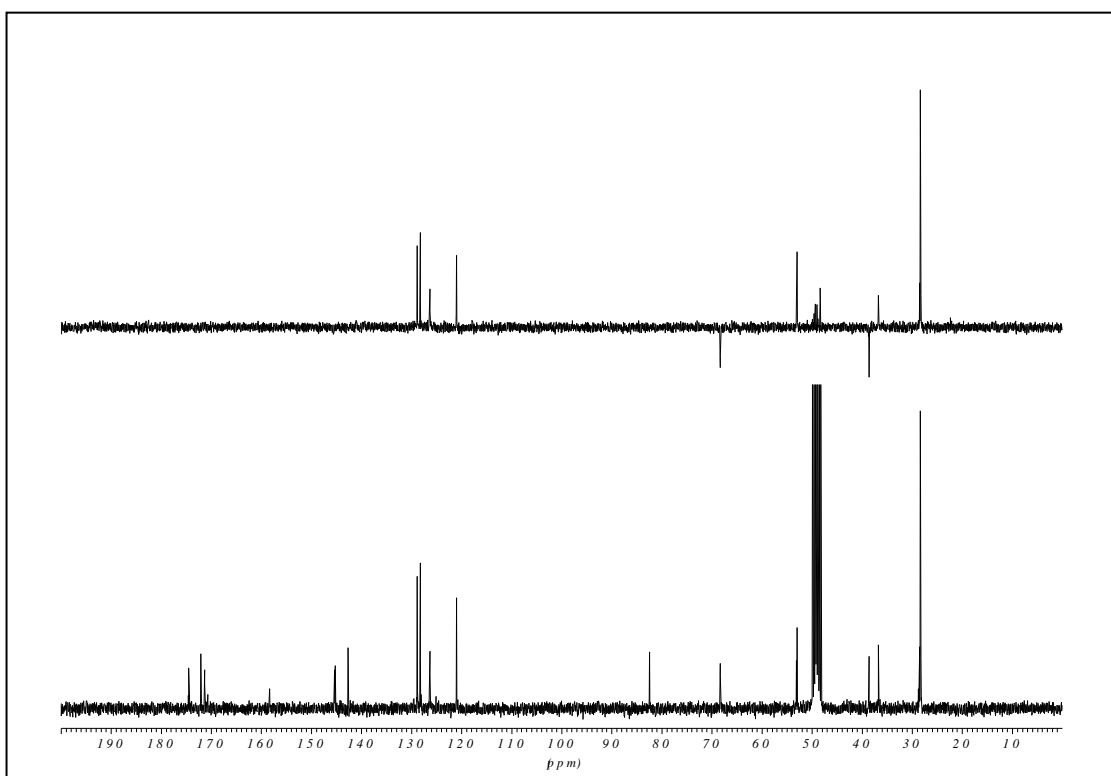
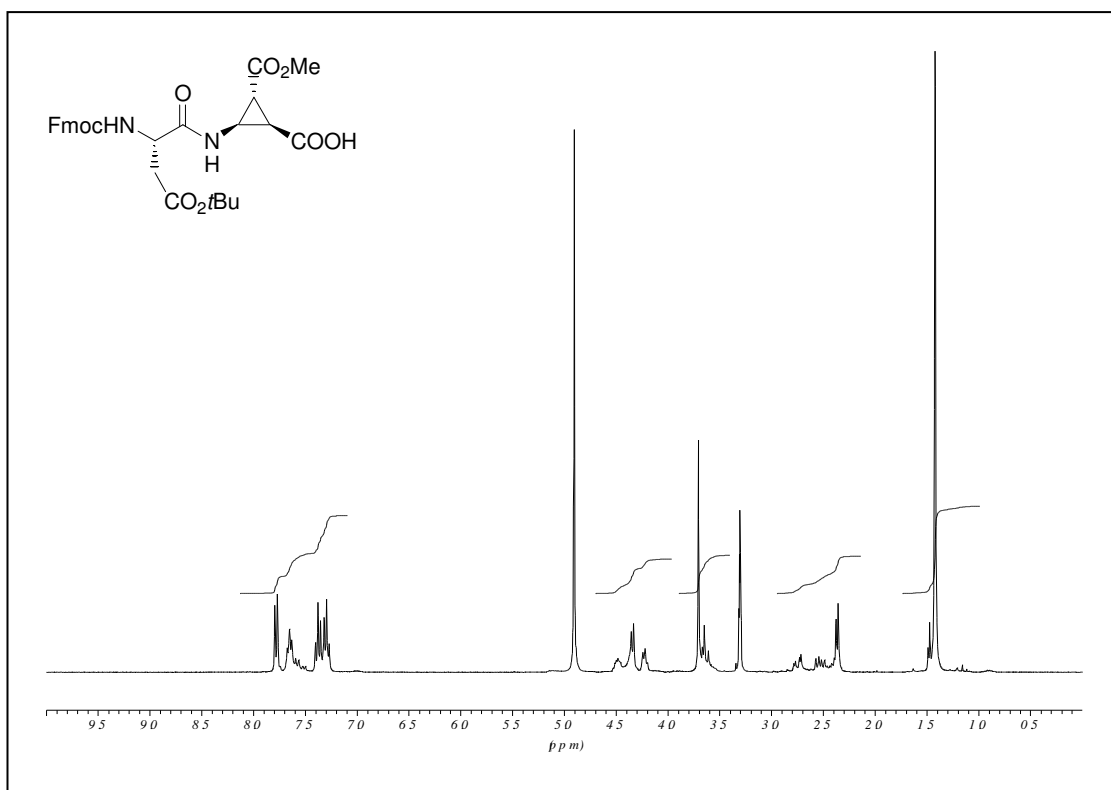
Fmoc-Val-(+)- β ACC-OH, (+)-**16a** measured in CD₃OD/CDCl₃ 10:1.



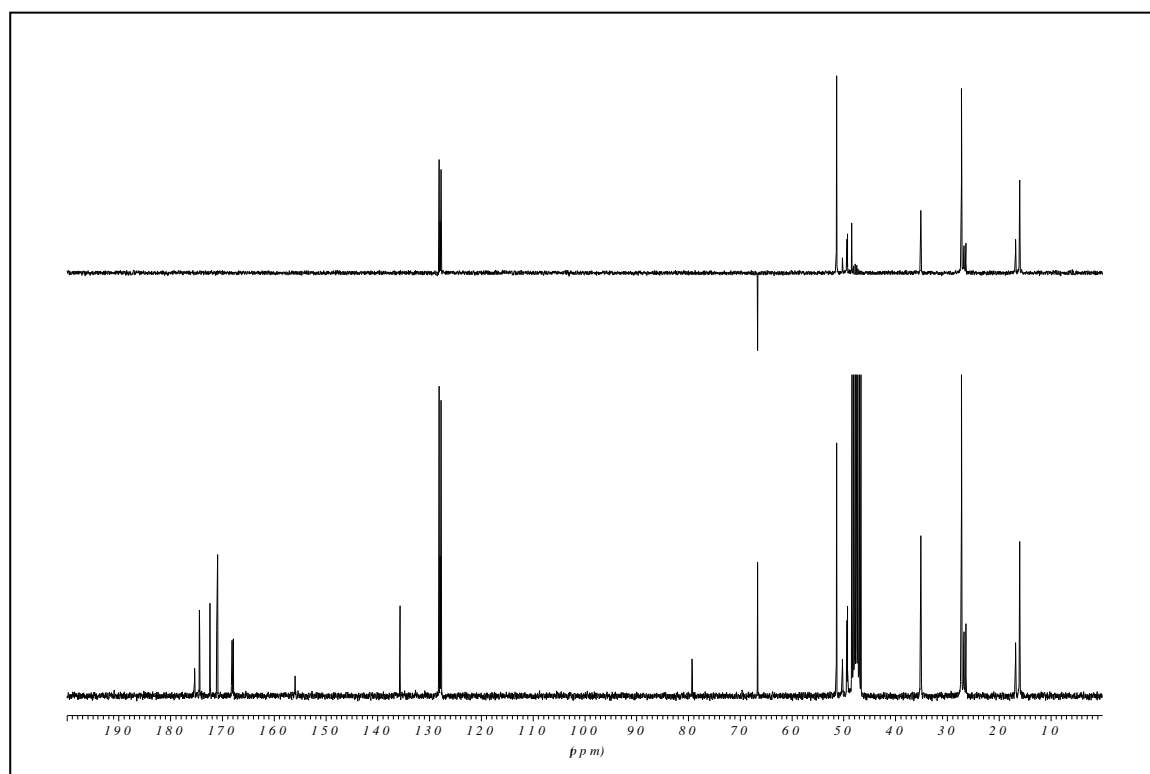
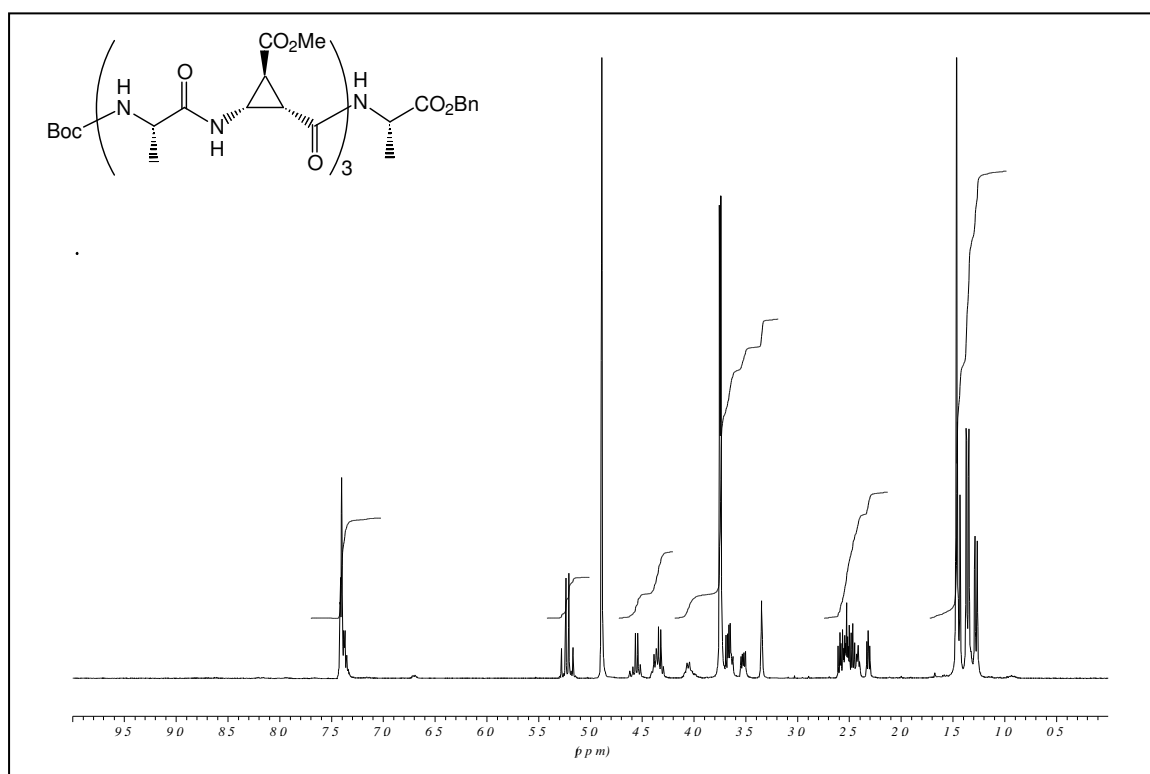
Fmoc-Asp(OtBu)-(+) - β ACC-OBn, (+)-**17** measured in CDCl₃.



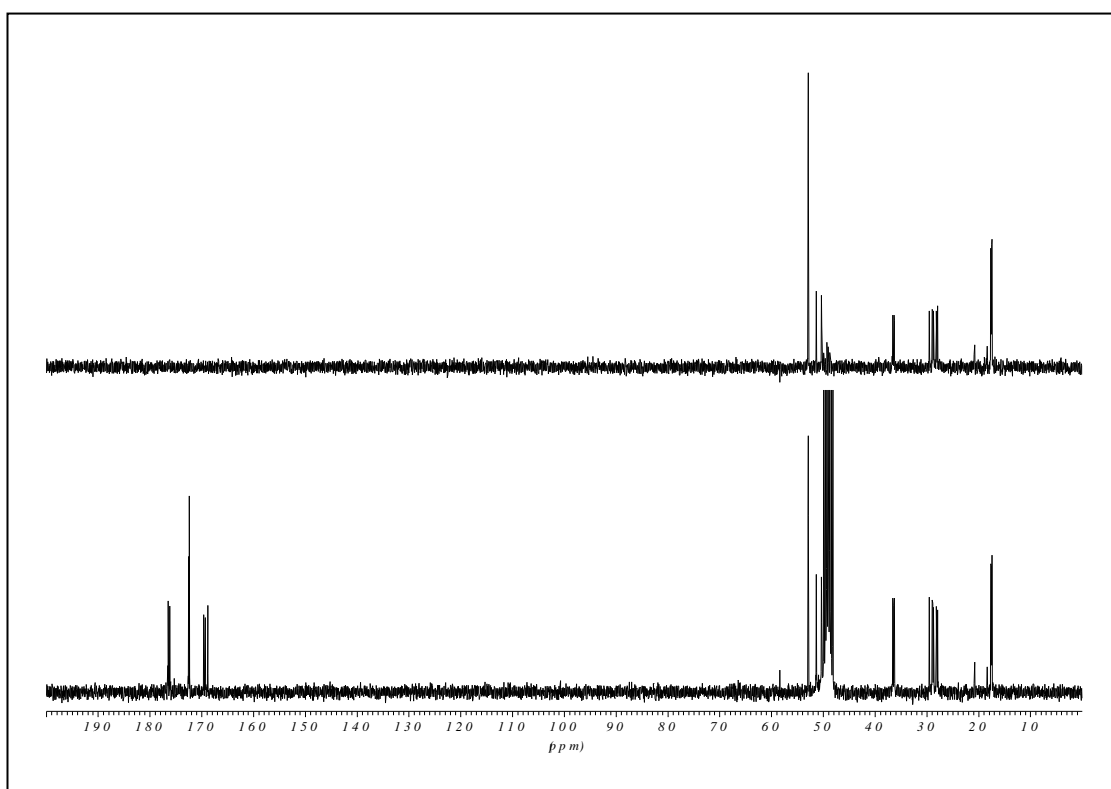
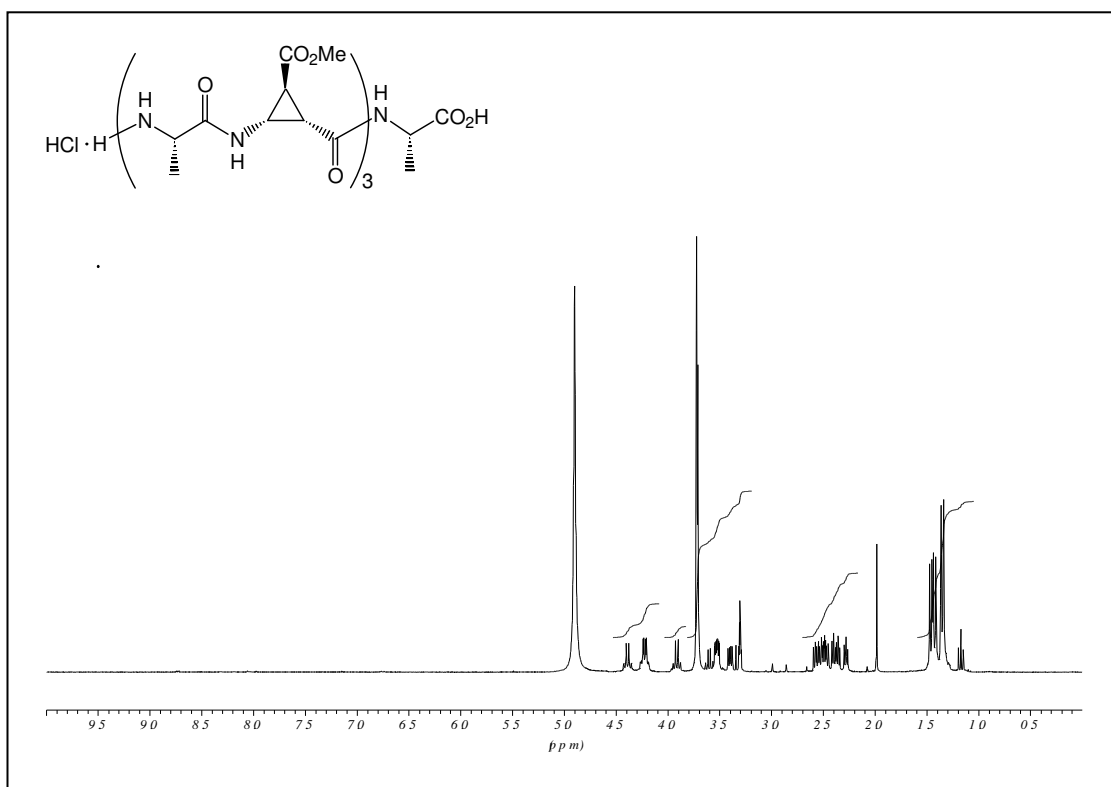
Fmoc-Asp(OtBu)-(+)- β ACC-OH, (+)-**17a** measured in CD₃OD.



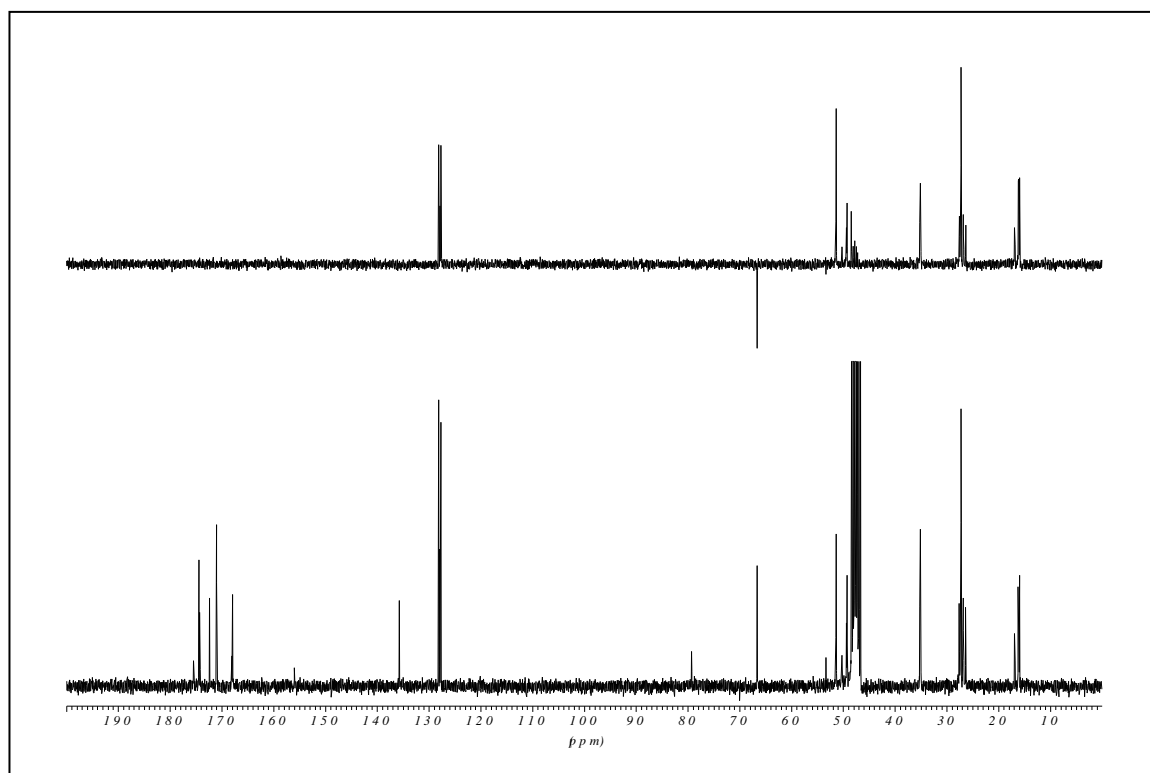
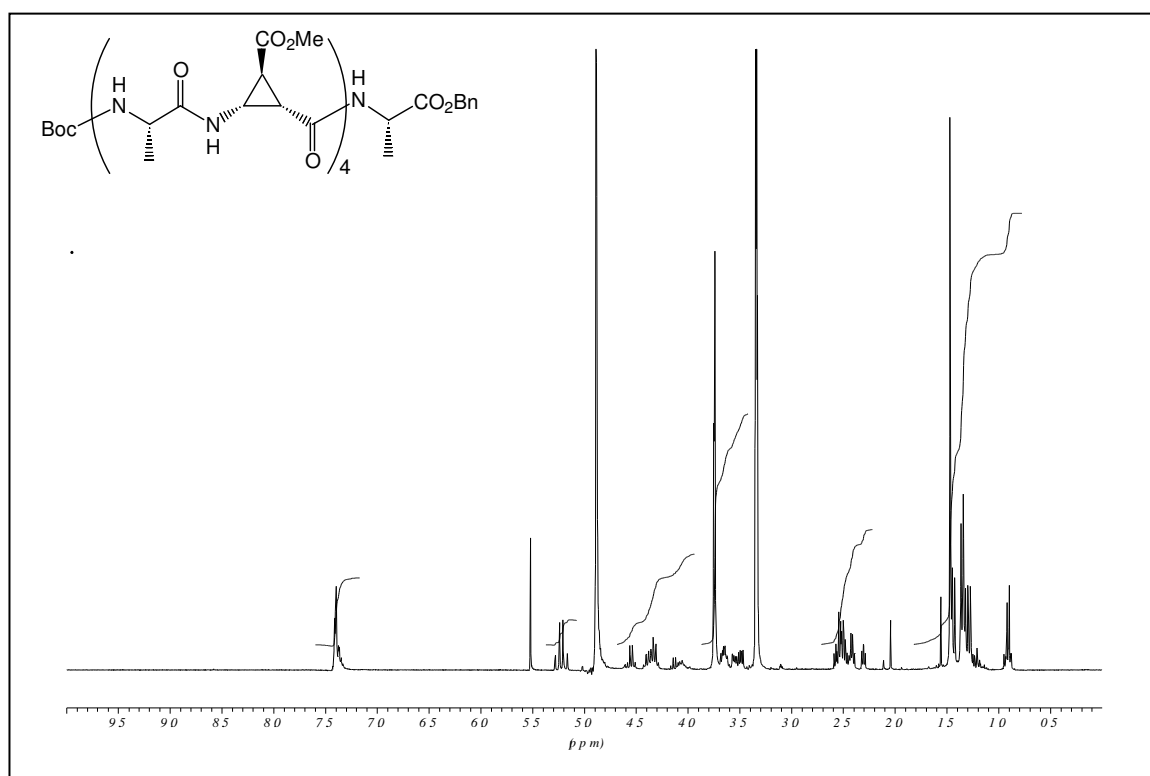
Boc-[Ala(-)- β -ACC]₃-Ala-OBn, (-)-**5** measured in CD₃OD.



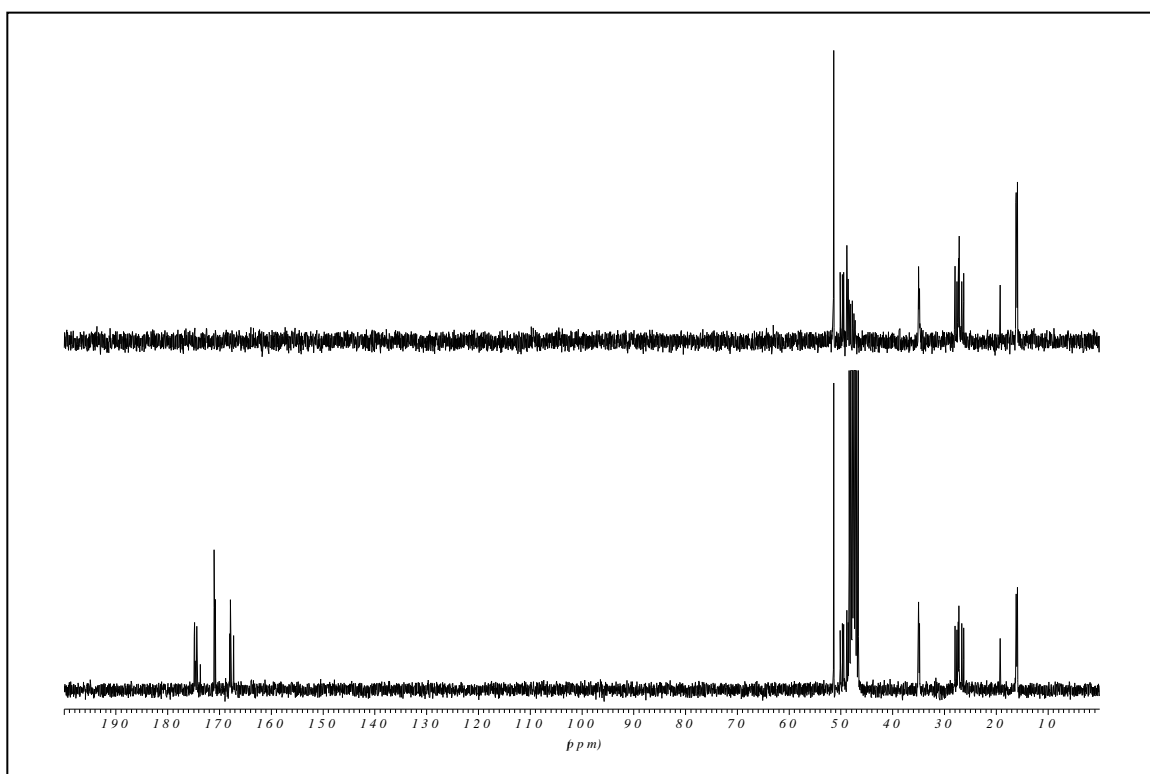
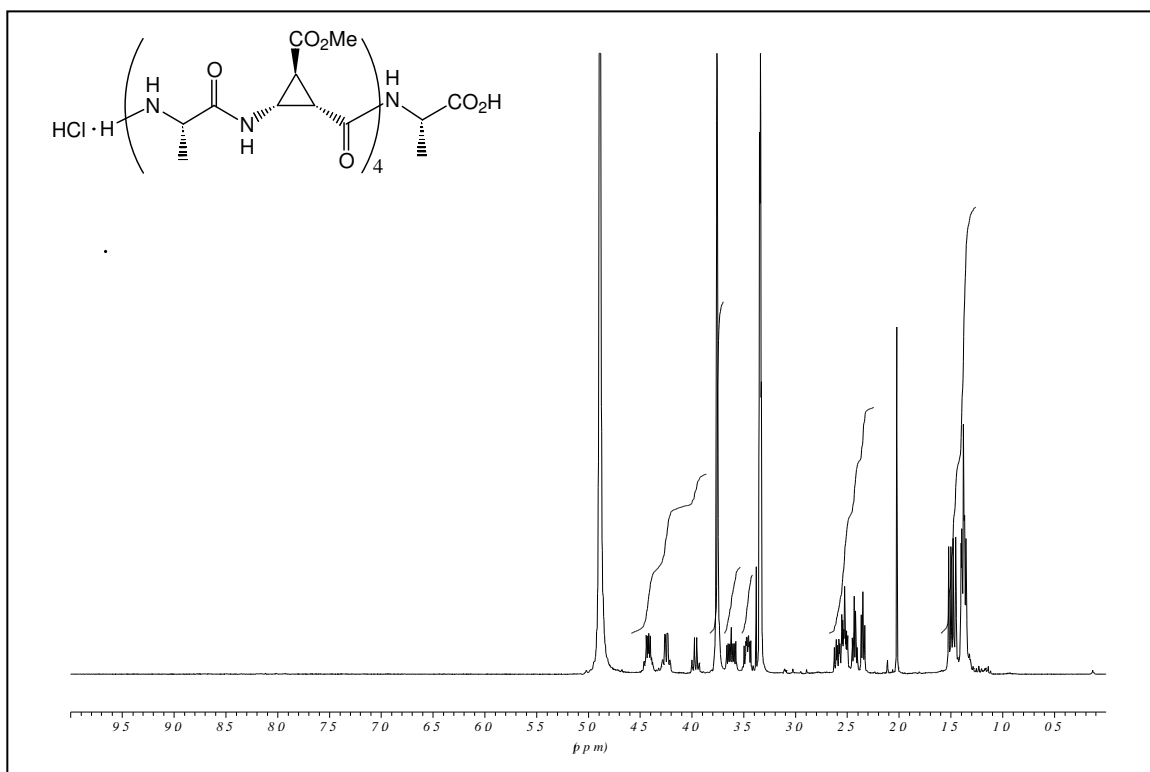
HCl·H-[Ala(-)-β-ACC]₃-Ala-OH, (-)-**5a** measured in CD₃OD.

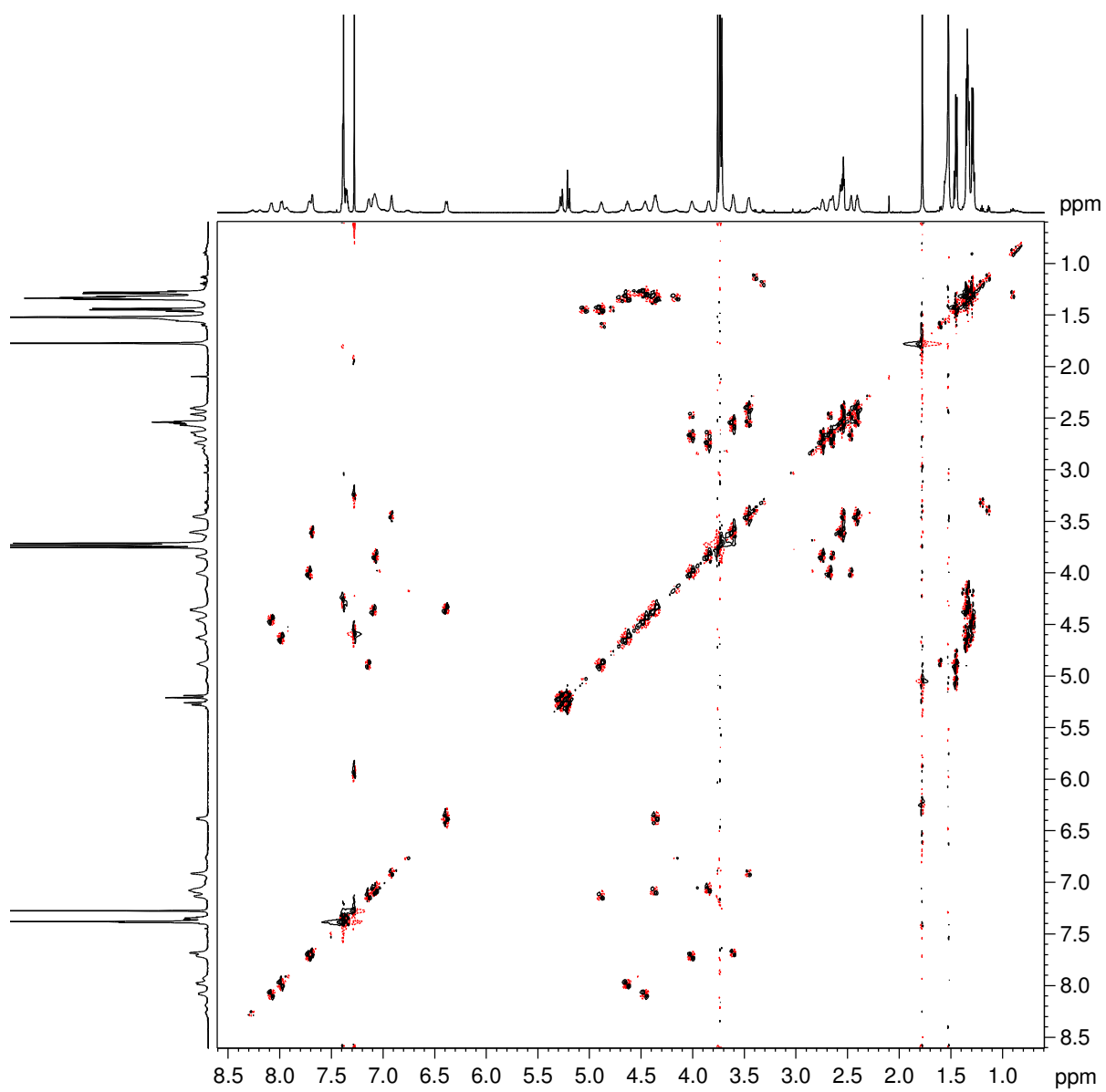


Boc-[Ala(-)-β-ACC]₄-Ala-OBn, (-)-**6** measured in CD₃OD.



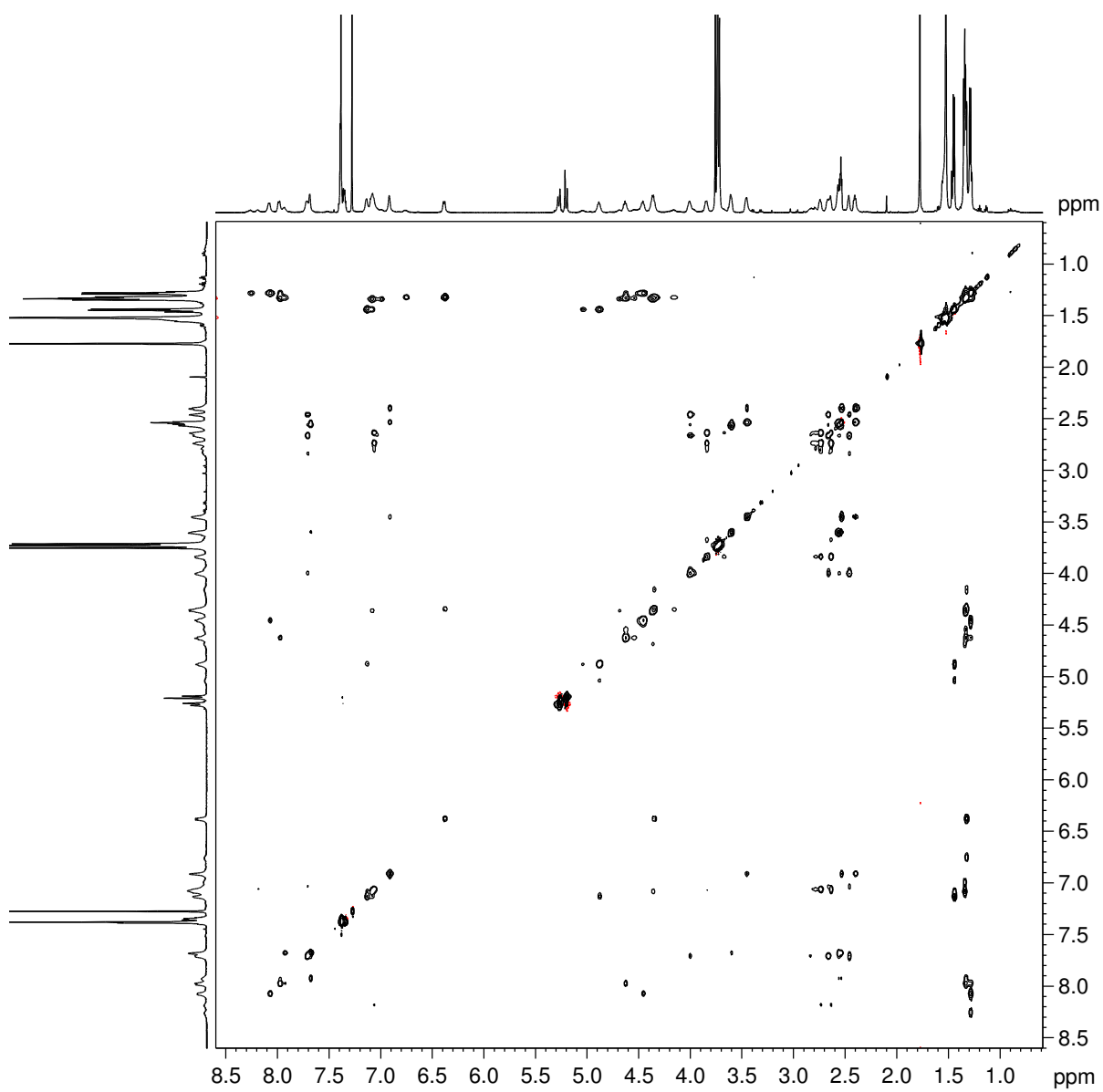
HCl·H-[Ala(-)-β-ACC]₄-Ala-OH, (-)-**6a** measured in CD₃OD.





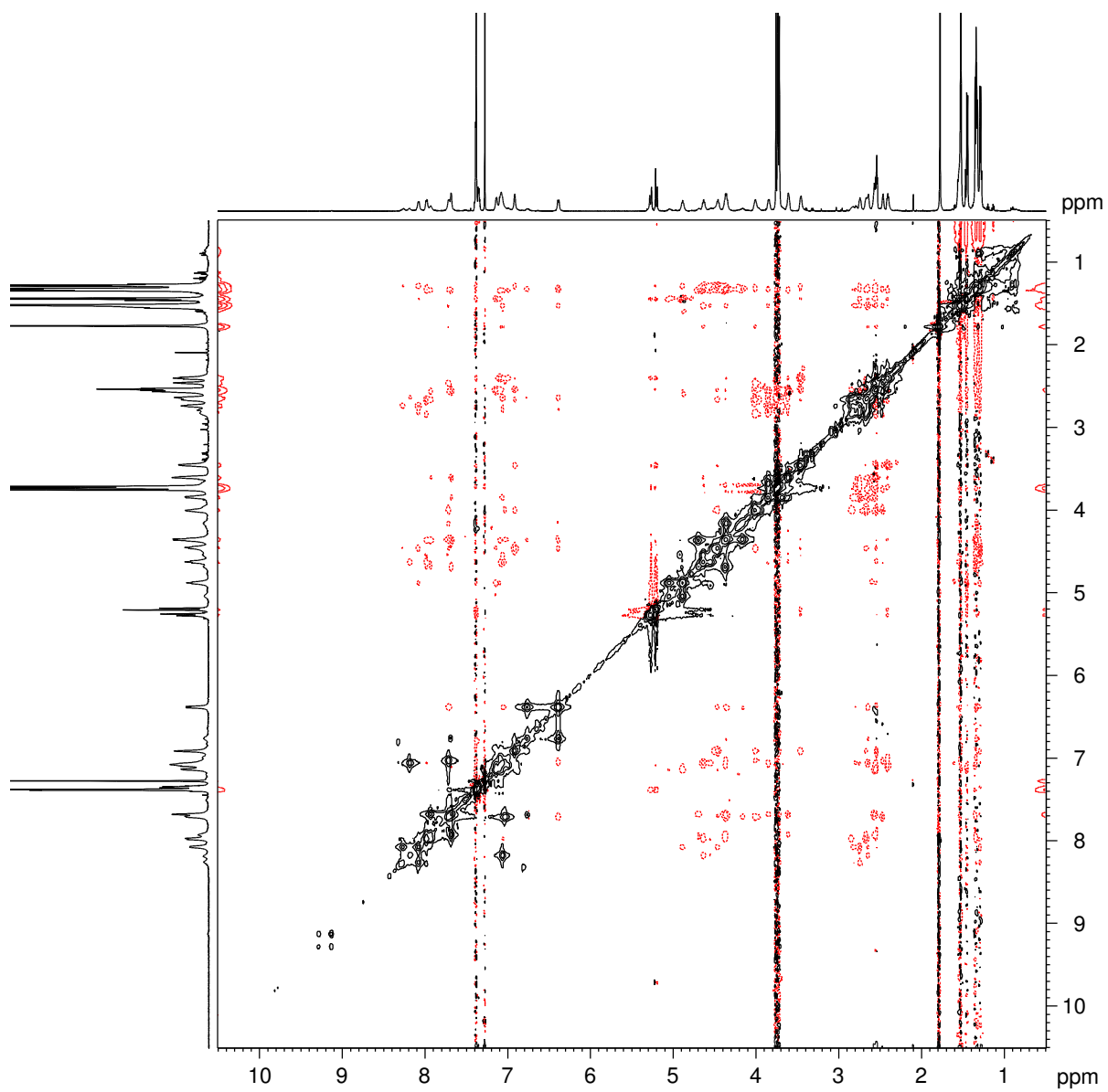
HCl·H-[Ala(-)-β-ACC]₄-Ala-OH, (-)-**6a**

DQF-COSY 600 MHz, 300 K, 4.5 mg in 0.8 ml in CDCl₃



HCl·H-[Ala(-)-β-ACC]₄-Ala-OH, (-)-**6a**

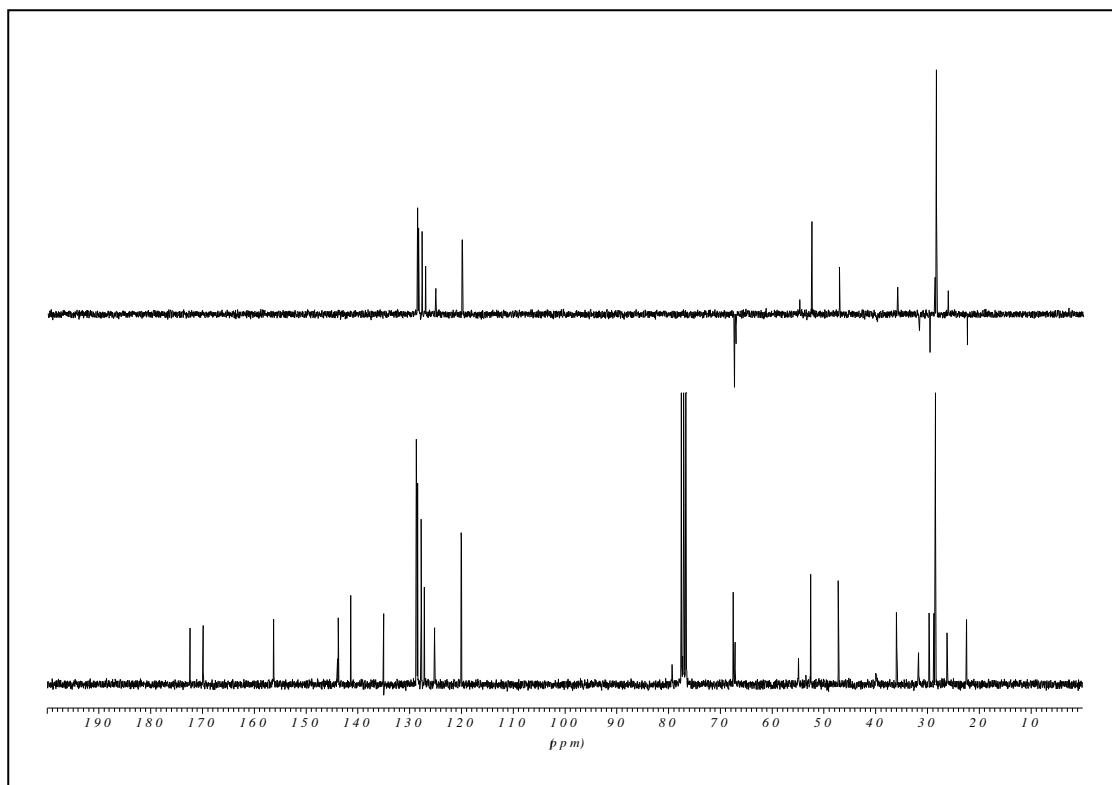
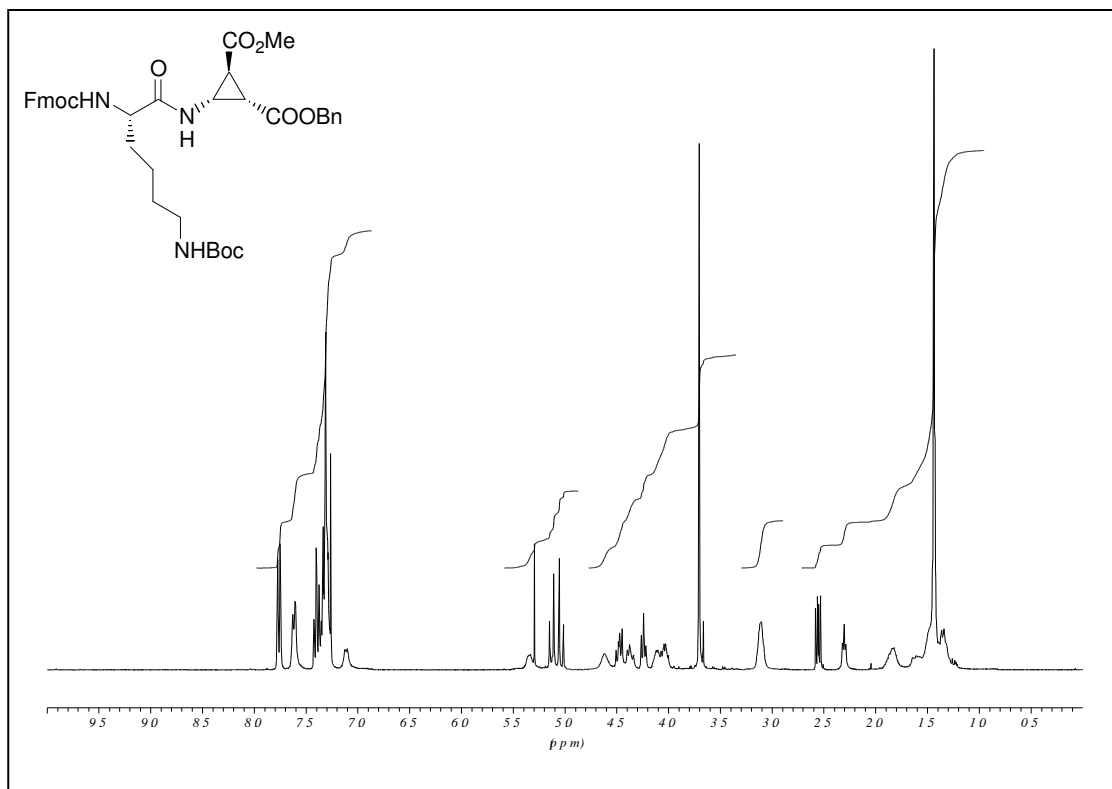
TOCSY 600 MHz, 300 K, 4.5 mg in 0.8 ml in CDCl₃



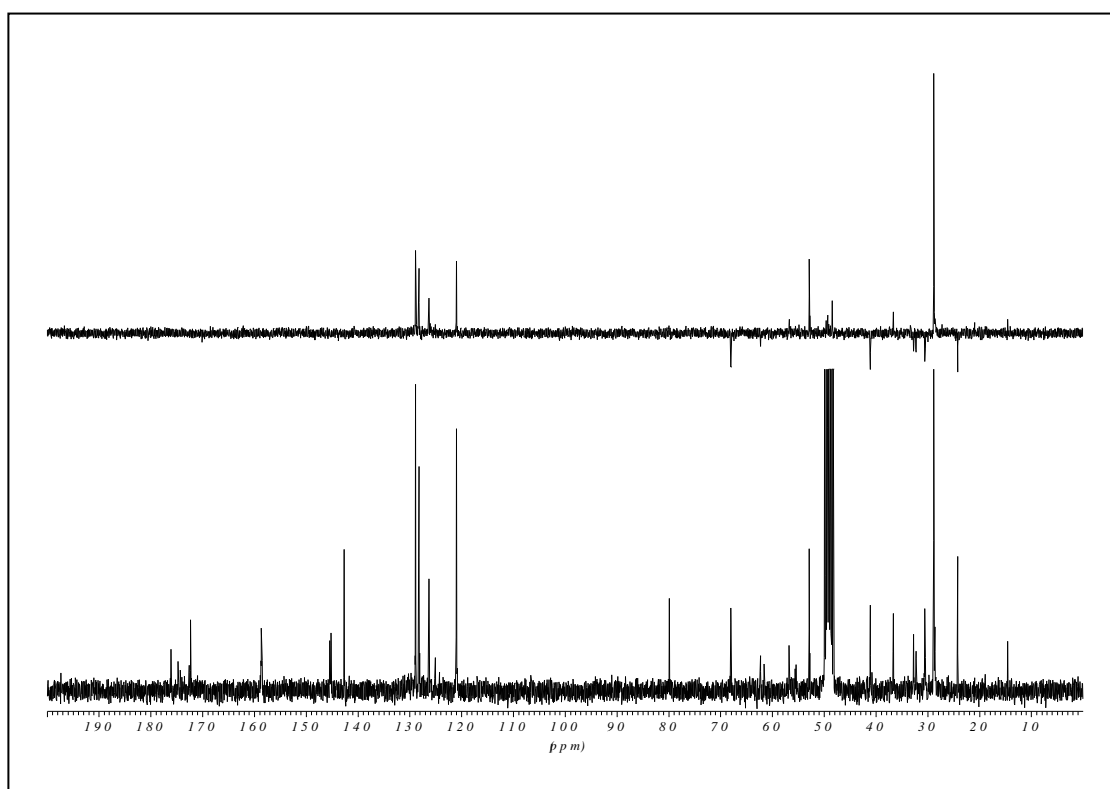
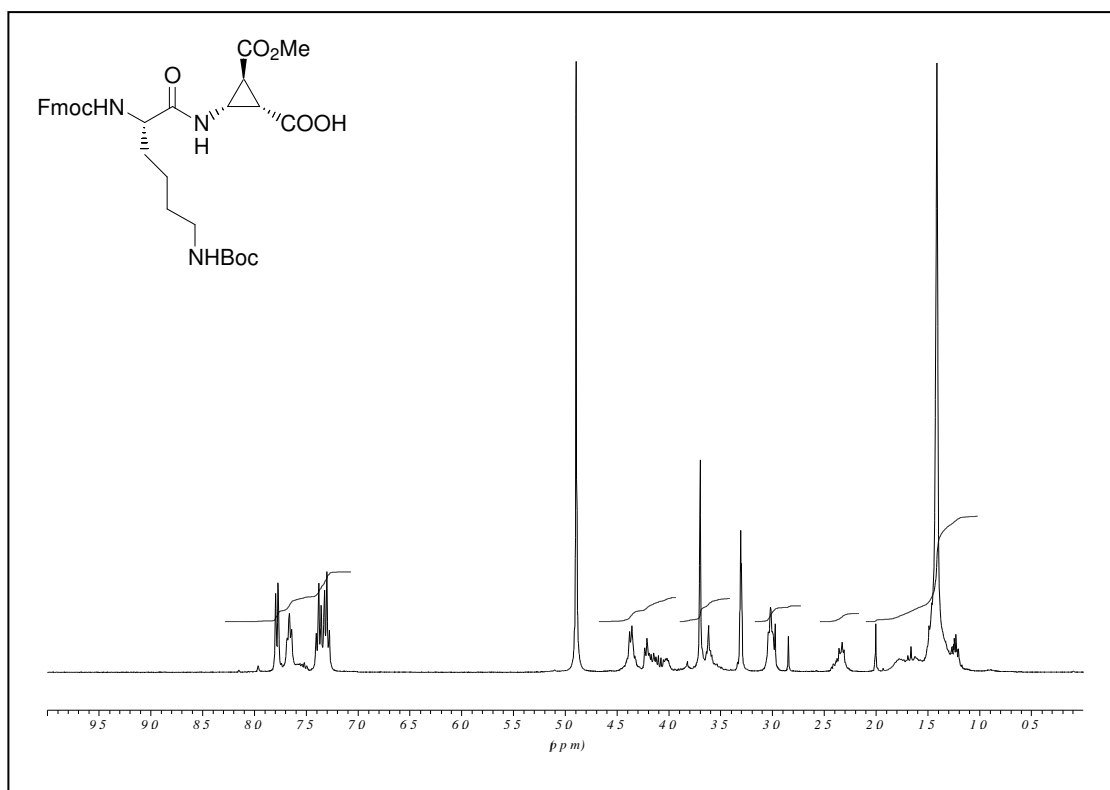
HCl·H-[Ala-(-)-β-ACC]₄-Ala-OH, (-)-**6a**

ROESY 600 MHz, 300 K, 4.5 mg in 0.8 ml in CDCl₃

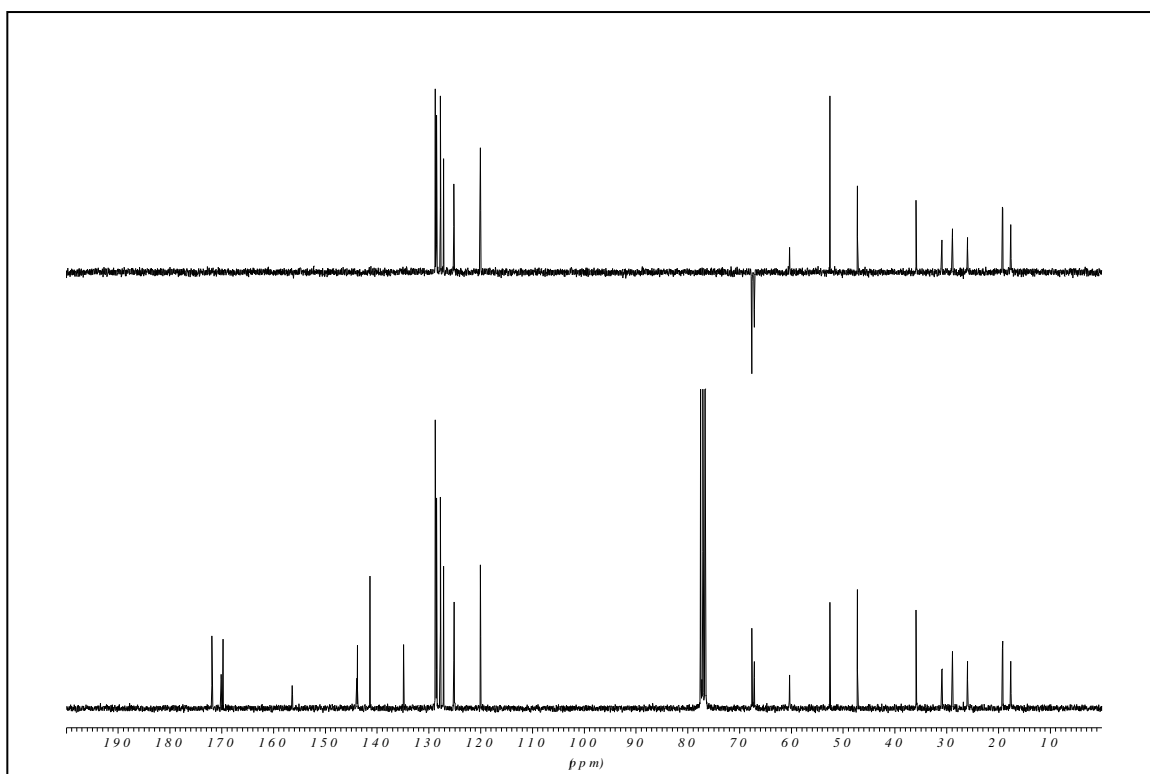
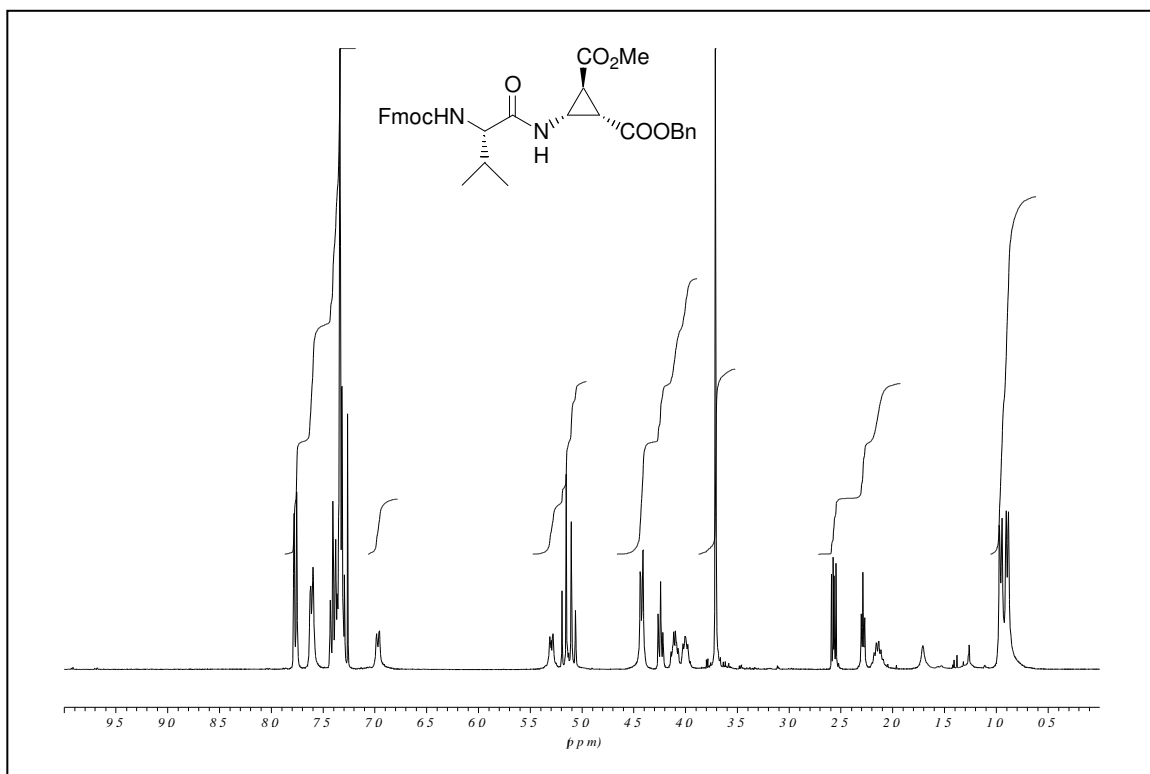
Fmoc-Lys(Boc)-(-)- β ACC-OBn, (-)-**14** measured in CDCl_3 .



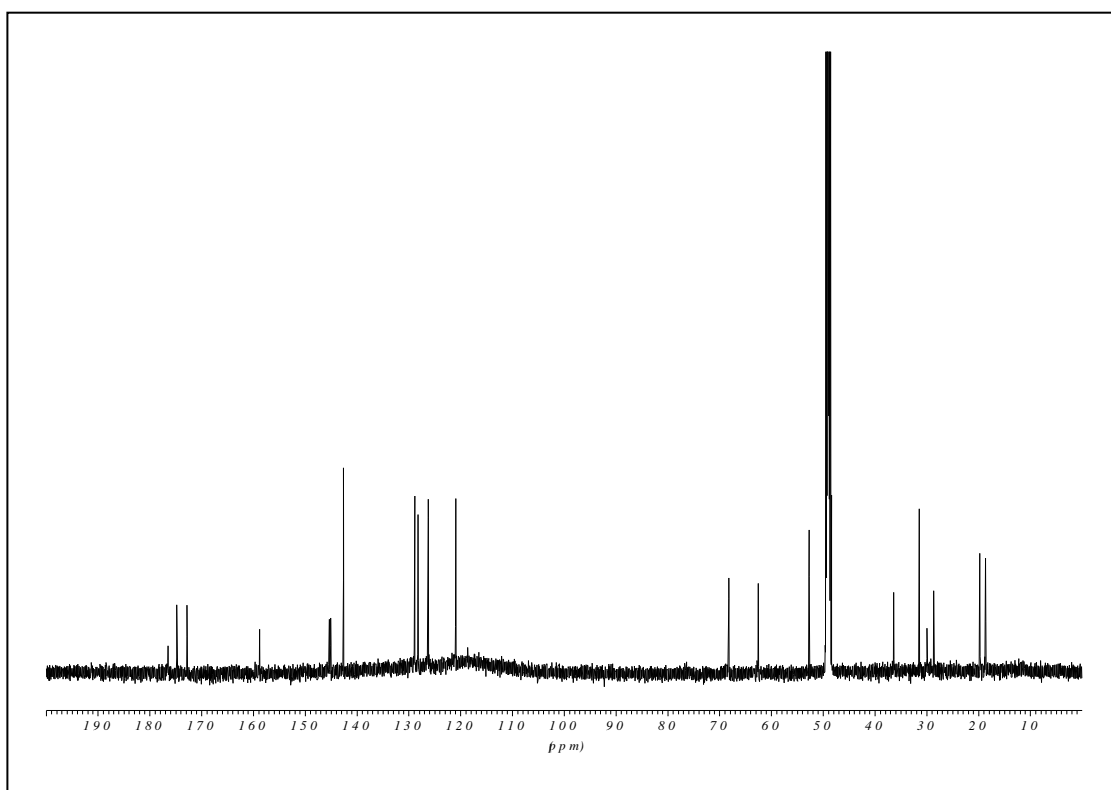
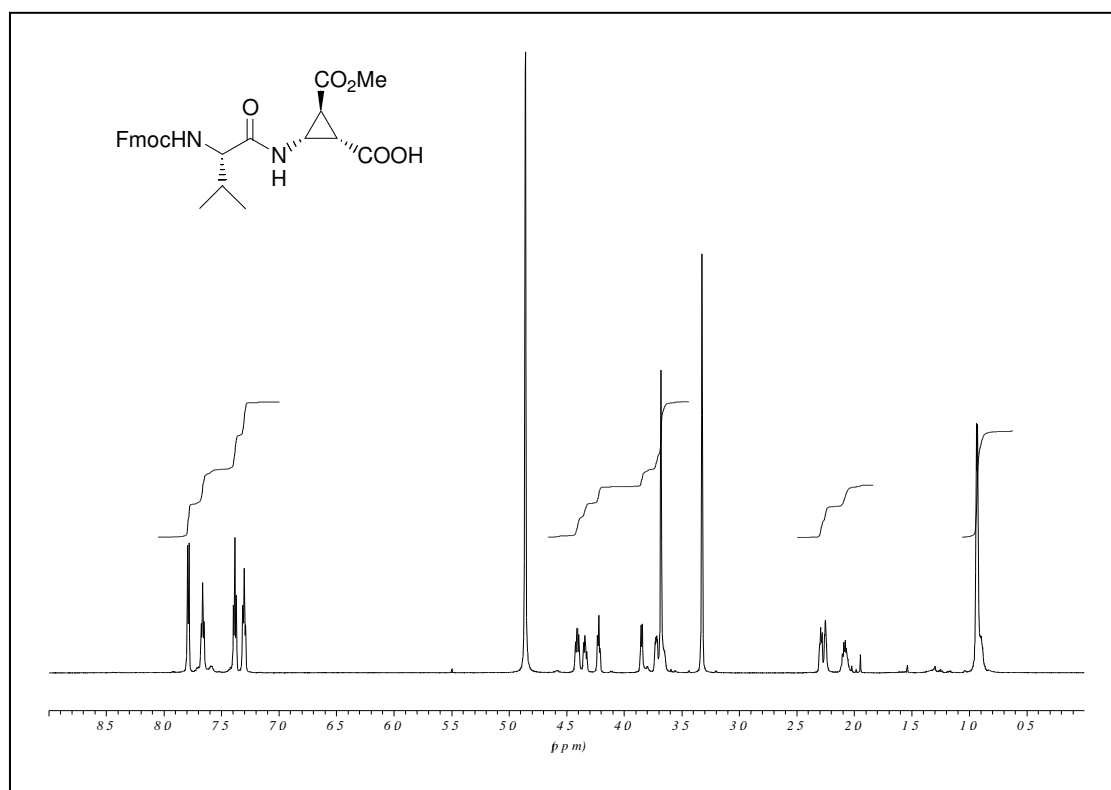
Fmoc-Lys(Boc)-(-)- β ACC-OH, (-)-**14a** measured in CD₃OD.



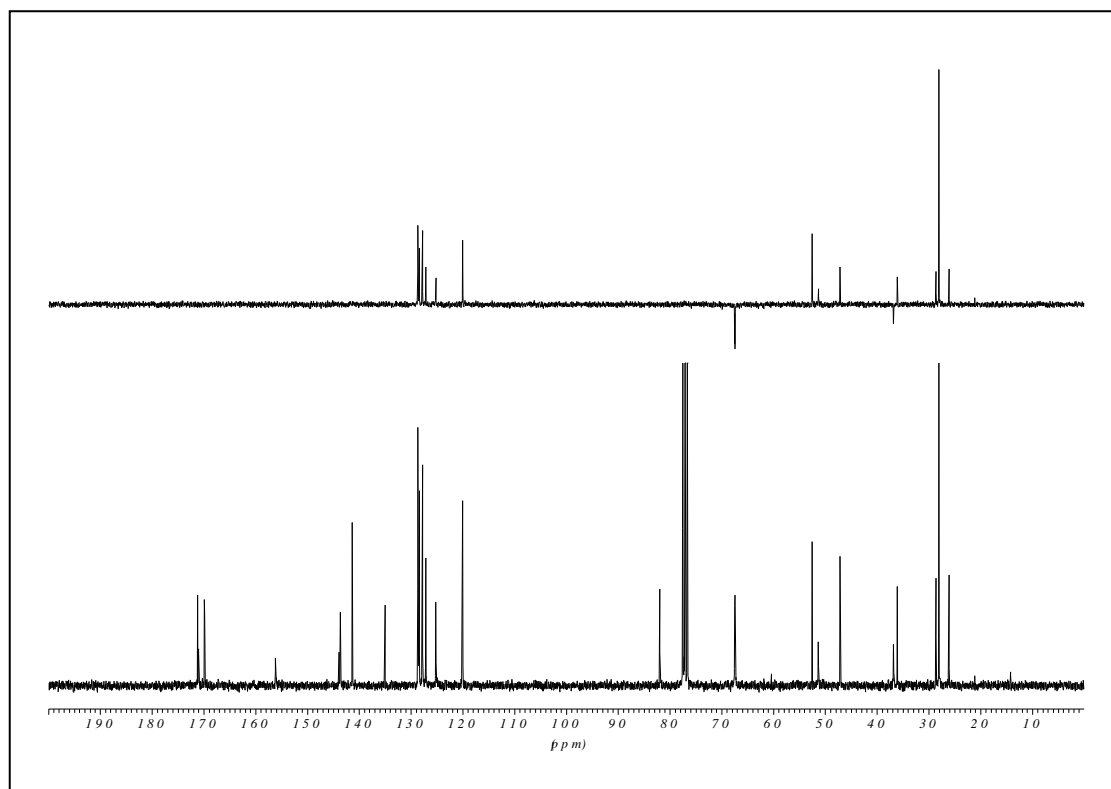
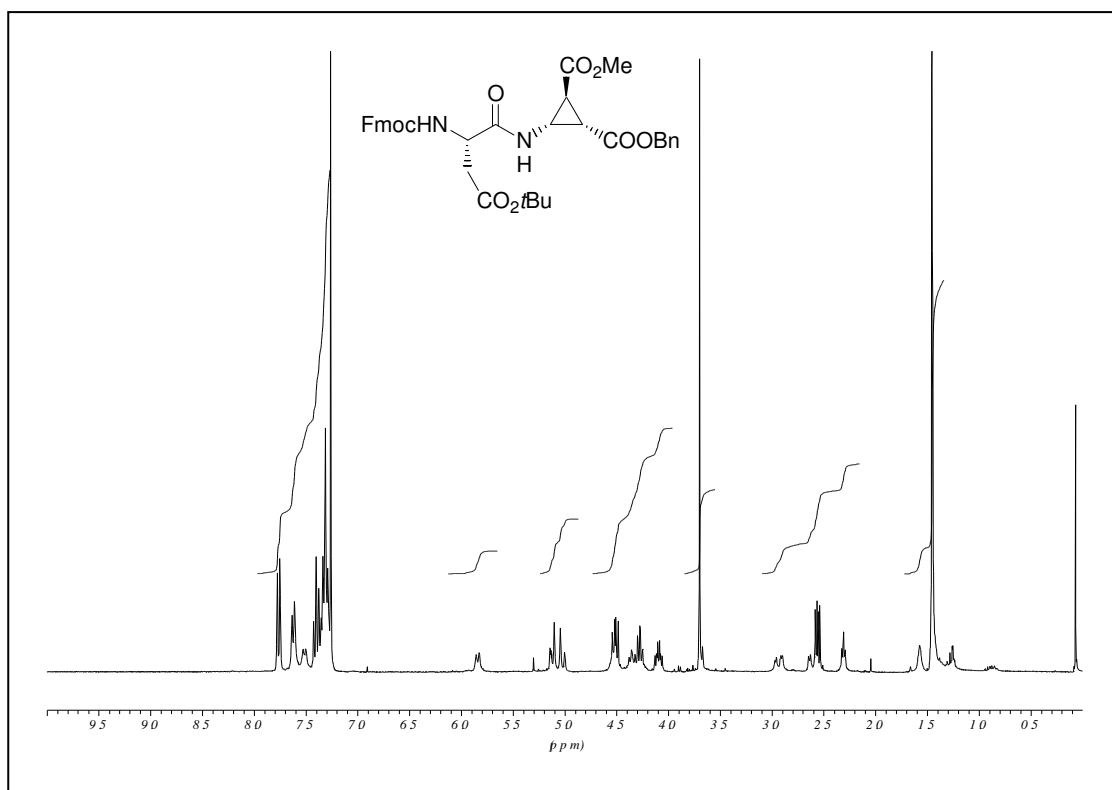
Fmoc-Val(-)- β ACC-OBn, (-)-**16** measured in CDCl₃.



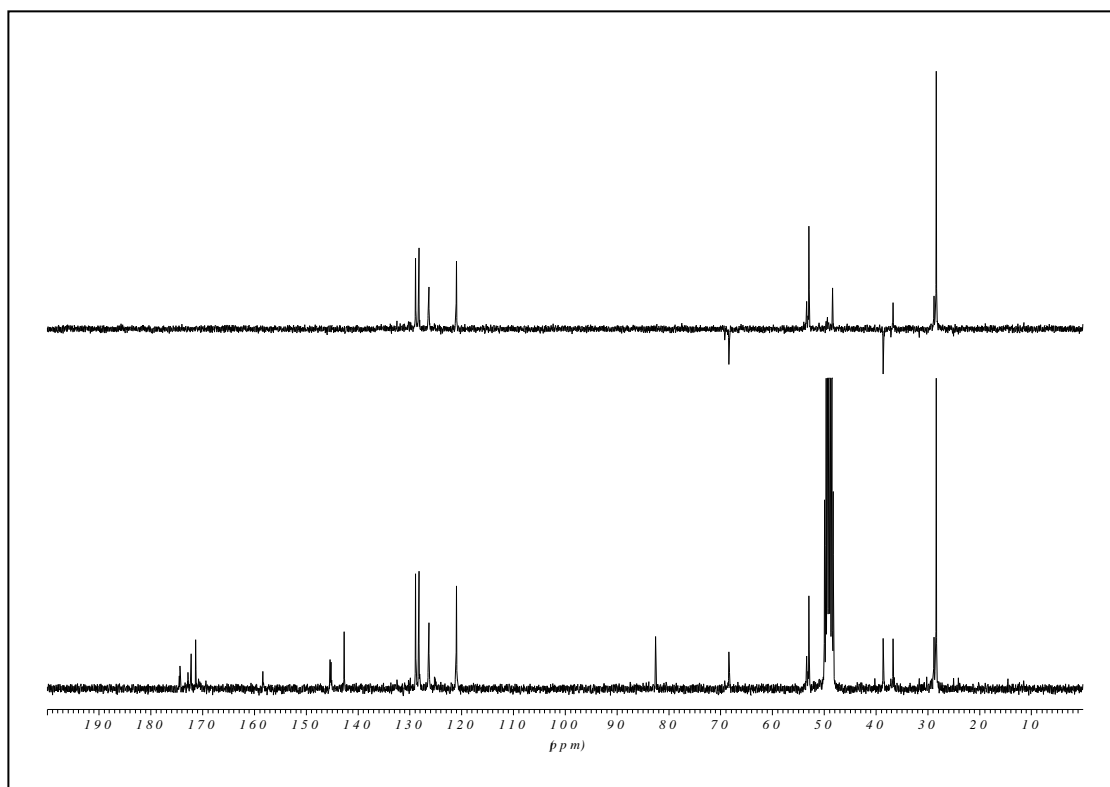
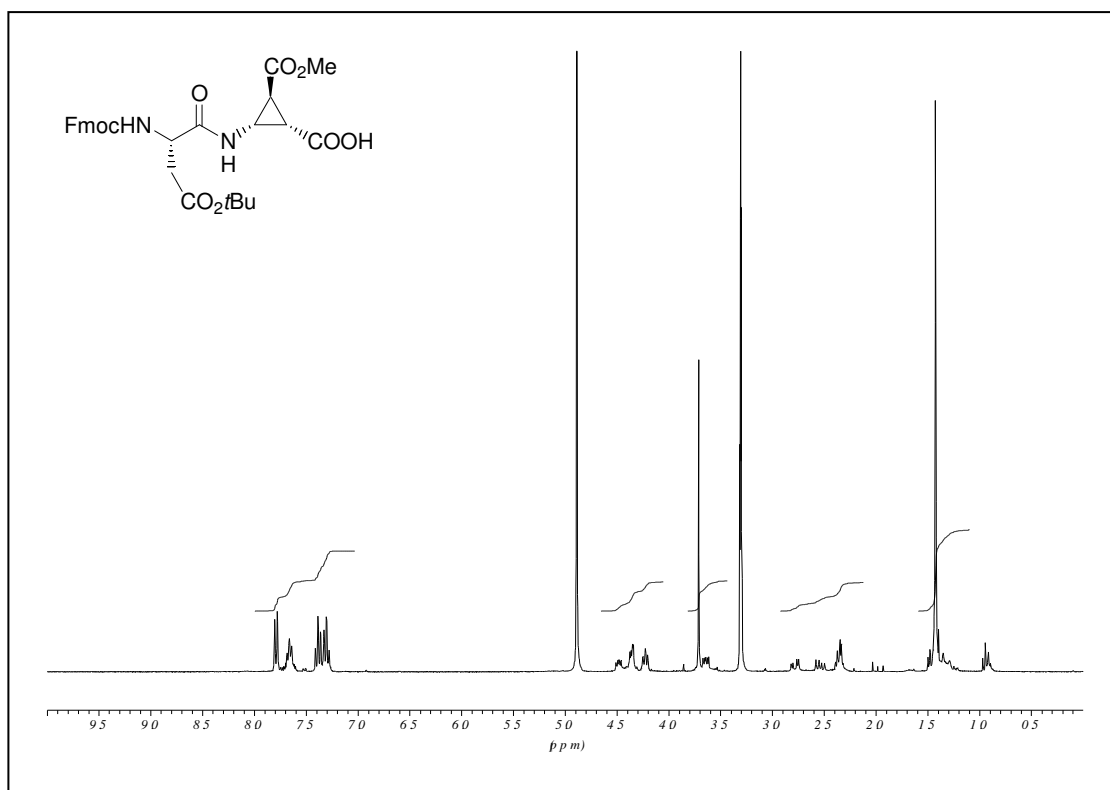
Fmoc-Val(-)- β ACC-OH, (-)-**16a** measured in CD₃OD.



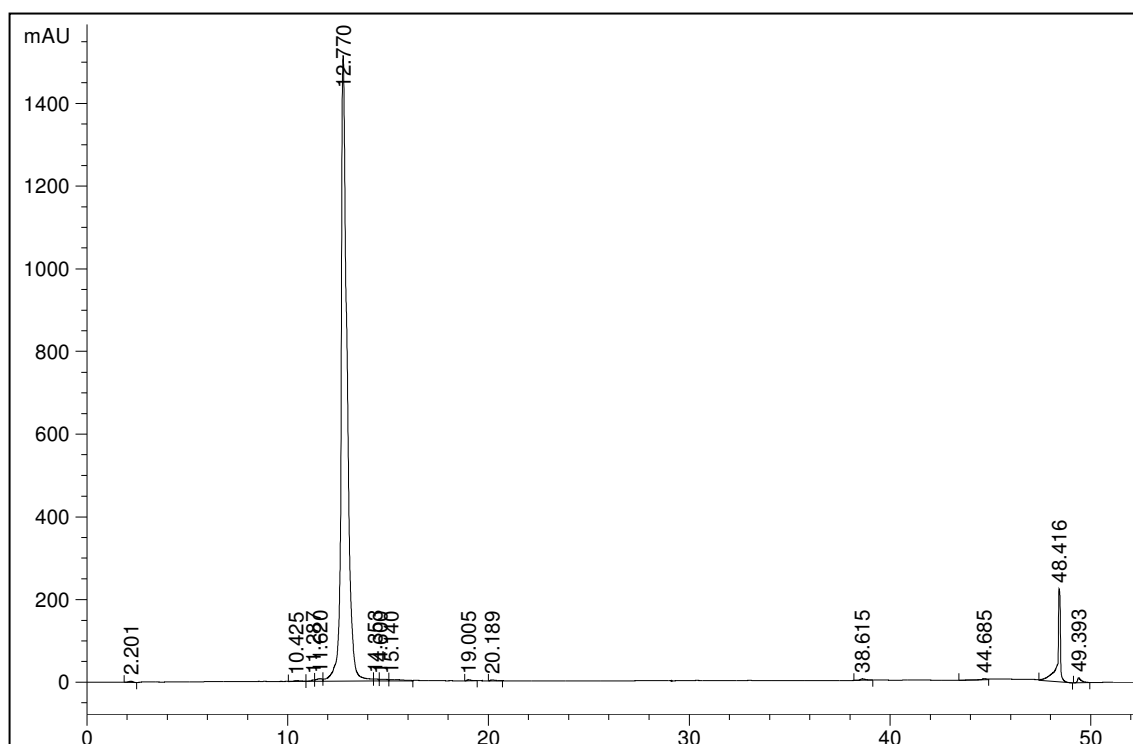
Fmoc-Asp(O^tBu)-(-)-βACC-OBn, (-)-**17** measured in CDCl₃.



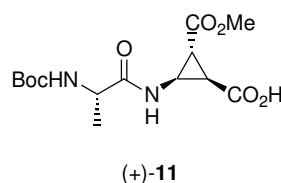
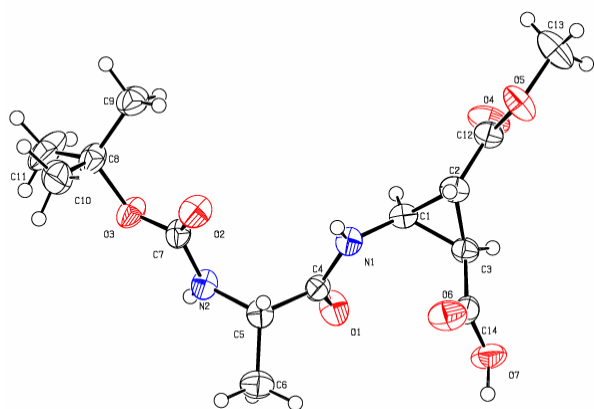
Fmoc-Asp(O^tBu)-(-)-βACC-OH, (-)-**17a** measured in CD₃OD.



H-Lys-(-)- β ACC-Phe-(-)- β ACC-Ala-(-)- β ACC-Phe-(-)- β ACC-Lys-(-)- β ACC-Phe-(-)- β ACC-Ala-OH, (-)-7



HPLC chromatogram, after purification, using Phenomenex luna C18; Injection 20 μ l; Gradient 5-95%ACN in 40 min, 95% for 5 min; Wavelength = 220 nm.



Crystal data of (+)-11:

Empirical formula	C ₁₄ H ₂₂ N ₂ O ₇
Formula weight	330.34
Crystal size	0.48 x 0.32 x 0.12 mm
Crystal description	bar
Crystal colour	colourless
Crystal system	Monoclinic
Space group	C 2
Unit cell dimensions	a = 20.847(2) Å alpha = 90°. b = 5.1817(3) Å beta = 107.825(11)°. c = 16.9359(16) Å gamma = 90°.
Volume	1741.6(3) Å ³
Z, Calculated density	4, 1.260 Mg/m ³
Absorption coefficient	0.101 mm ⁻¹
F(000)	704

Data Collection

Measurement device type	STOE-IPDS diffractometer
Measurement method	rotation
Temperature	173(1) K
Wavelength	0.71073 Å
Monochromator	graphite
Theta range for data collection	2.05 to 25.17°.
Index ranges	-24 ≤ h ≤ 24, -6 ≤ k ≤ 6, -20 ≤ l ≤ 20
Reflections collected / unique	8027 / 8033 [R(int) = 0.0000]
Reflections greater I > 2σ(I)	6620
Absorption correction	None
Refinement	
Refinement method	Full-matrix least-squares on F ²
Hydrogen treatment	:
Data / restraints / parameters	8033 / 1 / 226
Goodness-of-fit on F ²	0.994
Final R indices [I > 2σ(I)]	R1 = 0.0532, wR2 = 0.1435
R indices (all data)	R1 = 0.0651, wR2 = 0.1516
Absolute structure parameter	0.2(12)
Largest diff. peak and hole	0.225 and -0.164 e.Å ⁻³

	<i>x</i>	<i>y</i>	<i>z</i>	<i>U(eq)</i>
O(1)	-2514(1)	-2251(4)	-2606(1)	43(1)
O(2)	-1377(1)	4258(3)	-852(1)	46(1)
O(3)	-1251(1)	1177(3)	147(1)	42(1)
O(4)	-4788(1)	2789(4)	-3367(1)	53(1)
O(5)	-4682(1)	6612(4)	-3922(1)	49(1)
O(6)	-2712(1)	2769(4)	-4404(1)	51(1)
O(7)	-3196(1)	-1076(4)	-4851(1)	51(1)
N(1)	-2663(1)	2037(4)	-2641(1)	32(1)
N(2)	-1364(1)	8(4)	-1146(1)	34(1)
C(1)	-3368(1)	1794(5)	-3046(2)	30(1)
C(2)	-3750(1)	3860(5)	-3605(2)	33(1)
C(3)	-3636(1)	1291(5)	-3971(1)	32(1)
C(4)	-2271(1)	-77(5)	-2458(1)	31(1)
C(5)	-1515(1)	355(5)	-2037(2)	32(1)
C(6)	-1103(1)	-1497(6)	-2386(2)	45(1)
C(7)	-1337(1)	2014(5)	-631(2)	33(1)
C(8)	-1165(2)	3045(5)	838(2)	43(1)
C(9)	-1785(2)	4735(6)	678(2)	47(1)
C(10)	-514(2)	4541(8)	967(2)	63(1)
C(11)	-1100(3)	1262(6)	1575(2)	78(2)
C(12)	-4457(1)	4307(5)	-3612(2)	35(1)
C(13)	-5375(1)	7196(7)	-3973(2)	62(1)
C(14)	-3137(1)	1133(6)	-4437(1)	37(1)

Table 2. Atomic coordinates ($\times 10^4$) and equivalent isotropic displacement parameters ($\text{\AA}^2 \times 10^3$).

$U(eq)$ is defined as one third of the trace of the orthogonalized U_{ij} tensor.

O(1)-C(4)	1.229(3)	C(6)-H(6A)	0.9801
O(2)-C(7)	1.217(3)	C(6)-H(6B)	0.9797
O(3)-C(7)	1.345(3)	C(6)-H(6C)	0.9793
O(3)-C(8)	1.486(3)	C(9)-H(9A)	0.9805
O(4)-C(12)	1.200(3)	C(9)-H(9B)	0.9800
O(5)-C(12)	1.331(3)	C(9)-H(9C)	0.9800
O(5)-C(13)	1.453(4)	C(10)-H(10A)	0.9796
O(6)-C(14)	1.214(4)	C(10)-H(10B)	0.9792
O(7)-C(14)	1.328(4)	C(10)-H(10C)	0.9801
O(7)-H(7O)	0.91(4)	C(11)-H(11A)	0.9805
N(1)-C(4)	1.344(3)	C(11)-H(11B)	0.9789
N(1)-C(1)	1.425(3)	C(11)-H(11C)	0.9803
N(2)-C(5)	1.455(3)	C(13)-H(13A)	0.9795
N(2)-C(7)	1.348(3)	C(13)-H(13B)	0.9805
N(1)-H(1N)	0.82(3)	C(13)-H(13C)	0.9808
N(2)-H(2N)	0.93(3)		
C(1)-C(2)	1.488(4)	C(7)-O(3)-C(8)	120.54(18)
C(1)-C(3)	1.517(3)	C(12)-O(5)-C(13)	115.7(2)
C(2)-C(3)	1.518(4)	C(14)-O(7)-H(7O)	113(2)
C(2)-C(12)	1.490(4)	C(1)-N(1)-C(4)	120.2(2)
C(3)-C(14)	1.487(4)	C(5)-N(2)-C(7)	122.0(2)
C(4)-C(5)	1.535(4)	C(4)-N(1)-H(1N)	120.6(17)
C(5)-C(6)	1.522(4)	C(1)-N(1)-H(1N)	119.2(17)
C(8)-C(9)	1.516(4)	C(7)-N(2)-H(2N)	117.4(14)
C(8)-C(10)	1.520(5)	C(5)-N(2)-H(2N)	119.7(14)
C(8)-C(11)	1.526(4)	C(2)-C(1)-C(3)	60.67(17)
C(1)-H(1)	1.0000	N(1)-C(1)-C(2)	120.9(2)
C(2)-H(2)	1.0004	N(1)-C(1)-C(3)	120.7(2)
C(3)-H(3)	1.0001	C(3)-C(2)-C(12)	114.3(2)
C(5)-H(5)	1.0004	C(1)-C(2)-C(3)	60.60(16)

C(1)-C(2)-C(12)	116.8(2)	N(2)-C(5)-H(5)	108.81
C(1)-C(3)-C(14)	117.5(2)	C(4)-C(5)-H(5)	108.80
C(1)-C(3)-C(2)	58.73(16)	C(6)-C(5)-H(5)	108.73
C(2)-C(3)-C(14)	119.2(2)	C(5)-C(6)-H(6A)	109.47
O(1)-C(4)-N(1)	121.1(2)	C(5)-C(6)-H(6B)	109.49
O(1)-C(4)-C(5)	121.9(2)	C(5)-C(6)-H(6C)	109.47
N(1)-C(4)-C(5)	116.9(2)	H(6A)-C(6)-H(6B)	109.48
N(2)-C(5)-C(6)	110.8(2)	H(6A)-C(6)-H(6C)	109.50
C(4)-C(5)-C(6)	110.5(2)	H(6B)-C(6)-H(6C)	109.41
N(2)-C(5)-C(4)	109.2(2)	C(8)-C(9)-H(9A)	109.42
O(2)-C(7)-O(3)	125.8(2)	C(8)-C(9)-H(9B)	109.44
O(2)-C(7)-N(2)	123.5(2)	C(8)-C(9)-H(9C)	109.47
O(3)-C(7)-N(2)	110.6(2)	H(9A)-C(9)-H(9B)	109.55
O(3)-C(8)-C(11)	102.1(2)	H(9A)-C(9)-H(9C)	109.49
C(9)-C(8)-C(10)	114.0(3)	H(9B)-C(9)-H(9C)	109.46
C(9)-C(8)-C(11)	110.7(3)	C(8)-C(10)-H(10A)	109.49
O(3)-C(8)-C(9)	110.2(2)	C(8)-C(10)-H(10B)	109.45
O(3)-C(8)-C(10)	109.4(2)	C(8)-C(10)-H(10C)	109.47
C(10)-C(8)-C(11)	109.8(3)	H(10A)-C(10)-H(10B)	109.50
O(4)-C(12)-O(5)	123.7(2)	H(10A)-C(10)-H(10C)	109.45
O(4)-C(12)-C(2)	124.6(2)	H(10B)-C(10)-H(10C)	109.47
O(5)-C(12)-C(2)	111.8(2)	C(8)-C(11)-H(11A)	109.50
O(6)-C(14)-C(3)	123.7(3)	C(8)-C(11)-H(11B)	109.57
O(7)-C(14)-C(3)	111.1(2)	C(8)-C(11)-H(11C)	109.41
O(6)-C(14)-O(7)	125.1(2)	H(11A)-C(11)-H(11B)	109.51
N(1)-C(1)-H(1)	114.64	H(11A)-C(11)-H(11C)	109.40
C(2)-C(1)-H(1)	114.69	H(11B)-C(11)-H(11C)	109.43
C(3)-C(1)-H(1)	114.69	O(5)-C(13)-H(13A)	109.42
C(1)-C(2)-H(2)	117.53	O(5)-C(13)-H(13B)	109.49
C(3)-C(2)-H(2)	117.51	O(5)-C(13)-H(13C)	109.49
C(12)-C(2)-H(2)	117.60	H(13A)-C(13)-H(13B)	109.46
C(1)-C(3)-H(3)	116.39	H(13A)-C(13)-H(13C)	109.50
C(2)-C(3)-H(3)	116.38	H(13B)-C(13)-H(13C)	109.46
C(14)-C(3)-H(3)	116.32		

Table 3. Bond lengths [Å] and angles [°] for c048a.

	<i>U11</i>	<i>U22</i>	<i>U33</i>	<i>U23</i>	<i>U13</i>	<i>U12</i>
O(1)	43(1)	20(1)	55(1)	1(1)	1(1)	-7(1)
O(2)	70(1)	21(1)	45(1)	5(1)	17(1)	2(1)
O(3)	66(1)	23(1)	32(1)	-3(1)	10(1)	1(1)
O(4)	45(1)	41(1)	88(2)	6(1)	40(1)	0(1)
O(5)	29(1)	49(1)	68(1)	20(1)	13(1)	5(1)
O(6)	49(1)	55(1)	62(1)	-3(1)	37(1)	-12(1)
O(7)	38(1)	64(1)	58(1)	-26(1)	26(1)	-9(1)
N(1)	38(1)	22(1)	34(1)	1(1)	9(1)	-5(1)
N(2)	46(1)	19(1)	32(1)	3(1)	6(1)	-3(1)
C(1)	34(1)	25(1)	36(1)	-1(1)	16(1)	-3(1)
C(2)	35(1)	29(1)	40(1)	4(1)	18(1)	-1(1)
C(3)	29(1)	32(1)	36(1)	0(1)	13(1)	-2(1)
C(4)	38(1)	26(1)	28(1)	1(1)	9(1)	2(1)
C(5)	36(1)	24(1)	36(1)	3(1)	10(1)	-4(1)
C(6)	47(2)	44(2)	51(2)	1(1)	25(1)	1(1)
C(7)	38(1)	25(1)	32(1)	-1(1)	4(1)	-3(1)
C(8)	62(2)	30(1)	32(1)	-3(1)	6(1)	4(1)
C(9)	57(2)	40(2)	45(1)	-7(1)	17(1)	2(1)
C(10)	50(2)	61(2)	64(2)	-25(2)	-3(1)	3(2)

C(11)	156(4)	39(2)	33(1)	-4(2)	20(2)	22(2)
C(12)	32(1)	34(1)	41(1)	1(1)	16(1)	-2(1)
C(13)	30(1)	59(2)	92(2)	16(2)	14(2)	5(1)
C(14)	29(1)	53(2)	29(1)	-1(1)	9(1)	-4(1)

Table 4. Anisotropic displacement parameters ($\text{\AA}^2 \times 10^3$). The anisotropic displacement factor exponent takes the form: $-2 \pi^2 [h^2 a^{*2} U_{11} + \dots + 2 h k a^* b^* U_{12}]$

	<i>x</i>	<i>y</i>	<i>z</i>	<i>U(eq)</i>
H(1)	-3623	911	-2710	36
H(1N)	-2499(11)	3480(50)	-2528(13)	9(5)
H(2)	-3489	5382	-3704	40
H(2N)	-1360(11)	-1640(50)	-930(13)	14(5)
H(3)	-4035	122	-4162	38
H(5)	-1399	2165	-2148	39
H(6A)	-1200	-3277	-2263	54
H(6B)	-622	-1142	-2131	54
H(6C)	-1221	-1264	-2987	54
H(7O)	-2879(17)	-1270(60)	-5113(19)	56(9)
H(9A)	-1769	5676	1186	57
H(9B)	-2190	3653	510	57
H(9C)	-1797	5968	235	57
H(10A)	-574	5812	522	75
H(10B)	-152	3345	960	75
H(10C)	-396	5431	1503	75
H(11A)	-1010	2292	2083	94
H(11B)	-729	49	1629	94
H(11C)	-1521	300	1487	94
H(13A)	-5675	5905	-4321	74
H(13B)	-5495	8913	-4217	74
H(13C)	-5424	7165	-3415	74

Table 5. Hydrogen coordinates ($\times 10^4$) and isotropic displacement parameters ($\text{\AA}^2 \times 10^3$).

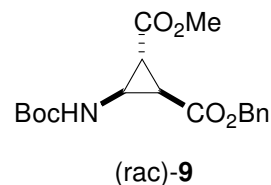
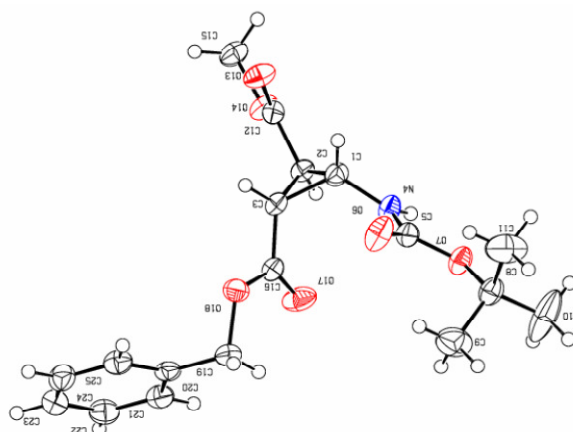
C(7)-O(3)-C(8)-C(9)	61.4(3)
C(7)-O(3)-C(8)-C(10)	-64.8(3)
C(7)-O(3)-C(8)-C(11)	179.0(3)
C(8)-O(3)-C(7)-N(2)	176.4(2)
C(8)-O(3)-C(7)-O(2)	-2.7(4)
C(13)-O(5)-C(12)-C(2)	178.5(2)
C(13)-O(5)-C(12)-O(4)	-1.6(4)
C(4)-N(1)-C(1)-C(2)	-150.2(2)
C(1)-N(1)-C(4)-C(5)	178.9(2)
C(4)-N(1)-C(1)-C(3)	-78.1(3)
C(1)-N(1)-C(4)-O(1)	-2.6(3)
C(5)-N(2)-C(7)-O(2)	-6.6(4)
C(7)-N(2)-C(5)-C(4)	-95.2(3)
C(5)-N(2)-C(7)-O(3)	174.4(2)
C(7)-N(2)-C(5)-C(6)	142.9(2)
N(1)-C(1)-C(3)-C(14)	-1.6(4)
N(1)-C(1)-C(3)-C(2)	-110.6(3)
C(2)-C(1)-C(3)-C(14)	109.1(3)
N(1)-C(1)-C(2)-C(12)	-145.6(2)
N(1)-C(1)-C(2)-C(3)	110.3(3)
C(3)-C(1)-C(2)-C(12)	104.2(2)
C(12)-C(2)-C(3)-C(14)	145.4(2)
C(1)-C(2)-C(3)-C(14)	-106.3(2)
C(12)-C(2)-C(3)-C(1)	-108.3(2)

C(1)-C(2)-C(12)-O(5)	161.2(2)
C(3)-C(2)-C(12)-O(4)	49.3(3)
C(1)-C(2)-C(12)-O(4)	-18.7(4)
C(3)-C(2)-C(12)-O(5)	-130.8(2)
C(2)-C(3)-C(14)-O(7)	-167.5(2)
C(1)-C(3)-C(14)-O(6)	-51.8(4)
C(1)-C(3)-C(14)-O(7)	124.8(2)
C(2)-C(3)-C(14)-O(6)	15.9(4)
O(1)-C(4)-C(5)-N(2)	-80.7(3)
O(1)-C(4)-C(5)-C(6)	41.4(3)
N(1)-C(4)-C(5)-N(2)	97.9(2)
N(1)-C(4)-C(5)-C(6)	-140.0(2)

Table 6. Torsion angles [°].

D-H...A	d(D-H)	d(H...A)	d(D...A)	<(DHA)
N(1)-H(1N)...O(1)#1	0.82(3)	2.22(3)	2.975(3)	154(2)
N(2)-H(2N)...O(2)#2	0.93(3)	2.13(3)	3.022(3)	160.7(19)
O(7)-H(7O)...O(6)#3	0.91(4)	1.75(4)	2.646(3)	170(3)
C(1)-H(1)...O(4)	1.0000	2.5400	2.887(3)	100.00
C(3)-H(3)...O(5)#2	1.0000	2.3700	3.280(3)	150.00
C(5)-H(5)...O(2)	1.0000	2.4400	2.802(3)	101.00
C(9)-H(9C)...O(2)	0.9800	2.4300	2.975(3)	114.00
C(10)-H(10A)...O(2)	0.9800	2.5500	3.059(4)	113.00

Table 7. Hydrogen-bonds [Å and °].



Crystal data of (rac)-9

Empirical formula	C ₁₈ H ₂₃ NO ₆
Formula weight	349.37
Crystal size	0.48 x 0.40 x 0.16 mm
Crystal description	platelike
Crystal colour	translucent colourless
Crystal system	Orthorhombic
Space group	P 21 21 21
Unit cell dimensions	a = 5.4517(3) Å alpha = 90°. b = 16.3923(11) Å beta = 90°. c = 20.2978(12) Å gamma = 90°
Volume	1813.93(19) Å ³
Z, Calculated density	4, 1.279 Mg/m ³
Absorption coefficient	0.096 mm ⁻¹
F(000)	744

Data Collection

Measurement device type	STOE-IPDS diffractometer
Measurement method	rotation
Temperature	173(1) K
Wavelength	0.71073 Å
Monochromator	graphite
Theta range for data collection	2.36 to 25.73 °
Index ranges	-6 <= h <= 6, -19 <= k <= 20, -24 <= l <= 24
Reflections collected / unique	17998 / 3445 [R(int) = 0.0486]
Reflections greater I > 4σ(I)	3102
Absorption correction	None
Refinement	
Refinement method	Full-matrix least-squares on F ²
Hydrogen treatment	mixed
Data / restraints / parameters	3445 / 0 / 246
Goodness-of-fit on F ²	1.049
Final R indices [I > 2σ(I)]	R1 = 0.0339, wR2 = 0.0849
R indices (all data)	R1 = 0.0386, wR2 = 0.0868
Absolute structure parameter	0.2(8)
Largest diff. peak and hole	0.231 and -0.198 e.Å ⁻³

	<i>x</i>	<i>y</i>	<i>z</i>	<i>U(eq)</i>
O(6)	-3014(2)	-2089(1)	-3686(1)	48(1)
O(7)	-6041(2)	-3012(1)	-3909(1)	35(1)
O(13)	-7499(2)	789(1)	-3267(1)	39(1)
O(14)	-10933(2)	528(1)	-2690(1)	34(1)
O(17)	-6798(2)	-1928(1)	-2030(1)	46(1)
O(18)	-3049(2)	-1386(1)	-1916(1)	34(1)
N(4)	-7044(3)	-1797(1)	-3529(1)	33(1)
C(1)	-6564(3)	-968(1)	-3348(1)	30(1)
C(2)	-8269(3)	-564(1)	-2873(1)	28(1)
C(3)	-5651(3)	-759(1)	-2663(1)	27(1)
C(5)	-5153(3)	-2289(1)	-3709(1)	31(1)
C(8)	-4391(3)	-3669(1)	-4144(1)	35(1)
C(9)	-2618(4)	-3918(1)	-3607(1)	58(1)
C(10)	-6154(5)	-4357(1)	-4270(2)	88(1)
C(11)	-3057(6)	-3400(2)	-4755(1)	70(1)
C(12)	-8818(3)	321(1)	-2975(1)	27(1)
C(15)	-11622(3)	1382(1)	-2739(1)	37(1)
C(16)	-5298(3)	-1424(1)	-2173(1)	28(1)
C(19)	-2367(3)	-2013(1)	-1427(1)	35(1)
C(20)	-2238(3)	-1639(1)	-754(1)	29(1)
C(21)	-4071(3)	-1774(1)	-290(1)	34(1)
C(22)	-3920(3)	-1429(1)	333(1)	39(1)
C(23)	-1917(3)	-952(1)	499(1)	41(1)
C(24)	-74(3)	-817(1)	45(1)	39(1)
C(25)	-235(3)	-1157(1)	-578(1)	36(1)

Table 2. Atomic coordinates ($\times 10^4$) and equivalent isotropic displacement parameters ($\text{\AA}^2 \times 10^3$).

$U(eq)$ is defined as one third of the trace of the orthogonalized U_{ij} tensor.

O(6)-C(5)	1.212(2)	C(1)-H(1)	0.923(19)
O(7)-C(5)	1.343(2)	C(2)-H(2)	0.949(16)
O(7)-C(8)	1.482(2)	C(3)-H(3)	0.936(18)
O(13)-C(12)	1.2058(19)	C(9)-H(9A)	0.9804
O(14)-C(12)	1.334(2)	C(9)-H(9B)	0.9794
O(14)-C(15)	1.4528(19)	C(9)-H(9C)	0.9801
O(17)-C(16)	1.198(2)	C(10)-H(10A)	0.9800
O(18)-C(16)	1.333(2)	C(10)-H(10B)	0.9794
O(18)-C(19)	1.476(2)	C(10)-H(10C)	0.9806
N(4)-C(1)	1.432(2)	C(11)-H(11A)	0.9797
N(4)-C(5)	1.359(2)	C(11)-H(11B)	0.9800
N(4)-H(4A)	0.8799	C(11)-H(11C)	0.9796
C(1)-C(3)	1.516(2)	C(15)-H(15A)	0.9801
C(1)-C(2)	1.493(2)	C(15)-H(15B)	0.9809
C(2)-C(12)	1.496(2)	C(15)-H(15C)	0.9805
C(2)-C(3)	1.524(2)	C(19)-H(19A)	0.97(2)
C(3)-C(16)	1.488(2)	C(19)-H(19B)	0.98(2)
C(8)-C(10)	1.504(3)	C(21)-H(21A)	0.9497
C(8)-C(11)	1.505(3)	C(22)-H(22A)	0.9499
C(8)-C(9)	1.512(3)	C(23)-H(23A)	0.9498
C(19)-C(20)	1.499(2)	C(24)-H(24A)	0.9503
C(20)-C(25)	1.394(2)	C(25)-H(25A)	0.9495
C(20)-C(21)	1.392(2)		
C(21)-C(22)	1.387(3)	C(5)-O(7)-C(8)	121.32(12)
C(22)-C(23)	1.385(2)	C(12)-O(14)-C(15)	116.02(12)
C(23)-C(24)	1.381(2)	C(16)-O(18)-C(19)	117.52(12)
C(24)-C(25)	1.386(3)	C(1)-N(4)-C(5)	119.59(15)

C(5)-N(4)-H(4A)	120.19	C(2)-C(3)-H(3)	116.4(10)
C(1)-N(4)-H(4A)	120.21	C(16)-C(3)-H(3)	116.2(11)
N(4)-C(1)-C(3)	120.67(13)	C(8)-C(9)-H(9A)	109.47
N(4)-C(1)-C(2)	118.22(14)	C(8)-C(9)-H(9B)	109.45
C(2)-C(1)-C(3)	60.85(11)	C(8)-C(9)-H(9C)	109.42
C(3)-C(2)-C(12)	115.46(13)	H(9A)-C(9)-H(9B)	109.49
C(1)-C(2)-C(3)	60.31(11)	H(9A)-C(9)-H(9C)	109.52
C(1)-C(2)-C(12)	117.72(13)	H(9B)-C(9)-H(9C)	109.47
C(1)-C(3)-C(16)	119.39(13)	C(8)-C(10)-H(10A)	109.48
C(1)-C(3)-C(2)	58.84(10)	C(8)-C(10)-H(10B)	109.44
C(2)-C(3)-C(16)	117.54(13)	C(8)-C(10)-H(10C)	109.43
O(6)-C(5)-N(4)	123.98(16)	H(10A)-C(10)-H(10B)	109.50
O(6)-C(5)-O(7)	126.65(15)	H(10A)-C(10)-H(10C)	109.46
O(7)-C(5)-N(4)	109.37(14)	H(10B)-C(10)-H(10C)	109.51
O(7)-C(8)-C(10)	102.24(15)	C(8)-C(11)-H(11A)	109.50
O(7)-C(8)-C(11)	110.19(15)	C(8)-C(11)-H(11B)	109.44
C(9)-C(8)-C(11)	111.36(18)	C(8)-C(11)-H(11C)	109.42
C(10)-C(8)-C(11)	112.9(2)	H(11A)-C(11)-H(11B)	109.49
C(9)-C(8)-C(10)	109.14(18)	H(11A)-C(11)-H(11C)	109.49
O(7)-C(8)-C(9)	110.67(15)	H(11B)-C(11)-H(11C)	109.48
O(14)-C(12)-C(2)	111.05(13)	O(14)-C(15)-H(15A)	109.52
O(13)-C(12)-C(2)	124.41(15)	O(14)-C(15)-H(15B)	109.48
O(13)-C(12)-O(14)	124.53(14)	O(14)-C(15)-H(15C)	109.47
O(17)-C(16)-C(3)	125.29(15)	H(15A)-C(15)-H(15B)	109.40
O(17)-C(16)-O(18)	124.45(15)	H(15A)-C(15)-H(15C)	109.46
O(18)-C(16)-C(3)	110.26(13)	H(15B)-C(15)-H(15C)	109.50
O(18)-C(19)-C(20)	109.87(13)	O(18)-C(19)-H(19A)	106.4(13)
C(19)-C(20)-C(21)	121.24(14)	O(18)-C(19)-H(19B)	102.5(11)
C(21)-C(20)-C(25)	118.62(15)	C(20)-C(19)-H(19A)	110.7(12)
C(19)-C(20)-C(25)	120.13(15)	C(20)-C(19)-H(19B)	112.9(11)
C(20)-C(21)-C(22)	120.64(15)	H(19A)-C(19)-H(19B)	113.8(17)
C(21)-C(22)-C(23)	119.95(16)	C(20)-C(21)-H(21A)	119.69
C(22)-C(23)-C(24)	120.08(17)	C(22)-C(21)-H(21A)	119.67
C(23)-C(24)-C(25)	119.92(16)	C(21)-C(22)-H(22A)	120.03
C(20)-C(25)-C(24)	120.78(16)	C(23)-C(22)-H(22A)	120.01
N(4)-C(1)-H(1)	114.9(11)	C(22)-C(23)-H(23A)	119.94
C(2)-C(1)-H(1)	116.0(12)	C(24)-C(23)-H(23A)	119.98
C(3)-C(1)-H(1)	115.5(12)	C(23)-C(24)-H(24A)	120.05
C(1)-C(2)-H(2)	118.1(10)	C(25)-C(24)-H(24A)	120.03
C(3)-C(2)-H(2)	117.0(10)	C(20)-C(25)-H(25A)	119.61
C(12)-C(2)-H(2)	116.4(10)	C(24)-C(25)-H(25A)	119.61
C(1)-C(3)-H(3)	116.1(11)		

Table 3. Bond lengths [Å] and angles [°].

	<i>U11</i>	<i>U22</i>	<i>U33</i>	<i>U23</i>	<i>U13</i>	<i>U12</i>
O(6)	35(1)	37(1)	73(1)	-15(1)	6(1)	-3(1)
O(7)	32(1)	27(1)	44(1)	-9(1)	1(1)	2(1)
O(13)	39(1)	28(1)	49(1)	9(1)	12(1)	2(1)
O(14)	31(1)	23(1)	47(1)	2(1)	7(1)	2(1)
O(17)	34(1)	36(1)	68(1)	20(1)	-4(1)	-8(1)
O(18)	34(1)	33(1)	36(1)	7(1)	-7(1)	-4(1)
N(4)	33(1)	27(1)	39(1)	-9(1)	0(1)	0(1)
C(1)	34(1)	25(1)	31(1)	-2(1)	3(1)	1(1)
C(2)	27(1)	23(1)	33(1)	1(1)	1(1)	-1(1)
C(3)	27(1)	21(1)	33(1)	-1(1)	1(1)	-3(1)
C(5)	35(1)	29(1)	30(1)	-3(1)	0(1)	1(1)
C(8)	35(1)	29(1)	43(1)	-8(1)	3(1)	5(1)
C(9)	67(1)	56(1)	51(1)	4(1)	2(1)	27(1)
C(10)	47(1)	49(1)	167(3)	-58(2)	0(2)	4(1)

C(11)	104(2)	58(1)	47(1)	9(1)	29(1)	36(1)
C(12)	28(1)	26(1)	27(1)	-1(1)	-1(1)	0(1)
C(15)	42(1)	25(1)	45(1)	-1(1)	7(1)	5(1)
C(16)	29(1)	23(1)	31(1)	-3(1)	1(1)	1(1)
C(19)	39(1)	28(1)	38(1)	4(1)	-4(1)	5(1)
C(20)	28(1)	25(1)	35(1)	6(1)	-3(1)	5(1)
C(21)	28(1)	32(1)	42(1)	8(1)	-3(1)	-2(1)
C(22)	40(1)	41(1)	37(1)	8(1)	7(1)	-1(1)
C(23)	50(1)	37(1)	36(1)	2(1)	-5(1)	0(1)
C(24)	36(1)	34(1)	47(1)	1(1)	-6(1)	-5(1)
C(25)	31(1)	35(1)	43(1)	6(1)	2(1)	0(1)

Table 4. Anisotropic displacement parameters ($\text{\AA}^2 \times 10^3$). The anisotropic displacement factor exponent takes the form: $-2 \pi^2 [h^2 a^{*2} U_{11} + \dots + 2 h k a^* b^* U_{12}]$

	<i>x</i>	<i>y</i>	<i>z</i>	<i>U(eq)</i>
H(1)	-5970(40)	-643(11)	-3683(9)	31(4)
H(2)	-9540(30)	-883(10)	-2684(8)	21(4)
H(3)	-4570(30)	-317(11)	-2633(9)	26(4)
H(4A)	-8554	-1986	-3525	40
H(9A)	-3527	-4027	-3200	70
H(9B)	-1741	-4412	-3743	70
H(9C)	-1438	-3477	-3532	70
H(10A)	-5241	-4843	-4408	105
H(10B)	-7064	-4478	-3865	105
H(10C)	-7305	-4199	-4618	105
H(11A)	-2018	-2929	-4652	83
H(11B)	-2034	-3848	-4918	83
H(11C)	-4252	-3247	-5094	83
H(15A)	-10357	1720	-2531	45
H(15B)	-11781	1534	-3204	45
H(15C)	-13193	1468	-2514	45
H(19A)	-3630(40)	-2425(13)	-1445(10)	43(5)
H(19B)	-770(40)	-2199(11)	-1588(9)	31(5)
H(21A)	-5439	-2106	-400	41
H(22A)	-5189	-1520	645	47
H(23A)	-1811	-717	926	49
H(24A)	1303	-491	160	47
H(25A)	1035	-1062	-889	43

Table 5. Hydrogen coordinates ($\times 10^4$) and isotropic displacement parameters ($\text{\AA}^2 \times 10^3$).

C(5)-O(7)-C(8)-C(11)	-63.1(2)
C(5)-O(7)-C(8)-C(9)	60.5(2)
C(5)-O(7)-C(8)-C(10)	176.66(18)
C(8)-O(7)-C(5)-O(6)	-0.9(3)
C(8)-O(7)-C(5)-N(4)	179.12(14)
C(15)-O(14)-C(12)-C(2)	178.12(13)
C(15)-O(14)-C(12)-O(13)	-0.6(2)
C(16)-O(18)-C(19)-C(20)	-108.22(15)
C(19)-O(18)-C(16)-C(3)	-178.90(13)
C(19)-O(18)-C(16)-O(17)	0.4(2)
C(1)-N(4)-C(5)-O(7)	-174.99(13)
C(1)-N(4)-C(5)-O(6)	5.1(3)
C(5)-N(4)-C(1)-C(3)	-80.7(2)
C(5)-N(4)-C(1)-C(2)	-151.74(15)
N(4)-C(1)-C(3)-C(2)	-107.38(17)

C(2)-C(1)-C(3)-C(16)	106.24(16)
N(4)-C(1)-C(2)-C(12)	-143.65(15)
N(4)-C(1)-C(3)-C(16)	-1.1(2)
N(4)-C(1)-C(2)-C(3)	111.32(16)
C(3)-C(1)-C(2)-C(12)	105.03(16)
C(12)-C(2)-C(3)-C(1)	-108.76(15)
C(1)-C(2)-C(3)-C(16)	-109.36(15)
C(3)-C(2)-C(12)-O(13)	44.6(2)
C(1)-C(2)-C(12)-O(13)	-23.7(2)
C(3)-C(2)-C(12)-O(14)	-134.14(14)
C(1)-C(2)-C(12)-O(14)	157.55(14)
C(12)-C(2)-C(3)-C(16)	141.88(14)
C(1)-C(3)-C(16)-O(18)	127.76(15)
C(2)-C(3)-C(16)-O(18)	-164.32(13)
C(1)-C(3)-C(16)-O(17)	-51.5(2)
C(2)-C(3)-C(16)-O(17)	16.4(2)
O(18)-C(19)-C(20)-C(21)	105.11(17)
O(18)-C(19)-C(20)-C(25)	-76.13(18)
C(19)-C(20)-C(21)-C(22)	179.54(15)
C(25)-C(20)-C(21)-C(22)	0.8(2)
C(19)-C(20)-C(25)-C(24)	-179.10(16)
C(21)-C(20)-C(25)-C(24)	-0.3(2)
C(20)-C(21)-C(22)-C(23)	-0.7(3)
C(21)-C(22)-C(23)-C(24)	0.2(3)
C(22)-C(23)-C(24)-C(25)	0.3(3)
C(23)-C(24)-C(25)-C(20)	-0.2(3)

Table 6. Torsion angles [°].

<i>D-H...A</i>	<i>d(D-H)</i>	<i>d(H...A)</i>	<i>d(D...A)</i>	<i>∠(DHA)</i>
N(4)-H(4A)...O(6)#1	0.8799	2.4590	3.305(2)	161.45
C(3)-H(3)...O(14)#2	0.936(18)	2.421(17)	3.3270(19)	162.8(15)
C(9)-H(9C)...O(6)	0.9801	2.4520	3.011(3)	115.79
C(11)-H(11A)...O(6)	0.9797	2.4572	3.054(3)	118.97
C(19)-H(19A)...O(17)	0.97(2)	2.25(2)	2.712(2)	108.3(15)
C(19)-H(19B)...O(17)#2	0.98(2)	2.39(2)	3.277(2)	151.0(15)

Table 7. Hydrogen-bonds [Å and °].

Publications

- Ceretti, S.; Luppi, G.; De Pol, S.; Formaggio, F.; Crisma, M.; Toniolo, C.; Tomasini, C. "Total Synthesis of Sequential Retro-Peptide Oligomers" *Eur. J. Org. Chem.* **2004**, 20, 4188-4196.
- De Pol, S.; Zorn, C.; Klein, D. C.; Zerbe, O.; Reiser O. "Surprisingly Stable Helical Conformations in α -/ β -Peptides by Incorporations of *cis*- β -Aminocyclopropane Carboxylic Acids" *Angew. Chem. Int. Ed.* **2004**, 43, 511-514.
"Überraschend stabile helicale Strukturen in α -/ β -Peptides durch Einbau von *cis*- β -Aminocyclopropan-carbosäuren" *Angew. Chem.* **2004**, 116, 517-520.
- Lang, M.; De Pol, S.; Baldauf, C.; Hofmann, H.-J.; Reiser, O.; Beck-Sickinger, A. G. "Identification of the key residue of Calcitonin Gene Related Peptide (CGRP) 27-37 to obtain antagonists with picomolar affinity at the CGRP receptor" *J. Med. Chem.* **2006**, 49, 616-624.
- Lang, M.; Bufe, B.; De Pol, S.; Reiser, O.; Meyerhof, W.; Beck-Sickinger, A. G. "Identification of prerequisites for activation of the orexin 1 and the orexin 2 receptor" *J. Peptide Sci.* **2006**, 12, 258-266.
-
- De Pol, S.; Khan, I. U.; Koglin, N.; Cabrele, C.; Zorn, C.; Zerbe, O.; Beck-Sickinger, A.; Reiser, O. "Investigation on Peptidic Neuropeptide Y Ligands Containing β -Aminocyclopropanecarboxylic Acids" manuscript in preparation.

Oral presentations

- "Investigation on NPY analogues containing conformationally restricted β -amino acids" *Evaluation of the Graduate College GRK 760* **01/2006**, Regensburg, Germany.
- "Introduction of β -ACC units into α -Peptides, Conformational Studies and Applications" *Summer School Medicinal Chemistry* **09/2005**, Shanghai, China.

Poster presentations

- De Pol, S.; Sahr, F.; Khan, I. U.; Haque, M. M.; Hoffman, H.-J.; Beck-Sickinger, A. G.; Zerbe, O.; Cabrele, C.; Reiser, O. *Evaluation of the Graduate College GRK 760* **01/2006**, Regensburg, Germany. "Foldamers from unnatural amino acids as selective ligands for neuropeptide Y receptors"
- De Pol, S.; Zerbe, O.; Reiser, O. *Summer School Medicinal Chemistry* **09/2005**, Shanghai, China. "Introduction of β -ACC units into α -Peptides, Conformational Studies and Applications"
- De Pol, S.; Zerbe, O.; Reiser, O. *7th German Peptide Symposium* **02/2005**, Braunschweig, Germany. "Studies on α -Peptides containing β -ACC units and their Applications"
- De Pol, S.; Zerbe, O.; Reiser, O. *Summer School Medicinal Chemistry* **09/2004**, Regensburg, Germany. "Stable Secondary structures of Peptides induced by β -ACC units"
- De Pol, S.; Zerbe, O.; Reiser, O. *Annual Chemistry GDCh Congress* **10/2003**, München, Germany. "Conformational studies on α -/ β -alternating Peptides containing β -ACC units"
- De Pol, S.; Zorn, C.; Gnad, F.; Zerbe, O.; Reiser, O. *Tag der Naturwissenschaft* **06/2003**, Regensburg, Germany. "Synthesis and structural studies of oligopeptides containing β -ACC units"
- De Pol, S.; Zorn, C.; Zerbe, O.; Reiser, O. *6th German Peptide Symposium* **05/2003**, Berlin, Germany. "Structural studies on α -/ β -alternating Oligopeptides containing β -ACC units"
- Zorn, C.; De Pol S.; Zerbe O.; Reiser, O. *Summer School Medicinal Chemistry* **09/2002**, Regensburg, Germany. "Synthesis and conformational studies of α -peptides containing β -ACC"

Curriculum Vitae

Silvia De Pol

28. August 1975 in Venezia, Italy

Email: silviadpm@hotmail.com

Education and qualifications

- 2002- 2006 Ph.D. work in Organic Chemistry (Prof. Dr. O. Reiser's research group)
University of Regensburg, Germany
"Synthesis, conformational investigations and applications of α -peptides containing cis- β -aminocyclopropane carboxylic acid"
- 2000-2001 Diploma (laurea) thesis in Organic Chemistry (Prof. C. Toniolo's research group) University of Padova, Italy
"Synthesis of Sequential Retro-Peptide Oligomers"
Result of final examination: 110/110
- 1994-2000 Chemistry studies; University of Padova, Italy
- 1989-1994 Istituto Tecnico A. Pacinotti (Mestre-Ve, Italy)
(high school for qualified industrial chemists)
Result of final examination: 60/60

Further educational experiences

- Jan 2002-Jan 2006 University of Regensburg, Germany
associated to the research training group *Graduate College GRK 760*.
- December 2004 University of Zürich, Switzerland.
Conformational investigations by 2D-NMR under the supervision of Prof. Dr. O. Zerbe.
- October 2004 University of Bielefeld, Germany.
Biological investigations under the supervision of Prof. Dr. N. Sewald.
- Jan-Mar 1999 Georg-August-University Göttingen, Germany.
ERASMUS, EU student exchange program.

Acknowledgements

I would like to thank my Ph.D. tutor, Prof. Dr. *Oliver Reiser*, who gave me the opportunity to perform my Ph.D. in Germany. He offered me an interesting research project in the world of peptides and supported its development at any time.

I am grateful to Prof. Dr. *Zerbe*, who taught me patiently the techniques for the 2D-NMR structural investigation analysis; to Prof. Dr. *Sewald* and Ms. *Urman* concerning the RGD Project; to Prof. Dr. *Beck-Sickinger*, Prof. Dr. *Buschauer*, Prof. Dr. *Bernhardt* and Ms. *Schreiber* concerning the NPY Project and to Prof. Dr. *Dove* for helping me with molecular modelling techniques.

Thanks to Dr. *Peter Kreitmeier* for his help and his precious answers to all my questions; to Mr. *Klaus Döring*, Mr. *Georg Adolin*, Ms. *Andrea Roithmeier* and Mr. *Robert Tomahogh* for our German-Italian exchange of views and for the helpful contribution to some reactions.

I am especially grateful to Dr. *Chiara Cabrele* and Dott.sa *Noemi Colombo* for their help with HPLC, MALDI analysis and for the interesting and helpful peptide-discussions.

For the indispensable bureaucratic organization, a special thanks to Mrs. *Rotermund*, Mr. *Hirtreiter*, Mr. *Reinhold*, Ms. *Ohli* and Mrs. *Kratochwil*.

I thank Dr. *Burgermeister*, Mr. *Kastner*, Ms. *Schramm* and Ms. *Stülher* for recording NMR spectra and for the many tips on NMR data; Dr. *Vasold* and Mr. *Lautenschlager* for HPLC analysis and for the help during peptide HPLC-purifications; Dr. *Zabel* und Ms. *Stempfhuber* for recording X-ray spectra; Dr. *Mayer*, Mr. *Keirmeier* and Mr. *Söllner* and Mr. *Wandinger* for recording mass-spectra and elemental analysis.

For the financial support I am grateful to the *DAAD* (International Quality Network Medicinal Chemistry), the *Deutsche Forschungsgemeinschaft (DFG)*, the *Graduiertenkolleg GRK 760 Medicinal Chemistry* and the *Fondazione Gini*.

For the correction of my Ph.D. thesis I would like to thank *Declan MacDonnell*, *Won Boo Jeong*, *Thorsten Graf* and *Andrea Salvetti*.

I am especially grateful to all my ex- and current colleagues for their helpfulness and friendship in the lab-time, in particular Dr. *Frieder Gnad*, Dott.sa *Tamara Danelli*, Dr. *Mohammad Mahbubul Haque*, Dr. *Marko Poleschak*, Dr. *Changkuo Zhao* and *Andreas Schall* for the nice mood in our lab.

Moreover I would like to thank all those friends that give, with their kind friendship, an important contribution to my experience in Regensburg, inside but also outside the labs:

Won Boo, Weimin, Mahbubul, his wife *Salma* and his child *Redwan*, Mrs. *Rotermund, Maria Kamm, Radek, Yukitaka, Yongwen* and her husband, *Htay, Patil* and his wife *Archana, Luo, Sanjay, Eva Engel, Yogesh, Prasanta, Srinivas, Rakesh, Anu, Ai, Alexander, Milli, Ralf, Kristina, Jiri und Jaroslava, Frieder* and *Conny*, who allow me to experience their cultures with chats, typical meals and presents from their countries.

Won Boo for his vitality, sympathy, helpfulness and extraordinary kindness; *Conny* and *Frieder* for their kind and infinite hospitality and moral support at any time; *Tamara*, because I will never forget our shopping-time on Saturdays and our dinners together in the first months of my staying here!; *Leda*, for her unforgettable, delicious dinners and the helpful discussions preparing the seminars; *Anna*, for her vitality, our interminable chats and our unforgettable weekend in Prague; *Giovanni*, for our interesting trips exploring Europe, for his generosity, hospitality and the delicious dinners; *Alexander, Florian, Yogesh, Patil, Srinivas* and *Hans* for our amusing bowling, billiard and “Tequila” challenges!; *Noemi, Elena Sancassiani, Elena Silva* and *Alessandro* for the good time we had together trying Bavarian gastronomic specialities and during the Gio’s dinners!

For the support from a distance, I would like to thank:

Eleonora Colombo in *Viale (!)*, whose friendship never failed;
Prof. *Leone*, Prof. *Veronese*, my grandfather *Guerrino* and *Umberto Zaffanella*, who deleted all my hesitations before the departure;
Andrea Salvetti for visiting me in Regensburg many times, for the all kind of presents and for the many tips concerning Computers, softwares and so on.
Walter, Sime, Bianca, Eva and *Jürgen, Cristina* and *Jacopo, Dorina* and *Valda, Ugo* and *Adele, Patrizia, Don Silvio, Lello, Indo, Wonder, Maria* and *Giordano, Vitaliano, Berta* and *Mauro* for Emails, Phone calls, presents and letters arrived during these years.

My parents *Betty* and *Giorgio* receive my greatest wholeheartedly thank for their support, understanding, helpfulness and encouragement they gave me at any time during this experience.